UNIVERSITY OF LIVERPOOL

Novel approaches in the management of bladder cancer

Richard Malcolm Douglas Greensmith

November 2016

Submitted in partial fulfilment of the requirements for the degree of Doctor of Philosophy

I, Richard Greensmith, confirm that the research included within this thesis is my own work or that where it has been carried out in collaboration, or supported by others that this is duly acknowledged below and my contribution indicated. Previously published material is also acknowledged within.

I attest that I have exercised reasonable care to ensure that the work is original, and does not to the best of my knowledge break any UK law, infringe any third parties copyright or other intellectual property right, or contain any confidential information.

I accept that The University of Liverpool has the right to use plagiarism detection software to check the electronic version of this thesis.

I confirm that this thesis has not been previously submitted for the award of a degree by this, or any other university.

Name: **Richard Malcolm Douglas Greensmith**

Signature: 

Date: 29/11/2016

Table of Contents

Table of Figures ..... **vii**
List of Tables ..... **xi**
Abstract ..... **xii**
Acknowledgements ..... **xv**
Publications ..... **xvi**
Papers xvi
Abstracts xvi
Grants xvi
Abbreviations ..... **xvii**
Chapter One – General Introduction **1**
1.1 Principles of cancer **2**
1.2 Bladder cancer **4**
1.2.1 Bladder cancer: the urinary bladder 4
1.2.2 Bladder cancer: epidemiology, aetiology and carcinogenesis 8
1.2.3 Bladder cancer: diagnosis 15
1.2.4 Bladder cancer: treatment 20
1.3 The NRF2-KEAP1 axis **28**
1.3.1 NRF2 in cancer 31
1.4 Cluster of differentiation 40 ..... **38**
1.4.1 CD40 expression in bladder cancer 40
1.4.2 CD40-ligand 41
1.4.3 TRAFs facilitate CD40 signal transduction 43
1.4.4 Clinical application of CD40 targeted therapies in bladder cancer 45
1.5 Matrix metalloproteinase-1 ..... **46**
1.6 Fibronectin **48**
1.7 Family with sequence similarity 83, member D **50**
1.8 Anillin **51**
1.9 Biomarkers in bladder cancer **53**
1.9.1 Biomarkers 54
1.10 Thesis hypotheses **57**
Chapter Two – Materials and Methods **58**
2.1 Tissue culture techniques **59**
2.1.1 Maintenance of cell lines 59
2.1.2 Cryopreservation and thawing of cell stocks 61

2.1.3 Cell counting and cell seeding 61
2.1.4 Cell viability assay 61
2.1.5 Short tandem repeat profiling 62
2.1.6 Treatment of cells with compounds 64
2.1.7 Transfection with NRF2 targeting short interfering RNA 64
2.1.8 Organotypic model of invasion 65
2.2 Protein biochemistry techniques 68
2.2.1 Preparation of protein extracts 68
2.2.2 Western Immunoblotting techniques 68
2.2.3 Immunohistochemistry 72
2.3 Nucleic acid techniques 76
2.3.1 Reverse transcription polymerase chain reaction 76
2.4 Gene expression analysis methods 81
2.4.1 Patients and tissue samples 81
2.4.2 Study ethical considerations 81
2.4.3 Tissue biopsy sample preparation 84
2.4.4 Human Gene 1.0 ST Microarray hybridisation analysis 84
2.4.5 Statistical analysis of microarray data 85
2.4.6 Meta-analysis 86
Chapter Three – An *in vitro* investigation into brusatol as a potentiating adjunct to cisplatin based chemotherapy 88
3.1 Introduction 89
3.1.2 Chapter aims 90
3.2 Results 91
3.2.1 Evaluation of the sensitivity of a panel of 5 UCC cell lines to the cytotoxic effects cisplatin 91
3.2.2 Determination of the sensitivity of 5 UCC cell lines to the cytotoxic effects of brusatol 94
3.2.3 DMSO at a concentration of 1:1000 does not alter the sensitivity of UCC cell lines to cisplatin 96
3.2.4 Investigation into the effects of 2-hour pre-treatment with a range of concentrations of brusatol with respect to the sensitivity to cisplatin 98
3.2.5 Optimisation of brusatol concentration and pre-treatment time prior to cisplatin addition 105
3.2.6 Brusatol as an inhibitor of protein synthesis 118

3.3 Discussion **123**

Chapter Four – The effect of CD40-ligation on urothelial cell carcinoma cell line invasion in an organotypic model of bladder cancer **129**

4.1 Introduction **130**

4.1.1 Chapter aims 133

4.2 Results **134**

4.2.1 UCC cells differentially express CD40 134

4.2.2 EJ transfection with AdNclCD40L 136

4.2.3 CD40-ligation attenuates tumour cell invasion in an organotypic model of bladder cancer 138

4.2.4 RNA microarray in EJ cells displays differential expression in genes implicated in tumour invasion by bladder gene expression profiling. 149

4.3 Discussion **158**

Chapter Five – Gene expression profiling identifies distinct segregation between histological subtypes of bladder cancer **163**

5.1 Introduction **164**

5.1.2 Chapter aims 165

5.2 Results **166**

5.2.1 Bladder cancer tissue exhibits specific gene expression signatures 166

5.2.2 Further functional analysis employing Database for Annotation, Visualization, and Integrated Discovery (DAVID) 189

5.2.3 Meta-analysis of publicly available datasets 191

5.2.4 Osteopontin protein is overexpressed in MIBC tissue compared to normal urothelium * 192

5.3 Discussion **202**

Chapter Six – General discussion **206**

6.1 Introduction **207**

6.2 The utility of brusatol in BC and the future of NRF2 inhibition in cancer .. **208**

6.3 The significance of CD40-signalling in bladder cancer **211**

6.4 The importance gene expression analysis and biomarker identification in the advancement of bladder cancer care **213**

6.5 Insight into the near and distant future of bladder cancer care **215**

6.6 Concluding statements **218**

Chapter Seven – Bibliography **220**

Appendix I – Publication: Gene expression profiling in bladder cancer identifies potential therapeutic targets.....244

Appendix II – Grant: Characterisation of dendritic cell function in the three-dimensional model of urothelial carcinoma in response to soluble CD40L based immunotherapy.....257

Table of Figures

Chapter One

Figure 1.1. The hallmarks of cancer. 3
Figure 1.2. The urinary bladder, displaying different stages of urothelial cell carcinoma 5
Figure 1.3. Structure of the urothelium 6
Figure 1.4. Age standardised five-year relative survival rates for England and Wales 1971-2009, based on cancer type 9
Figure 1.5. Bladder cancer: stage at diagnosis. 16
Figure 1.6. The NRF2-KEAP1 axis 30
Figure 1.7. Mechanism of CD40L induced cell death 39

Chapter Two

Figure 2.1. An organotypic model of bladder cancer 66

Chapter Three

Figure 3.1. Cisplatin exerts its cytotoxicity in a concentration dependent manner on 5 UCC cell lines 92
Figure 3.2. Brusatol exerts concentration-dependent cytotoxic effects in UCC cells 95
Figure 3.3. The comparative cytotoxicity of cisplatin alone and cisplatin in combination with 1:1000 DMSO 97
Figure 3.4. Pre-treatment with 400nM brusatol for 2 hours significantly increases the sensitivity of EJ cells to the cytotoxic effects of cisplatin 100
Figure 3.5. Pre-treatment with 400nM brusatol for 2 hours significantly increases the sensitivity of 253-J cells to the cytotoxic effects of cisplatin 101
Figure 3.6. Pre-treatment with brusatol for 2 hours does not significantly increases the sensitivity of MGH-U3 cells to the cytotoxic effects of cisplatin 102
Figure 3.7. Pre-treatment with concentrations at 100nM and greater of brusatol for 2 hours significantly increases the sensitivity of RT112 cells to the cytotoxic effects of cisplatin 103

Figure 3.8. Pre-treatment with concentrations at 200nM of brusatol and higher for 2 hours significantly increases the sensitivity of RT112-CP cells to the cytotoxic effects of cisplatin 104
Figure 3.9. Comparison of NRF2 targeting antibodies, and evaluation of HO-1 as a downstream marker of NRF2 activity by western blot 106
Figure 3.10. Differential levels of NRF2, KEAP1 and NQO1 in EJ, 253-J, MGH-U3, RT112 and RT112-CP cells 108
Figure 3.11. Brusatol exposure reduces NRF2 levels in UCC cell lines in a concentration dependent manner 111
Figure 3.12. Brusatol exposure decreases NRF2 levels in a time dependent manner, although causes no significant change in NQO1 expression over 48 hours 114
Figure 3.13. NQO1 is sensitive to NRF2 depletion by siRNA knockdown, although brusatol does not significantly alter NQO1 levels 117
Figure 3.14. Exposure to Brusatol and CHX reduces NRF2 levels in RT112-CP cells 119
Figure 3.15. Brusatol slows the growth of RT112 and RT112-CP cells 122
Figure 3.16. Correlation between cell doubling time and brusatol IC50 in EJ, 253-J, MGH-U3, RT112 and RT112-CP 126

Chapter Four

Figure 4.1. Diagram of homologous recombination, and adenovirus packaging in HEK293 cells 131
Figure 4.2. UCC cells express CD40 in a differential manner 135
Figure 4.3. Infection with 1 MOI AdNclCD40L initiates CD40L protein expression in UCC cells 137
Figure 4.4. Comparison of basal RT112 (A) and EJ (B) cell growth characteristics in a three-dimensional organotypic model of bladder cancer 139
Figure 4.5. H&E stained cross sections of EJ cell three-dimensional organotypic invasion assays 141
Figure 4.6. H&E stained cross sections of RT112 cell three-dimensional organotypic invasion assays 142

Figure 4.7. CD40-ligation limits EJ cell invasion and leads to marked cell death in an organotypic model of bladder cancer 143
Figure 4.8. Western blot of EJ cell lysates treated as indicated 146
Figure 4.9. Non-invading EJ cells express mCD40L 148
Figure 4.10. CD40-ligation induced changes in expression 153
Figure 4.11. Consequences of CD40-ligation on FN1 and MMP1 expression 155
157
Figure 4.12. Confirmation of *MMP1*, *FAM83D*, *ANLN* and *FN1* RNA expression in EJ and RT112 cells 157
Figure 4.13. In vitro behaviour of RT112 cells is similar to that in the parent tumour of RT112. (A) Parent Tumour H&E, papillary transitional cell carcinoma of the human bladder [272]. (B) RT112 cell line in an organotypic model of BC, H&E. Shares papillary morphology of parent tumor. 160

Chapter Five

Figure 5.1. Hierarchal clustering separates BC samples from normal tissue samples 167
Figure 5.2. Genes implicated in mitosis are upregulated in BC ($p = 2.59 \times 10^{-9}$) 169
Figure 5.3. Genes implicated in myogenesis arte downregulated in BC samples ($p = 1.22 \times 10^{-10}$) 171
Figure 5.4. Downregulation of genes involved in EMT in BC samples ($p = 1.41 \times 10^{-9}$) 172
Figure 5.5. Hierarchical clustering displays clustering of NMIBC and normal bladder tissue with further branching 174
Figure 5.6. Genes implicated in the classical complement pathway are downregulated in NMIBC when compared to normal tissue ($p = 5.12 \times 10^{-10}$) 177
Figure 5.7. Hierarchical clustering of genes and tissue samples displays segregation of MIBC and normal bladder samples into distinct clusters 179
Figure 5.8. Pathway Enrichment: MIBC vs normal tissue control samples. 180
Figure 5.9. Hierarchical clustering displays well defined segregation between grade 1 and grade 3 NMIBC samples 184

Figure 5.10. Pathway enrichment: Grade 3 NMIBC vs grade 1 NMIBC. 185
Figure 5.11. Hierarchal clustering displays a clear disparity between grade 3 NMIBC and MIBC 187
Figure 5.12. OPN expression in 253-J and RT112 cells 193
Figure 5.13. Osteopontin antibody optimisation in advanced colon adenocarcinoma 195
Figure 5.14. OPN staining in clear cell renal carcinoma (CCRC) and normal kidney tissue 197
Figure 5.15. OPN staining in bladder using 1:100 anti-OPN. 199
Figure 5.16. Osteopontin is overexpressed in MIBC when compared to normal bladder urothelium 201

List of Tables

Chapter Two

Table 2.1. Cell lines and their tissue origins.....60
Table 2.2. Results of STR-profiling of human bladder carcinoma cell lines.....63
Table 2.3. Western blot antibody conditions.....71
Table 2.4. Primary antibody concentrations for IHC.....73
Table 2.5. PCR primers targeting MMP1, FAM83D, ANLN and FN1. 79
Table 2.6. Patient demographics for gene expression analysis.....82
Table 2.7. Tumour information for immunohistochemical analysis.....83

Chapter Four

Table 4.1. Gene's dysregulated in MIBC when compared to grade 3 NMIBC or normal bladder tissue.....150

Chapter Five

Table 5.2. Genes displaying greater than 5-fold increased expression in MIBC when compared to normal tissue samples.....181
Table 5.3. Genes displaying greater than 5-fold differential expression between grade 3 NMIBC and MIBC samples ($p<0.05$ FDR).....188
Table 5.4. Summary of DAVID analysis: functional annotation clusters. 190

Abstract

Background:

In recent decades, despite survival improvements in the majority of high incidence cancers, survival rates for patients with bladder cancers have remained static. Key challenges in the treatment of bladder cancer are the acquisition of chemotherapy resistance, and progression to lethal muscle-invasive bladder cancer.

Aims:

This thesis aims to explore methods of pharmacological inhibition of chemotherapy resistance, mechanisms of bladder tumour invasion, and gene expression in bladder cancer.

Rationale:

Nuclear factor (erythroid-derived 2)-like 2 (NRF2) overexpression has been associated with chemotherapy resistance in a number of cancers including bladder. Therefore, the utility of the purported specific inhibitor of NRF2, brusatol in the attenuation of cisplatin chemotherapy resistance was investigated.

In bladder cancer, cluster of differentiation-40 (CD40)-ligation with membrane bound CD40-Ligand (CD40L) has been shown to induce marked cell death. However, little is known about the role of CD40-ligation in tumour cell invasion. With CD40 currently under investigation as a putative target for anti-cancer therapy, it was a timely goal of this thesis to understand more about its role in tumour cell invasion.

Until recently, knowledge of gene expression profiles in bladder cancer has been limited. Understanding of gene expression patterns in cancer may allow for enhanced prognostication, identification of potential drug targets and move the management of bladder cancer towards the ideal of personalised medicine.

Methods:

In vitro cytotoxicity assays were employed to determine the effect of brusatol on cisplatin sensitivity. Western blotting was employed to determine the effects of brusatol on proteins downstream of NRF2.

An organotypic model of bladder cancer was used to investigate the effect of CD40-ligation on bladder tumour cell invasion. Non-cleavable membrane bound CD40-ligand delivered by adenoviral vector was used in CD40 expressing cell lines of invasive and non-invasive origin. The effect of CD40-ligation was investigated downstream by western analysis and RNA microarray.

Whole-transcript based microarray analysis was performed on bladder biopsies obtained from 19 patients, and 10 controls. Unsupervised hierarchical clustering was used to identify samples with similar expression profiles. Hypergeometric analysis was used to identify canonical pathways and curated networks with statistically significant enrichment of differentially expressed genes. Samples from a further 6 patients (muscle invasive bladder cancer (MIBC) n = 3, normal tissue n = 3) were tested for osteopontin expression by immunohistochemistry.

Results:

Brusatol increased the sensitivity of bladder cancer cell lines to cisplatin in a dosage and cell line dependent manner. Furthermore, brusatol exhibited marked toxicity as a standalone treatment. However, evidence suggests that brusatol does not act as a specific inhibitor of NRF2.

CD40-ligation with non-cleavable membrane-bound CD40-ligand led to marked cell death in CD40-positive non-muscle invasive cell lines. However, in muscle-invasive CD40-positive cell lines marked inhibition of tumour invasion was also observed. Expression analysis of family with sequence similarity member 83 d (*FAM83D)*, fibronectin (*FN1)*, matrix metalloproteinase 1 (*MMP1)* and anillin (*ANLN)* revealed downregulation of *FN1, FAM83D, and ANLN*, and upregulation of *MMP1*, with a concurrent upregulation of MMP1 and a paradoxical increase of FN1 in EJ cells, with no change in FN1 and MMP1 expression in RT112 cells.

Pathways associated with cell cycle and proliferation were markedly upregulated in muscle-invasive and grade 3 cancers. Genes associated with the classical complement pathway were downregulated in non-muscle invasive cancer. Osteopontin was significantly overexpressed in invasive cancer compared to healthy tissue.

Conclusions:

It is unlikely that brusatol is a specific inhibitor of NRF2 however its marked cytotoxicity as a stand-alone agent and potentiating effects in combination with cisplatin are rationale for further investigation.

CD40-ligation attenuates the invasion of MIBC cells in an organotypic model of bladder cancer. However, it is unclear whether the attenuation of invasion is due to the inhibition of invasive pathways, or direct induction of apoptosis. Nevertheless, with the usage of CD40-agnoistic antibodies currently in clinical trials, attenuation of tumour invasion is a promising effect.

Gene expression analysis identifies divergent pathways that may be useful in the stratification of bladder cancers, and the identification of drug targets. Furthermore, this study supports a key role for osteopontin in bladder cancer, which warrants further investigation as a marker prognostic of muscle invasive disease.

Acknowledgements

Firstly, thank you to my parents, Malcolm and Sonjia Greensmith. Your unending support has been invaluable. I dedicate this thesis to you both, with all my love.

Thank you to my supervisory team, Dr Syed Hussain, Dr Ian Copple and Professor Daniel Palmer; for allowing me this opportunity and your kind support.

Dr Taha Elmitwalli, thank you for your generous guidance and mentorship, both as a colleague and friend.

Professor Chris Goldring, thank you for your support during my PhD, and for being a source of inspiration throughout my time at this university.

Professor Ross Sibson, thank you kindly for your support and teaching.

To Dr Anthony Evans, thank you for spending an age scanning a ridiculous number of slides on my behalf.

Finally, thanks to all in my group, the Department of Clinical and Molecular Cancer Medicine, and Clinical and Molecular Pharmacology, it has been a pleasure working with you all, and I wish everyone the best for the future.

Publications

Papers

- Gene expression profiling in bladder cancer identifies potential therapeutic targets.

  SA Hussain*, DH Palmer*, WK Syn, JJ Sacco, **RMD Greensmith**, T Elmetwali, V Aachi, B Lloyd, PV Jithesh, JR Arrand, D Barton, J Ansari, DR Sibson, ND James

  Published in The International Journal of Oncology 02/03/2017

Abstracts

- Pharmacological inhibition of NRF2 as a novel strategy for overcoming cisplatin resistance in bladder cancer.

  RMD Greensmith, OMS El-Taji, ZX Lin, IM Copple, CE Goldring, SA Hussain. 2014 NCRI Cancer Conference, 2-5 November 2014, BT Convention Centre Liverpool UK. Poster presentation.
- Pharmacological inhibition of NRF2 as a novel strategy for overcoming cisplatin resistance in bladder cancer.

  RMD Greensmith, OMS El-Taji, ZX Lin, IM Copple, CE Goldring, SA Hussain. The Keap1/Nrf2 Pathway in Health and Disease, 6-8 January 2015, Robinson College, Cambridge, UK. Poster presentation.

Grants

- Characterisation of dendritic cell function in the three-dimensional model of urothelial carcinoma in response to soluble CD40L based immunotherapy.

  Main applicant: SA Hussain. Collaborators: DH Palmer, DR Sibson, T Elmitwali, A Salman, **RMD Greensmith (author)**. Clatterbridge Cancer Centre charitable funds for early / novel R&D projects, March 2014.

Abbreviations

5- FU – 5-flourouracil

AdMock – Mock Adenovirus
AdNclCD40L – Adenoviral non-cleavable CD40L
AJ – Adherens junction
ALL – Acute lymphoblastic leukaemia
ANLN – Anillin
ANOVA – Analysis of variance
APC – Anaphase promoting complex
APCs – Antigen presenting cells
AUM – Asymmetric unit membrane

BBN – N-butyl-N-(4-hydroxybutyl) nitrosamine
BC – Bladder cancer
BCG – Bacillus Calmette – Guérin
BCL2 – B-cell lymphoma 2
BCL_{XL} – B-cell lymphoma-extra large
BCR-ABL – The Philadelphia translocation
BRAF – B-Raf
BRCA1 – Breast cancer type 1 susceptibility protein
BRCA2 – Breast cancer type 2 susceptibility protein
BSA – Bovine serum albumin

CA-125 – Cancer antigen 125
CA19-9 – Cancer antigen 19-9
CASC5 – Cancer susceptibility candidate 5
CCND1 – Cyclin D1
CCND3 – Cyclin D3
cDNA – Complementary DNA
CD40 – Cluster of differentiation 40
CD40L – Cluster of differentiation 40 ligand

CD44 – Cluster of differentiation 44

CDC25C – M-phase inducer phosphatase 3

CDK1 – Cyclin-dependent kinase 1

CDKN2A – Cyclin dependent kinase 2A

cDNA – Coding DNA

CFH - Compliment factor H

CHX – Cycloheximide

Cis – Carcinoma *in situ*

CLL – Chronic lymphocytic leukaemia

CpG – 5'-C-phosphate-G-3'

CT – Computed Tomography

CTLA4 – Cytotoxic T-lymphocyte-associated protein 4

CUL3 – Cullin-3

CYP – Cytochrome P450 family of enzymes

CYP2D6 – CYP family member 2D6

DAVID – Database for annotation, visualisation and integrated discovery.

DCs – Dendritic cells

DMEM – Dulbecco's modified Eagles medium

DMF – Dimethylformamide

DMSO – Dimethyl sulfoxide

DNA – Deoxyribonucleic acid

DUSP – Dual-specificity phosphatase

ECM – Extra cellular matrix

EDTA – Ethylenediaminetetracetic acid

EGFR – Epidermal growth factor receptor

EMT – Epithelial to mesenchymal transition

ERCC1 – DNA excision repair protein ERCC1

ERK – Extracellular signal-regulated kinases

ESRP1 - Epithelial splicing regulatory protein 1

ESRP2 - Epithelial splicing regulatory protein 2

FAM83D – Family with sequence similarity 83 member D
FBXW7 – F-box/WD repeat-containing protein 7
FC – Final concentration
FDR – False discovery rate
FGFR2 – Fibroblast growth factor receptor 2
FN1 – Fibronectin
FOXM1 – Forkhead box protein M1

GAPDH – Glyceraldehyde 3-phosphate dehydrogenase
GC – Gemcitabine and cisplatin combination chemotherapy
GFR – Glomerular filtration rate
GSH – Glutathione
GST – Glutathione-S-transferase
GSTM1 – Glutathione-S-transferase Mu 1
GSTπ – Glutathione-S-transferase Pi

H&E – Haematoxylin and eosin staining
HCC – Hepatocellular carcinoma
hCNT – Human concentrative nucleoside transporter
hENT1 – Human equilibrative nucleoside transporter 1
HER2/NEU – Human epidermal growth factor receptor 2
HER3 – Human epidermal growth factor receptor 3
HFF1 – Human foreskin fibroblast 1
HRP – Horseradish peroxidase

IC50 – Half maximal inhibitory concentration
IHC – Immunohistochemistry
IL-12 – Interleukin-12
IL-2 – Interleukin-1
IJO – International Journal of Oncology

JNK – c-Jun N-terminal kinases

Keap1 - Kelch-like ECH-associated protein 1

KIT – c-KIT

KLH – Keyhole limpet hemocyanin

KNSL1 – kinesin family member 1

LOH – Loss of heterozygosity

mAbs – Monoclonal antibodies

MAPK – Mitogen-activated protein kinase

MBC – Metastatic bladder cancer

mCD40L – Membrane-bound CD40-Ligand

MDM2 – Mouse double minute 2 homolog

MDR1 – Multi-drug resistance protein 1 / p-Glycoprotein

MEF2 – Myocyte enhancer factor-2

MEM – Modified Eagles medium

MENSA – 2-mercaptoethanesulfonic acid

MET – c-MET

MIBC – Muscle invasive bladder cancer

MMC – mitomycin C

MMP1 – Matrix metalloproteinase 1

MMP16 – Matrix metalloproteinase 16

MMPs – Matrix metalloproteinases

MOI – Multiplicity of infection

MRI – Magnetic resonance imaging

MRP2 – Multidrug resistance-associated protein 2

mTOR – Mechanistic target of rapamycin

MTT – 3-[4,5-dimethylthiazol-2-yl]-2,5- diphenyltetrazolium bromide; thiazolyl blue

MVAC – Methotrexate, vinblastine, adriamycin (doxorubicin) and cisplatin combination chemotherapy

MyoD – Myogenic differentiation 1

NAT – N-acetyl-transferase

NAT-2 – N-acetyl-transferase 2

NCBI – National Center for Biotechnology Information

NF-κB – Nuclear factor kappa-light-chain-enhancer of activated B cells

NHS – The National Health Service

NK – Natural killer cells

NMIBC – Non-muscle invasive bladder cancer

NRF2 – Nuclear factor (erythroid-derived 2)-like 2

NSCLC – Non-small cell lung cancer

OPN – Osteopontin

P53 – Tumour protein P53

PBS – Phosphate buffered saline

PCR – Polymerase chain reaction

PD-L1 – Programmed death-ligand 1

PD1 – Programmed cell death protein 1

PDGFR – Platelet derived growth factor receptor

PELO – Protein pelota homolog

PFS – Progression free survival

PI3K – Phosphatidylinositide 3-kinase

PKC – Protein kinase C

PLK1 – Polo-like kinase 1

PSA – Prostate specific antigen

PUNLMP – Papillary urothelial neoplasm of low malignant potential

RB – Retinoblastoma protein

RBX1 – Ring-box 1

RHOA – Ras homolog gene family, member A

RHOG – Ras homolog gene family, member G

RNA – Ribonucleic acid

RNAi – RNA interference

ROS – Reactive oxygen species

RPMI – Roswell Park Memorial Institute 1640 medium

RRM1 – Ribonucleoside-diphosphate reductase large subunit

rsCD40L – Recombinant soluble CD40-ligand

RT – Reverse transcription

RT-PCR – Reverse transcription polymerase chain reaction

RTK – Receptor tyrosine kinase

SABC – Schistosomiasis associated bladder cancer

SCC – Squamous cell carcinoma

sCD40L – Soluble CD40-ligand

SCF – Skp-Cullin-F-box E3 ubiquitin ligase

SD – Standard deviation

SDS-PAGE – Sodium dodecyl sulphate polyacrylamide gel electrophoresis

SERPINB13 - Serpin peptidase inhibitor, clade B (ovalbumin), member 13

siRNA – Short-interfering RNA

SMAF – Small maf

STAT – Signal transducer and activator of transcription

STR – Short tandem repeat

TBST – 1 x Tris-Buffered Saline with 0.01% Tween-20

TCC - transitional cell carcinoma

TCGA – The Cancer Genome Atlas

TEMED – Tetramethylethylenediamine

TJ – Tight junction

TNF – Tumour necrosis factor

TNM – Tumour, Node, Metastasis system

TOP2A - topoisomerase 2-alpha

TP53 – P53 gene

TPX2 - targeting protein for Xklp2

TRAFs – Tumour necrosis factor receptor associated factors, family members include TRAFs 1-6

TRAIL – Tumour necrosis factor related apoptosis inducing ligand

TSC1 – Tuberous sclerosis protein 1

TSP – Tumour suppressor protein

TURBT – Transurethral resection of the bladder tumour

UCC – Urothelial Cell Carcinoma

UPK1B – Uroplakin 1B

VEGFRs – Vascular endothelial growth factor receptors

WGS – Whole genome sequencing

WHO – World health organisation

Chapter One – General Introduction

1.1 Principles of cancer **2**
1.2 Bladder cancer **4**
1.2.1 Bladder cancer: the urinary bladder 4
1.2.2 Bladder cancer: epidemiology, aetiology and carcinogenesis 8
1.2.3 Bladder cancer: diagnosis 15
1.2.4 Bladder cancer: treatment 20
1.3 The NRF2-KEAP1 axis **28**
1.3.1 NRF2 in cancer 31
1.4 Cluster of differentiation 40 ..... **38**
1.4.1 CD40 expression in bladder cancer 40
1.4.2 CD40-ligand 41
1.4.3 TRAFs facilitate CD40 signal transduction 43
1.4.4 Clinical application of CD40 targeted therapies in bladder cancer 45
1.5 Matrix metalloproteinase-1 ..... **46**
1.6 Fibronectin **48**
1.7 Family with sequence similarity 83, member D **50**
1.8 Anillin **51**
1.9 Biomarkers in bladder cancer **53**
1.9.1 Biomarkers 54
1.10 Thesis hypotheses **57**

1.1 Principles of cancer

The development of cancer is a progressive process, where cells evolve in a multi-step manner progressively into a malignant state. In 2000 Hanahan and Weinberg displayed that during the process of carcinogenesis, cells acquire an essential succession six of cancer-associated hallmarks (Fig 1.1) [1].

More recently, an increasing body of work has begun to characterise the role of the tumour-microenvironment, and the ability of non-cancer cells such as cancer associated fibroblasts to support malignant spread, aiding in invasion, angiogenesis, and evasion of immune surveillance [2]. Based on this increasing body of research in 2011 Hanahan and Weinberg unveiled the sequel to their seminal work, highlighting the roles of inflammation, genomic instability and mutation, dysregulated cellular energetics and immune evasion in the development and progression of cancers (Fig 1.1) [2].

This thesis focuses on novel approaches in the management of the most deadly genitourinary malignancy, bladder cancer (BC) [3]. Investigating: methods used to attenuate resistance to first line systemic chemotherapy for muscle-invasive BC; prognostic biomarkers which may aid the early detection of the most malignant BC subtypes; and mechanistic work unravelling the role of cell-surface receptors and ligands often found chiefly in the immune system, and their role in tumour cell invasion.

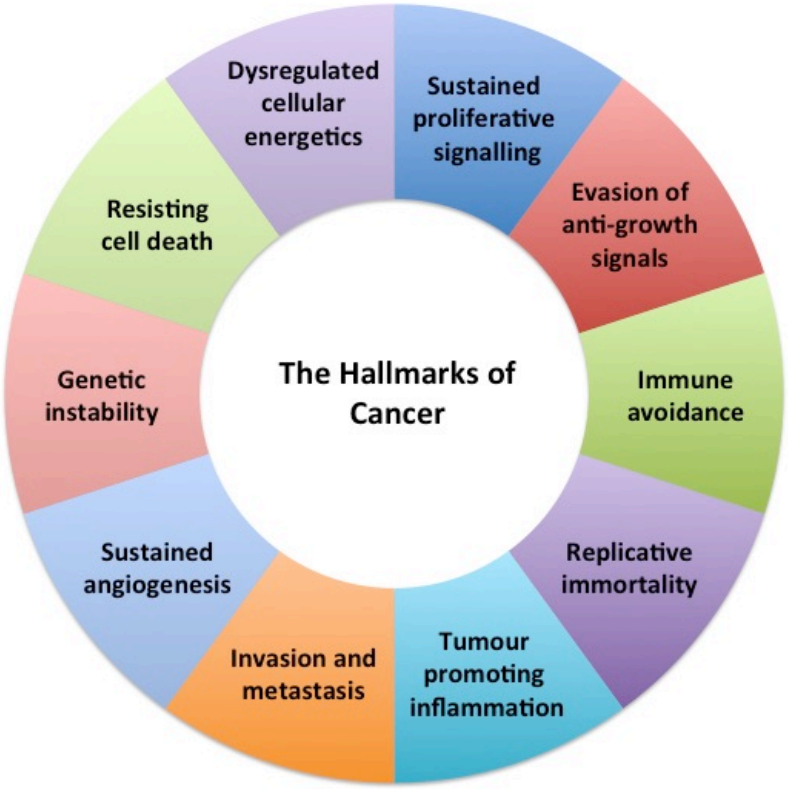

Figure 1.1. The hallmarks of cancer. In the sequel to their seminal work, Hanahan and Weinberg identified a further four essential hallmarks of cancer in addition to the six original cancer hallmarks: sustaining proliferative signals, evasion of anti-growth signals, activation of invasion and metastasis, limitless replicative potential, induction of angiogenesis and resistance of cell death. The four more recently identified hallmarks of cancer are the presence of tumour promoting inflammation, genetic instability and mutation, avoidance of immune surveillance and dysregulated cellular energetics. (adapted from Hanahan and Weinberg 2000, 2011) [1, 2].

1.2 Bladder cancer

This section outlines: physiological and anatomical elements of the urinary bladder; epidemiological and aetiological factors involved in bladder carcinogenesis; BC diagnosis and treatment.

1.2.1 Bladder cancer: the urinary bladder

The urinary bladder (Fig 1.2) is hollow distensible muscular organ, situated in the pelvic cavity posterior to the pubic symphysis, used for the storage of urine for extended periods of time [4]. As such, the bladder has adapted in several ways to protect the blood in underlying vessels and itself from pathologies associated with contact with pathogenic microbes and toxic waste products contained in urine. The composition of urine is vastly different to that of the blood, with a pH of 4.5 and osmolality ranging from 50-1000 mOsmol/kg, including high concentrations of urea and potential carcinogens [5]. The urothelium acts as the protective barrier between the urine, blood and underlying muscle.

Urothelium consists of three stratified layers of transitional epithelium, usually no greater than eight cells thick (Fig 1.3) [6]. Connected to the basement lamina lie small basal cells (10μm), 10% are stem cells, these have the highest potential to proliferate and serve as precursors to the cells above [6]. Upward from the basement layer, with thin connections to the basement lamina exists a region of larger (10-25μm) intermediate transit-amplifying cells, which will eventually replace their protective top layer, the large (25-250μm) polyhedral umbrella cells [7]. The umbrella cells have adapted their morphology so they are wider than the cells beneath, forming a protective blood-urine barrier, and are able to adjust their diameter to adapt to the changing volume of the bladder [6]. The ability of the transitional epithelium to adapt to such conditions is likely due to a dense cytokeratin network below the apical membrane, and urothelial tight junctions.

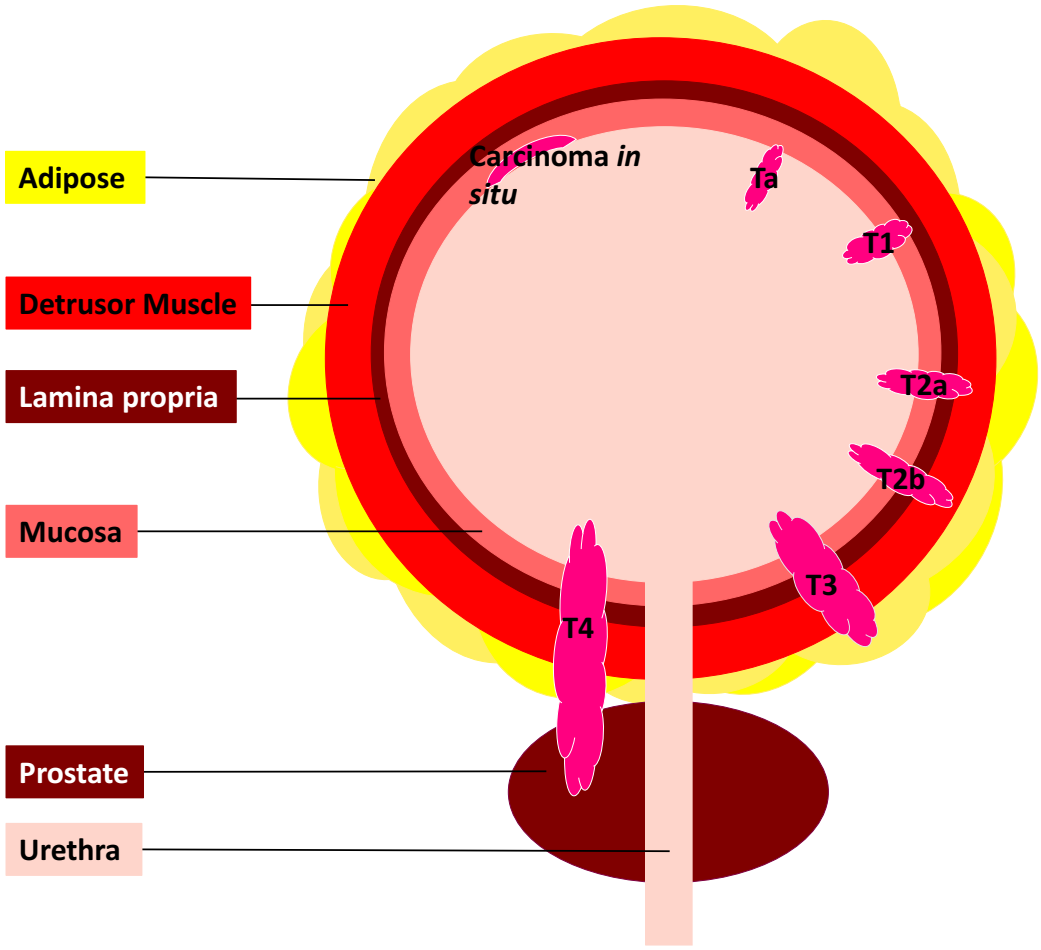

Figure 1.2. The urinary bladder, displaying different stages of urothelial cell carcinoma. Ta refers to non-invasive papillary carcinoma – raised tumours growing into the bladder; carcinoma *in situ* (*Cis*), flat tumours, which do not invade past the mucosa. At stage T1 the tumour has spread through the mucosa into the lamina propria, but does not invade the underlying detrusor muscle. By stage T2 tumours have spread into the muscle of the bladder wall, T2a tumours are confined to the inner half of the muscle, whereas T2b have spread to the outer half of the muscle. Tumours at stage T3 have spread into the perivesicular adipose tissue (fat) – T3a is microscopically apparent, where at T3b the invasion is evident macroscopically via imaging or palpation. Stage T4 tumours have spread to the surrounding organs, with T4a accounting for spread into genitourinary organs (prostate, uterus or vagina), where as T4b denotes spread beyond T4a into the pelvic or abdominal wall.

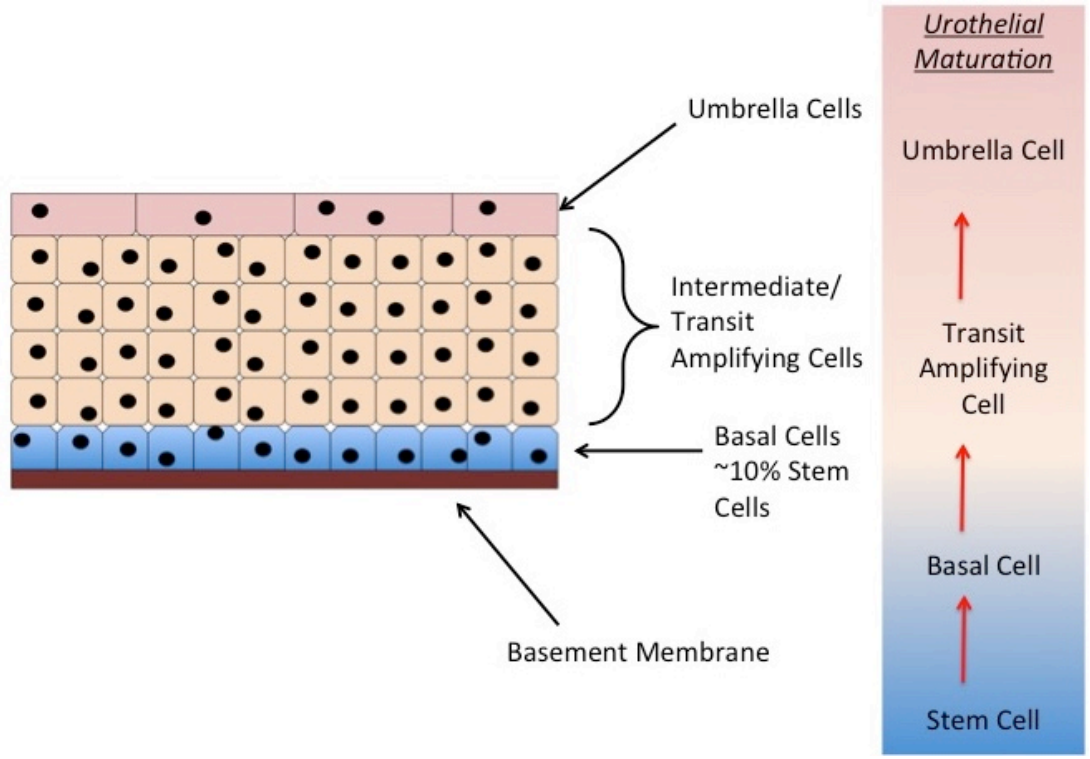

Figure 1.3. Structure of the urothelium. The urothelium is a stratified transitional epithelium, consisting of three distinct layers. The basal layer attached to the basement lamina consists of small basal cells (10μm), above this exists larger (10-25μm) transit amplifying cells, above the intermediate strata of transit amplifying cells lies the large (25-250μm) umbrella cells. With a turnover rate of ~200 days, and a tritium-thymidine labelling index of ~0.01%, urothelium is one of the slowest cycling epithelia in the human body [8].

Beneath the urothelium lies a basal lamina, consisting of collagen, adhesive glycoproteins and glycosaminoglycans [4, 6, 9]. Below this basement membrane lies the lamina propria (sub-mucosa), consisting of loose connective tissue and a sparse number of smooth muscle fibres [4, 6]. Outside the lamina propria lies the muscularis propria; this layer is formed out three distinct layers of muscle (inner longitudinal, outer circular, and outermost longitudinal), this triad of muscular layers are known as the detrusor muscle, when contracted their function is to expel urine from the bladder [4, 6]. The outermost, and thickest layer of the bladder wall is serosa, consisting of loose connective tissue, and perivesicular fat [4, 6].

Cancers of the urothelium are characterised by the loss of the mature, differentiated morphology normal urothelial tissue, and gain of aberrant molecular function [10]. Changes in protective morphology of the urothelium leave the underlying tissue and bloodstream susceptible to damage from urine, through the leeching of toxins and carcinogens, or microbes, which may lead to sepsis and potentially increased localised inflammation, allowing for a suitable environment for cancer growth and progression [4, 11].

1.2.2 Bladder cancer: epidemiology, aetiology and carcinogenesis

There are various factors, which determine the incidence, distribution, possible control and health implications of BC. The study and understanding of these causative factors as an adjunct to clinical and translational research can aid in the advancement of BC treatment and the understanding of bladder carcinogenesis.

1.2.2.1 Epidemiology

BC is the 7th commonest malignancy in the United Kingdom, where there were 10,335 new cases of BC and 4,907 associated deaths in 2008 [12]. Although men have an 8% increased 5-year survival advantage over women, BC is three- to four- times more common in males [13]. The vast majority (90%) of cases are classified as urothelial cell carcinoma (UCC), however other cancers of the bladder include, squamous cell carcinoma (SCC) (8%), Adenocarcinoma (1-2%) and the remaining <1% of cases being accounted for by small cell cancers, and sarcomas [12]. This remarkably heterogeneous disease is the only top-twenty cancer to have a significant decrease its relative survival between 1990 and 2009, however this is due to a decrease in the number of cases in males, whilst the death rate remains stable (Fig 1.4) [13].

Locally contained BC is stratified into muscle-invasive (≥T2) and non-muscle invasive disease (≤T1); Non-muscle invasive BC (NMIBC) is associated with a good prognosis with 92% of patients surviving 5-years post-diagnosis [10, 12]. NMIBC can be managed effectively through transurethral resection of the bladder tumour and Bacillus Calmette-Guérin (BCG) instillation, although 70% of patients with NMIBC have recurrent lesions, lending the need for regular surveillance using diagnostic cystoscopy. The high potential for recurrence and necessity of repeat treatment in BC makes it the most expensive cancer to treat, costing US$3.7 Billion in 2001 in the USA [14, 15]. One fifth of NMIBC patients will progress to muscle-invasive BC (MIBC) over time, this number rises to half if the patient presents with Carcinoma *in situ* (*Cis)*.

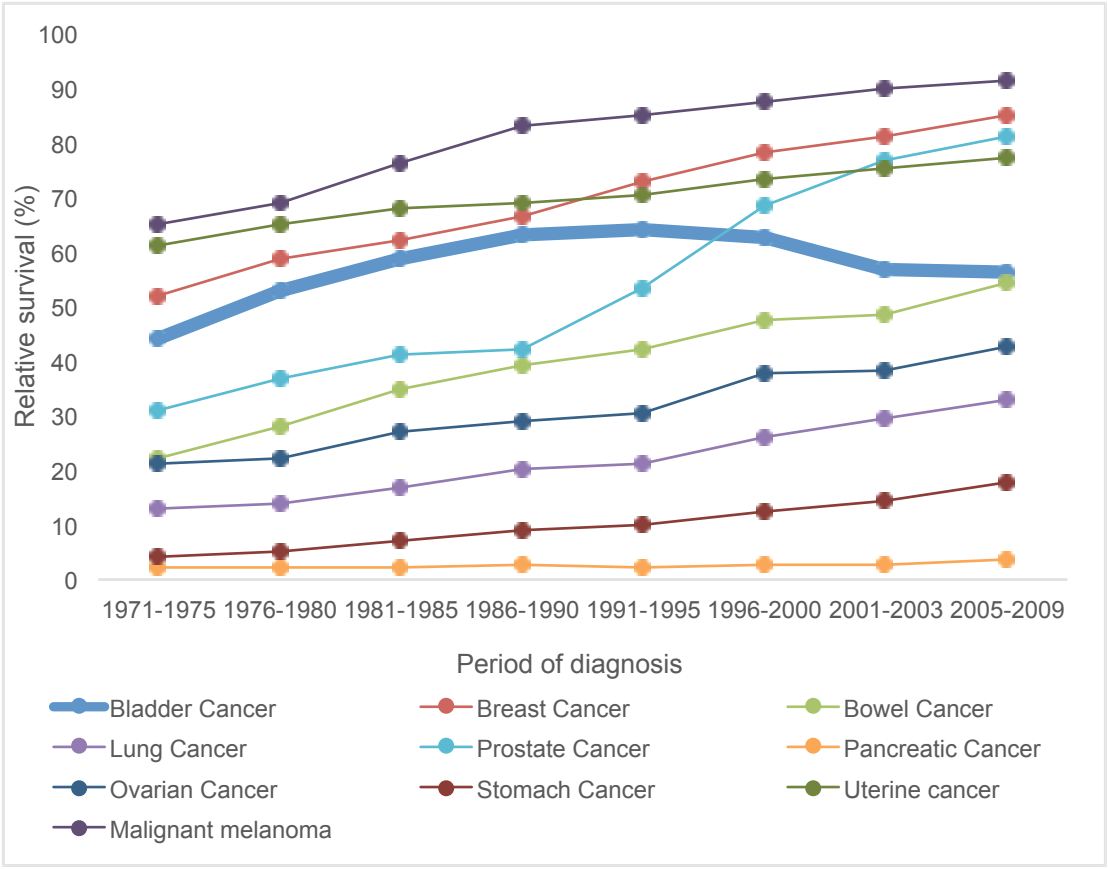

Figure 1.4. Age standardised five-year relative survival rates for England and Wales 1971-2009, based on cancer type. BC is the only top 10 cancers that has decreased in terms of relative survival over recent decades. This is believed to be due to decreasing incidence rates in males with the mortality rate remaining unchanged, combined with the implementation of the World Health Organisation (WHO) 2004 guidelines for BC risk stratification [12].

The 5-year survival for patients with MIBC is under half that of a NMIBC diagnosis, with only 45% surviving [12]. This is, in part, believed to be due to tumour cell clones undergoing epithelial-to-mesenchymal transition, entering a more motile, malignant state with a much higher propensity to form metastatic lesions [10, 16]. First line treatment options for MIBC include radical/partial cystectomy, cisplatin based chemotherapy with gemcitabine, and chemoradiotherapy [17, 18].

Metastatic BC (MBC), is a devastating disease, leaving only 6% of patients alive after 5-years [12, 19]. Treatment options will be discussed later, although in the first line setting, treatment for MBC includes palliative cisplatin-based chemotherapy with gemcitabine, radiotherapy, chemoradiation, neo-adjuvant chemotherapy, and surgical tumour resection when possible.

With primary diagnosis of BC most likely between the ages of 65 and 84, and a high incidence of co-morbidities, often related to tobacco smoking [13]. A significant challenge is present in the treatment of MIBC, as the single most efficacious agent in the treatment of BC, cisplatin, is highly nephrotoxic, leading to contraindication in patients with low (glomerular filtration rate) GFR [10].

BC is most prevalent in the Western world, with the incidence rate in Western Europe being over 4-times that of that in large parts of Africa [12]. Although North Africa is an exception, here there is a high rate of Schistosomiasis induced SCC of the bladder, where 90% of cases are SCC and only 10% of patients present with UCC and other less common disease subtypes [12].

1.2.2.2 Aetiology

There are several aetiological factors which have been implicated in the development of bladder carcinomas, these are discussed below.

1.2.2.2.1 Smoking

Tobacco smoking is linked with a greater than four-fold increased chance of developing BC, accounting for 47% and 33% of cases in American males and females, respectively [20, 21]. There are a number of causative agents which are believed to be secreted into the urine including benzo(a)pyrene, and a range of alpha- and beta-naphthylamines [22, 23].

1.2.2.2.2 Occupational

In the early 20th century the increased incidence of BC in people working in the textile industry led to several studies, which revealed that oral ingestion of 2-naphthylamine (a once key arylamine used in the production of aniline dyes) induced BC in canines. It was also found that these workers had a 20-fold increased chance of BC development when compared to the general population [24].

More recently, it has become apparent that workers from many different trades were subject to the chemical induction of BC. These include people working in the chemical, dye, rubber, petrochemical, aluminium production, leather, and printing industries. A number of chemicals have been implicated in the increased incidence of BC, including polycyclic aromatic hydrocarbons, fluorides, aromatic amines, benzidine, beta-napthylamine, o-toluidine and 4-amino-biphenyl [25-27].

1.2.2.2.3 Dietary Factors

There is some anecdotal evidence that the consumption of coffee may increase the chance of BC, as there is the number of coffee drinkers within BC cohorts is unusually high, however there is no established dose-response relationship [28-30].

The artificial sweetener saccharin, in excess of normal dietary intake levels has been shown in animal models to increase the chance of BC, however there has been no evidence of this being the case in humans[31, 32].

Conversely consumption of foods high in selenium, vitamin D and vitamin E may shown decrease the risk of contracting BC [33-35].

1.2.2.2.4 Iatrogenic

There are a triad of instances where the development of urothelial carcinoma can be due to side effects of medical examination, or treatment. These are known as iatrogenic side effects.

Phenacetin

The analgesic phenacetin (acetophenetidin), which has structural homology to aniline dyes, has been shown to be associated with a two- to six-fold increase in the development of urothelial cancers in the bladder and urinary tract [36]. The increase in BC incidence is most strongly associated with heavy usage of phenacetin in young patients [36, 37]. The iatrogenic induction of BC by phenacetin is the key reason for the drugs withdrawal, its usage has now been replaced with safer agents such as paracetamol, which is not associated with an increased risk of BC [37, 38].

Cyclophosphamide

The oxazophosphorine, cyclophosphamide, is a chemotherapeutic drug that uses alkylation as its primary mode of cytotoxicity. Its usage leads to haemorrhagic cystitis and is associated with a 9-fold increase in the development of BC, in the region of 6-13 years post-treatment [39]. These effects are caused by a metabolite of cyclophosphamide, acrolein. 2-mercaptoethanesulfonic acid (MENSA) is an organosulfur uroprotective compound, which is co-administered with cyclophosphamide to limit the negative effects on the bladder [40]. MENSA

reacts with acrolein and other urotoxic metabolites leading the formation of harmless compounds [40, 41].

Radiotherapy

One of the few iatrogenic risk factors, which is not chemically induced is the usage of radiotherapy in women who have been treated for cancers of the ovary or uterine cervix associated with a 2- to 4-fold increased chance of developing BC after a decade, in comparison to patients who underwent surgical tumour management [42, 43].

1.2.2.2.5 Chronic bladder inflammation

Chronic inflammation, or chronic cystitis of the bladder is associated with an increase incidence of BC [44]. Conversely to the majority of bladder tumours, the lesions tend to be SCC, rather than the more commonly seen UCC [44].

As a result of chronic catheter cystitis, 2-10% of paraplegics will ultimately develop SCC of the bladder, however there are reports of up to 81% of spinal cord injury patients with BC developing urothelial cell carcinomas [45-47]. Forms of physical trauma to the bladder through infection, calculi formation and chronic catheter usage in this patient group may also lead to the formation of cancerous lesions of the bladder [45, 47, 48].

Globally, schistosomiasis is the most prevalent waterborne parasitic infection, and after smoking it is the second leading cause of BC [49]. The *Schistosoma haematobium* digenetic trematode, which effects at least 76 countries and is endemic in Egypt and the Middle East, infecting 200 million people, is the cause of schistosomiasis associated BC (SABC), which accounts for >30% of all cases of BC in Egypt, for the most part leading to SCC [50, 51]. In comparison to smoking associated BCs, the mean age of onset of SABC is much lower and there is a much greater proportion of males who suffer from the disease [51]. It is believed that an increased concentration of N-Nitroso compounds in the bladder of people

infected by *S. haematobium* is the cause of SCC, through deoxyribonucleic acid (DNA) damage, leading to pro-malignant point mutations [51].

1.2.2.2.6 Hereditary factors

Apart from radiotherapy and parasite infection, the key aetiological factors that lead to BC are exposure to a several chemicals, either by direct action or after the metabolic activation of inert compounds into mutagens.

Humans are equipped with a range of enzymes that are involved in the detoxification of compounds with biological activity. These enzymes facilitate processes including acetylation, hydroxylation and conjugation to neutralise compounds with biologically active chemical groups [4, 52]. This group of enzymes including N-acetyl-transferase (NAT), cytochrome P450 (CYP) and glutathione transferase (GST) are subject to a range of polymorphisms within the population, due to the two allelic forms derived from maternal and paternal DNA [4, 52]. A common polymorphism, implicated in the metabolism of toxic compounds of cigarette smoking is the NAT-2 slow acylator phenotype, which increases the duration of arylamine exposure leading to increased incidences of cancer formation [53, 54]. High expression of GSTs is linked to a lower susceptibility to carcinogens from cigarette smoke; unsurprisingly glutathione-s-transferase-Mu 1 (GSTM1) null patients are more likely to contract BC. Furthermore, individuals with Cytochrome P450 2D6 (CYP2D6) polymorphisms may have an increased chance of developing BC [55-58].

There are limited reported cases of inherited BC, the few that do exist are primarily due to the inheritance of hereditary cancer syndromes such as Retinoblastoma, Costello syndrome, Facio-Cutaneous Skeletal syndrome, Cowden syndrome and Lynch syndrome [59-63].

1.2.2.2.7 Other aetiological factors

There are a number of other aetiological factors which can result in an increased risk of BC, these include: exposure to arsenic in well water and inorganic arsenic compounds such as gallium arsenide [26, 64, 65]; exposure to chlorinated aliphatic hydrocarbons and chlorination by-products in treated water [66]; and finally chronic usage of Chinese herbal medicines containing aristolochic acids, extracted from the *Aristolochia fangchi* plant [67, 68].

1.2.3 Bladder cancer: diagnosis

BC is often identified due to the presence of visible blood in the urine (haematuria), or blood detected upon urinalysis (microscopic haematuria). Emergency admission due to BC related complications is a common mode of disease presentation and is often associated with poor prognosis. Stage 1 BC is the most frequently diagnosed (Fig 1.5), however if MIBC is suspected at cystoscopy, computed tomography (CT) or magnetic resonance imaging (MRI) will be employed to query muscle invasion.

With treatment and surveillance involving the urogenital tract, BC often has a high psychological impact, in addition to the profound physical impact of the disease.

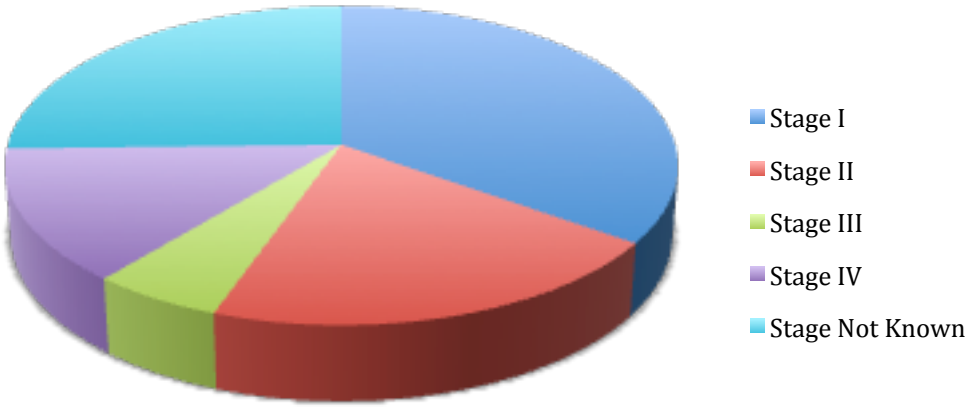

Figure 1.5. Bladder cancer: stage at diagnosis. Stage 1 (34.9%), stage II (20.6%), stage III (5.6%), stage IV (13.6%) and stage not known (25.4%)[12].

1.2.3.1 Histological staging and grading of bladder cancer

The tumour-node-metastasis (TNM) system is used to categorise the stage at which a cancer is at within a patient. Tumour (T) denotes the size and location of the primary tumour, Node (N) informs as to whether the tumour has spread to the lymph nodes, and the extent of lymph involvement, Metastasis (M) indicates whether the tumour has spread to distant sites [12] (Fig 1.2).

Tumour (T):

In the TNM system, T is used plus a denomination to describe the extent of tumour invasion.

TX: The tumour is unable to be assessed.

T0: No evidence of BC.

Ta: Non-invasive papillary BC.

Tis: Carcinoma in situ, a flat, non-invasive lesion found on, or near the surface of the bladder.

T1: The tumour invades up to an including the lamina propria.

T2: The tumour has spread into the detrusor muscle.

T2a: The tumour spread is confined to the inner half of the muscle.

T2b: The tumour invades the outer half of the muscle.

T3: The tumour invades the perivesicular adipose tissue.

T3a: Invasion into perivesicular tissue is only apparent microscopically.

T3b: Invasion into perivesicular tissue is apparent macroscopically, through imaging or palpation.

T4: The tumour has spread to near-by organs:

T4a: The invasion is confined to the prostate, uterus or vagina.

T4b: The tumour infiltrates the pelvic or abdominal diaphragm.

Node (N):

Several lymph nodes are local to the bladder. These regional lymph nodes include the hypogastric, obturator, iliac, perivesical, pelvic, sacral and presacral lymph nodes.

NX: Regional lymph nodes cannot be assessed.
N0: No cancer is present in the regional lymph nodes.
N1: The malignancy has spread to one regional lymph node in the pelvis.
N2: The malignancy has spread to greater than one lymph node in the pelvis.
N3: The disease has spread beyond regional lymph nodes of the pelvis, to the common iliac lymph nodes.

Metastasis (M):

The final category in this classification system denotes whether metastasis is present. Common sites for distant metastasis of urothelial cell carcinomas include bone, liver and the lung [69]. This classification does not consider micrometastases.

M0: There is no detectable metastatic disease.
M1: Distant metastases are present.

Grade:

In conjunction with the TNM staging system, the grade considers the neoplastic potential of certain cancers. There are three classifications of BC cancer grade.

Papilloma: Also known as a benign papillary urothelial neoplasm of low malignant potential (PUNLMP), there is a high chance this lesion will recur, however PUNLMPs are unlikely to progress to a more advanced disease.

Low Grade: Well differentiated, with a higher chance of recurrence and progression when compared to a papilloma.

High Grade: Poorly differentiated, there is the highest chance of recurrence and progression to advanced disease.

The 1973 advice of the World Health Organisation (WHO), the system used prior to the 2004 revision mentioned above, designated grades from 1 to 3, with stage 1 showing the least degree of cellular anaplasia compatible with a cancer diagnosis, and stage 3 showing the most severe degrees of cellular anaplasia, the histological features of grade 2 malignancies lying between grades 1 and 3 [70]. This thesis will use both the 1973, and 2004 revision, depending on the age of the sample used, and/ or the preference of the pathologist.

1.2.4 Bladder cancer: treatment

This section discusses current approaches in the treatment of NMIBC and MIBC.

1.2.4.1 Muscle invasive bladder cancer and non-muscle invasive bladder cancer

Stratification between aggressive and more conservative modes of treatment is normally determined by the presence, or absence of BC muscle invasion [71].

The vast majority of cases (90%) are histologically classified as urothelial cell carcinomas. Localised disease can be stratified into NMIBC and MIBC [12]. NMIBC can be effectively managed through transurethral resection and Bacillus Calmette-Guérin (BCG) vaccine bladder instillation, whereas MIBC often requires aggressive surgical management of surgery with radiotherapy, often with concurrent neoadjuvant platinum based chemotherapy consisting of the nucleoside analogue gemcitabine and alkylating agent cisplatin [12].

Intravesical mitomycin C instillation is often offered during the first (diagnostic) cystoscopy, as there is evidence for reduced recurrence [72].

1.2.4.1.1 Treatment of non-muscle invasive bladder cancer

With an 80% success rate the mainstay of treatment for NMIBC is transurethral resection of the bladder tumour (TURBT), with adjuvant intravesical therapy [73]. BCG is the most common and effective form of intravesical therapy used in the treatment of non-muscle invasive BC, however other agents such as mitomycin C and interferon-α can be administered in the same manner with fair therapeutic efficacy [74].

Trans-urethral resection of the bladder tumour

TURBT is the first-line surgical treatment for NMIBC. Bladder tumours are first located using a cystoscope, and resected with an electrosurgical excision loop, allowing for tumour resection whilst sealing underlying blood vessels [75, 76]. Tissue is then histologically staged and graded by a pathologist. TURBT is often followed by intravesical chemotherapy, most commonly using BCG [75]. A period of at least two weeks post TURBT is allowed before BCG instillation to allow time urothelial repair, limiting systemic exposure to the attenuated *Mycobacterium bovis [77].*

One potential drawback of TURBTs is an increased number of circulating tumour cells in peripheral blood post-surgery, which may lead to dissemination of UCCs to organs and tissues within the body [78]. However a consensus has not been reached on this topic [79].

Bacillus Calmette-Guérin and other intravesical immunomodulators

Originally formulated as a vaccination against tuberculosis, BCG is an attenuated form of the bovine tuberculosis bacillus, *Mycobacterium bovis* [80]. Since the first reported successful usage of BCG in BC by Morales, Eidinger and Bruce in 1976, BCG has become the most efficacious agent used in the treatment of high-risk NMIBC [81, 82].

BCG is delivered into the bladder as an intravesical treatment, and so bypasses many of the side effects associated with systemic chemotherapy, with many patients reporting mild to moderate side effects. BCG treatment is superior to intravesical treatment with conventional chemotherapy drugs in terms of progression, specifically displaying greater effect on tumour progression in comparison to the DNA crosslinker, mitomycin C [72, 83, 84]. On average this form of immunotherapy reduces the recurrence rate by 40% and the chance of progression by 20% in patients presenting with papillary lesions [85]. For

patients with *Cis*, more than 40% of patients respond to therapy, there is also a 25% decrease in progression when *Cis* patients undergo BCG treatment [85].

The exact mechanism behind the anti-tumour effects of BCG has not been characterised although theories suggest that efficacy may be due to a local immune response, mediated by a concert of immune cells including $CD4^+$ and $CD8^+$ lymphocytes, natural killer (NK) cells, granulocytes, macrophages and dendritic cells (DCs). As a result of this immune response BC cells potentially undergo apoptosis due to direct cytotoxicity possibly mediated through CD40L, secretion of soluble factors such as tumour necrosis factor-related apoptosis-inducing ligand (TRAIL) and direct action of BCG [86, 87]. BCG is the gold standard in intravesical treatment for high-risk NMIBC although its use can cause treatment-contraindicating adverse reactions and there has been a shortage in supply in recent years, highlighting the requirement for a well-tolerated efficacious alternative [88].

Aside from BCG other forms of immune therapy used in the treatment of NMIBC includes interferon-α instillation. Although, as a sole agent interferon-α is less effective and more expensive than BCG, there is no evidence to show that BCG plus interferon-α exhibits superior efficacy to BCG alone, with the same applying for its use alongside chemotherapy [89-92]. Interestingly, Interferon-α does occasionally show efficacy in patients who are unresponsive to BCG therapy, with 15-20% completely responding [74]. In addition to interferon-α, similar levels of efficacy have been seen with Interleukins -2 and -12 (IL-2, IL-12), tumour necrosis factor (TNF), keyhole limpet hemocyanin (KLH) and rubratin [73].

Intravesical chemotherapy

There are a number of chemotherapy drugs, which have been used in the intravesical treatment of BC, these include: mitomycin C, doxorubicin, thritepa, ethoglucid, valrubicin, epirubicin, cisplatin and gemcitabine or their combinations [73]. There is no apparent superior agent, the addition of

intravesical chemotherapy to TURBT yields a 14-17% reduction in recurrence, however there is little benefit in terms of disease progression [73]. Generally, the side effects of intravesical chemotherapy are less than that of BCG instillation, making intravesical chemotherapy an attractive treatment in patients who are least likely to progress.

1.2.4.1.2 Treatment of muscle invasive bladder cancer

Treatments for patients presenting with MIBC are much more radical than for patients presenting with NMIBC. This is due to there being an increased likelihood of progression to stage 3 or 4, associated with poor five-year survival rates of just 30% and 10% respectfully [13]. These treatments vary from surgical resection of the whole bladder (cystectomy), or affected portions of the bladder (partial cystectomy), with adjuvant or neo-adjuvant chemotherapy and chemoradiotherapy.

Surgery

Surgical management of MIBC is limited to cystectomy, partial cystectomy and initial debulking by TURBT, depending on the amount of the bladder affected by the cancer and patient preference. Surgery is paired with chemotherapy to target micro-metastases.

Radical cystectomy

Radical cystectomy is the removal of the entire bladder, surrounding nearby lymph nodes, the prostate, part of the urethra, surrounding tissue and organs infiltrated by tumour [93].

Partial cystectomy

A partial cystectomy is an option in unifocal MIBCs. Part of the bladder is removed, allowing for retention of bladder function, although with a reduced volume [94].

Radiotherapy and Chemoradiotherapy

Radiotherapy is a alternative to cystectomy in patients with MIBC. It allows for locoregional control of the disease whilst preserving bladder function. Cisplatin is used in many cancers as a radio-sensitising agent, however its use in BC is not practical due to the low renal function and performance status of a large portion of patients. Although, the usage of 5-flurouracil (5-FU) and Mitomycin C (MMC) has been shown to significantly improve locoregional control in MIBC, when compared to radiotherapy alone, with no significant increase in adverse events [95].

Chemotherapy

First line chemotherapy in BC is a combination of cisplatin and gemcitabine (GC). Neoadjuvant cisplatin based GC chemotherapy is offered suitable patients with newly diagnosed MIBC, prior to cystectomy or radiotherapy [96]. MIBC patients are offered adjuvant cisplatin after radical cystectomy, wherever neoadjuvant chemotherapy is not possible.

Cisplatin

Cis-diaminedichlorldoplatinum(II) is the first member in the class of platinum-containing anti-cancer drugs, which also includes carboplatin and oxaliplatin, and is the single most efficacious agent in the treatment of MIBC [97, 98]. Upon entering the tumour cells, the chloride ions of cisplatin are subject to aquation in

the cytosol where the chloride content is 3-20% of the 100mM present in the extracellular fluid [97]. The resultant activated compound forms highly reactive platinum complexes and creates of intra and inter-strand crosslinks. Specifically 1,2-intrastrand crosslinks with the N7 position on purine bases, including GpG and ApG adducts [97]. These crosslinks interfere with DNA repair mechanisms, leading to DNA damage and the subsequent induction of apoptosis in tumour cells, or indeed most quickly dividing cells, such as cells involved in haematopoiesis within the bone marrow [97].

Cisplatin is used in the treatment of a wide variety of cancers including bladder, head and neck, lung, ovarian, and most notably testicular cancers [96, 98-103]. It shows efficacy against carcinomas, germ cell tumours, lymphomas, and sarcomas. The renally excreted compound is intravenously administered and binds highly (>95%) to plasma proteins [104]. Cisplatin is a poor penetrator of the blood-brain barrier and accumulates most significantly within the kidneys, although accumulation is also observed in the testes and intestine. Side effects include nephrotoxicity, neurotoxicity, ototoxicity, electrolyte disturbance, haemolytic anaemia, nausea and vomiting. Unfortunately, BCs often acquire resistance to cisplatin.

Gemcitabine

Gemcitabine is a hydrophilic nucleoside analogue pro-drug that is intracellularally converted into the active metabolites gemcitabine bi- and tri-phosphate[105]. It blocks the *de novo* synthesis pathway inhibiting ribonucleotide reductase by replacing cytidine during replication, leading to cell cycle arrest and apoptosis [105]. The membrane transport proteins human equilibrative nucleoside transporter 1 (hENT1) and human concentrative nucleoside transporter (hCNT) are responsible for the transport of gemcitabine into the cell, underexpression of the 50KDa transmembrane protein hENT1 has been linked to gemcitabine resistance in a range of cancers as has overexpression of the R1 subunit of ribonucleotide reductase [105-109].

The addition of gemcitabine to cisplatin allowed for a similar survival advantage to the previous gold-standard first line therapy for BC - methotrexate, vinblastine, doxorubicin, and cisplatin (MVAC) - but GC is better tolerated with a lower incidence of adverse events, and as such is the current standard of care for patients with MIBC and MBC [99].

Chemotherapy Resistance

Most patients initially respond well to cisplatin-based chemotherapy, however 90% of patients will acquire resistance to cisplatin. Interestingly, a small proportion of patients will present with intrinsically cisplatin resistant BC.

Modes of cisplatin resistance are facilitated by decreased intracellular concentrations of cisplatin, increased DNA repair, and decreased mitotic checkpoint surveillance.

Decreased intracellular concentrations of cisplatin are achieved through: increased efflux – multidrug resistance-associated protein 2 (MRP2), with an antioxidant response element (ARE) in its promoter region, has been implicated in cisplatin accumulation, and cisplatin resistance [110]; increased detoxification – glutathione (GSH) overexpression, also containing an ARE in its promoter, has been linked to cisplatin resistance, furthermore GSH-cisplatin conjugates are substrates for MRP2 efflux [111-113]. DNA excision repair protein 1 (ERCC1), which functions within the nucleotide excision repair pathway, has been implicated in cisplatin resistance in several cancers, where increased expression leads to the repair of platinum adducts formed by cisplatin, attenuating its cytotoxic effects [114-118]. Interestingly, dysregulation of checkpoint proteins at the G2/M phase mitotic checkpoint has been implicated in cisplatin resistance, mediated by overexpression of cyclin-dependent kinase 1 (CDK1), and M-phase inducer phosphatase 3 (CDC25C) in lung cancer cells [119].

There is much to be understood about the modes of cisplatin resistance, however it is likely that resistance is due to a combination of the above factors. Finding a

target that governs a range of proteins implicated in cisplatin detoxification may be useful in mitigating cisplatin resistance in BC.

1.3 The NRF2-KEAP1 axis

Nuclear factor (erythroid-derived 2)-like 2 (NRF2) is a basic leucine zipper transcription factor encoded by the *NFE2L2 gene*, and the master regulator of a battery of proteins involved in intracellular redox homeostasis [120]. NRF2 expression is ubiquitous throughout the body, with the highest levels of activity being observed in tissues exposed to high concentrations of environmental toxicants, reactive oxygen species (ROS), and carcinogens such as the kidney and liver [121].

In normally functioning cells NRF2 pathway activation elicits strong anti-inflammatory and anti-apoptotic effects, limiting macromolecular damage by intracellular chemical and oxidative stress [122, 123]. Under basal conditions NRF2 is kept transcriptionally inactive by kelch-like ECH-associated protein 1 (KEAP1) binding [124]. Subsequent ubiquitination facilitated by cullin 3 ubiquitin ligase (CUL3), promoting proteasomal degradation (Fig 1.6) [124]. When the cell is subject to oxidative or electrophilic stress, it is hypothesised that cysteine thiol groups are modified on KEAP1 and NRF2 undergo phosphorylation, inhibiting ubiquitination, leading to KEAP1 saturation, allowing newly synthesised NRF2 to accumulate in the nucleus and transactivate a plethora of cytoprotective genes [124].

KEAP1 is the chief regulator of NRF2 activation, although NRF2 activation may be mediated in a KEAP1-independent manner such as phosphorylation by a number of kinases including protein kinase C (PKC), mitogen-activated protein kinase (MAPK)/ extracellular signal-regulated kinase (ERK)/ c-Jun N-terminal kinase (JNK), and phosphatidylinositide 3-kinase (PI3K) [125].

Furthermore, NRF2 expression is also dependent on autoregulation. For example, an autoregulatory loop is formed with CUL3 and RING-box protein 1 (RBX1), whereby NRF2 expression triggers the transcription of CUL3 and RBX1 [126]. Interestingly, NRF2 can autoregulate its expression through an ARE

located in the proximal region of its promoter, allowing for NRF2 replenishment in times of cellular stress, upon NRF2 nuclear translocation [127].

Studies in transgenic NRF2 knockout mice have highlighted the physiological significance of NRF2 mediated cytoprotective effects, where these mice have demonstrated increased susceptibility to drug induced toxicities [128]. Unsurprisingly, the NRF2-KEAP1 axis has been implicated in many disease processes including cancer.

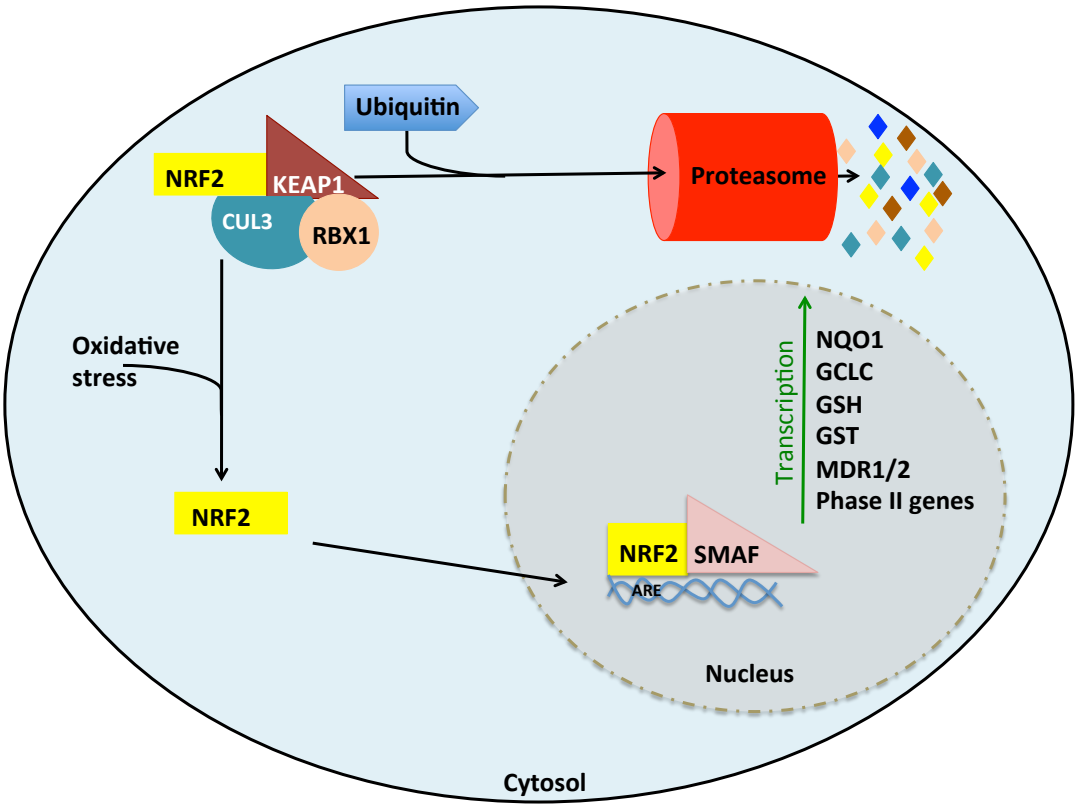

Figure 1.6. The NRF2-KEAP1 axis. Under basal conditions KEAP1 sequesters NRF2 in a complex with CUL3 and RBX1 that facilitates ubiquitin ligation. Polyubiquitinylation of NRF2 results in proteasomal degradation. Under conditions of cellular stress cysteine residues on KEAP1 are disrupted, leading to decreased NRF2 binding, resulting in NRF2 release, followed by translocation to the nucleus, ARE binding and heterodimerisation with small MAF (SMAF) facilitating the upregulation of a battery of cytoprotective genes.

1.3.1 NRF2 in cancer

Since the discovery of NRF2, there has been an increasing body of evidence indicating a positive role of NRF2 in cancer. In healthy cells NRF2 transcription factor binding mediates cellular detoxification, furthermore NRF2 induction by compounds such as sulforaphane, found in broccoli, has been hypothesised as a mechanism of chemoprevention [129, 130]. The chemopreventitive nature of such compounds is due to induction of the NRF2-mediated adaptive response, leading to increased expression of phase II detoxifying enzymes, antioxidants, and transporters responsible for cytoprotection from mutagens. Interestingly, in NRF2-null mice an increased incidence of cancer was noted compared to wild type, further highlighting the tumour suppressor protein (TSP) role of NRF2, as a result for many years NRF2 has been viewed as a positive factor in terms of cancer prevention[131, 132].

However, the NRF2-mediated response is a double-edged sword, beneficial in the context of protecting cells from damaging oxidative stress, whilst in cancer overexpression of NRF2 can lead to chemotherapy resistance through increased cellular efflux and detoxification, and the promotion of proliferation, and a more aggressive cancer phenotype [133].

Increased levels of NRF2 are associated with cisplatin resistance in a range of cancers including pancreatic cancer, ovarian cancer, and BC [134-139]. The result of high NRF2 levels in cancer is the upregulation of a battery of genes with an ARE in their promoter region. Upregulated genes that result in decreased sensitivity to cisplatin are those involved in efflux, and intracellular detoxification. MRP2, regulated by NRF2, may be responsible for the efflux of cisplatin [140]. Interestingly, in oesophageal SCC MRP2 expression strongly positively correlates with patients' sensitivity to cisplatin-based therapy [141]. The multidrug resistance protein 1 (MDR1) transport protein, moderated by NRF2, has also been implicated in cisplatin resistance, where in ovarian cancer MDR1 expression was associated with reduced sensitivity to cisplatin [142]. High resistance to cisplatin in ovarian cancer cell lines is associated with high

levels of glutathione synthesis [143]. Furthermore, glutathione s-transferase pi (GSTπ) amplification has been linked with cisplatin resistance in head and neck cancers, further implicating genes downstream of NRF2 in cisplatin resistance [144]. Notably, cisplatin treatment has been shown to increase the level of cellular oxidative stress [145]. This effect has potential to lead an increase in the expression of NRF2 and downstream proteins that may render cisplatin chemotherapy treatment ineffective, whilst still inflicting marked systemic adverse toxicity on the patient.

Some cancers have activating mutations in NRF2, which may alter its KEAP1 binding affinity, whilst inactivating mutations in KEAP1 have been associated with increased NRF2 expression, as has KEAP1 epigenetic suppression through promoter hypermethylation, and KEAP1 mutation in NRF2 binding sites [146-148]. Without KEAP1-mediated regulation, NRF2 levels can greatly increase due to its positive autoregulatory action [127]. Furthermore, disruption of the KEAP1-RBX1-CUL3 complex has been associated with highly malignant invasive UCCs [149].

Aside from its role in the regulation of drug efflux and metabolism, there is evidence for an oncogenic role of NRF2 in a number of cancers, associated with a more aggressive, proliferative phenotype [133, 150-153]. Interestingly, hyperactivation of NRF2 has also been implicated in the onset of the Warburg effect, a phenomenon where the majority of cancer cells produce energy primarily through glycolysis, rather than mitochondrial pyruvate oxidisation as in normal cells under aerobic conditions [154]. The Warburg effect is hypothesised to be associated with a tumour promoting microenvironment, defined by lactate acidosis, where H^+ ions secreted by cancer cells cause breakdown surrounding parenchyma, enhancing invasiveness [155, 156]. Furthermore, increased glucose demand by tumour cells can lead to glucose starvation in the surrounding environment, giving tumour cells a selective advantage [157]. Interestingly, NRF2-null mice produce tumours that are significantly less malignant than tumours in wild-type mice, further indicating a multifaceted role of NRF2 in cancer [158]. Indeed, when comparing NRF2 wild-

type with NRF2-null mice in a urethane induced multistep model of lung cancer *Satoh et al*, demonstrated an initial chemoprotective role of NRF2, where tumour onset time was longer in wild-type mice [158].

1.3.1.1 NRF2 in bladder cancer

Several proteins regulated by the NRF2 pathway are directly linked to cisplatin resistance or clinical parameters, including the negative correlation of pre-treatment GSH levels with response to cisplatin-based chemotherapy [159]. Furthermore, several proteins involved in GSH synthesis (including GSH reductase and γ-glytamylcysteine synthetase), and other mediators of the antioxidant response (such as GSH peroxidase and superoxide dismutase) are overexpressed in BC samples compared to normal urothelium, aberrant expression of these factors correlates with tumour stage and grade [160]. Compellingly, a cisplatin resistant variant of the T24 UCC cell line with increased levels of GSH or GST presented a less sensitive phenotype, whilst chemical depletion of GSH and GST block led to increased cisplatin cytotoxicity [161]. Moreover, expression of metallothionein, proteins central to heavy metal metabolism, correlates with cisplatin resistance in BC cell lines, and a poor prognosis clinically [162, 163]. Additionally, expression of the inducible heme-degradation enzyme, heme oxygenase-1 (HO-1), involved in the response to heavy metals and oxidative stress, correlates with chemotherapy resistance and increased tumour grade [164]. The involvement of HO-1 in BC is further exemplified by increased chemosensitivity in cell line models of BC, resulting from HO-1 inhibition [164, 165]. Interestingly, overexpression of the multidrug resistance-associated proteins (e.g. MRP1/2, which have been directly implicated in cisplatin efflux), and MDR1 are predictive of chemotherapy resistance and a poor prognosis [166, 167]. Conversely, an oncoprotective role of NRF2 has been demonstrated a murine N-butyl-N-(4-hydroxybutyl) nitrosamine (BBN)-induced model of BC, highlighting the context-dependent effects of NRF2-ARE signalling [168].

Further rationale for pharmacological targeting of NRF2 in BC has been demonstrated using *in vitro* expression silencing techniques. An interesting investigation by Hayden *et al,* using RT112 and RT112-CP UCC cells in an *in vitro* model of cisplatin resistance, demonstrated a marked increase in NRF2 expression, with a concurrent decrease in KEAP1 expression in the cisplatin

resistant RT112-CP cell line [134]. Furthermore, siRNA knockdown of NRF2 markedly increased the cisplatin-sensitivity of RT112-CP cells, although sensitivity to cisplatin was not fully restored to that of the parent cell line, RT112, indicating a multifaceted mechanism of cisplatin resistance in these cells [134]. Interestingly, Hayden *et al* reported unfavourable overall, BC-specific, and recurrence free survival in neoadjuvant cisplatin treated patients treated with cystectomy, but not in patients treated with cystectomy alone [134]. With evidence of NRF2 implication in cisplatin resistance in a range of cancers, now including a mechanistic rationale in UCC, the usage of a selective inhibitor of NRF2 may be clinically useful management of cisplatin resistance in patients with advanced BC.

1.3.1.2 Targeting NRF2

There are many specific inducers of NRF2 activity, including CDDO-Me and numerous phytochemicals, implicated in the management of a number of diseases including neurodegenerative disorders and cancer prevention [169]. Unfortunately, there has been little success in the development of specific inhibitors of the NRF2 pathway. Amongst the limited number of identified NRF2 inhibitors include: trigonelline, a coffee alkaloid which has been shown to inhibit NRF2 in chemotherapy resistant pancreatic cancer cells with high basal NRF2 activity, increased sensitivity to chemotherapy drugs was noticed in Panc1, Colo357 and MiaPaca2 cells, resulting in TRAIL-induced apoptosis [170]; ascorbic acid is a key antioxidant, and has been shown to suppress NRF2 expression, leading to decreased NRF2-DNA binding and partial restoration of imatinib sensitivity in a myelogenous leukaemia cell line [171]; brusatol, which is discussed in more detail below has been shown to reduce NRF2 protein level without affecting KEAP1 status, sensitises to chemotherapy drugs including carboplatin, 5-fluorouracil, etoposide and paclitaxel in HeLa, MDA-MB-231, and A549 cells. Furthermore, murine xenograft models have highlighted a marked anticancer effect, indicating brusatol may be clinically useful in the management of chemotherapy resistant cancers [172].

1.3.1.3 Brusatol

Brusatol is a quassinoid extracted from the South East Asian plant, *Brucea Javanica*. Brusatol displays promise as a specific inhibitor of NRF2 protein levels, with associated inhibitory affects downstream, increasing sensitivity to chemical stresses [173, 174]. Furthermore, robust effects have been displayed in cancer, where in a murine xenograft model of lung adenocarcinoma brusatol treatment initiated potent and transient inhibition of the NRF2 pathway, causing a reduction in tumour size when combined with cisplatin compared to the single use of either agent, providing rationale for the usage of brusatol in combination with cisplatin in BC [172].

1.4 Cluster of differentiation 40

Cluster of differentiation 40 (CD40) is a 48 kDa glycoprotein member of the TNF-receptor super-family. Originally identified in BC, since its role in immune biology has been well characterised, where CD40 plays a central role in the regulation of the immune response [175-179]. Mediation of humoral and cellular immune responses is facilitated by binding of CD40 with CD40-Ligand (CD40L) which acts between T-cells and antigen presenting cells in a bi-directional manner [176, 177].

The expression of CD40 is not only confined to the immune system, but also to a plethora of cells including, endothelial cells, fibroblasts, and epithelial cancer cells – where it regulates processes such as cell proliferation, growth suppression and cell death [178, 180, 181].

CD40 cytoplasmic domain lacks any intrinsic kinase activity, therefore, signal transduction is reliant on recruitment of a number of adaptor proteins known as TNFR-associated factors (TRAFs) (Fig 1.7) [180]. Two domains critical for TRAF association and signal transduction, reside in the cytoplasmic tail of CD40: a region proximal to the membrane, where amino acids Gln^{234} and Glu^{235} reside, responsible for TRAF6 binding, a Pro^{250} $XGlu^{252}$ and $XThr^{254}$ motif which directly binds TRAF2 and TRAF3 and indirectly binds TRAF5 [180]. Depending on the nature of CD40-ligation, recruitment of the TRAFs triggers the activation of a number of signalling pathways, including JNK, ERK, p38, MAPK, the transcription factors nuclear factor kappa-light-chain-enhancer of activated B cells (NF-κB) and signal transducer and activator of transcription (STAT), and the PI3K signalling module, which acts collaboratively to modulate the many pleiotropic effects of CD40 dependent on cell type and context [180].

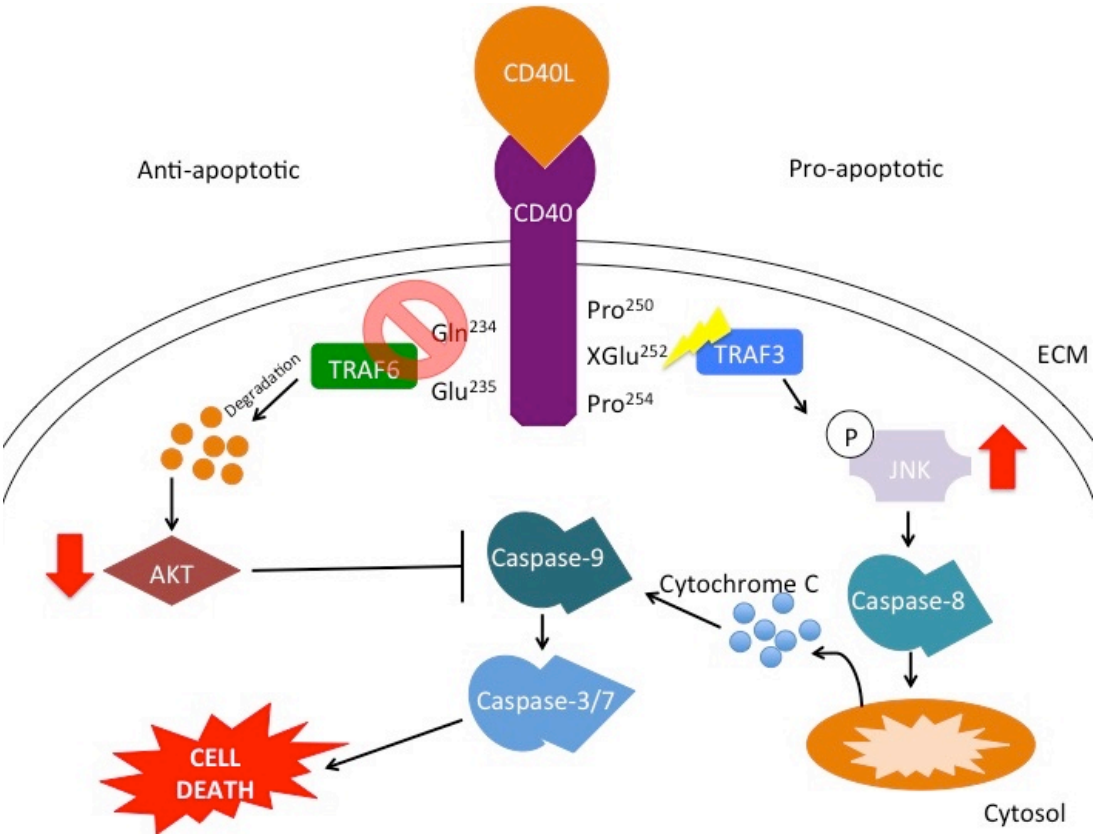

Figure 1.7. Mechanism of CD40L induced cell death. CD40-ligation results in pro- and anti-apoptotic signals, the balance between which decides cell fate. When CD40L is not present, the conformation of CD40 facilitates binding of TRAF6, promoting cell survival via Akt signalling. This conformation does not allow for TRAF3 binding, leading to its degradation. CD40 ligation causes receptor trimerisation, which leads to TRAF6 dissociation and degradation leading to the loss of Akt-dependent pro-survival signals, and TRAF3 binding, leading to TRAF3 mediated phosphorylation of JNK, which leads to caspase induction and apoptotic cell death [180].

1.4.1 CD40 expression in bladder cancer

CD40 is highly expressed in a number of epithelial cancers, including BC, with undetectable expression of CD40 in normal epithelial tissue at the site of tumour origin [182, 183].

In BC expression of CD40 is associated with lower stage and lower grade UCCs, with 89% of Ta and T1 tumours expressing CD40, and 62% of tumours at T2 or higher expressing CD40, compared to predominately negative normal urothelium [178]. Although, expression of CD40 is not an independent marker of prognosis, nor does it link with other clinicopathological factors such as the expression of P53 or BCL2 [178]. Interestingly, the high incidence of CD40 expression in non-muscle invasive BCs is likely a significant contributing factor in the excellent response to BCG therapy [178].

With CD40 being expressed in the majority of BCs, but not surrounding urothelium it is attractive target for potential therapies. The consequences of ligation with the membrane bound derivative of its ligand, CD40L add further to its therapeutic potential. The consequences of CD40-ligation in BC are discussed next.

1.4.2 CD40-ligand

CD40L is a member of the TNF superfamily of molecules and is most commonly expressed on activated T cells [184, 185]. The 32 kDa plasma membrane-bound protein (mCD40L) is subject to cleavage by MMPs, forming soluble CD40L (sCD40L).

In cancer cells, research into the effect of CD40L binding in epithelial cells shows outcome of CD40 ligation is multifaceted, with the type of ligand and cellular context influencing the physiological consequence [180]. Sustained CD40 engagement induces growth arrest and apoptosis, whereas transient CD40 ligation promotes proliferation and cell survival signalling [180]. The most profound effects are elicited by mCD40L, with sCD40L only inducing transient survival signalling. This disparity in effect is believed to be due to differential recruitment of TRAFs – however there is much to be learned about the results of CD40 ligation by both forms of CD40L [180].

In epithelial cells there is no detectable expression of CD40, however in a number of epithelial cancers, including bladder, CD40 expression is present [178]. In order to determine more about the consequences of CD40-ligation with mCD40L and sCD40L, a cleavage resistant CD40L construct, delivered via conditionally replicating adenoviral vector (AdNclCD40L), and recombinant soluble CD40L (rsCD40L) have been utilised.

In vitro work into the comparative effects of rsCD40L and AdNclCD40L on the CD40-positive EJ urothelial cell carcinoma cell line exhibited contrasting effects, with AdNclCD40L displaying the most potent response through sustained signalling inducing cell death, whereas sCD40L induced signalling was transient [180, 186]. Additionally, stimulation of CD40 with rsCD40L in carcinoma cell lines induces PI3K and ERK/MAPK mediated survival signals, with the induction of apoptosis only occurring in the presence of cytotoxic drugs, PI3K/ mammalian target of rapamycin (mTOR) and/or ERK pathway inhibitors, or in the presence of the protein synthesis inhibitor cycloheximide (CHX) [180]. This is a stark

contrast to the effects of AdNclCD40L, when delivered through co-culture of the CD40-positive UCC cell line EJ with AdNclCD40L expressing fibroblasts, where marked apoptosis is observed without the addition of other agents [180]. Similarly, high levels of cell death are reported when EJ cells are directly infected with AdNclCD40L [180].

1.4.3 TRAFs facilitate CD40 signal transduction

CD40 lacks intrinsic kinase ability on its cytoplasmic tail therefore a group of TRAFs are essential for the propagation of ligation-dependent signalling [187]. Interestingly, the nature of ligation affects the level of TRAFs recruitment leading to divergent outcomes discussed below.

CD40 ligation with AdNclCD40L leads to an increase in the expression of TRAF1 and TRAF3 with a concurrent decrease in the expression of TRAF6, the two former projecting pro-apoptotic signals, whilst the latter is responsible for pro-survival signalling [180]. This contrasts with rsCD40L, which induces only a modest increase in the expression of TRAF1 [180]. Intriguingly, changes in the expression of TRAF3 and TRAF6 as a result of CD40-ligation are due to post-translational modifications, as mRNA levels are not affected [180]. Conversely, TRAF1 mRNA increases as a result of CD40 ligation, indicating transcriptional regulation [180]. Interestingly, ligation with AdNclCD40L but not rsCD40L has been shown in a number of cases to increase the expression of TRAF3 in UCC cells, but not in normal urothelial cells, further indicating the potential of CD40-ligation as a specific therapy for the management of BC [180, 188, 189].

Evidence suggests that TRAF3 induces apoptosis through sustained phosphorylation of JNK post ligation with AdNclCD40L [180]. Two key pieces of evidence implicate JNK pathway in CD40-ligaiton induced cell death in UCC cells. These are a decrease in cell death when a JNK inhibitor is introduced; whilst cytochrome c is released from the mitochondria – JNK dependent process mediated by the phosphorylation of c-JUN, B-cell lymphoma 2 (BCL2) and B-cell lymphoma-extra-large (BCL_{xL}) [180]. Interestingly, the transient nature of the signal resulting from CD40 ligation with rsCD40L is believed to explain the lack of JNK mediated apoptosis, as sustained activation of JNK is required for cell death induction [180, 190].

TRAF6 is key in the propagation of survival signals through the PI3K/Akt-

pathway. Interestingly, TRAF6 has been shown to be downregulated upon CD40 ligation with mCD40L, and subsequent TRAF3 stabilisation [180]. Notably, whilst siRNA knockdown of TRAF3 maintained TRAF6 expression, artificial overexpression of TRAF6 could not divert the cells from an apoptotic fate, indicating that TRAF3 binding may inhibit TRAF6 localisation to the cytoplasmic tail of CD40 [180].

1.4.4 Clinical application of CD40 targeted therapies in bladder cancer

CD40 is an attractive target in BC due to its direct cell death inducing effects on BC cells and its activating effects on the immune system may also increase the response to therapy. Recent investigations in BC have unveiled local immunotherapy as a potential method of treatment for localised and MBC with more limited toxic effects when compared to traditional chemotherapy.

The usage of intravesical instillation of CD40L-expressing adenoviruses has been demonstrated to mediate antitumor effects in NMIBC, with a low incidence of adverse events [191]. Furthermore, agonistic CD40 antibodies have shown promise in the treatment of solid tumours [191, 192]. However, this thesis aims to understand more about the role of CD40-ligation in BC invasion.

1.5 Matrix metalloproteinase-1

Controlled remodelling of the ECM is key for tumour progression and dissemination [193]. The matrix metalloproteinases (MMPs) are a family of calcium-dependent zinc-containing endopeptidases that are capable of degrading many different kinds of extracellular matrix (ECM) proteins [194]. Further to their role in ECM remodelling, MMPs are involved in the proteolytic activation of proproteins.

The interstitial collagenase, MMP1, has substrates that include collagens (I, II, III, VII, and X), proteoglycans, entactin, ovostatin, MMP2 and MMP9 [195]. In normal physiology MMP1 is involved in a number of processes including development, angiogenesis, reproduction and tissue morphogenesis [194, 196]. As a result of their proteolytic activity, MMPs can release growth factors from the ECM, facilitating receptor binding [196]. Pathologically MMP1 is known to be involved in rheumatoid arthritis and cancer metastasis [197].

MMPs have been implicated in the progression of several cancers. In a breast cancer cell line murine xenograft model elevated MMP1 expression has been implicated in local growth and brain tumour metastases in [198]. Furthermore, MMP1 has also been suggested as a predictive marker of breast cancer and metastatic colorectal cancer [199, 200]. In BC, increased urinary expression of MMP1 is associated with advanced disease [201]. Finally, MMP1 single nucleotide polymorphisms (SNPs) have been associated with an increased susceptibility to BC [202-204].

Despite a lack of success in early-stage clinical trials for broad-range MMP inhibitors, MMPs remain a potential target for cancer therapeutics [196, 205-211]. Early drugs were designed at a time where only three out of 24 MMPs had been identified, prior to knowledge of the roles of MMPs in cancer. With hindsight, the poor trial performance of MMP inhibitors can be reasoned to lack of knowledge of the roles of MMPs in cancer. Furthermore, the importance of context must be addressed as MMPs clearly have multifaceted roles in the human

body, especially with evidence of MMP inhibition linked with a worse prognosis. Two tansomastat trials in small-cell lung cancer and pancreatic cancer were halted early after patients taking the inhibitor had a significantly poorer survival than those receiving placebo [212, 213]. New efforts in targeting MMPs must focus using molecular data to develop targeted agents, with high accumulation in cancerous tissues and low systemic adverse effects. Moreover, compared to previous approaches where MMP inhibitors were unsuccessfully trailed in advanced stage cancers, where marked invasion and dissemination had already occurred, a novel approach where MMP inhibitors are administered prior to disease advancement to mitigate the effects of MMPs in invasion and metastasis.

1.6 Fibronectin

Fibronectin (FN1) is a ubiquitous ECM glycoprotein, which exists as a dimer of two ~250kDa subunits, that binds to receptors in the integrin family [214]. Integrins are heterodimeric cell-surface receptors that connect the ECM with the intracellular cytoskeleton; they sense the cell microenvironment and modulate numerous signalling pathways [214]. Similarly to integrins, FN1 binds ECM constituents including collagen, fibrin, and syndecans. FN1 mediates a large array of cellular interactions within the ECM including roles in cell cycle regulation, cell adhesion, differentiation, growth, and migration [214-219]. Under normal physiological conditions FN1 is expressed predominantly by fibroblasts and hepatocytes, and is essential for cell-cell crosstalk, interaction with the cellular microenvironment, and development and wound healing [214].

The *FN1* gene is subject to alternative splicing creating different truncated copies of full length FN1 [214]. Resultantly, FN1 exists in both insoluble and soluble (plasma) forms [214]. Under normal conditions insoluble FN1 is primarily produced by fibroblasts where it is produced as a major component of the ECM, whilst plasma FN1 is produced by hepatocytes and is involved in blood clotting [215]. Plasma FN1 has been suggested as a prognostic marker in several cancers [220-222]. Notably, *Yiätupa et al* demonstrated that 86% of patients with digestive tract malignancies had elevated blood FN1 levels compared to the healthy group, potentially indicating merit as a blood biomarker [220].

In the tumour microenvironment, endocrine growth factors from the primary tumour facilitate the upregulation of FN1 secretion by fibroblasts preparing sites for distant metastasis known as premetastatic niches [223-225]. Furthermore, the co-injection of FN1 with tumour-cells increased tumour cell adhesion and metastasis, whilst mesothelial cell secreted FN1 has been implicated in the promotion of early metastasis in an organotypic model of ovarian cancer [226] [227].

Interestingly, integrin α5β1, a FN1 receptor involved in development and neoangiogenesis, has been suggested as a therapeutic target in a number of advanced cancers including those of the colon, breast, ovary and brain [228].

1.7 Family with sequence similarity 83, member D

The family with sequence similarity 83, member D (*FAM83D*), gene is located on chromosome 20q, where amplifications are present in cancers including bladder, breast, colorectal, ovarian, pancreatic and prostate [229-234]. First identified as a mitotic spindle associated protein, FAM83D interacts with the chromkinesin KID22 to allow for proper chromosome congression in metaphase [235, 236]. During mitosis, the mitotic spindle is essential for precise distribution of sister chromatids; functional alterations to components of the mitotic spindle may be a source of the chromosomal aberrations, and aneuploidy observed in advanced cancer. Interestingly, microarray studies have identified overexpression in hepatocellular carcinoma, ovarian cancer and lung adenocarcinoma metastases however there are few mechanistic studies into the role of FAM83D in cancer [231, 237, 238].

An *in vitro* study in breast cancer by *Wang* et al suggests *FAM83D* as a novel oncogene that inhibits the expression of the tumour suppressor protein (TSP) F-box/WD repeat-containing protein 7 (FBXW7), leading to hyperactive mTOR-signalling and a resultant increase in cell proliferation and motility [239]. With the addition of the mTOR inhibitor, rapamycin, mTOR dependent oncogenicity was markedly depleted, indicating a possible therapeutic option in FAM83D overexpressing malignancies [239]. Furthermore, the TSP FBXW7 is reported to be downregulated in a large number of malignancies, including BC [240]. In concert with Skp-Cullin-F-box (SCF) E3 ubiquitin ligase, FBXW7 is essential for the ubiquitin-mediated degradation of an array of oncoproteins including, c-JUN, c-MYC, Cyclin E, NOTCH, and mTOR [241-246].

1.8 Anillin

Anillin (ANLN) is a ubiquitously expressed 124 kDa protein centrally involved in formation of the contractile ring and cleavage furrow, acting as a scaffold linking ras homolog gene family, member A (RHOA), actin and myosin during cytokinesis [247]. In healthy neurones, ANLN is associated with neuronal migration and neurite growth through linkage of ras homolog gene family, member A (RHOG) and the actin cytoskeleton [248]. Furthermore, ANLN is implicated in the regulation of tight junctions (TJ) and adherens junctions (AJ) [249]. The referenced study reports AJ and TJ disassembly, without change to the expression of junction proteins, as a result of downregulation of ANLN expression, indicating a key regulatory role [249]. Overexpression of ANLN has been linked with poor survival in a number of cancers including colorectal [250, 251].

Further examples of the involvement of ANLN in tumour invasion and progression are presented by Liang *et al* who reported a significant positive correlation between nuclear ANLN levels and tumour stage, grade, and invasion patterns in upper urinary tract UCCs [252]. Furthermore, they reported a significant association between nuclear ANLN levels and poor disease-specific survival and metastasis free survival. Whereas overexpression of cytosolic ANLN was negatively correlated with tumour grade and vascular invasion, whilst low total ANLN levels were strongly associated with poor disease-specific survival, and metastasis free survival [252]. Furthermore, ANLN has been identified as a marker of poor survival in hepatocellular carcinoma [253]. Additionally, high ANLN is one of three markers in a signature of poor prognosis in breast cancer [254]. Moreover, ANLN levels were 19.8-fold higher in pancreatic cancer patients, than in normal pancreas [255]. Conversely ANLN expression is a marker of a favourable prognosis in patients with renal cell carcinoma [256].

Interestingly, *in vitro* studies have reported lentiviral knockdown of ANLN leading to the inhibition of cell growth and migration in a model of breast cancer, suggesting usefulness as a therapeutic target [257]. Furthermore, the referenced study reported increased accumulation at G2/M phase as a result of CDK1

phosphorylation and Cyclin D1 suppression, suggesting inhibition of cytokinesis as a mechanism of action [257].

1.9 Biomarkers in bladder cancer

MBC and MIBC are the deadliest variants of BC, associated with meagre outcomes. Patients who can be treated at an earlier stage are more likely to survive for a longer period. However, beyond TNM staging and grading there are little tools to predict the chance of a BC developing into muscle invasive disease. A marker or signature indicative of MIBC, which can be obtained in a minimally invasive manner could allow for more accurate and timely treatment stratification.

1.9.1 Biomarkers

Biomarkers are molecules, genes or characteristics associated with an increased risk of a certain disease event, for example progression to MIBC. Alterations may include germline or somatic mutations, transcriptional changes and post-translational modifications [258].

A 'molecular signature' is are a collection of alterations indicative of a particular physiological state, altered components making up molecular signatures may be, genetic (gene expression and/or mutation), proteomic, and/or metabolomic [258]. Such panels of biomarkers can offer increased specificity than single biomarkers. Biomarkers can be detected by non-invasive means, in the blood (whole blood, serum or plasma), or in secretions or excretions (sputum, nipple discharge, faeces or urine), these can be assessed regularly in comparison to tissue-derived biomarkers, which require a biopsy such as those taken during TURBTs [258]. Biomarkers are used by three principal means: as diagnostic markers, e.g. identification of early stage cancers, prognostic i.e. to forecast how aggressive a cancer is and predictive, for example to predict how well a patient will respond to treatment. A small number of biomarkers are currently used in different cancers, giving the medical oncologist more insight into the tumour biology, aiding in the determination of treatment regimens. These include prostate-specific antigen (PSA) a prostate cancer related marker, and the breast cancer susceptibility genes breast cancer related genes -1 and -2 (*BRCA1)* and (*BRCA2)* [259].

In BC, there is a dire need for a non-invasive marker of MIBC, as patients with aggressive BC who are treated more radically from the outset, have the best chance of long-term survival in comparison to those patients whose aggressive disease has progressed. An early marker of muscle invasive BC could inform the medical oncologist whether the patient can have their disease managed by minimally invasive methods such as TURBT and BCG instillation, rather than cystectomy and systemic chemotherapy, potentially enhancing patient outcomes, whilst reducing treatment costs.

1.9.1.1 Osteopontin

Osteopontin (OPN) is a highly negatively charged phosphorylated glycoprotein secreted by activated T lymphocytes, activated macrophages, leukocytes and is present at sites of inflammation in the interstitial fluid, and at the matrix of mineralized tissues such as bone [259]. There are a number of physiological functions where OPN has been shown to be involved, it has roles in inflammation and immune function, in mineralized tissues, in vascular tissue as well as in the kidney [259]. OPN elicits its physiological effects through binding with a diverse range of cell surface receptors including several integrins and CD44 [259]. Receptor binding mediates specific signalling functions leading to cell adhesion and migration [259]. More recently it has been discovered that OPN is overexpressed in a number of cancers including BC, breast cancer, colorectal cancer, lung cancer, ovarian cancer and melanoma where it promotes tumour proliferation, differentiation, invasion and metastasis, and is associated with a poor prognosis [259-261]. Interestingly it has been observed that OPN is also elevated in the blood of patients with metastatic cancers [259].

In a model of invasive BC using the T24 cell line RNAi inhibition of OPN significantly inhibited proliferation and invasion, whilst study examining the role of OPN in BC, which enrolled 225 patients with UCC, and 230 age- and sex-matched healthy volunteers as control subjects, demonstrated significantly higher plasma OPN levels in patients with UCC compared to healthy volunteers [260, 261]. It was also found that high levels of OPN correlated significantly with high-grade UCCs when compared to low grade UCC [261]. Patients with disease confined to the bladder had the lowest levels of OPN, whereas those with lymph node positive UCC showed higher expression, with the highest level of OPN being present in metastatic disease [261]. Intriguingly, the overall survival rate in MIBC patients expressing high levels OPN was significantly lower than those with lower expression of OPN [261]. Further studies in hepatocellular carcinoma, head and neck squamous cell carcinoma, lung and prostate cancer have shown that OPN level is highly associated with prognosis [261-267].

The mechanism whereby OPN increases tumour invasion and metastasis is essentially unclassified. Although, *in vitro* data suggests OPN mediates tumour invasiveness. For example, breast cancer cell lines lacking OPN expression form tumours in nude mice much more slowly than wild type [268]. Also, as previously mentioned, inhibition of OPN expression in T24 BC cells significantly limits their invasive capacity [260]. Conversely, some data suggests that OPN may indirectly contribute to the survival of cancer cells through the upregulation of hyaluronic acid synthase, another prominent feature in metastatic cancer cells [269].

1.10 Thesis hypotheses

Chapter 3: Brusatol, via inhibition of NRF2 will increase the sensitivity of UCC cell lines to cisplatin.

Chapter 4: CD40-ligation will modulate UCC cell invasion in An organotypic model of BC.

Chapter 5: Gene expression analysis will identify molecularly distinct subtypes of BC.

Chapter Two – Materials and Methods

2.1 Tissue culture techniques 59
2.1.1 Maintenance of cell lines 59
2.1.2 Cryopreservation and thawing of cell stocks 61
2.1.3 Cell counting and cell seeding 61
2.1.4 Cell viability assay 61
2.1.5 Short tandem repeat profiling 62
2.1.6 Treatment of cells with compounds 64
2.1.7 Transfection with NRF2 targeting short interfering RNA 64
2.1.8 Organotypic model of invasion 65
2.2 Protein biochemistry techniques 68
2.2.1 Preparation of protein extracts 68
2.2.2 Western Immunoblotting techniques 68
2.2.3 Immunohistochemistry 72
2.3 Nucleic acid techniques 76
2.3.1 Reverse transcription polymerase chain reaction 76
2.4 Gene expression analysis methods 81
2.4.1 Patients and tissue samples 81
2.4.2 Study ethical considerations 81
2.4.3 Tissue biopsy sample preparation 84
2.4.4 Human Gene 1.0 ST Microarray hybridisation analysis 84
2.4.5 Statistical analysis of microarray data 85
2.4.6 Meta-analysis 86

Unless stated otherwise, all reagents and materials were sourced from Sigma-Aldrich, Poole, UK

2.1 Tissue culture techniques

2.1.1 Maintenance of cell lines

The human urothelial cell carcinoma cell lines, EJ, 253-J, MGH-U3, RT112, RT112-CP and the human colorectal, carcinoma cell line HCT116 were maintained in either Roswell Park Memorial Institute medium (RPMI), Dulbecco's modified Eagles medium (DMEM) or modified Eagles medium MEM supplemented with 2mM glutamine, 10% foetal calf serum and 1% antibiotic antimycotic solution (final concentrations 100U/ml penicillin, 0.1mg/ml streptomycin and 0.25μg/ml). RT112-CP cells were supplemented with an additional 5μM of freshly prepared cisplatin in dimethylformamide (DMF). Cells were grown in vented 75cm^2 flasks (Corning, USA) at 37°C in 5% CO_2, and routinely passaged when 90% confluent. The media was discarded, cells washed once with phosphate buffered saline (PBS), and trypsin-ethylenediaminetetracetic acid (EDTA) (0.5% w/v trypsin, 0.02% w/v EDTA) added to cover the cells. Cells were transferred to complete culture media and pelleted through centrifugation at 1300rpm for 5min. The supernatant was discarded and the cell pellet was resuspended in fresh complete media and plated into a 75cm^2 flask.

Table 2.1. Cell lines and their tissue origins.

Cell Line	Tumour Description	Stage	Grade	Sex	Established	Ref
EJ	Bladder Primary	≥T3	G3	M	1972	[270]
253-J	Retroperitoneal lymph node metastasis	T4	G4	M	1972	[271]
MGH-U3	Papillary UCC	≤T1	G1	M	1977	[270]
RT112	Well differentiated UCC	≤T1	G1	F	1973	[272]
RT112-CP	Cisplatin resistant RT112	≤T1	G1	F	1990	[273]

2.1.2 Cryopreservation and thawing of cell stocks

Approximately $2x10^6$ pelleted cells were resuspended in 1ml of freezing down media (DMEM supplemented with 20% FBS, and 10% DMSO) and transferred to a 1ml cryovial (Nunc, Fisher Scientific UK Ltd, Loughborough, UK). The vials were placed at -70°C overnight in a freezing container immersed in isopropyl alcohol, before being transferred into liquid nitrogen for long-term storage. Cells were recovered by thawing the cryovials quickly at 37°C and transferring cells into 10ml warm complete media. Cells were pelleted, resuspended in complete media and transferred to a $75cm^2$ flask.

2.1.3 Cell counting and cell seeding

Cells were counted using a haemocytometer. Briefly, cells were dissociated from the culture flasks and resuspended as described above. 10µl of the cell suspension was pipetted onto a haemocytometer. Cells in the central grid were visualised using a Zeiss Axiovert 40 C inverted microscope and counted.

2.1.4 Cell viability assay

The 3-[4,5-dimethylthiazol-2-yl]-2,5-diphenyltetrazolium bromide; thiazolyl blue (MTT) assay was used to determine cell viability in response to various treatments. Leaving 4 wells blank, cells were plated into each well of a 96-well microtiter plate at a density of $3x10^3$ cells per well, and incubated overnight at 37°C 5% CO_2. Cells were treated with appropriate titre of compound, with four wells reserved for an untreated control, a vehicle control and only cell culture media in the 4 wells with no cells. After 48-hours MTT reagent was added to each well at a final concentration of 0.5mg/ml in cell culture media, and is incubated at 37°C 5% CO_2 for 3-hours. The MTT reagent is then removed, the plates are dried and the insoluble formazan is solubilised in DMSO prior to being read by a microtiter plate reader (Turner Biosystems) at 570nM and a reference wavelength of 650nM.

2.1.5 Short tandem repeat profiling

To determine the provenance of the cell lines used in this thesis, short tandem repeat (STR) profiling was undertaken. One million cells were plated in a 60 mm dish, incubated overnight at 37°C 5% CO_2. DNA was prepared as follows: Cells were detached with trypsin and centrifuged for 5 minutes at 500g, 4°C prior to washing with ice cold PBS and re-suspension in digestion buffer (100mM NaCl, 10mM Tris-HCl (pH 8), 25mM EDTA (pH 8), 0.5% SDS, 0.1mg/ml proteinase K). Lysates were then incubated overnight at 50°C with agitation. One volume of phenol/chloroform/isoamyl alcohol was added prior to centrifugation at 1700g for 10 minutes. The aqueous layer was then transferred to a fresh tube, with 0.5 volumes of 7.5M ammonium acetate, and 2 volumes of absolute ethanol, and centrifuged for 2 minutes at 1700g. The DNA pellet was then washed with 70% ethanol, prior to air-drying and re-suspension at 1µg/µl in TE buffer. STR profiling was performed by departmental technical laboratory staff.

Table 2.2. Results of STR-profiling of human bladder carcinoma cell lines. Where data was available, provenance of cell lines was confirmed to be a 100% match to published data. However, there is no published STR data (NR) for two cell lines, MGH-U3 and RT112-CP. As RT112 and RT112-CP almost completely match, loss of TPOX 11 in RT112-CP could be a result of selective pressures in the cisplatin resistant RT112 clone, due to cisplatin-induced genomic instability.

Marker	EJ	253-J	MGH-U3	RT112	RT112-CP
THO1	6	6, 9.3	8, 9	7	7
D21S11	29	28, 29	28, 31	27, 30	27, 30
D5S818	10, 12	10, 12	10, 11	10, 13	10, 13
D135317	12	9	8, 11	13, 14	13, 14
D7S820	10, 11	9	8, 9	11, 12	11, 12
D165539	9	9, 12	9, 11	11, 13	11, 13
CSF1PO	10, 12	10, 12	10, 12	10, 11	10, 11
AMEL	X	X	XY	X	X
vWA	17	17, 18	17, 19	14, 17	14, 17
TPOX	8, 11	8, 11	8, 11	8, 11	8
Match	100%	100%	NR	100%	NR
Reference	[274]	[275, 276]	-	[277, 278]	-

2.1.6 Treatment of cells with compounds

For cell viability assays, UCC cells were seeded at a density of 3000 cells/well prior to overnight incubation at 37°C, 5% CO_2.

For protein and nucleic acid extraction cells were plated in 60mm petri dishes at a density of 600,000 cells/dish, and incubated overnight prior to treatment.

Samples were treated with the required concentration, for the required time as follows. Cisplatin was dissolved in DMF at 1000x the final concentration (FC) for FCs at ≤50μM. For FCs >50μM cisplatin was dissolved in DMEM. The FC of DMF in all samples was 0.1%. Brusatol, CDDO-Me, CHX and MG132 were dissolved in DMSO, to 1000x the FC, with a final dimethyl sulfoxide (DMSO) concentration across all samples of 0.1%. Once appropriately treated cells were incubated at 37°C, 5% CO_2, for the required time. Following incubation cells were processed as required and where appropriate data was normalised to a 1/1000 vehicle control.

2.1.7 Transfection with NRF2 targeting short interfering RNA

Cells were plated to 20% confluence, and incubated overnight at 37°C and 5% CO_2. Transfection solutions were prepared. Solution 1 (S1) comprises of 200μl optimem and 2μl Lipofectamine 2000 per well, S1 is mixed and allowed to rest for 5 minutes. Meanwhile solution 2 (S2) was prepared by combining 200μl optimem media, and either 1.5μl NRF2 short interfering RNA (siRNA) 20μM (Dharmacon siGenome Smart Pool NRF2), or 1.5μl 20μM non-targeting siRNA (Dharmacon Control Pool Non-Targeting #1) per well. Equal volumes of S1 and S2 were then combined and allowed to stand for 20 minutes (S3). Cells were then treated in a 6-plate, in 2.6ml culture medium; 0.4ml S3 was added to the appropriate wells drop wise. Cells were cultured for 72-hours prior to lysis and subsequent western blotting, where NRF2 siRNA data was compared to non-targeting siRNA.

2.1.8 Organotypic model of invasion

Organotypic cultures of UCCs were assembled as described by and detailed in Figure 2.1. [279]. Concisely, $1x10^6$ human foreskin fibroblast (HFF1) cells were suspended in a matrigel and collagen, rat tail type 1 matrix (1:1), incubated at 37°C 5% CO_2 overnight. Prior to being overlaid with $5x10^5$ UCC cells (EJ, MGH-U3 or RT112) untreated, treated with AdMock or treated with AdNclCD40L. After a further 24 hours at 37°C 5% CO_2, the gels were raised onto steel gauzes with a collagen membrane acting as an air-media interface. After 10-days, the gels were formalin fixed and paraffin embedded before staining by haematoxylin and eosin (H&E) or immunohistochemistry (IHC) for further analysis. All cultures were conducted in triplicate.

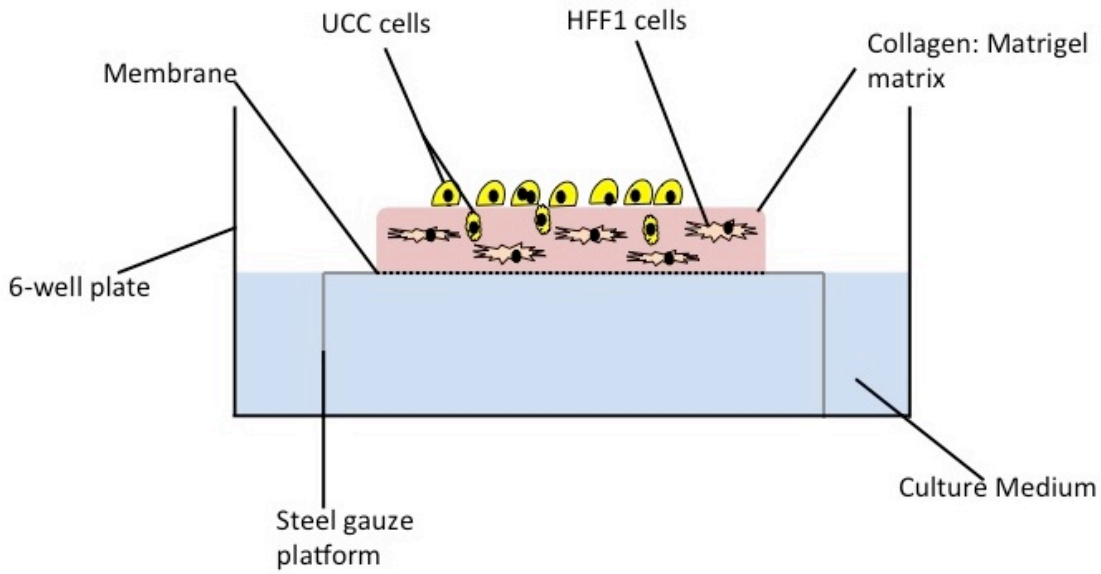

Figure 2.1. An organotypic model of bladder cancer. This organotypic forms an air-liquid interface to emulate growth conditions in the bladder. A pseudostroma consisting of collagen, matrigel (1:1) and HFF1 cells lies under a colony of urothelial cell carcinoma cell lines. Beneath the gel lies a collagen-coated membrane acting as an interface between the culture medium below, and the gel above. Suspending the gel above the culture medium is a steel gauze platform, performed in a 6-well plate.

2.1.8.1 Infection of cells with AdNclCD40L †

EJ, RT112 & MGH-U3 cells were incubated at 37°C 5% CO_2 for 2 hours, with constant agitation, in cell culture medium with 1 multiplicity of infection (MOI) of AdNclCD40L in parallel with a 1 MOI AdMock virus control, both replications deficient viruses. The cells were then centrifuged at 1,000 RPM for 5 minutes, the supernatant was discarded, the pellet was re-suspended in PBS, and the prior centrifugation step was then repeated, and the supernatant discarded. The cell pellet was then re-suspended in cell culture medium, prior to addition to organotypic experiments, with $1x10^6$ of cells being cultured for 24h before lysis and western blotting to confirm infection.

† Taha Elmitwalli, performed this work under the instruction of myself, as I did not have approval to undertake class II work with adenoviral vectors. I set up the experiment up until the infection of cells. Once fixed in formalin I continued my work with the samples.

2.1.8.2 Fixation

Complete organotypic assays were transferred to neutral buffered formalin for 24 hours at 4°C, prior to being transferred to 70% ethanol in dH_2O for a further 24 hours at 4°C.

2.2 Protein biochemistry techniques

2.2.1 Preparation of protein extracts

To extract protein from BC cells, cells were washed three times with ice cold PBS. Once the PBS wash was removed, cells were lysed *in situ* with an appropriate volume of radioimmunoprecipitation assay (RIPA) lysis buffer, and crude lysate collected into pre-chilled microfuge tubes. Cells were left on ice for 30 minutes to allow for complete lysis. Debris was removed from the lysis by centrifugation at 13,000 rpm for 5 minutes at 4°C, the supernatant transferred to a fresh pre-chilled microfuge tube and stored at -20°C.

2.2.1.1 Determination of protein concentration

Protein concentration was determined using the Bradford Protein assay kit (BioRad Lab Ltd., Hemel Hempstead, UK) by thoroughly mixing by vortex 2.5µl of clarified lysates with 1.2ml dH_2O and 300µl Bradford reagent (BioRad). Absorbance at λ_{595} was measured by a spectrophotometer, and protein concentrations were calculated in reference to the bovine serum albumin (BSA) standard curve.

2.2.2 Western Immunoblotting techniques

2.2.2.1 SDS-PAGE electrophoresis

Western blotting was performed using a mini-PROTEAN Tetra cell tank (BioRad) using the method of Laemmli. Glass plates were cleaned using ethanol and the apparatus was assembled according to the manufactures instructions. 10ml resolving gel (375mM Tris-HCl (pH 8.8), 0.1% SDS, 0.1% ammonium persulfate, 30% w/v acrylamide/ 0.8% w/v bis mix (National Diagnostics, Geneflow, Frandley, UK) and tetramethylethylenediamine (TEMED) depending on the

desired acrylamide of the gel) was poured. Methanol was layered on top of the resolving gel to remove air bubbles. Gels were set at room temperature until the hydrogel had solidified. Methanol was discarded and the gel was rinsed with dH_2O. 4ml of stacking gel was then prepared (125mM Tris-HCl (pH 6.8), 0.1% SDS, 0.1% ammonium persulfate, 0.01% TEMED and 670µl 30% (w/v) acrylamide/0.8% (w/v) bis mix) and poured on top of the set resolving gel, a comb was inserted and the gel was set at room temperature. Where increased separation was appropriate, 4-20% pre-cast mini-PROTEAN gels (BioRad) were used. Prior to gel loading, the comb was removed whilst submerged in running buffer; the wells were washed extensively with x1 sodium dodecyl sulfate-polyacrylamide gel electrophoresis (SDS-PAGE) running buffer (x10 stock solution; 0.25M Tris-HCl pH 8.3, 1.92M glycine, and 1% (w/v) SDS). Samples containing 15-100ug of total protein were denatured by incubating at 95°C with 3x concentrated protein sample buffer (PSB: 187.5mM, Tris-HCL pH 6.8, 6% (w/v) SDS, 30% glycerol, 0.03% (w/v) bromophenol blue, 10% (v/v) 2-Mercaptoethanol) for 5 minutes. Denatured samples were cooled on ice, centrifuged to remove condensation and loaded into the appropriate wells of the assembled PAGE gel. Gels were electrophoresed at 150-175V (constant volts) for 60-120 minutes.

2.2.2.2 Western Immunoblotting

After SDS-electrophoresis, the proteins are transferred onto nitrocellulose transfer membranes, methanol soaked 0.45µM PDVF membranes using the BioRad Trans-Blot Turbo system. Where pre-assembled BioRad transfer packs were not used, the filter paper and membranes were soaked in transfer buffer (50mM Tris-HCl, 190mM glycine, 20% (v/v) methanol) prior to assembly. The proteins were then transferred for 10 min at 25V/1.5A. Membranes were then washed in TBST (1x TBS; 20mM Tris-HCl pH 7.6, 136mM NaCl, supplemented with 0.1% Tween-20) for 5 minutes, followed by blocking in 10% skimmed milk or 10% BSA (phospho-proteins) for 1 hour at RT or overnight at 4°C. Blocked membranes were washed in TBST for 5 minutes, and incubated overnight in the

appropriate primary antibody diluted in TBST with 2% milk (Table 2.3.). Membranes were washed 6 times for 10 minutes each in TBST, incubated for 1 hour at RT in the relevant peroxidase conjugated secondary antibody (Table 2.2.) diluted in TBST with 2% milk. The membrane is washed a further 6 times for 10 minutes each in TBST, before being visualised by enhanced chemiluminescence (Amersham).

2.2.2.3 Reprobing membranes

Membranes were thoroughly washed in TBST, and horseradish peroxidase (HRP) was inactivated through incubation with 15ml PBS supplemented with 3 drops H_2O_2 and 3 drops Chromagen (Vector Labs) for 20 min in a light sealed box. Blots were then incubated with another primary antibody, overnight at 4°C.

Table 2.3. Western blot antibody conditions. RT: Room temperature.

Raised Against	Manufacturer	Clonality/ Species	Block	Primary Concentration	Primary incubation	Secondary Concentration	Secondary Incubation	Protein Loading (µg)
Nrf2	Santa-Cruz (H-300)	Polyclonal/ Rabbit	Overnight 4°C	1:400	Overnight 4°C	1:5000	1 hour RT	40
Nrf2	MBL (M200)	Monoclonal/ Mouse	Overnight 4°C	1:1000	Overnight 4°C	1:10000	1 hour RT	40
Nrf2	ProteinTech (16396-1-AP)	Polyclonal/ Rabbit	1 hour RT	1:1000	Overnight 4°C	1:5000	1 hour RT	40
Keap1	Santa-Cruz (H-190)	Polyclonal/ Rabbit	1 hour RT	1:2000	Overnight 4°C	1:2000	1 hour RT	40
Ho-1	Abcam (ab13248)	Monoclonal/ Mouse	1 hour RT	1:2000	1 hour RT	1:5000	1 hour RT	20
Nqo1	Abcam (ab195862)	Monoclonal/ Rabbit	1 hour RT	1:1000	Overnight 4°C	HRP-conjugated primary	N/A	20
CD40	Santa-Cruz	Polyclonal/ Rabbit	1 hour RT	1:1000	Overnight 4°C	1:2000	1 hour RT	50
CD40L	Santa-Cruz (SC-978)	Polyclonal/ Rabbit	1 hour RT	1:1000	Overnight 4°C	1:2000	1 hour RT	50
FN1	Sigma (F3648)	Polyclonal/ Rabbit	1 hour RT	1:1000	Overnight 4°C	1:10000	1 hour RT	50
β-Actin	Abcam (ab8227)	Polyclonal/ Rabbit	1 hour RT	1:20000	1 hour RT	1:20000	1 hour RT	5
OPN/ SPP1	R&D (AF1433)	Polyclonal/ Goat	1 hour RT	1:1000	Overnight 4°C	1:2000	1 hour RT	50
MMP1	R&D (BAF901)	Polyclonal/ Goat	1 hour RT	1:1000	Overnight 4°C	1:1000	1 hour RT	50

2.2.3 Immunohistochemistry

Antigen retrieval was performed using PT Link antigen retrieval machine (Dako) at pH 9. Prior to blocking, where TBST was removed, the slide was dried, and each section was incubated in peroxidase blocker (Envision, Dako) for 10-minutes, before three 1-minute washes in TBST. Primary antibody solutions were prepared to the appropriate concentration in Chemomate, and added to each slide for 1-hour at room temperature, prior to three 1-minute washes in TBST. The slides are then dried and secondary antibody (Envision, Dako) is then applied at room temperature, for 60 minutes, prior to a triplicate of 1-minute washes in TBST. DAB/Chromagen (Dako) were then made as per manufacturers instructions and was applied to each dried slide for 10-minutes, before washing in TBST three times for 1-minute. The slides were then counterstained in haematoxylin for 30 seconds, before being washed in distilled water for 5-seconds, then washed in acid water for 5 seconds, prior to a 5 second wash in 2% ammonium hydroxide. The slides were then incubated in 90% ethanol for 1 minute, before transferring to two separate 1-minute washes in absolute ethanol, prior to two subsequent 1-minute washes in xylene and cover-slip mounting using DPX mountant.

Table 2.4. Primary antibody concentrations for IHC.

Primary Antibody	Primary Antibody Concentration	Secondary Antibody Concentration
Osteopontin (R&D AF1433)	1:50	1/100
CD40-Ligand (SC-978)	1:1000	Stock

2.2.3.1 Histological processing

2.2.3.1.1 Paraffin embedding

Paraffin infiltration was performed overnight using a tissue processor.

2.2.3.1.2 Sectioning and slide preparation

Sections for IHC and H&E staining were prepared using a microtome, at a thickness of 4μm, on SuperFrost Plus slides (*ThermoFisher Scientific)***.** Slides were dried at 30°C overnight prior to staining, or storage in an anoxic cabinet.

2.2.3.1.3 Haematoxylin and eosin Staining

In the appropriate rack, slides were placed in xylene for 5 minutes, prior to two 30-second washes in fresh xylene. The slides were then washed in 100% ethanol three times for thirty seconds each, the previous step was then repeated with 95% ethanol, 70% ethanol and 30% ethanol respectively, before being agitated in water for 30-seconds. The slides were then placed in haematoxylin (30-seconds for cell pellets and organotypic assays, 1 minute for tissue sections), prior to being washed in running water until the solution ran clear. The slides were then agitated in acid water for 30-seconds, rinsed in running tap water for a further 30-seconds, then agitated in Scott's tap water for 30 seconds. Once the sections were clearly stained blue/ purple, the slides were washed in running tap water, followed by 30-seconds of agitation in 100% ethanol, prior to a 2-minute incubation in eosin. The slides were then transferred into 100% ethanol for 50 seconds, before being transferred into fresh absolute ethanol twice for 30-seconds, then xylene three-times for 30-seconds. Coverslips were mounted using DPX.

2.2.3.2 Scoring of immunohistochemical staining intensity

Staining intensity was scored by, consultant pathologist, Dr Vijay Aachi. Briefly, staining intensity was graded as 0 (negative), + (weak), ++ (moderate), +++ (strong).

2.3 Nucleic acid techniques

2.3.1 Reverse transcription polymerase chain reaction

2.3.1.1 RNA isolation

Following treatment, the media was discarded before washing the cells twice with ice-cold PBS, discarding each time. The cells were then subjected to digestion with RLT lysis buffer, and transferred to RNase-free microfuge-tubes. Lysates were centrifuged at 8,000g for 3 minutes; the supernatant was then transferred into fresh microfuge tubes (RNase free). 420µl absolute ethanol / 1 volume 70% ethanol was added to the supernatant prior to mixing by flicking the tube. <700µl of the supernatant including precipitate was transferred into a RNeasy mini column, and 2ml collection tube, before 15 seconds of centrifugation at 8,000g, discarding the flow-through. 350µl of buffer RW1 was added to the spin column prior to 15 seconds centrifugation at 8,000g. In each sample 10µl of DNAse I stock solution was added to 70µl RDD buffer, prior to mixing by inverting, then adding directly to the RNase silica-gel in the mini-column. The columns were then incubated at room temperature for 15 minutes, before the addition of 350µl of RW1 buffer, and a subsequent centrifugation for 15 seconds. The flow-through was then discarded. 500µl RPE buffer was added to the RNeasy mini spin column, prior 2 minutes' centrifugation at 8,000g, then discarding the flow-through. The column was then transferred into a fresh RNase free collection tube, prior to centrifugation at 8,000g for 1 minute to dehydrate the column. RNA was then solubilised in 30-50µl of RNase free water, prior to adding to the column, which in a fresh RNase-free collection tube was centrifuged at 8,000g, for 1 minute.

2.3.1.2 RNA quality control

The concentration and quality of RNA was assessed using the NanoDrop ND-1000 spectrophotometer. Here 1µl nuclease-free water was added to the

nanodrop, to calibrate a blank reading. After-which 1µl of each RNA sample was added to the sensor. The nanodrop measures the concentration using *Beer's Law*. Whereby, nucleic acid concentration (ng/µL) equals, absorbance (in AU) multiplied by wavelength-dependent extinction coefficient (ng-cm/µL) divided by the path length (cm). The calculated concentration is used to standardise RNA loading amount during cDNA synthesis.

The RNA quality is then assessed based on purity in relation to protein content (260/280nM) – where a value > 1.8 is acceptable, values below this are considered as contaminated with protein and discarded; or in relation to the solvent content (260/230nM) – where a value of >1.8 is accepted, any values below this are considered as contaminated with solvents and are discarded.

2.3.1.3 cDNA synthesis

Complementary DNA (cDNA) was prepared following the manufacturer's instructions (RETROscript® Kit, AMBION). Briefly, 2µg RNA and 2µl of Oligo(dT) were added 12µl (final volume) nuclease free water. Samples were heated at 85°C for 3 minutes, before adding reverse transcription (RT) components (2µl 10X RT Buffer, 4µl dNTP mix, 1µl RNase inhibitor and 1µl MMLV-RT) immediately at 44°C. Prior to 1 hour incubation at 44°C. Samples were heated at 92°C for 10 minutes to deactivate MMLV-RT.

2.3.1.4 PCR amplification

Amplification of MMP1, FAM83D, ANLN, FN1 and GAPDH cDNA fragments was performed by PCR. Reaction mixes were performed in a final volume of 25µl consisting of 1 volume of DreamTaq Green PCR Master Mix 2x (ThermoFisher Scientific, K1081), and 1 volume containing dH_2O, 2 pM forward primer, 2 pM reverse primer, and 1.5µl cDNA from the above cDNA synthesis. dH_2O replaces cDNA in no-cDNA control. The amplification was performed on a thermocycler (MJ Research PTC-200) as follows: 1) 93°C for 5 minutes, 2) 93°C for 30 seconds,

3) 60.3°C for 30 seconds, 4) 72°C for 1.5 minutes, repeat 2-4 29 times, to a total of 30 cycles.

Table 2.5. PCR primers targeting MMP1, FAM83D, ANLN and FN1.

Gene	Direction	Sequence 5'-3'
MMP1	FWD	aaggtctctgagggtcaagc
MMP1	REV	tgagctcaacttccgggtag
FAM83D	FWD	ggtaattctgtctggccaagtg
FAM83D	REV	gtttgagagcttgctatcctgg
ANLN	FWD	acgtccatcaataaagcaggtg
ANLN	REV	aagtacttgctaatggtgtggc
FN1	FWD	caggatcacttacggagagaca
FN1	REV	cagtgaatgccagtcctttagg
GAPDH	FWD	cctccaaaatcaagtggggcg
GAPDH	REV	accaccaggtgctcagtgtag

2.3.1.5 Agarose gel electrophoresis

A 1.2% suspension of agarose was prepared in Tris base, acetic acid, and EDTA (TAE) buffer, prior to heating with a domestic microwave until all agarose was in solution with the buffer. The solution was cooled to 50°C before adding SYBR® safe DNA gel stain according to manufacturer's instructions, gently mixing to avoid bubbles, then pouring into a midi-gel cassette to cast the gel. Once cast, samples were loaded to a final volume of 10µl. Electrophoresis was performed at 140V until sufficient separation of had occurred. The gel was visualised by UV-light detection using the ChemiDoc™ Touch Imaging System (BioRad).

2.4 Gene expression analysis methods

Unless marked with an asterisk (*) the following methods were performed by authors of the 2017 paper published in The International Journal of Oncology (IJO) "Gene expression profiling in bladder cancer identifies potential therapeutic targets" excluding I, Richard Greensmith.

2.4.1 Patients and tissue samples

Tissue biopsies, collected by cystoscope were collected between May 2004 and November 2005. Before cystoscopy, all participants gave written informed consent for additional samples to be taken for this study during their procedure. Eligible patients were aged 18 to 80 years, with a diagnosis of histologically confirmed NMIBC (n = 14) or MIBC (n = 5) urothelial cell carcinoma, who had not undergone any previous therapy. Control samples (n=11) were from histologically confirmed normal bladder tissue obtained from uninvolved tissues. Ten of the control samples were paired with corresponding UCC biopsies (4 NMIBC, 5 MIBC), the remaining sample was obtained from a patient with no diagnosis of BC. Patient demographic data is presented in table 2.6.

2.4.2 Study ethical considerations

Study approval was obtained from the South Birmingham Local Research Ethics Committee. All participants gave written informed consent for the usage of their respective biopsies in this study.

*Approval for further analysis was granted by the Liverpool Tissue Bank Ethics Committee (application number 12-09). All participants gave written informed consent for their respective biopsies to be used in biomedical analysis.

Table 2.6. Patient demographics for gene expression analysis. N/A: not applicable

		Controls (n=11)	**NMIBC (n=14)**	**MIBC (n=5)**
Age in years {median (range)}		79.2 (64-85.8)	70.8 (47.0 - 81.9)	80.14 (65.3-85.8)
Gender	Male	8 (72.2)	11 (78.6)	3 (60.0)
	Female	3 (27.2)	3 (21.4)	2 (40.0)
Grade	G1	N/A	6 (42.8)	0 (0)
	G2	N/A	1 (7.1)	0 (0)
	G3	N/A	7 (50.0)	5 (100)
T stage	PT1	N/A	5 (35.7)	0 (0)
	PT1B	N/A	1 (7.1)	0 (0)
	PTa	N/A	8 (57.1)	0 (0)
	PT2	N/A	0 (0)	5(100)
Recurrence	No	N/A	12 (92.3)	0 (0)
	Yes	N/A	1 (7.7)	5 (100)
Survival in Months (95% CI)		N/A	81.2 (73.3-not estimatable)	12.26 (0 - 35.6)

Table 2.7. Tumour information for immunohistochemical analysis. N/A: not applicable. *

		Controls (n=3)	MIBC (n=3)
Grade	G2	N/A	1
	G3	N/A	2
T Stage	pT2	N/A	1
	pT3	N/A	1
	pT4	N/A	1
Survival in Months		N/A	66.3 (20-120)

2.4.3 Tissue biopsy sample preparation

Tissue samples were snap frozen and stored in liquid nitrogen prior to RNA isolation.

2.4.3.1 RNA extraction

Total RNA was extracted from each biopsy with TRIzol (Invitrogen), before silica purification (RNAeasy Mini columns, QIAGEN) according to the manufacturer's instructions. RNA integrity was confirmed using the Agilent Bioanalyser, samples with a RIN of 6.0 were included in this study.

2.4.3.2 cDNA probe synthesis

200ng of total RNA was processed in to cDNA including targeted depletion of rRNA transcripts using the WT Expression kit (Ambion) according to the manufacturer's instructions. The cDNA was then fragmented and biotin end labelled with the WT Terminal Labelling Kit (Affymetrix).

2.4.4 Human Gene 1.0 ST Microarray hybridisation analysis

The resulting labelled cDNA was hybridised to Human Gene 1.0 ST whole transcript-based arrays (Affymetrix) prior to washing and staining on the FS450 fluidics station (Affymetrix). The Human Gene 1.0 ST Array (Affymetrix) was made up of 764.885 distinct 25nt probes, probing 28,869 annotated genes based on the March 2006 (UCSC hg18, NCBI Build 36) human genome sequence assembly with widespread coverage of RefSeq, Ensembl and putative whole CDS GeneBank transcripts.

2.4.4.1 Signal collection and analysis

A Scanner 3000 7G (Affymetrix) was used to scan the arrays and a Command Console (Affymetrix) was implemented in instrument control. Standard Affymetrix protocols were adhered to throughout. Raw microarray data was submitted to ArrayExpress (Accession: E-MTAB-1560).

2.4.5 Statistical analysis of microarray data

2.4.5.1 Data transformation

Robust multi-array averaging, adjustments for non-specific binding, Bioconductor GCRMA was used for data normalisation and summarisation of the probe intensity signals as described in the following referenced literature [280, 281]. RMA background correction and quantile normalisation across all chips was applied to the data as to ensure comparable mean, and standard deviation of probe intensities, Log2 transformation and median polish probe set summarisation was then undertaken.

2.4.5.2 Quality estimation of array data

The NUSE of each array was calculated in order to compare inter- and intra-array data variability as described in the referenced paper [282]. The upper limit for acceptable quality was a NUSE value of 1.05.

2.4.5.3 Data analysis

Principal Components Analysis applying a covariance dispersion matric was undertaken to map multidimensional data of each sample to three dimensions for clustering according to classification, and identification of outliers.

ANOVA including methods of moments estimation was applied to locate differential expression between normal bladder tissue, NMIBCs and MIBCs. Batch effects were accounted for within the model. When conducting ANOVA the

patient was designated as a factor, paired samples were taken into consideration. The t-test was applied to assess differences in gene expression between BCs of different grade and between samples. To adjust for multiple testing, genes were deliberated to be differentially expressed if a FDR adjusted p value of $p<0.05$ was attained. FDR was calculated as described here [283]. Genes selected for further analysis were those with a significant fold change in expression above 2-fold.

Unsupervised hierarchical agglomerative clustering (Euclidean distance with average linking clustering) was implemented to identify samples with similar expression profiles.

MetaCore version 6.7 (GenGo Unc, St. Joseph, MI, USA), IPA (Ingenuity systems, Redwood City, CA, USA) and DAVID Bioinformatics resource v6.7 were applied in the identification of canonical pathways and curated networks which had statistically significant levels of amplification of differentially expressed genes [284]. Unless otherwise stated, all pathways from metacore analysis in the results section are filtered with a FDR of <0.05. The association between disease progression and differential gene expression was analysed using univariate Cox proportional hazards regression analysis.

2.4.6 Meta-analysis

A meta-analysis was performed utilising publicly available gene expression data from NCBI Gene Expression Omnibus [285]. Out of 12 potential datasets, two datasets, which used the same microarray platform (Affymetrix Human Genome U133A array GSE3167, GSE5287), were used for further investigation, with a large sample number for further investigation. Raw CEL files from GSE3167 consisting of 60 samples, and from GSE5287 consisting of 30 samples, were imported into Partek Genomic Suite (Partek Inc.), data was processed and differential genes were identified following the same protocol applied to the in-

house microarray data [19, 286]. The authors kindly provided clinic-pathological data for each dataset. The GSE3167 data set consisted of NMIBC with surrounding *Cis* (n = 13), NMIBC without surrounding *Cis* (n = 15), MIBC (n = 13), *Cis* alone (n = 5) and normal bladder tissue (n = 14). The GSE2587 dataset consisted entirely of MIBC cases (n = 30).

Chapter Three – An *in vitro* investigation into brusatol as a potentiating adjunct to cisplatin based chemotherapy

3.1 Introduction 89

3.1.2 Chapter aims 90

3.2 Results 91

3.2.1 Evaluation of the sensitivity of a panel of 5 UCC cell lines to the cytotoxic effects cisplatin 91

3.2.2 Determination of the sensitivity of 5 UCC cell lines to the cytotoxic effects of brusatol 94

3.2.3 DMSO at a concentration of 1:1000 does not alter the sensitivity of UCC cell lines to cisplatin 96

3.2.4 Investigation into the effects of 2-hour pre-treatment with a range of concentrations of brusatol with respect to the sensitivity to cisplatin 98

3.2.5 Optimisation of brusatol concentration and pre-treatment time prior to cisplatin addition 105

3.2.6 Brusatol as an inhibitor of protein synthesis 118

3.3 Discussion 123

3.1 Introduction

The platinum containing anti-cancer drug, cisplatin, is the single most efficacious agent in the treatment of MIBC, although 90% of patients acquire resistance associated with disease progression and a very poor prognosis. In recent years, there has been an increased focus on NRF2 and its role in chemotherapy resistance in several cancers, including those of the bladder.

The Basic Leucine Zipper transcription factor, NRF2, is the chief mediator of the antioxidant response, and is responsible for cytoprotection and redox homeostasis in normally functioning cells. However, in many cancers increased levels of NRF2 are associated with chemoresistance and a more aggressive phenotype. The hypothesised mechanism of NRF2 mediated chemoresistance is through increased transactivation of NRF2 mediated genes, which include GSH, MDR1/2 and metallothionein, together it is believed that these proteins facilitate increased metabolism and efflux of chemotherapeutic agents, including cisplatin, lowering intracellular drug concentrations into a sub-toxic range, whilst still exerting considerable toxicities on the body. In this context, it may be therapeutically useful to inhibit NRF2 activity to potentiate the cytotoxic effects of cisplatin-based chemotherapy.

In this chapter brusatol, a quassinoid extracted from the South East Asian plant *Brucea Javancia,* which has shown to cause a marked reduction in NRF2 levels in several cell line models, is investigated with respect to its capacity to increase the sensitivity of BC cell lines to cisplatin. A panel of cell lines (Table 2.1.) originating from a range of stages and grades of bladder cancer, and a model of cisplatin resistant UCC were selected to test the hypothesis stated below.

3.1.2 Chapter aims

- To determine whether brusatol enhances the sensitivity of urothelial cell carcinoma cells to cisplatin.

- Define the response in terms of inhibition of NRF2 levels and downstream effects.

Hypothesis: Brusatol, via inhibition of NRF2 levels will increase the sensitivity of UCC cell lines to cisplatin.

3.2 Results

3.2.1 Evaluation of the sensitivity of a panel of 5 UCC cell lines to the cytotoxic effects cisplatin

A titre of 10 cisplatin concentrations ranging from 10nM to 1mM was employed to decipher its concentration-dependent cytotoxic effects on EJ, 253-J, MGH-U3, RT112 and RT112-CP cells (Fig 3.1). Cells were treated for 48 hours, with the cytotoxicity being determined using the MTT assay and displayed as a percentage of viable cells when normalised to the vehicle control. The mean IC50s range from 17.08μM for EJ cells to 136.7μM for cisplatin resistant RT112-CP, 5.9-fold higher than the 23.11μM IC50 observed in its parent cell line, RT12, significantly higher than all cisplatin sensitive cell lines (RT112 $p=0.0007$, EJ $p=0.0005$, 253-J $p=0.0006$, MGH-U3 $p=0.0006$). There was no significant difference between the IC50 values of all cisplatin-sensitive cell lines*, with the most and least sensitive cell lines being separated by only 6.03μM.

*Cisplatin-sensitive cell lines are defined as EJ, 253-J, MGH-U3 and RT112 cells. RT112-CP cells are considered cisplatin resistant.

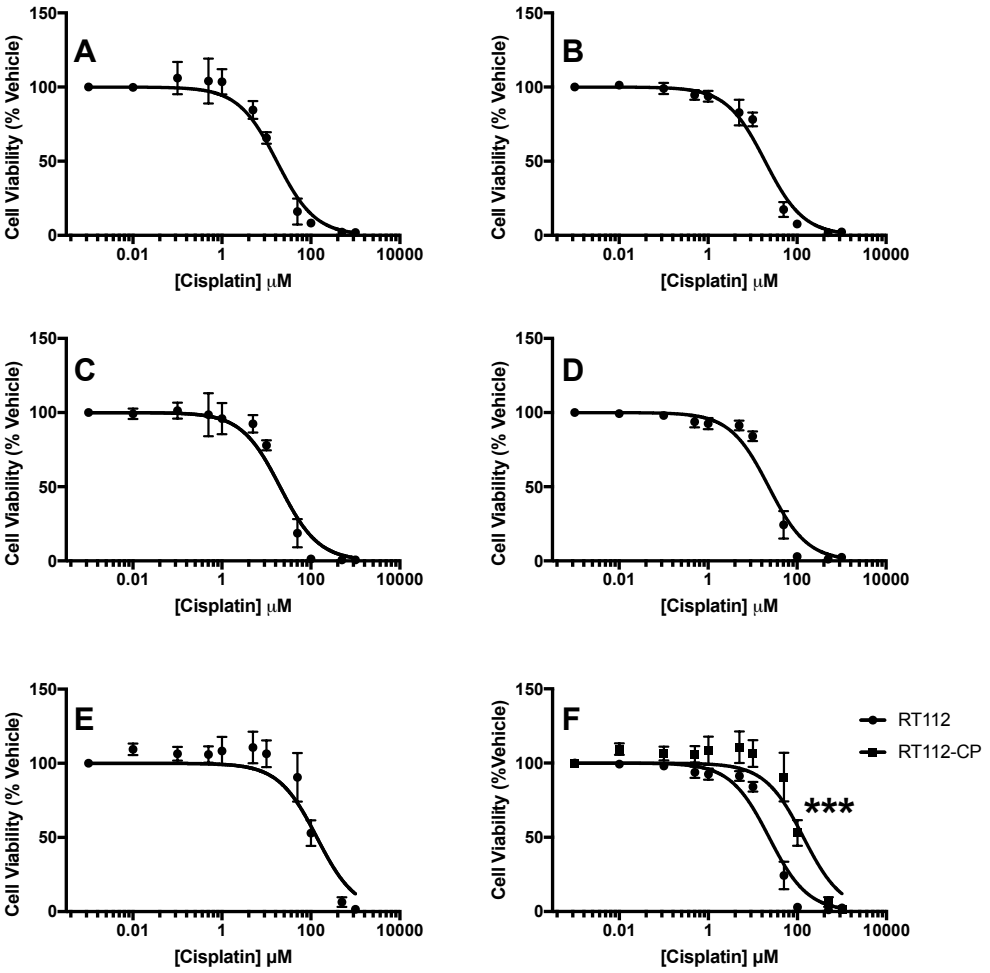

G

***

Cell Line	EJ	253-J	MGH-U3	RT112	RT112-CP
Mean IC50 (μM)	17.08 (±4.59)	19.15 (±7.23)	20.26 (±6.02)	23.11 (±5.92)	136.7 (±39.00)

Figure 3.1. Cisplatin exerts its cytotoxicity in a concentration dependent manner on 5 UCC cell lines. After 48-hours exposed to cisplatin, the cell viability was determined in EJ (A), 253-J (B), MGH-U3 (C), RT112 (D), RT112-CP (E), cells using the MTT assay. (F) A comparison of cisplatins cytotoxic effects on RT112 cells when compared to the cisplatin resistant RT112-CP sub-line. (G) Mean IC50 values + standard deviation (SD) (μM). All dose-response data was normalised to vehicle control, data shown is mean of three independent experiments + SD. The average IC50 values are plotted with SD. Statistical

analysis was performed using a one-way ANOVA (***p<0.001 vs EJ, 253-J, MGH-U3, and RT112 cells).

3.2.2 Determination of the sensitivity of 5 UCC cell lines to the cytotoxic effects of brusatol

To understand more about the effects of brusatol on UCC cell lines the effect of brusatol on UCC cell viability was investigated on the same panel of 5 cell lines (Fig 3.2). Here the UCC cell lines were cultured for 48 hours in a titre of brusatol concentrations ranging from 10pM to 1μM, before the MTT assay was employed to determine the effect on cell viability as a percentage of the mean. IC50 values range from 78.11nM in 253-J cells, to 282nM ($p=0.0324$) in the slowest dividing cell line in the panel, MGH-U3.

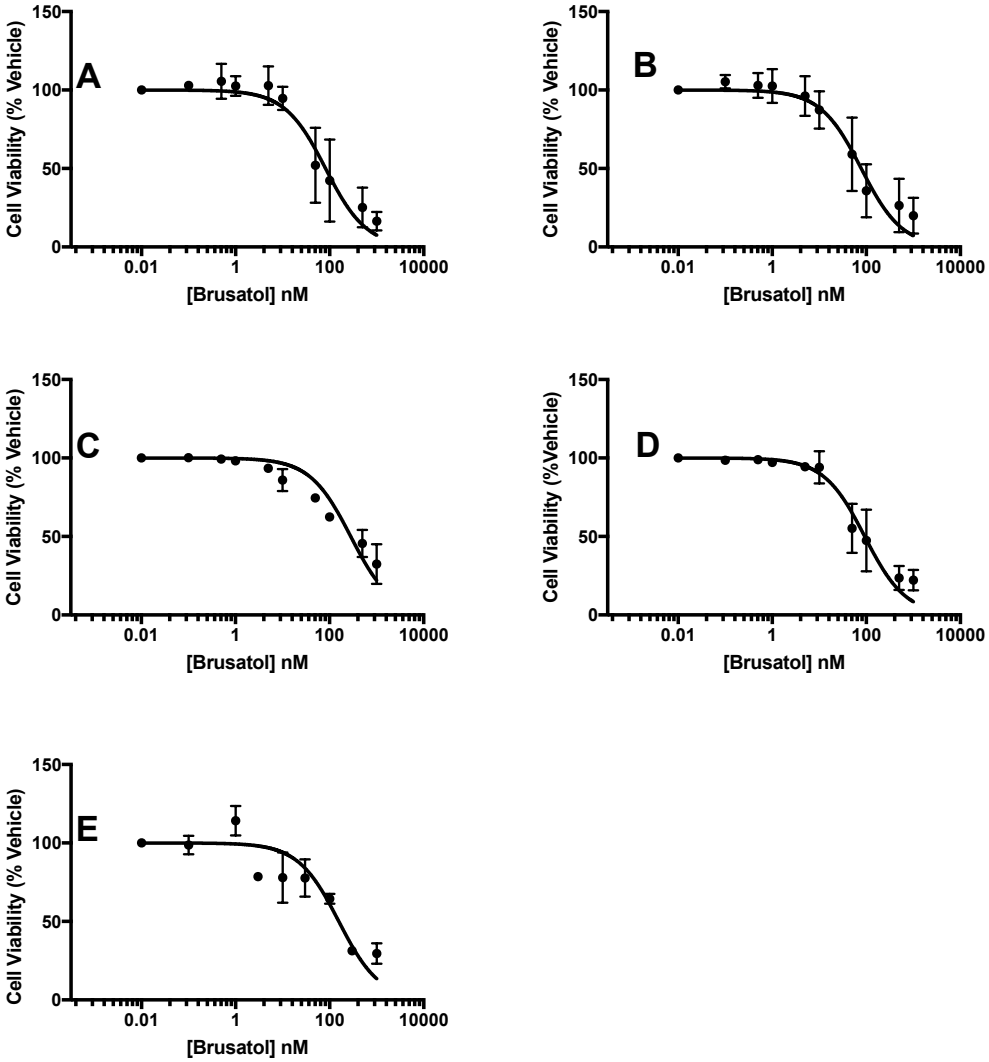

F

Cell Line	EJ	253-J	MGH-U3	RT112	RT112-CP
Mean IC50 (nM)	82 (±27.89)	78.21 (±26.62)	282.6 (±78.8)	92.69 (±25.46)	156.6 (±58.5)

Figure 3.2. Brusatol exerts concentration-dependent cytotoxic effects in UCC cells. 5 UCC cell lines (A) EJ, (B) 253-J, (C) MGH-U3, (D) RT112, (E) RT112-CP) were treated with a range of concentrations of brusatol from 1pM to 1μM for 48-hours. The effect on cell viability was determined using the MTT assay, with all dose response data being represented as a percentage of the vehicle control, and is mean of three independent experiments + SD. (F) Average IC50 values (with SD).

3.2.3 DMSO at a concentration of 1:1000 does not alter the sensitivity of UCC cell lines to cisplatin

It has been reported that DMSO binds with cisplatin in a manner that severely attenuates its efficacy as a cytotoxic agent [287]. However, brusatol used in this investigation was only available in solution with DMSO, so the effect of the maximum concentration of DMSO (1:1000) was assessed in terms of its effect on cisplatin toxicity. In all UCC cell lines tested there was no negative effect, in terms of attenuated cytotoxicity, of adding 1:1000 DMSO to cisplatin dose response experiments (Fig 3.3).

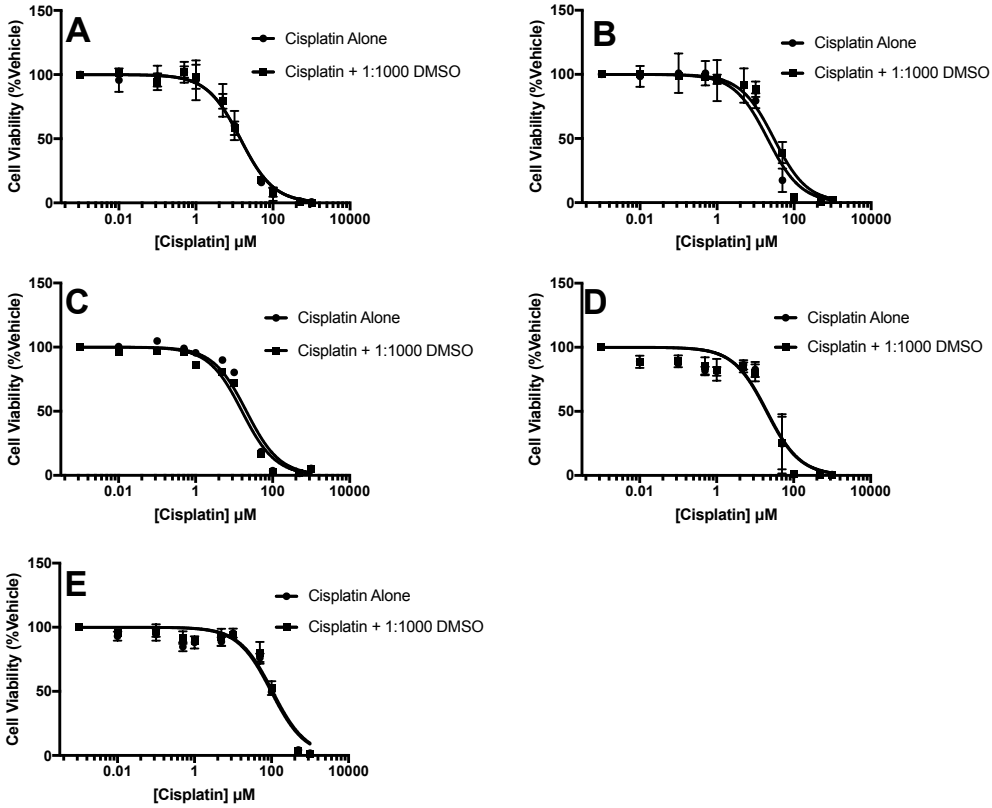

F

Cell Line	EJ	253-J	MGH-U3	RT112	RT112-CP
Cisplatin Alone (µM)	14.31 (±3.77)	20.47 (±7.1)	20.89 (±7.18)	24.41 (±8.89)	97.44 (±21.95)
Cisplatin + DMSO (µM)	14.21 (±2.42)	29.94 (±7.5)	16.03 (±5.73)	19.66 (±7.88)	106.7 (±28.5)

Figure 3.3. The comparative cytotoxicity of cisplatin alone and cisplatin in combination with 1:1000 DMSO. After 48-hours exposed to cisplatin, the cell viability was determined in (A) EJ, (B) 253-J, (C) MGH-U3, (D) RT112, (E) RT112-CP cells using the MTT assay. (F) Mean IC50 values (µM). All dose-response data was normalised to vehicle control, data shown is mean of three independent experiments. The average IC50 values are plotted with SD.

3.2.4 Investigation into the effects of 2-hour pre-treatment with a range of concentrations of brusatol with respect to the sensitivity to cisplatin

To determine whether brusatol increases the sensitivity of urothelial cell carcinoma cell lines to cisplatin, the full panel of 5 cell lines were employed to allow for a pathologically diverse cross-section of BC disease grades and stages. Based on prior observations a 2-hour brusatol pre-treatment time was selected as it has been noted in the literature that maximum depletion of NRF2 protein expression occurs at this time-point [172]. There are reports of brusatol concentrations as low as 40nM and as high as 300nM inhibiting NRF2, thus a range of concentrations of brusatol were selected from 5nM, which over 48 hours exhibits negligible toxicity on UCC cell lines, up-to a concentration of 400nM where marked toxicity was observed. After the 2-hour pre-treatment with brusatol, a titre of cisplatin was added to the plate from 1nM to 1mM. The MTT assay was use for read out, and each treatment was normalised to a vehicle control. Statistical analysis was performed using a one-way ANOVA.

In EJ cells (Fig 3.4), the addition of brusatol to cisplatin allowed for a significant increase in sensitivity to cisplatin at the 400nM brusatol concentration point ($p=0.0125$).

The response to 2-hour brusatol pre-treatment in 253-J cells (Fig 3.5) was similar to that in EJ cells. Here a small shift to the left was observed with the addition of 200nM and a significant change in the IC50 is observed at 400nM ($p=0.0494$).

2-hour pre-treatment with 5-400nM brusatol does not significantly increase the sensitivity of MGH-U3 cell lines to the cytotoxic effects of cisplatin (Fig 3.6).

In the NMIBC cell line, RT112 (Fig 3.7), a significant decrease in the IC50 was observed when compared to cisplatin plus vehicle at brusatol concentrations greater than 100nM (100nM $p=0.0003$, 200nM $p=0.0118$, 400nM $p=0.0111$).

Interestingly, in the cisplatin resistant RT112-CP cell line (Fig 3.8), an increase in sensitivity to cisplatin was noted to be significant at concentrations above 200nM of brusatol (200nM 0.0326, 400nM 0.0373). Although a non-significant shift to the left was evident at 100nM of brusatol.

The most profound effects were displayed in the NMIBC cell lines RT112 and RT112-CP, where cisplatin is unlikely to be used as a treatment option in the clinic, these data show that co-treatment of brusatol and cisplatin may be a more effective option than cisplatin alone.

I hypothesise that whilst NRF2 may be inhibited at 2-hours, this does not leave enough time for the downstream consequences of NRF2 inhibition to be realised. Hence the next step should be to optimise a time-point where NRF2 regulated proteins are downregulated due to brusatol mediated NRF2 inhibition. Once optimised, cells will be treated with cisplatin when defence proteins regulated by NRF2 are at their lowest levels, hypothetically allowing for enhanced cisplatin cytotoxicity.

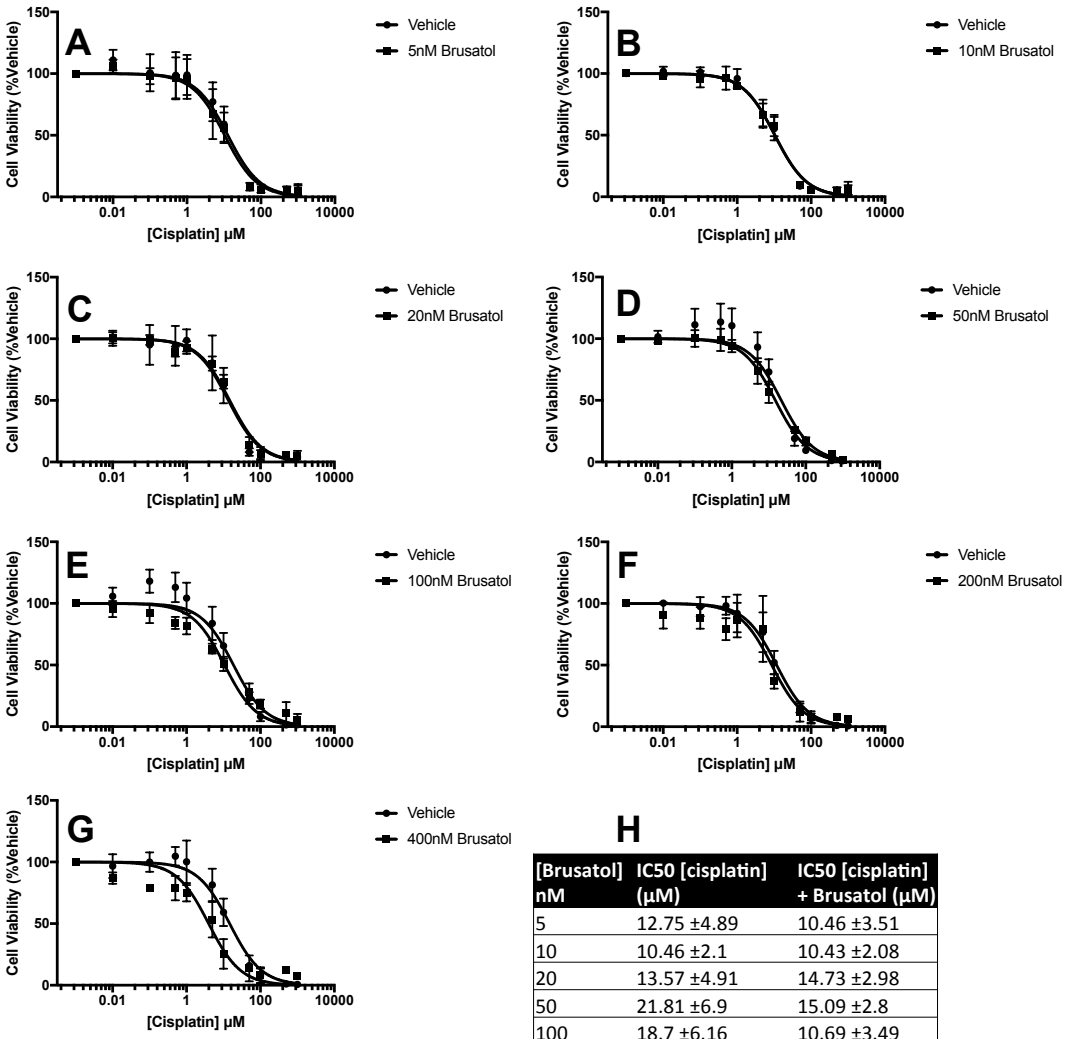

H

[Brusatol] nM	IC50 [cisplatin] (µM)	IC50 [cisplatin] + Brusatol (µM)
5	12.75 ±4.89	10.46 ±3.51
10	10.46 ±2.1	10.43 ±2.08
20	13.57 ±4.91	14.73 ±2.98
50	21.81 ±6.9	15.09 ±2.8
100	18.7 ±6.16	10.69 ±3.49
200	11.71 ±2.28	8.648 ±3.47
400	14.71 ±3.74	3.975 ±1.56 *

Figure 3.4. Pre-treatment with 400nM brusatol for 2 hours significantly increases the sensitivity of EJ cells to the cytotoxic effects of cisplatin. EJ cells were cultured either with vehicle or brusatol at 5nM (A), 10nM (B), 20nM (C), 50nM (D), 100nM (E), 200nM (F) and 400nM (G) for 2-hours prior to a 48-hour exposure to a titre of cisplatin concentrations ranging from 10nM to 1mM. The cell viability was then determined using the MTT assay and data was normalised to control (brusatol plus cisplatin: vehicle and brusatol; vehicle plus cisplatin: vehicle only). (H) A comparison of cisplatin IC50 values in combination with cisplatin or vehicle. Data shown is mean of three independent experiments. The average IC50 values are plotted with SD. Statistical analysis was performed using a one-way ANOVA (*p=0.05).

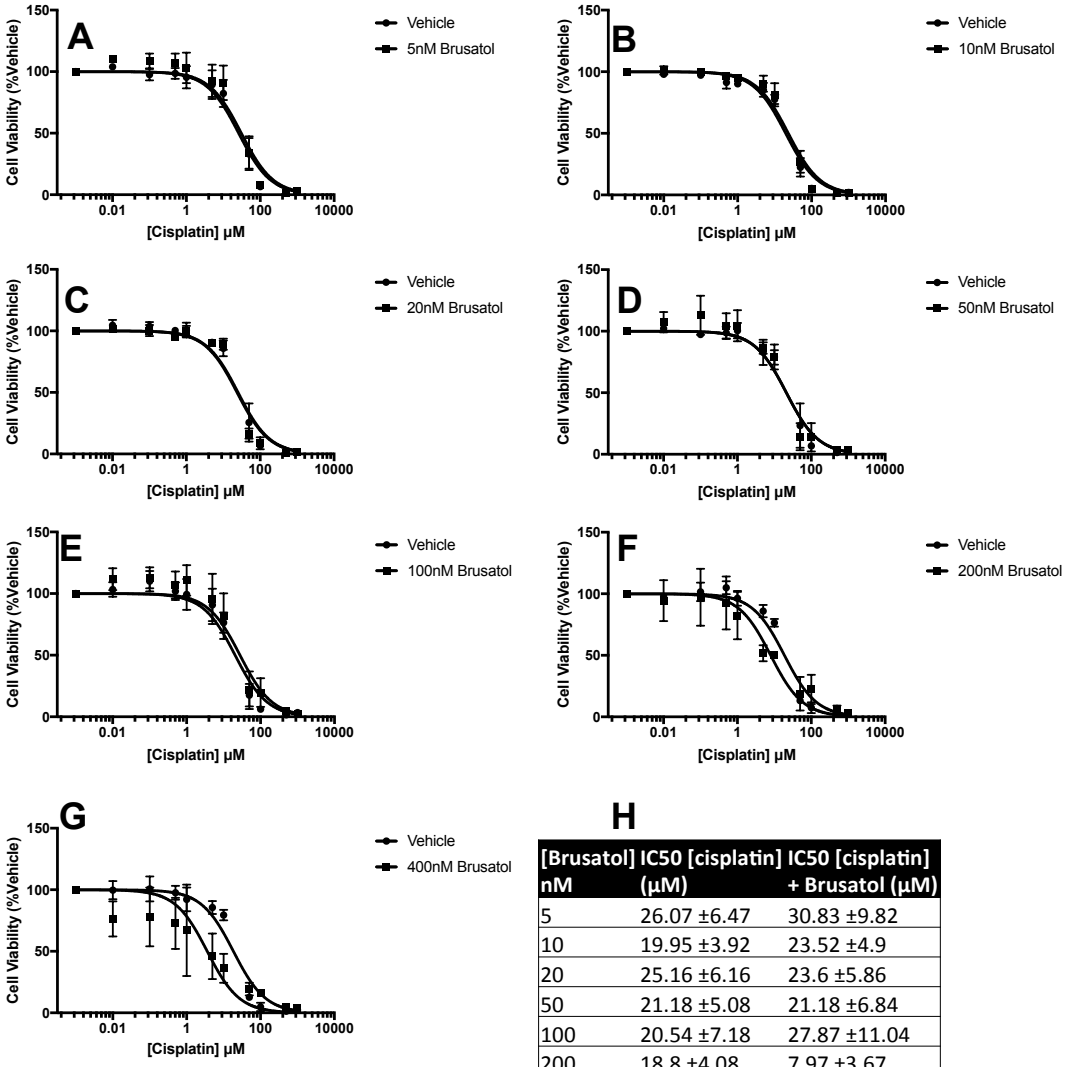

H

[Brusatol] nM	IC50 [cisplatin] (µM)	IC50 [cisplatin] + Brusatol (µM)
5	26.07 ±6.47	30.83 ±9.82
10	19.95 ±3.92	23.52 ±4.9
20	25.16 ±6.16	23.6 ±5.86
50	21.18 ±5.08	21.18 ±6.84
100	20.54 ±7.18	27.87 ±11.04
200	18.8 ±4.08	7.97 ±3.67
400	18.5 ±4.57	3.62 ±2.82 *

Figure 3.5. Pre-treatment with 400nM brusatol for 2 hours significantly increases the sensitivity of 253-J cells to the cytotoxic effects of cisplatin. 253-J cells were cultured either with vehicle or brusatol at 5nM (A), 10nM (B), 20nM (C), 50nM (D), 100nM (E), 200nM (F) and 400nM (G) for 2-hours prior to a 48-hour exposure to a titre of cisplatin concentrations ranging from 10nM to 1mM. The cell viability was then determined using the MTT assay and data was normalised to control (brusatol plus cisplatin: vehicle and brusatol; vehicle plus cisplatin: vehicle only). (H) A comparison of cisplatin IC50 values in combination with cisplatin or vehicle. Data shown is mean of three independent experiments. Statistical analysis was performed using a one-way ANOVA. The average IC50 values are plotted with SD. (*p=0.05).

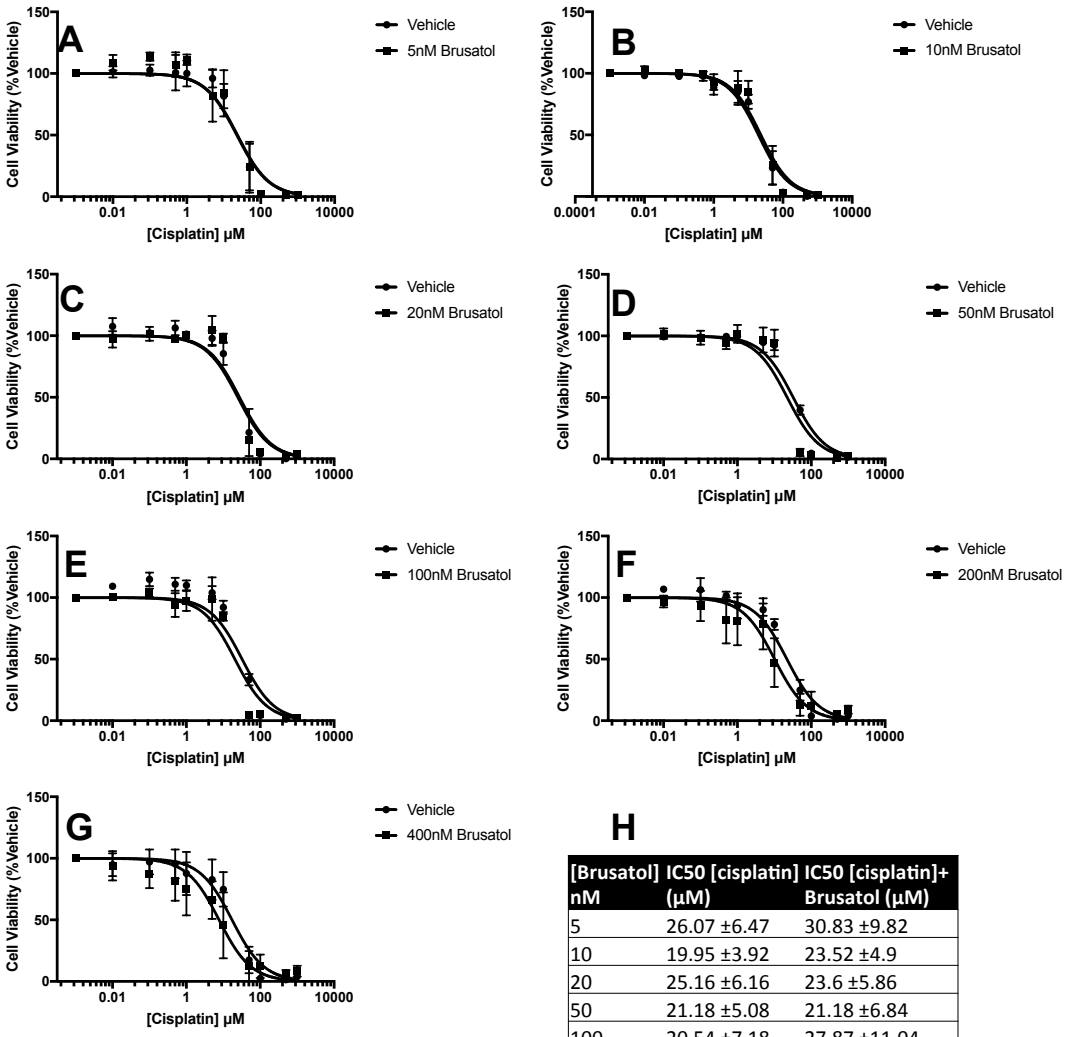

H

[Brusatol] nM	IC50 [cisplatin] (µM)	IC50 [cisplatin]+ Brusatol (µM)
5	26.07 ±6.47	30.83 ±9.82
10	19.95 ±3.92	23.52 ±4.9
20	25.16 ±6.16	23.6 ±5.86
50	21.18 ±5.08	21.18 ±6.84
100	20.54 ±7.18	27.87 ±11.04
200	18.8 ±4.08	7.97 ±3.67
400	18.5 ±4.57	3.62 ±2.82

Figure 3.6. Pre-treatment with brusatol for 2 hours does not significantly increases the sensitivity of MGH-U3 cells to the cytotoxic effects of cisplatin. MGH-U3 cells were cultured either with vehicle or brusatol at 5nM (A), 10nM (B), 20nM (C), 50nM (D), 100nM (E), 200nM (F) and 400nM (G) for 2-hours prior to a 48-hour exposure to a titre of cisplatin concentrations ranging from 10nM to 1mM. The cell viability was then determined using the MTT assay and data was normalised to control (brusatol plus cisplatin: vehicle and brusatol; vehicle plus cisplatin: vehicle only). (H) A comparison of cisplatin IC50 values in combination with cisplatin or vehicle. Data shown is mean of three independent experiments. Statistical analysis was performed using a one-way ANOVA. The average IC50 values are plotted with SD.

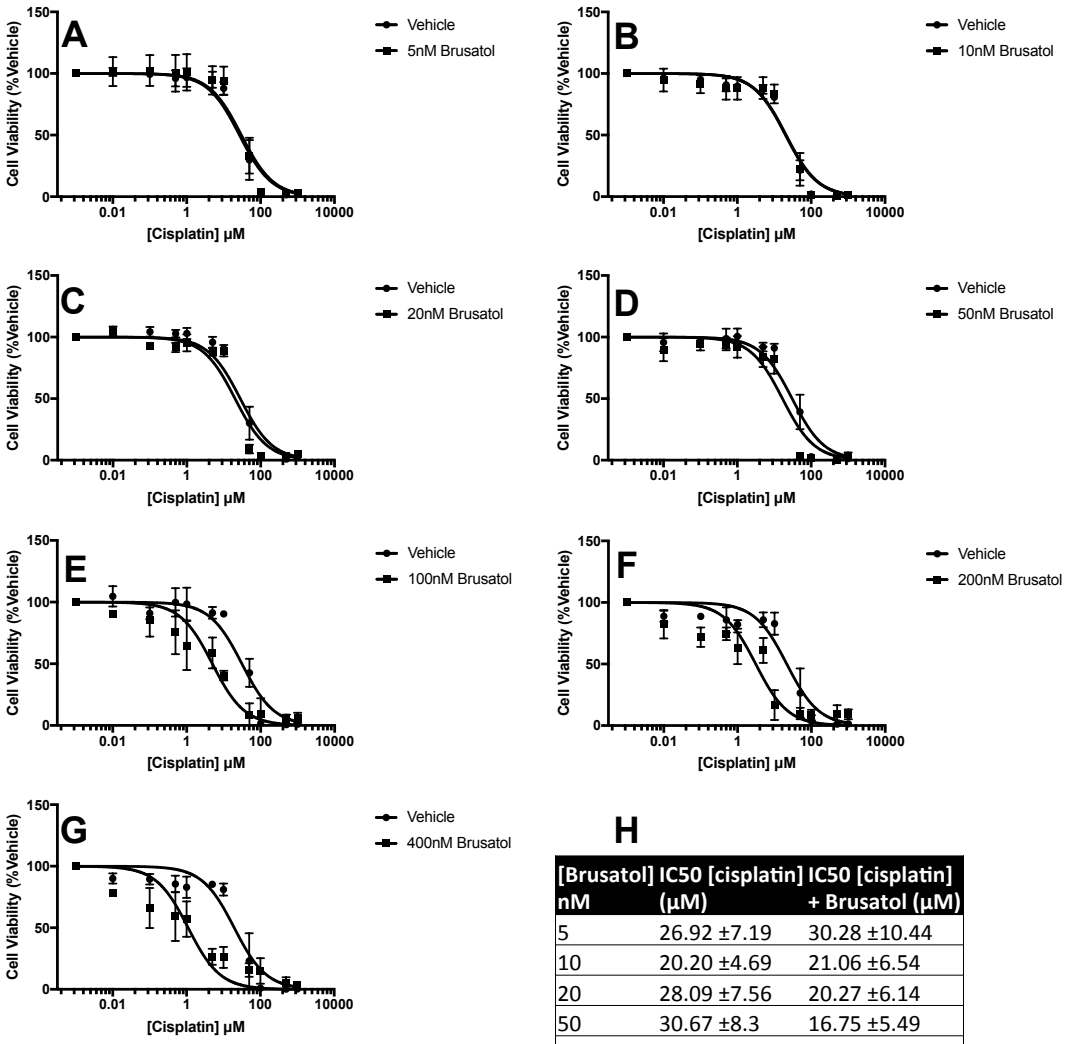

H

[Brusatol] nM	IC50 [cisplatin] (µM)	IC50 [cisplatin] + Brusatol (µM)	
5	26.92 ±7.19	30.28 ±10.44	
10	20.20 ±4.69	21.06 ±6.54	
20	28.09 ±7.56	20.27 ±6.14	
50	30.67 ±8.3	16.75 ±5.49	
100	31.21 ±9.45	4.95 ±2.44	***
200	21.56 ±7.48	3.11 ±1.82	*
400	19.64 ±6.77	1.11 ±0.73	*

Figure 3.7. Pre-treatment with concentrations at 100nM and greater of brusatol for 2 hours significantly increases the sensitivity of RT112 cells to the cytotoxic effects of cisplatin. RT112 cells were cultured either with vehicle or brusatol at 5nM (A), 10nM (B), 20nM (C), 50nM (D), 100nM (E), 200nM (F) and 400nM (G) for 2-hours prior to a 48-hour exposure to a titre of cisplatin concentrations ranging from 10nM to 1mM. The cell viability was then determined using the MTT assay and data was normalised to control (brusatol plus cisplatin: vehicle and brusatol; vehicle plus cisplatin: vehicle only). (H) A comparison of cisplatin IC50 values in combination with cisplatin or vehicle, Data shown is mean of three independent experiments. Statistical analysis was performed by one-way ANOVA (***p=<0.001, *p=0.05).

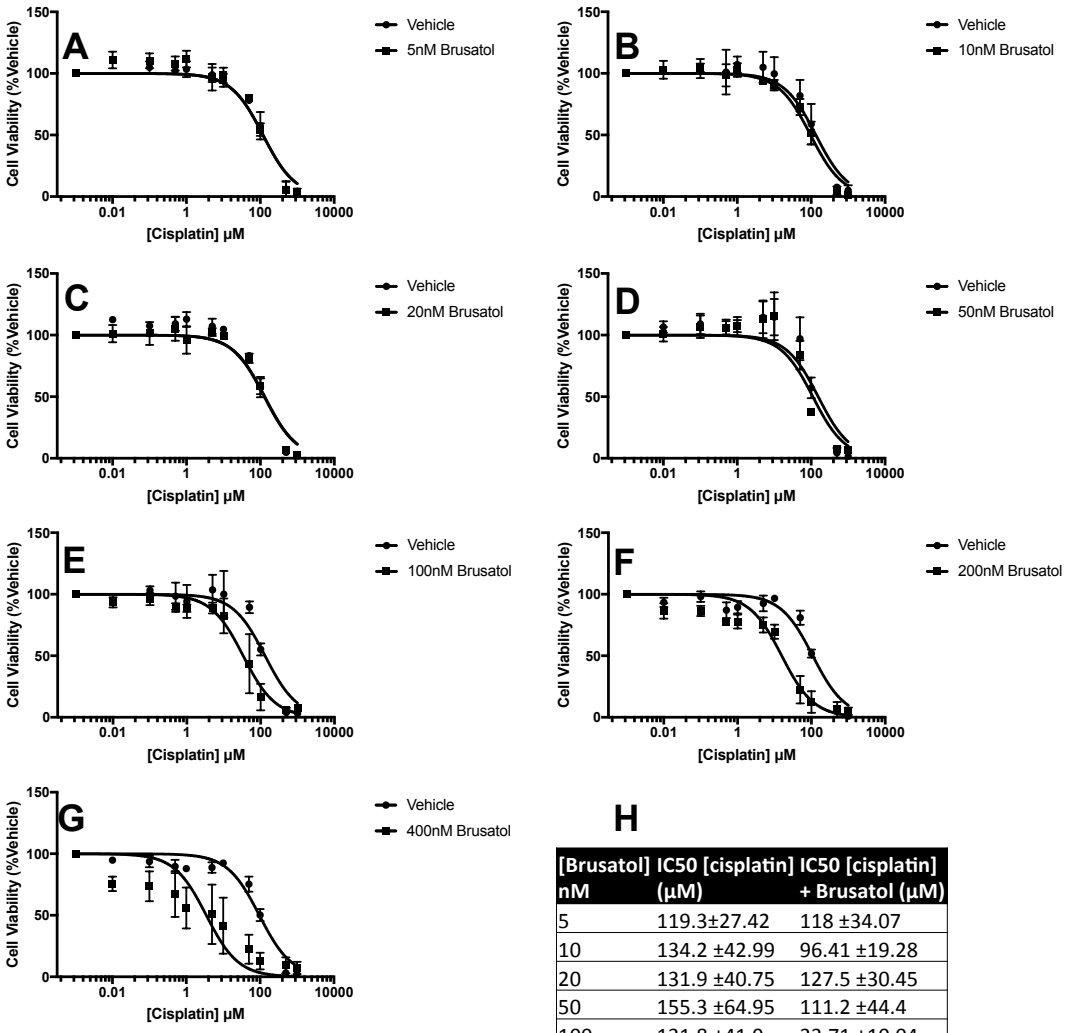

H

[Brusatol] nM	IC50 [cisplatin] (µM)	IC50 [cisplatin] + Brusatol (µM)
5	119.3±27.42	118 ±34.07
10	134.2 ±42.99	96.41 ±19.28
20	131.9 ±40.75	127.5 ±30.45
50	155.3 ±64.95	111.2 ±44.4
100	131.8 ±41.9	33.71 ±10.04
200	109.1 ±21.87	15.76 ±5.91 *
400	95.83 ±22.91	3.50 ±3.39 *

Figure 3.8. Pre-treatment with concentrations at 200nM of brusatol and higher for 2 hours significantly increases the sensitivity of RT112-CP cells to the cytotoxic effects of cisplatin. RT112-CP cells were cultured either with vehicle or brusatol at 5nM (A), 10nM (B), 20nM (C), 50nM (D), 100nM (E), 200nM (F) and 400nM (G) for 2-hours prior to a 48-hour exposure to a titre of cisplatin concentrations ranging from 10nM to 1mM. The cell viability was then determined using the MTT assay and data was normalised to control (brusatol plus cisplatin: vehicle and brusatol; vehicle plus cisplatin: vehicle only). (H) A comparison of cisplatin IC50 values in combination with cisplatin or vehicle. Data shown is mean of three independent experiments. Statistical analysis was performed by one-way ANOVA (*p=0.05).

3.2.5 Optimisation of brusatol concentration and pre-treatment time prior to cisplatin addition

3.2.5.1 Optimisation of NRF2 *antibodies for western blot*

In order to optimise a time-point where NRF2 regulated proteins are at their lowest levels post-brusatol exposure, three antibodies against NRF2 were tested (Fig 3.9): ProteinTech 16396-1-AP (PT); Santa Cruz H300 (H300); MBL life sciences M200 (M200). An antibody raised against HO-1, a protein regulated by NRF2, was tested [288]. HO-1 is documented as being sensitive to changes in NRF2 levels, however it is reported as highly overexpressed in some BCs therefore there was benefit in checking its status within this cell line panel [135, 289-291]. The cell line panel consists of two MIBC cell lines (EJ, 253-J) and two NMIBC cell lines (MGH-U3 and RT112), under basal conditions and treated for 2-hours with CDDO-Me, a pharmacological inducer of NRF2 accumulation. Upon comparison of PT, H300, and M200 anti-NRF2 antibodies, PT was found to detect NRF2 the most reliably, with no non-specific binding at 75KDa as noted with H300 and M200, therefore PT will be used henceforth for NRF2 Immunoblotting. The cell lines originating from MIBC were shown to have marked differential expression of HO-1 when compared to NMIBC cell lines furthermore, no change in HO-1 levels was observed following stimulation with CDDO-Me, making HO-1 a poor choice as a downstream marker of NRF2 activity in this panel of cell lines. Therefore another protein regulated by NRF2, NQO1, was tested as a documented sensitive marker of NRF2 activity [292].

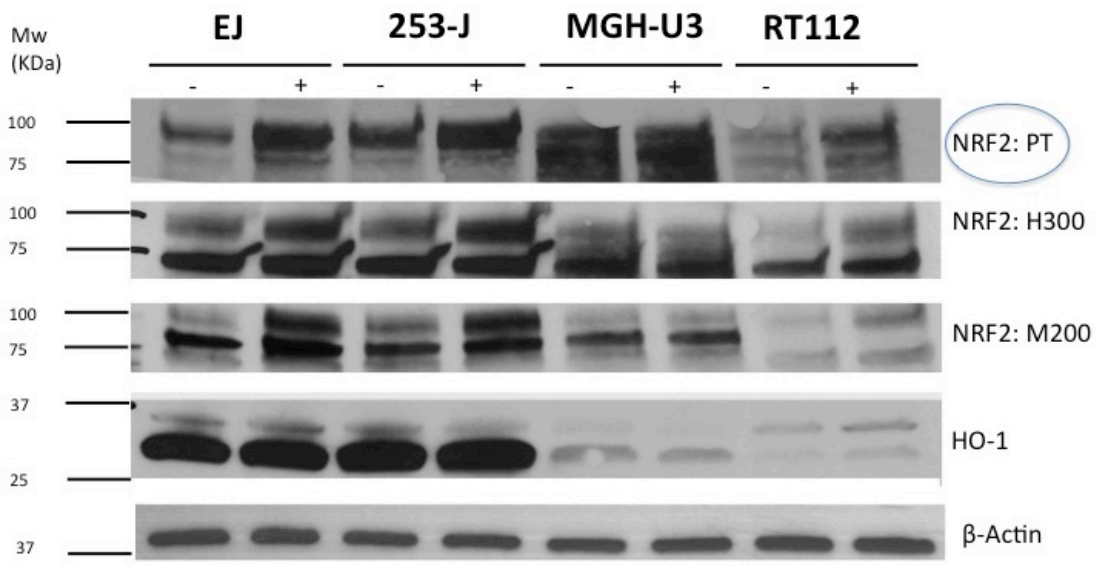

Figure 3.9. Comparison of NRF2 targeting antibodies, and evaluation of HO-1 as a downstream marker of NRF2 activity by western blot. PT: ProteinTech anti-NRF2 rabbit polyclonal 16396-1-AP, H300: Santa Cruz anti-NRF2 rabbit polyclonal sc-13032, M200: MBL life science anti-NRF2 mouse monoclonal. - Basal, + 2-hour treatment with 100nM CDDO-Me. Data is representative of three independent experiments.

3.2.5.2 Determination of basal **NRF2, KEAP1** *and* **NQO1** *levels in the 5 UCC cell line panel*

The relative basal expression of NRF2, its regulating partner KEAP1 and downstream protein NQO1 were determined by western blot (Fig 3.10). There was no significant difference in NRF2 levels between MIBC and NMIBC cell lines. However, upon comparison of the cisplatin naïve RT112 cell line and the cisplatin resistant RT112-CP cell line the later expressed NRF2 at a significantly greater level ($p=<0.0001$).

Interestingly there was an inversely proportional relationship between the expression of NRF2 in RT112 and RT112-CP cell lines and KEAP1 levels ($<p=0.01$). The low levels of KEAP1 in RT112-CP cells may explain the elevated levels of NRF2, potentially due to epigenetic silencing of KEAP1 [293].

NQO1 levels correlated well with NRF2 levels across the cell line panel. A marked difference in NQO1 levels was observed between RT112 and RT112-CP cells ($p=<0.0001$). Based on these findings NQO1 was used as a marker of NRF2 activity henceforth.

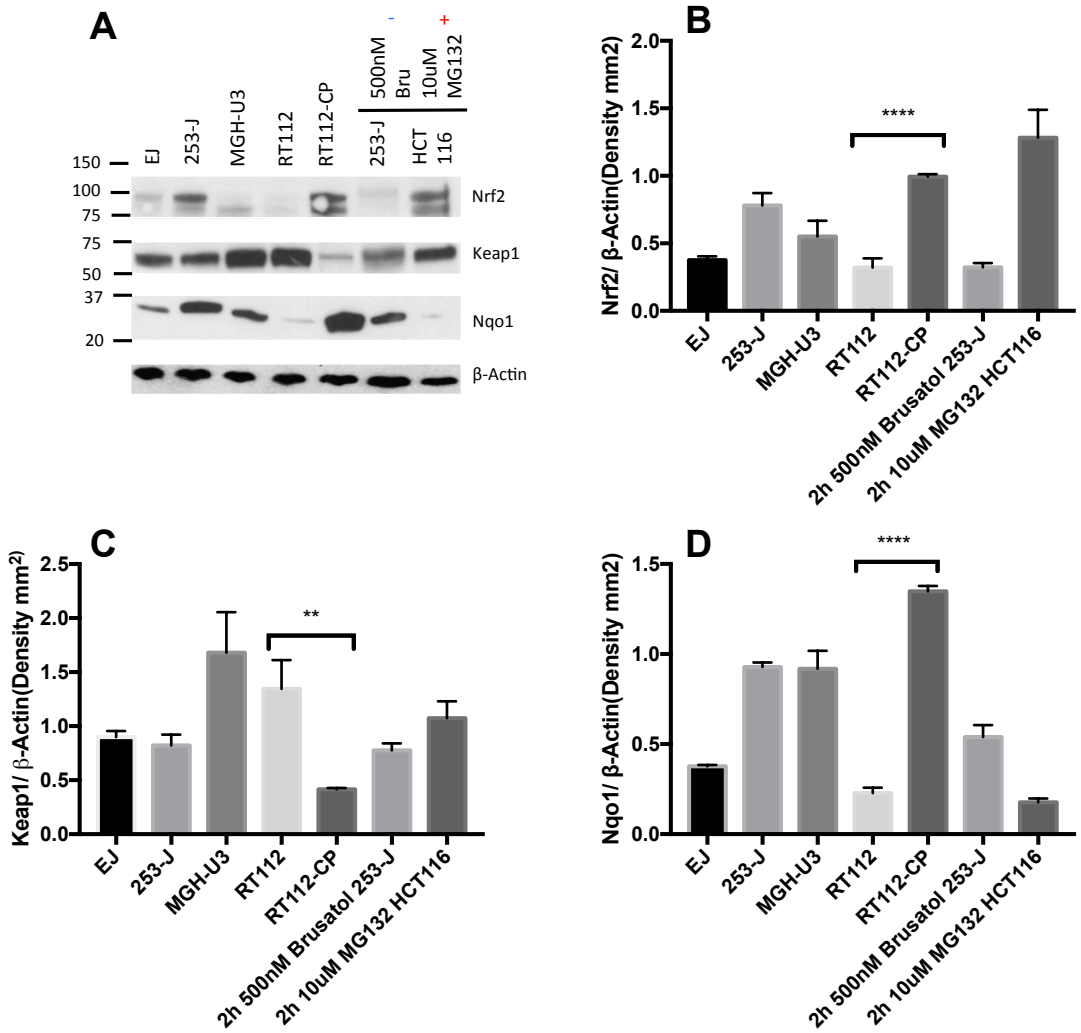

Figure 3.10. Differential levels of NRF2, KEAP1 and NQO1 in EJ, 253-J, MGH-U3, RT112 and RT112-CP cells. (A) Western blots for probing for NRF2, KEAP1, NQO1 and β-actin. Mean NRF2 (B), KEAP1 (C) and NQO1(D) expression. A is representative of three independent experiments, whilst B, C, D are mean of three independent experiments. Mean NRF2, NQO1 and KEAP1 expression was plotted after normalisation with actin + SD. One-way ANOVA was used to compare the statistical significance between the expression of NRF2, NQO1 and KEAP1 in RT112 compared to RT112-CP cells (**<p=0.01 **** p=<0.0001). 253-J cells treated for 2-hours with 500nM brusatol were used as a negative control of NRF2 expression, where as HCT116 cells treated with 10μM of the proteasome inhibitor MG132 were used as a positive control for NRF2 expression.

3.2.5.3 Investigation into the concentration-dependent effects of brusatol on **NRF2** *levels in the 5 UCC cell line panel*

Next the effect of increasing concentrations of brusatol on NRF2 levels was evaluated in the 5 UCC cell lines (Fig 3.11). Cells were treated for 2 hours with a titre of concentrations ranging from 5 to 1000nM, each normalised to a vehicle control.

When compared to the vehicle control, EJ cells (A, B) displayed a significant reduction in NRF2 levels at concentrations greater than 10nM of brusatol, with a 30% decrease in relative NRF2 levels being observed ($p=0.045$), with NRF2 levels decreasing further to 30% at 50nM ($p=<0.0001$). The 253-J cell line (C, D) followed a similar trend to EJ cells, however 253-J cells were less sensitive to brusatol, with 59% relative NRF2 levels being observed at 50nM ($p=0.0084$). MGH-U3 cells (E, F) exhibited a marked reduction in NRF2 levels at concentrations 50nM and greater, where a 77% decrease in the relative expression of NRF2 was noted ($p=0.0001$). Although NRF2 levels vary greatly between RT112 and RT112-CP cell lines, they respond in a similar concentration-dependent manner to each other, with the two cell lines displaying a highly significant ($p=<0.0001$) decrease in NRF2 levels at concentrations of 50nM and greater, where 14% and 7% relative expression was noted in RT112 and RT112-CP cells respectively.

Based on these data where all UCC cell lines show similar sensitivity to the inhibitory effects of brusatol on NRF2 levels, the similar cytotoxic effects of cisplatin (excepting the cisplatin resistant RT112-CP cell line) and the availability of a model of cisplatin resistance with high NRF2 levels and downstream proteins levels, RT112 and RT112-CP cell lines will be used for further investigation into the potential chemo-potentiating benefit of brusatol. This is despite the cell lines originating from NMIBC, rather than MIBC, where cisplatin is a common treatment option.

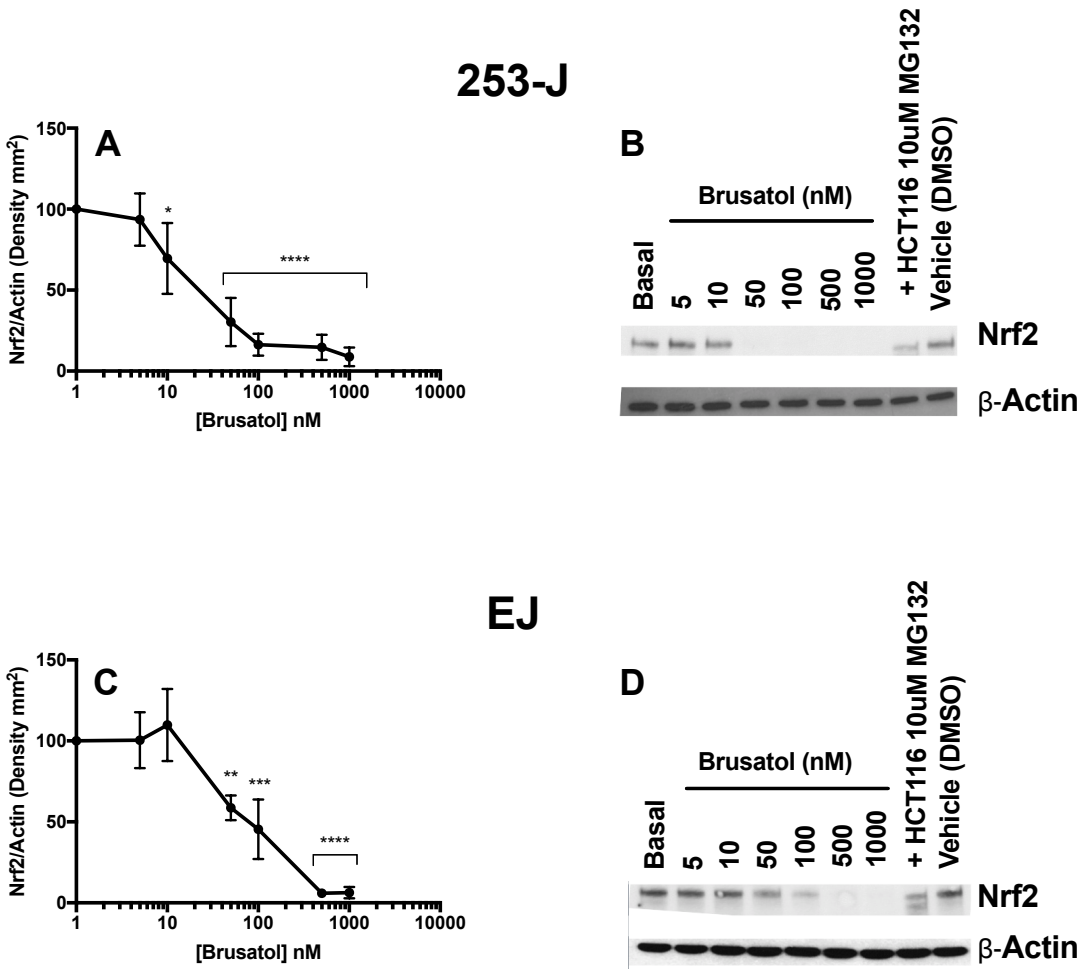
253-J
A
Nrf2/Actin (Density mm²)
150
100
50
0
1
10
100
1000
10000
[Brusatol] nM
*
****
B
Brusatol (nM)
Basal
5
10
50
100
500
1000
+ HCT116 10uM MG132
Vehicle (DMSO)
Nrf2
β-Actin
EJ
C
Nrf2/Actin (Density mm²)
[Brusatol] nM
**
***
****
D
Brusatol (nM)
Basal
5
10
50
100
500
1000
+ HCT116 10uM MG132
Vehicle (DMSO)
Nrf2
β-Actin
MGH-U3
E
Nrf2/Actin (Density mm²)
[Brusatol] nM
****
F
Brusatol (nM)
Basal
5
10
50
100
500
1000
+ HCT116 10uM MG132
Vehicle (DMSO)
Nrf2
β-Actin

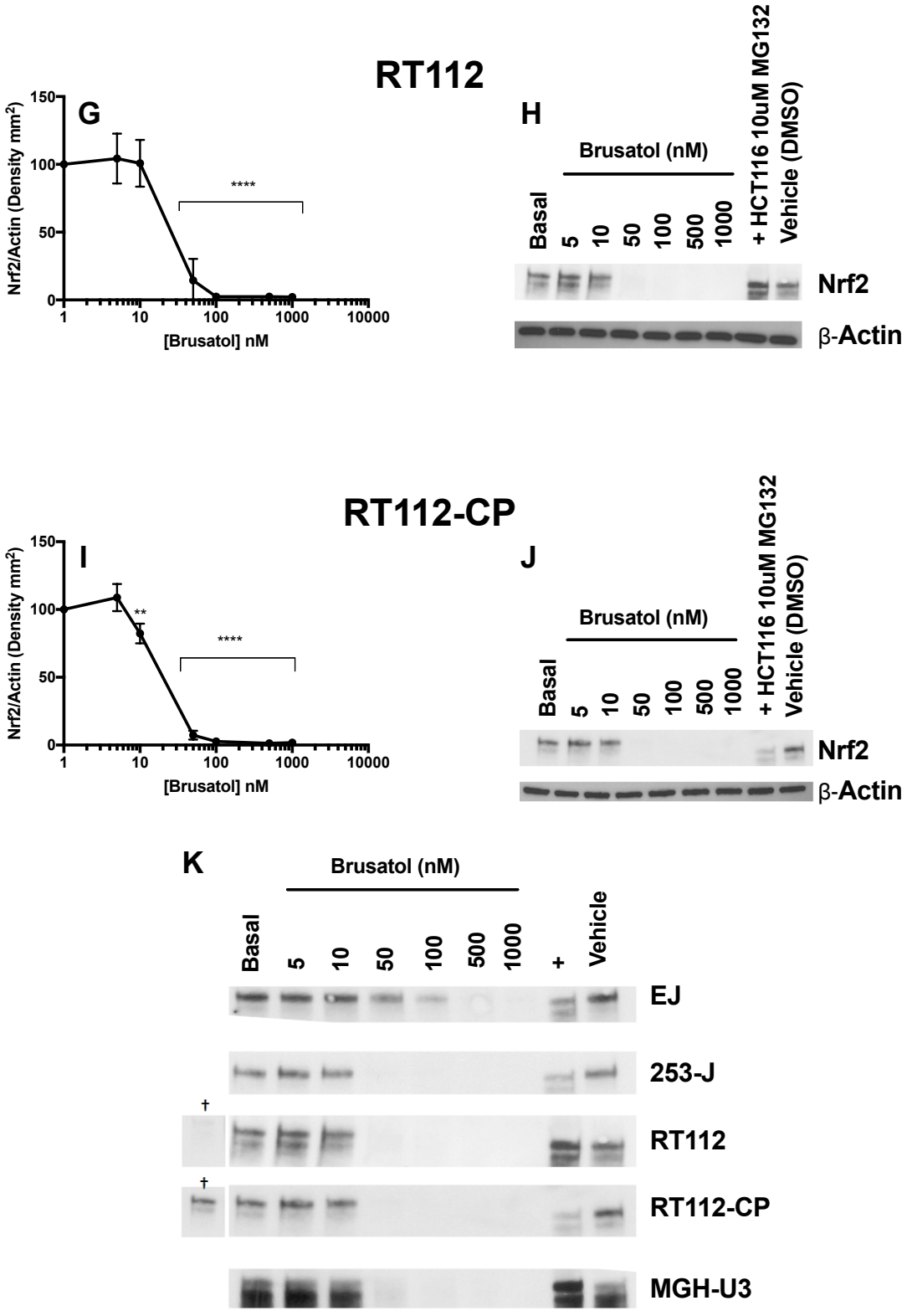

Figure 3.11. Brusatol exposure reduces NRF2 levels in UCC cell lines in a concentration dependent manner. 253-J (A, B), EJ (C, D), MGH-U3 (E, F), RT112 (G, H) and RT112-CP (I, J) cell lines were treated for 2-hours with a

titration of brusatol concentrations ranging from 5nM to 1μM, before being lysed and analysed via western blot. Dose-response data was expressed as a percentage of vehicle. Data shown in B, D, F, H, J, and K is representative of three independent experiments, whilst data shown in A, C, E, G and I is mean of three independent experiments, plotted with SD. HCT116 cells treated with 10μM of MG132 were used as a positive control of NRF2 expression. Statistical analysis was performed by one-way ANOVA (****p=<0.0001, *** p=<0.001, **p=<0.01, *p=<0.05).

3.2.5.4 Investigation into the time-dependent effects of brusatol on **NRF2** *and* **NQO1** *levels in RT112 and RT112-CP cells*

Theoretically, for cells to be maximally sensitive to cisplatin its defence proteins must be at their lowest possible levels. Here the effect of 50nM brusatol was assessed over a 48-hour time-course, where its effect on NRF2 and NQO1 levels was investigated (Fig 3.12). A significant decrease in NRF2 levels was observed at the 2-hour time point in both RT112 and RT112-CP cell lines ($p=<0.0001$). Although a slight decrease in NQO1 levels was observed at 12 hours this change was not significant (RT122 $p=0.49$, RT112-CP $p=0.57$). The lack of a significant change in NQO1 levels cast doubt over the sensitivity of NQO1 as a marker of NRF2 activity in these cell lines.

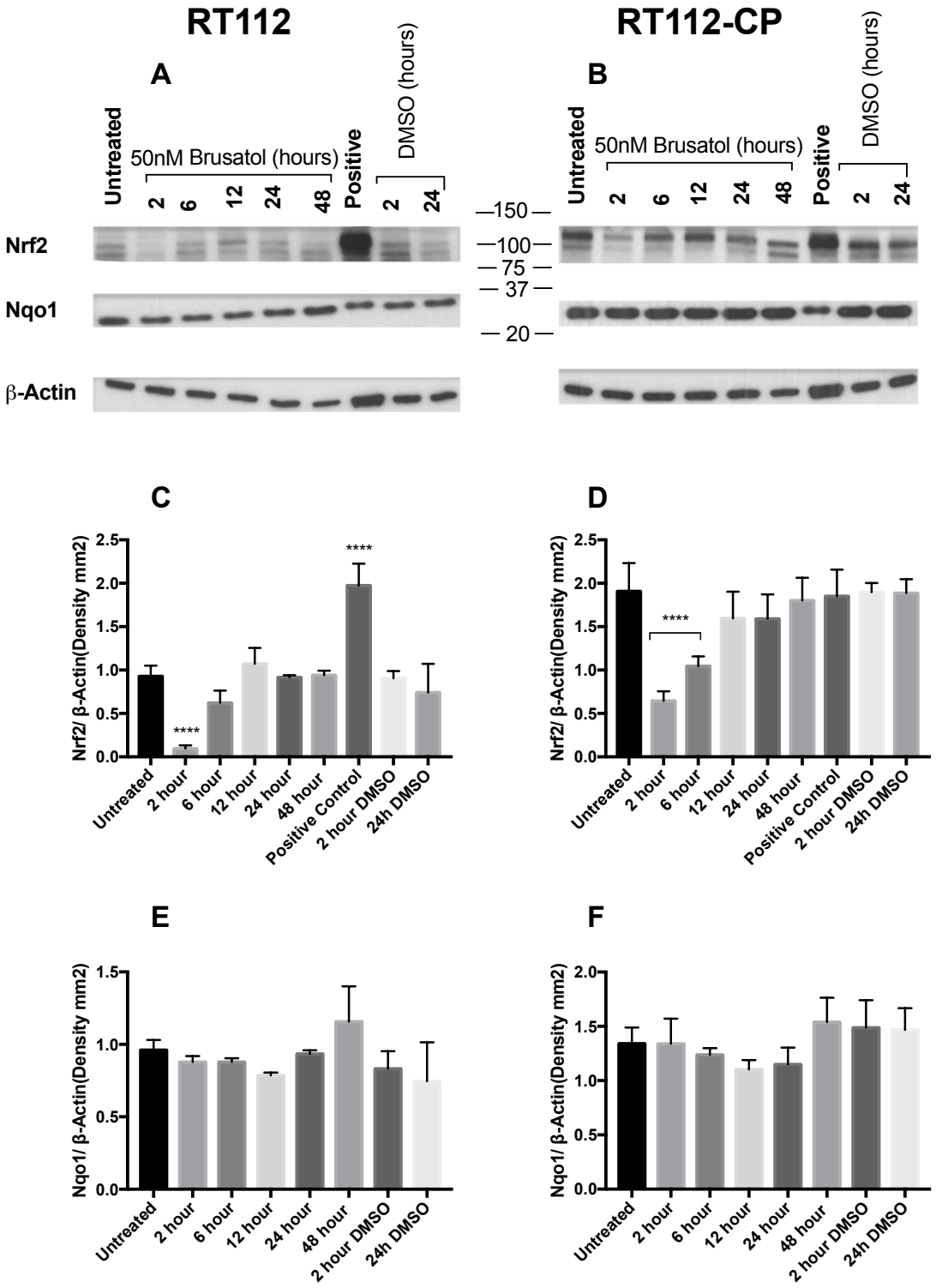

Figure 3.12. Brusatol exposure decreases NRF2 levels in a time dependent manner, although causes no significant change in NQO1 expression over 48 hours. RT112 and RT112-CP cell lines were treated with 50nM brusatol or vehicle and lysed at 2, 6, 12, 24 and 48 hours, prior to western blotting. RT112 (A) and RT112-CP (B) cells were probed for NRF2 (C, D), and NQO1 (E, F) respectively. Densitometry was used to quantify the western blot data which was

normalised to actin and is representative of three independent experiments + SD. A and B are representative of three independent experiments. Statistical analysis was performed via one-way ANOVA (**** p=<0.0001, *** p=<0.001, ** p=<0.01).

3.2.5.5 Investigation into the sensitivity of **NQO1** *as a marker of* **NRF2** *activity*

Next, the sensitivity of NQO1 as a marker of NRF2 activity was tested through the comparison of NRF2 siRNA Knockdown with a 24-hour treatment with 100nM brusatol (Fig 3.13). A 24-hour time point was chosen to allow for potential downstream effects of brusatol mediated NRF2 inhibition to be realised. Furthermore, a concentration of 100nM, double the concentration used in the prior experiment, was selected to increase the opportunity for downstream consequences of NRF2 inhibition to occur – NQO1 inhibition has been previously noted at a concentration of 80nM brusatol, although in A549 cells [172].

NRF2 siRNA significantly inhibited NRF2 levels ($p=0.0003$), whilst no change was observed in NRF2 levels following a 24-hour treatment of 100nM brusatol, in agreement with the previous time course experiment. Furthermore, no significant change in NQO1 levels was noted after a 24-hour exposure with 100nM brusatol, however, a significant decrease in NQO1 levels was observed when comparing control siRNA and NRF2 siRNA treatments (RT112 $p=0.0101$, RT112-CP $p=0.0003$).

These data confirm NQO1 as a sensitive marker of NRF2 pathway inhibition in RT112-CP cells. However, due to the 72-hour time period needed to induce sufficient NRF2 knockdown in these cells, it was not possible to compare the effects of NRF2 siRNA and brusatol at a common time point.

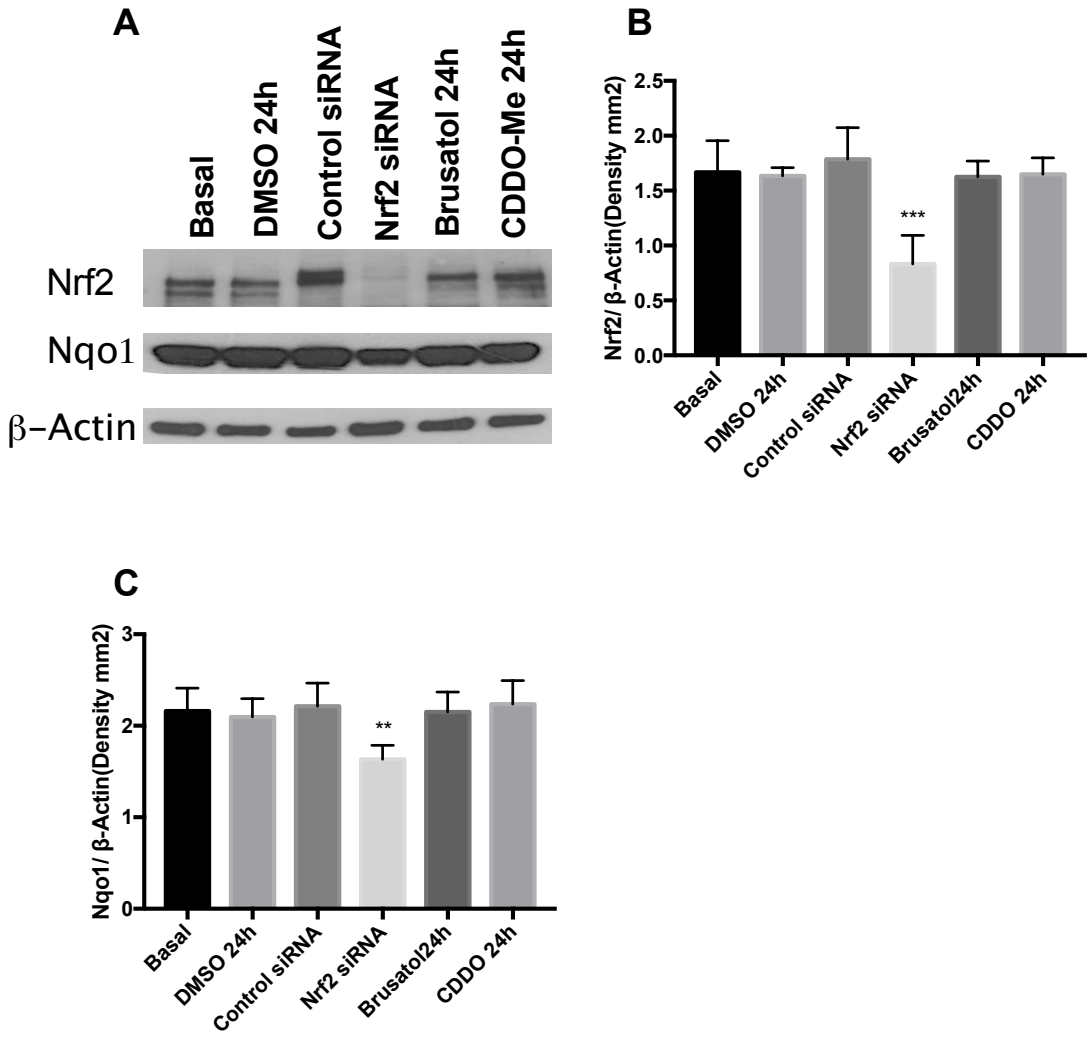

Figure 3.13. NQO1 is sensitive to NRF2 depletion by siRNA knockdown, although brusatol does not significantly alter NQO1 levels. RT112-CP cells were treated with NRF2 targeting siRNA, or brusatol for 24-hours, the effect on relative levels of NRF2 was examined (A, C), as was the effect of these treatments on NQO1 levels (B, C). A is representative of three independent experiments. NRF2 and NQO1 (B, C) western blotting data analysed by densitometry normalised to β-actin and is mean of three independent experiments. Statistical analysis was performed using a one-way ANOVA (***p=<0.001, **p=<0.01, *p=<0.05).

3.2.6 Brusatol as an inhibitor of protein synthesis

3.2.6.1 Comparison of the effects of brusatol and CHX on NRF2 *levels in RT112-CP cells*

With brusatol not causing any significant effects downstream of NRF2 and reports of brusatol potentially acting as an inhibitor of protein synthesis, rather than a specific inhibitor of NRF2, it is possible that NRF2 levels are reduced as a consequence of the short half-life of NRF2 and the inhibition of *de novo* synthesis of NRF2 by brusatol [294].

To determine whether concurrent results are observed in a UCC cell lines as stated in recent literature implicating brusatol as a global inhibitor of protein synthesis where A549 cells have been studied. The effect of the protein synthesis inhibitor CHX was compared to brusatol in terms of NRF2 inhibition, here RT112-CP cells were subject to a 2-hour exposure of 50nM brusatol and 5μg/ml CHX, both concentrations being used by *Vartanian et al* (Fig 3.14) [294]. A marked significant decrease in relative NRF2 levels was noted with both agents (Brusatol p=0.0001, CHX p=<0.0001) (Fig 3.14).

The similar levels of NRF2 inhibition, within the same time-point, by both CHX and brusatol are concurrent with recent literature implicating brusatol in inhibition of protein synthesis.

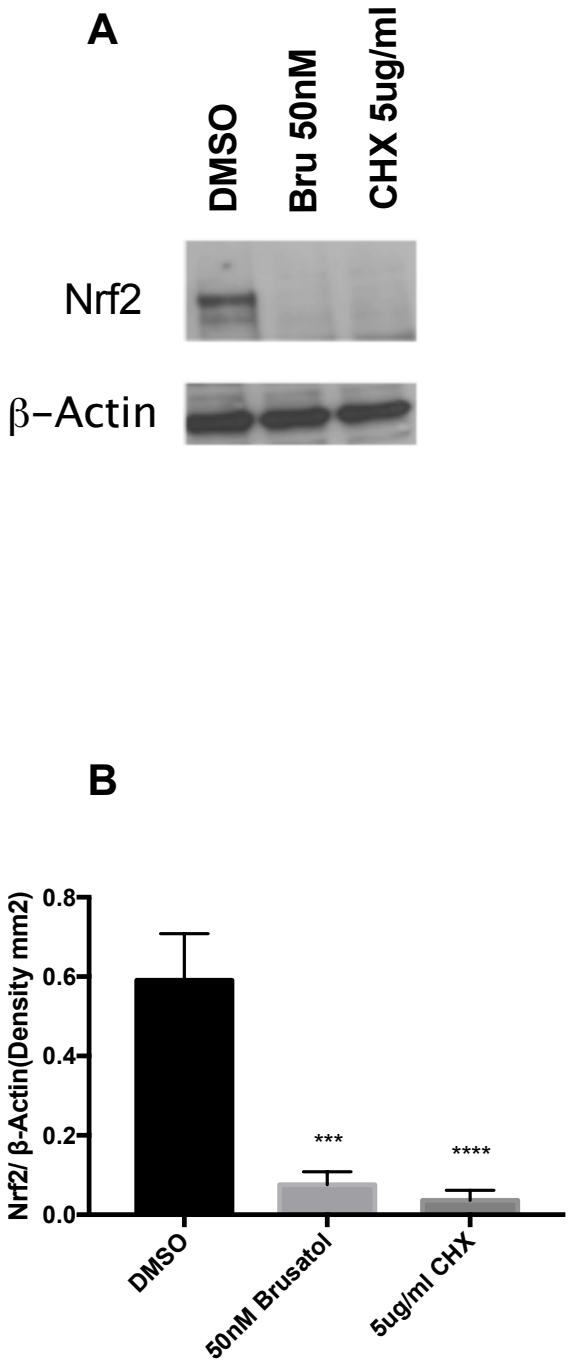

Figure 3.14. Exposure to Brusatol and CHX reduces NRF2 levels in RT112-CP cells. RT112 cells were dosed with either 50nM brusatol, 5µg/ml CHX or vehicle for 2-hours before being lysed and having the expression of NRF2 analysed by western immunoblot. Densitometry was used to quantify blots, with NRF2 expression being normalised to actin. Data is representative of three

separate experiments + SD. Statistical analysis was performed by one-way ANOVA. (***p=<0.001).

3.2.6.2 Brusatol inhibits growth of RT112 and RT112-CP cell lines.

Due to time limitations only one further parameter was investigated, firstly RT112 and RT112-CP cells were dosed with either 50nM brusatol and photographed at regular intervals for 48-hours (Fig 3.15). Here inhibition in growth was visible in brusatol treated cells, when compared to the vehicle control. This effect was most apparent at the 24- and 48-hour time points where the brusatol treated cells are 80% (RT112) and 90% (RT112-CP) confluent, in comparison to the cells in the vehicle control which were growing on top of the confluent monolayer.

These data support findings by Vartanian et al. However, with NRF2 being implicated in cell growth and proliferation in cancers, a reduction in proliferation would be anticipated with a specific inhibitor of NRF2 activity.

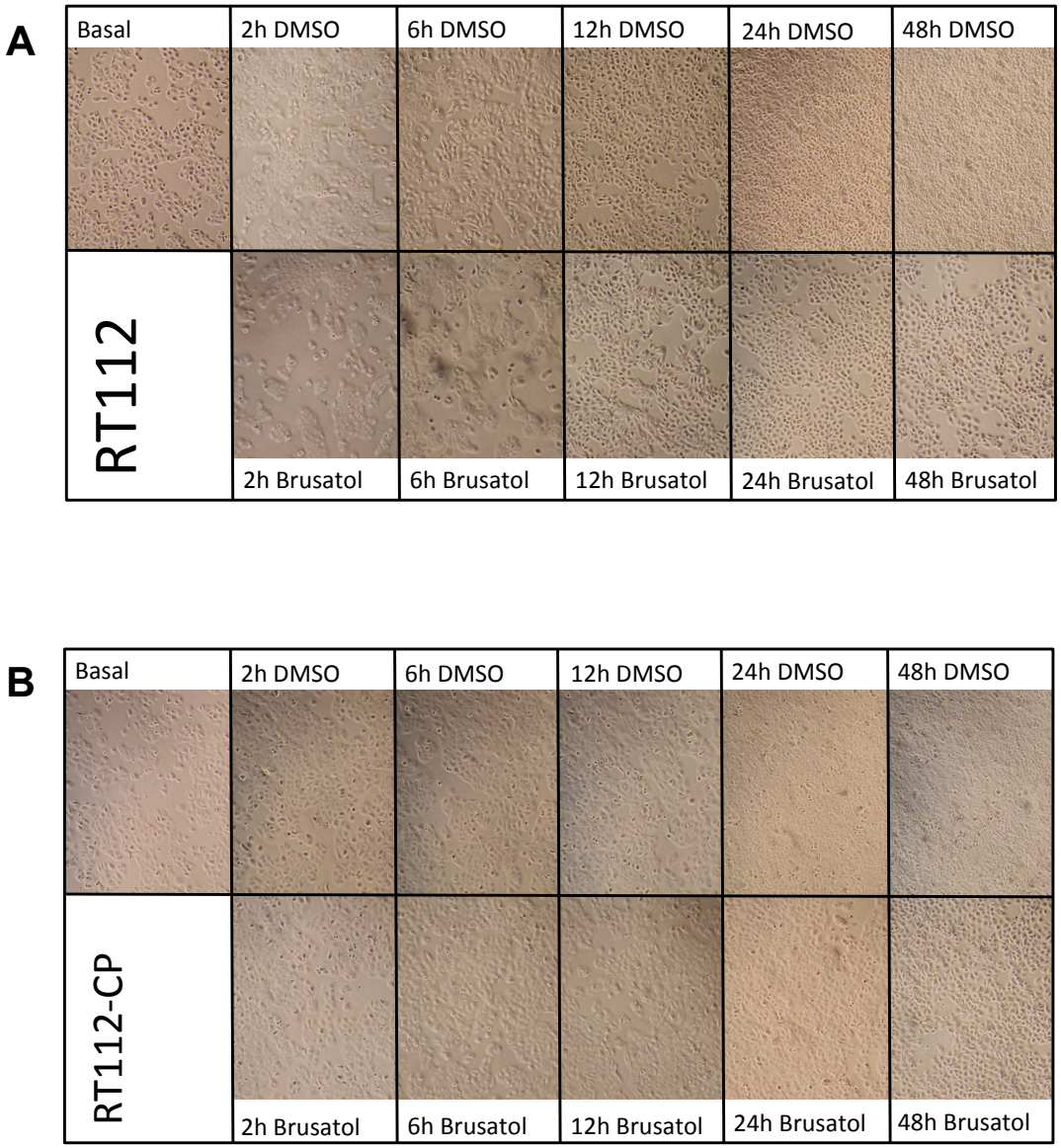

Figure 3.15. Brusatol slows the growth of RT112 and RT112-CP cells. RT112 (A) and RT112-CP (B) cells were treated with 50nM brusatol or vehicle (DMSO) and imaged at 0-hours, 2-hours, 6-hours, 12-hours, 24-hours and 48-hours. Data is representative of three separate experiments.

3.3 Discussion

In recent years, there has been an increasingly large interest in the role of NRF2 in cancer. Studies have implicated NRF2 in many cancers including those of the bladder, pancreas, stomach and skin [129, 133]. And whilst siRNA knockdown of NRF2 in RT112-CP cells has been previously shown to partially restore their sensitivity to cisplatin, a specific pharmacological NRF2 inhibitor has not been tested as a method of chemopotentiation in BC [134].

In this chapter brusatol, a compound originating from the South East Asian plant *Brucea Javanica,* has been investigated. Brusatol has been shown in a number of instances to cause potent, specific inhibition of NRF2 [172, 174].

The primary aim of this study was to define the response to brusatol in terms of sensitivity to the cytotoxic effects of cisplatin. A key secondary aim was to determine the response to brusatol in terms of cell viability, and NRF2 levels, to allow optimisation of a time point where cisplatin would be subject to minimal efflux or catabolism, theoretically maximising potentiation of its cytotoxic effects. It was found that brusatol inhibited NRF2 levels in a time and concentration dependent manner, with 50nM being sufficient for marked NRF2 inhibition in all UCC cell lines, with maximal effects at 2-hours, returning to baseline by 6-hours. These data are in line with observations by *Olayanju et al*, where a marked decrease in relative levels of NRF2 was reported at concentrations greater than 30nM in the mouse hepatoma cell line Hepa-1c1c7 [174]. The transient nature of NRF2 inhibition *in vitro* was also demonstrated in the same cell line, although the aforementioned work used a larger range of time points between 0- and 8-hours, demonstrating marked inhibition of NRF2 from 30-minutes, with replenished NRF2 levels being noted after 8 hour [174].

The low duration of brusatol induced NRF2 inhibition is attractive in the setting of BC as many patients who present with BC also have co-morbidities including kidney damage. With NRF2 being one of the chief cell defence pathways in the kidneys sustained NRF2 inhibition after systemic brusatol treatment with

nephrotoxic cisplatin based chemotherapy may lead to increased kidney damage [295]. Although, *Ren et al* have demonstrated sustained reduction of NRF2 levels by brusatol *in vivo,* with intratumoural NRF2 suppression being noted up to 48-huors post treatment in an A549 murine xenograft model [172]. Unfortunately, no studies to date have analysed the systemic consequences of brusatol treatment *in vivo*.

In the BC cell lines used in this thesis it was essential to determine whether brusatol induced disruptions in NRF2 signalling were translated into reduced levels of detoxification proteins with an ARE in their promoter region. Thus, NQO1 levels were evaluated over 48-hours in response to 50nM brusatol, with no significant change being observed. This cast doubt over the utility of NQO1 as a marker of NRF2 activity, as a result siRNA knockdown was performed to test the worth of NQO1 as a marker of NRF2 activity. This was tested alongside a 24-hour treatment with 100nM brusatol, in contrast to the significant response to NRF2 siRNA, brusatol caused no change in NQO1 levels.

Recently a vast proteomic analysis undertaken by Vartanian *et al* has revealed that brusatol may not function as a specific inhibitor of NRF2, but as a global inhibitor of protein synthesis [294]. The reasoning for the rapid inhibition of NRF2 protein expression being due to the short half-life of the NRF2 protein, and the inhibition of protein synthesis machinery essential for the synthesis of NRF2 [294]. Vartanian *et al* reached this conclusion through analysis of the effects of brusatol on the proteome of the A549 non-small cell lung cancer (NSCLC) cell line. They demonstrated the most dramatically decreased proteins being those with short half-lives, and in fact the only proteins to be upregulated were multiple components of the ribosome, suggesting a role in the regulation of protein synthesis [294]. Furthermore, their findings were compared with marked parity to the well-used protein synthesis inhibitor, CHX.

With no significant change in NQO1 levels in response to brusatol treatment, and gaining insight on brusatol from Vartanian *et al*, where they had demonstrated that CHX leads to similar potent inhibition of NRF2. It was then sought to draw

parallels between brusatol activity in NSCLC and UCC cell lines, thus the effect of CHX on NRF2 levels was compared with the effect of brusatol. A highly significant decrease in NRF2 levels was observed with both treatments. Indicating that inhibition of protein synthesis by CHX causes a similar effect to brusatol in terms of relative NRF2 protein expression.

Throughout the process of mitosis, the protein synthesis machinery is essential for successful proliferation, therefore the effects of brusatol on cell growth were analysed. RT112 and RT112-CP cells were treated with brusatol, and photographed for 48-hours. At the 24-hour and 48-hour time points, the difference in cell growth is very noticeable, with vehicle treated cells being crowded, and growing above the monolayer, whilst brusatol treated cells had yet to reach confluence. This qualitative data demonstrates that cell growth is partially inhibited in UCC cells, possibly due to inhibited protein synthesis. Although, NRF2 has been implicated in cell growth and proliferation in cancer [296].

Vartanian *et al* demonstrated a relationship between the doubling time of a cell line, and its susceptibility to the cytotoxic effects of brusatol – a trait which is supportive of the protein synthesis inhibitor hypothesis as cells which are dividing at a faster rate are more likely to have an increased dependency on the protein synthesis machinery.

To determine whether the relationship between sensitivity to the cytotoxic effects of brusatol and cell doubling time were similar when the work of *Vartanian et al* was comparable to the data in this thesis, published average cell doubling times were compared to the mean brusatol IC50s determined in this chapter. It was hypothesised that brusatol will exert increased cytotoxic effects on the fastest dividing cells, possibly due to the increased demand put on the hypothetically non-functional protein synthesis machinery. Near-significant ($p=0.0793$) positive linear correlation (Pearson $r = 0.8338$), as some correlation can be observed this may become a significant correlation if a larger panel of cell lines was utilised (Fig 3.16).

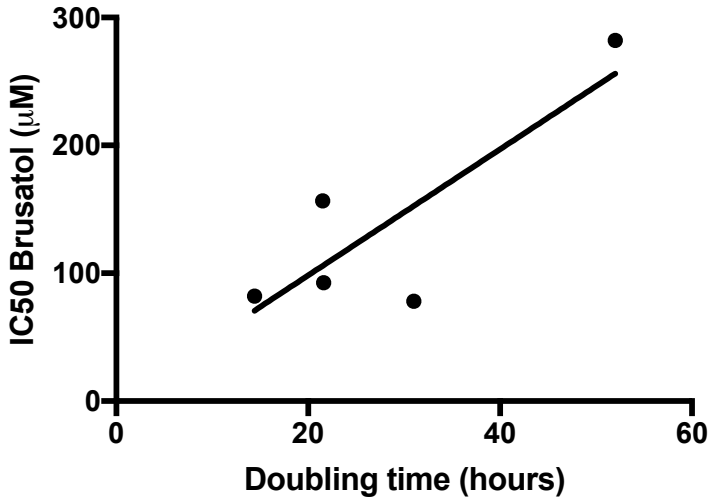

Figure 3.16. Correlation between cell doubling time and brusatol IC50 in EJ, 253-J, MGH-U3, RT112 and RT112-CP. Average brusatol IC50 values were compared to published mean cell doubling times for each cell line. The data was subject to two-tailed Pearson's correlation analysis (Pearsons r 0.8338, p=0.0793).

Collectively the data questioning the specificity of brusatol do not definitively prove that brusatol is an inhibitor of protein synthesis, however, these data do for the most part correspond with what has been observed by Vartanian *et al*, and offer a potential explanation for brusatol inability to inhibit NQO1, as NQO1 has a half-life of 18-hours compared to just 15-minutes for NRF2 [297, 298]. Additionally, these data may explain why no significant effect in terms of cisplatin potentiation is noted at 50nM of brusatol, a concentration that leads to drastic inhibition of NRF2 levels. Moreover, it might be expected that with the RT112-CP cell line expressing NRF2 at a considerably higher level than RT112 cells that the sensitivity to the combined effects of brusatol and cisplatin may be higher, especially considering the comparable efficiency of brusatol mediated NRF2 depletion in both cell lines, although the converse it true.

Interestingly brusatol did not inhibit proteins downstream of NRF2 however it did significantly increase the sensitivity of UCC cell lines to the cytotoxic effects of cisplatin. Although, at concentrations where brusatol addition is most

beneficial, brusatol is highly cytotoxic. In comparison to cisplatin brusatol is an order of magnitude more potently cytotoxic to UCC cells. So rather than brusatol acting synergistically with cisplatin, the observed effects are more likely to be additive cytotoxic effects. Although, further analysis would be required to determine this relationship.

CHX does not have therapeutic benefits due to its toxic side effects including DNA damage, teratogenesis, and other reproductive effects including sperm toxicity [299]. However, whilst brusatol may not be a specific inhibitor of NRF2, it may have some therapeutic benefit in the setting of BC. The early research into the therapeutic benefit of silvestrol, a compound isolated from the *Aglaia foveolata* plant, with potent cytotoxic effects is promising, demonstrating potential usefulness of translational inhibitors in the treatment of cancer [300]. Parallels may be drawn between brusatol and silvestrol in that they both show some effect when combined with therapeutic agents, with cisplatin being shown to combine well with brusatol both in this thesis and in work by Ren *et al,* whilst silvestrol has a synergistic effect with cisplatin in nasopharyngeal carcinoma cell lines [301]. Furthermore, both agents also have potent growth inhibitory effects in the Nanomolar range.

The therapeutic potential of the translation inhibitor silvestrol has been evaluated in a number of cancer models including: hepatocellular carcinoma (HCC) where silvestrol potently inhibited growth of HCC cell lines, mouse xenograft models showed similar potency with increased survival noted, and a synergistic relationship with other therapeutic agents sorafenib and rapamycin [302]; chronic lymphocytic leukaemia (CLL) and acute lymphoblastic leukaemia (ALL) where a significant increase in efficacy was noted *in vitro* whilst *in vivo* an increase in survival without discernible off target toxicity was noted in a xenograft mouse model [303].

In conclusion, brusatol is a potent inhibitor of UCC cell growth, and in combination with cisplatin at concentrations above 100nM in RT112 cells, 200nM in RT112-CP cells and 400nM for EJ and 253-J cells significantly inhibits

cell growth more than either agent alone. However, it is likely that brusatol is not a specific inhibitor of NRF2.

Further investigation beyond this must investigate the effect that brusatol has on normal urothelial cells, BC xenograft models and on murine health, considering liver function, cardiac function, renal function, and neurological function at a broad range of concentrations and durations to determine whether brusatol is a suitable candidate for human trials. With cancer cells being fast dividing cells, highly reliant on protein synthesis machinery, there is a good rationale for the usage of well tolerated inhibitors of protein synthesis. However, effects on high-turnover normal tissue in the human body may lead to side effects including myleosuppression, and neutropenia. Furthermore, sustained inhibition of proteins involved in cellular detoxification, and DNA repair may leave healthy tissue vulnerable when used in combination with cytotoxic chemotherapy agents.

Chapter Four – The effect of CD40-ligation on urothelial cell carcinoma cell line invasion in an organotypic model of bladder cancer

4.1 Introduction 130
4.1.1 Chapter aims 133
4.2 Results 134
4.2.1 UCC cells differentially express CD40 134
4.2.2 EJ transfection with AdNclCD40L 136
4.2.3 CD40-ligation attenuates tumour cell invasion in an organotypic model of bladder cancer 138
4.2.4 RNA microarray in EJ cells displays differential expression in genes implicated in tumour invasion by bladder gene expression profiling. 149
4.3 Discussion 158

4.1 Introduction

CD40-ligation has a multifaceted role in human physiology having a profound effect on a plethora of cells throughout the body. However, the effects of CD40L-binding are highly context dependent.

In cells of the immune system CD40-ligation leads to activation and maturation of dendritic cells from immature peripheral blood monocytes (PBMCs), whereas in the context of BC, CD40-ligation has been linked to tumour cell death. The downstream effects of CD40-ligation are mediated by a group of adaptor proteins named TRAFs.

In BC, CD40 expression is associated predominantly with NMIBCs, however a large proportion of MIBCs also express CD40. This contrasts with normal urothelium, which is predominantly CD40-negative. It is hypothesised that CD40 expression is central to the excellent response to BCG intravesical therapy in NMIBC patients.

The inability to control metastasis is the leading cause of death in patients with cancer, therefore, this chapter aims to determine whether CD40-ligation affects the invasive nature of BC cells, in an organotypic three-dimensional model of BC. The behaviour of two CD40-positive cell lines, RT112 and EJ, will be investigated in this model, originating from a papillary NMIBC and a MIBC, respectively. These cell lines were chosen as they will allow insight into whether CD40-ligation can increase the invasiveness of cells, or decrease the invasiveness. Furthermore, RNA-microarray data was cross-referenced to determine whether any genes involved invasion are differentially expressed as a result of CD40-ligation.

The non-cleavable mCD40L construct, delivered by an adenoviral vector, used in this chapter is described in detail in the referenced work [180]. Briefly, a replication-deficient E1, E3 deleted recombinant adenovirus was utilised to express either AdNclCD40L, or GFP control (AdMock) (Fig 4.1).

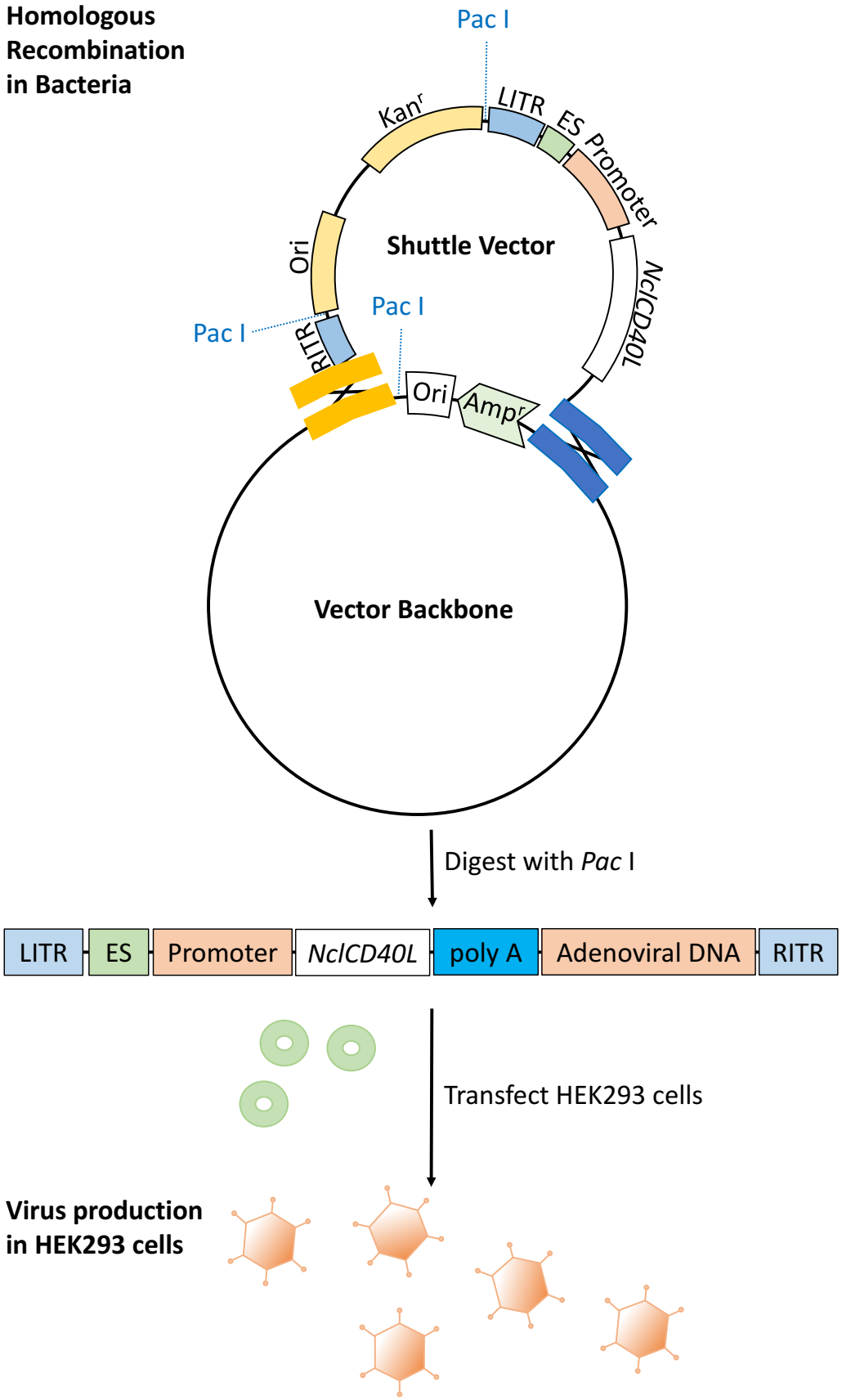

Figure 4.1. Diagram of homologous recombination, and adenovirus packaging in HEK293 cells. Three steps are involved: 1) Generation of the gene

expressing construct; 2) Constructing the adenovirus expressing the gene of interest; 3) Production of the virus in mammalian cells.

4.1.1 Chapter aims

- To determine whether CD40-ligation influences urothelial cell carcinoma cell invasion in a three-dimensional model of BC.
- To understand more about the mechanisms behind CD40-ligation dependent modulation of tumour cell invasion.

Hypothesis: CD40-ligation will modulate UCC cell invasion in an organotypic model of BC.

4.2 Results

4.2.1 UCC cells differentially express CD40

To select cell lines appropriate for further analysis the relative basal expression of CD40 was assessed by western immunoblot in EJ, 253-J, and RT112 cell lysates (Fig 4.2). All cell lines expressed CD40; with EJ expressing the highest levels and RT112 cells expressing the lowest levels.

EJ and RT112 cells were selected for further analysis, as both are CD40-positive, with EJ cells originating from a ≥T3G3 (MIBC) tumour whilst RT112 cells originate from a ≤T1 G1 (NMIBC) lesion.. This model allows comparison between the two disease states, and insight into whether CD40-ligation is a pro- or anti-tumour invasion event in UCC.

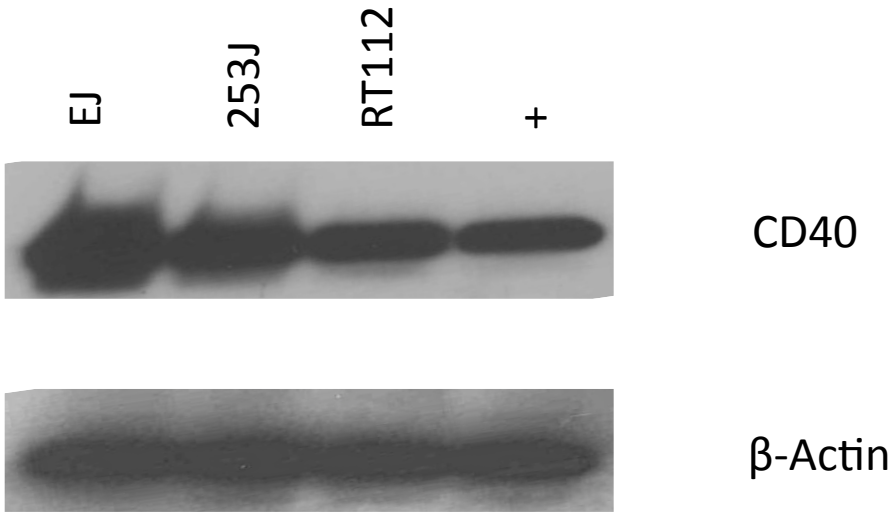

Figure 4.2. UCC cells express CD40 in a differential manner. 50μg of total protein lysates of EJ, 253J and RT112 were analysed by western blot for CD40 expression and β-actin as a loading control. (n=1).

4.2.2 EJ transfection with AdNclCD40L

The effect of CD40-ligation on BC invasion was studied in an organotypic model of BC. Initially, EJ cells were infected with either AdNclCD40L or AdMock virus at a low MOI (1MOI), to avoid a profound apoptotic induction and a saturated response). CD40L expression was confirmed by western blotting 24-hours post-infection (Fig 4.3), where CD40L expression was detected in AdNclCD40L but not AdMock-transfected cells. Furthermore, no significant difference in cell morphology between each condition was detected.

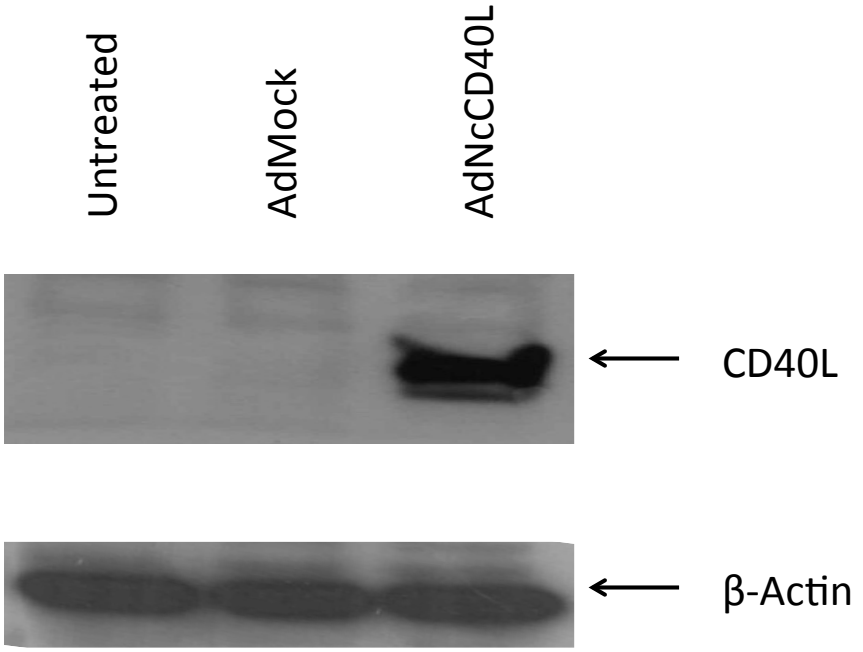

Figure 4.3. Infection with 1 MOI AdNclCD40L initiates CD40L protein expression in UCC cells. EJ cells were infected with 1 MOI AdNclCD40L or AdMock. Protein lysates were then prepared and analysed by western immunoblot. β-actin was used to demonstrate even protein loading. Data is representative of three independent experiments.

4.2.3 CD40-ligation attenuates tumour cell invasion in an organotypic model of bladder cancer

The effect of CD40-ligation on tumour cell invasion was assessed in an organotypic model of BC (Fig 4.4). Here, EJ and RT112 cells infected with 1 MOI AdNclCD40L were compared to AdMock and basal controls. Cells were infected overnight, before being applied to a pseudostroma consisting of HFFs, collagen, and matrigel, then being raised up onto a stainless-steel platform. This mimics the interface between the internal environment of the bladder and bladder tumour noted in vivo, furthermore, the media beneath is representative of underlying vasculature offering a supply of oxygen, moisture and nutrition. Organotypic models were formalin fixed and paraffin embedded after two weeks, before sectioning and H&E staining for microscopic observation.

Under basal conditions the EJ cell line invaded the stroma extensively, as single cells, and occasionally in small groups (Fig 4.4, 4.5, 4.7). Some cellular accumulation had occurred above the stroma, 1 cell thick under basal conditions and 2 cells thick when infected with AdMock, however most cells display marked invasiveness. Interestingly, invasiveness was attenuated partially by infection with AdMock. This contrasts with the behaviour of RT112 cells (Fig 4.4, 4.6), where under basal conditions no invasiveness was demonstrated, furthermore cellular accumulation occurred above the matrix, at 6 cells thick in some regions. The morphology of RT112 cell accumulation in this model is like papillary lesions *in vivo.*

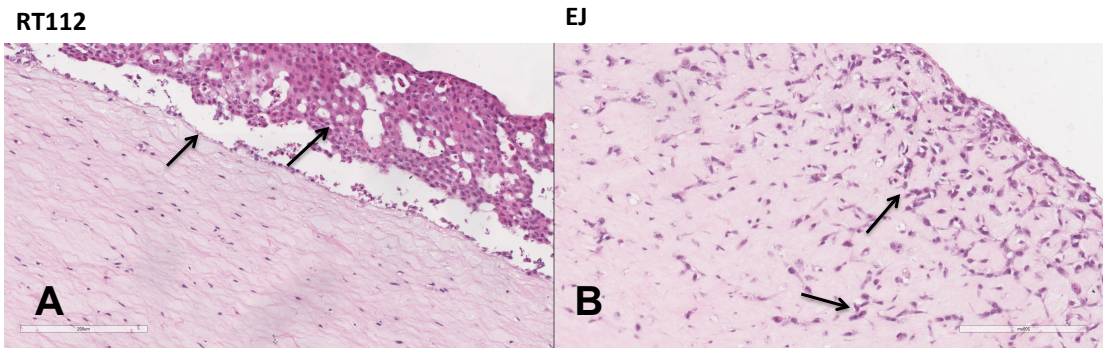

Figure 4.4. Comparison of basal RT112 (A) and EJ (B) cell growth characteristics in a three-dimensional organotypic model of bladder cancer. Black arrows indicate a defined tumour-stroma boarder (A), and invading tumour cells (B). Data is representative of 3 independent experiments.

The effects of CD40-ligation on both EJ (Fig 4.4, 4.5, 4.7) and RT112 (Fig 4.4, 4.6) cell growth were very evident. In RT112 cells, marked cell death occurred, making it impossible to discern between the no UCC control sample and the AdNclCD40L condition, whereas there was little difference in morphology between either AdMock infected or uninfected RT112 cells. Marked cell death was also observed in EJ cells, along with attenuated invasion, however a population of cells survived both above the stroma, and a small number also invaded. There was significant disparity between AdMock control and EJ cells under basal conditions, highlighting the growth-inhibitory effects of the adenoviral vector alone.

As the adenoviral vector is conditionally replicating, it was hypothesised that cells invading the stroma may be those that have replicated and no longer express CD40L, furthermore, as a low MOI used, it is possible a number of cells escaped sufficient CD40-ligation. To determine whether there was a difference in CD40L expression in invading cells when compared to non-invading cells, AdNclCD40L infected sections will be stained by IHC probing for CD40L.

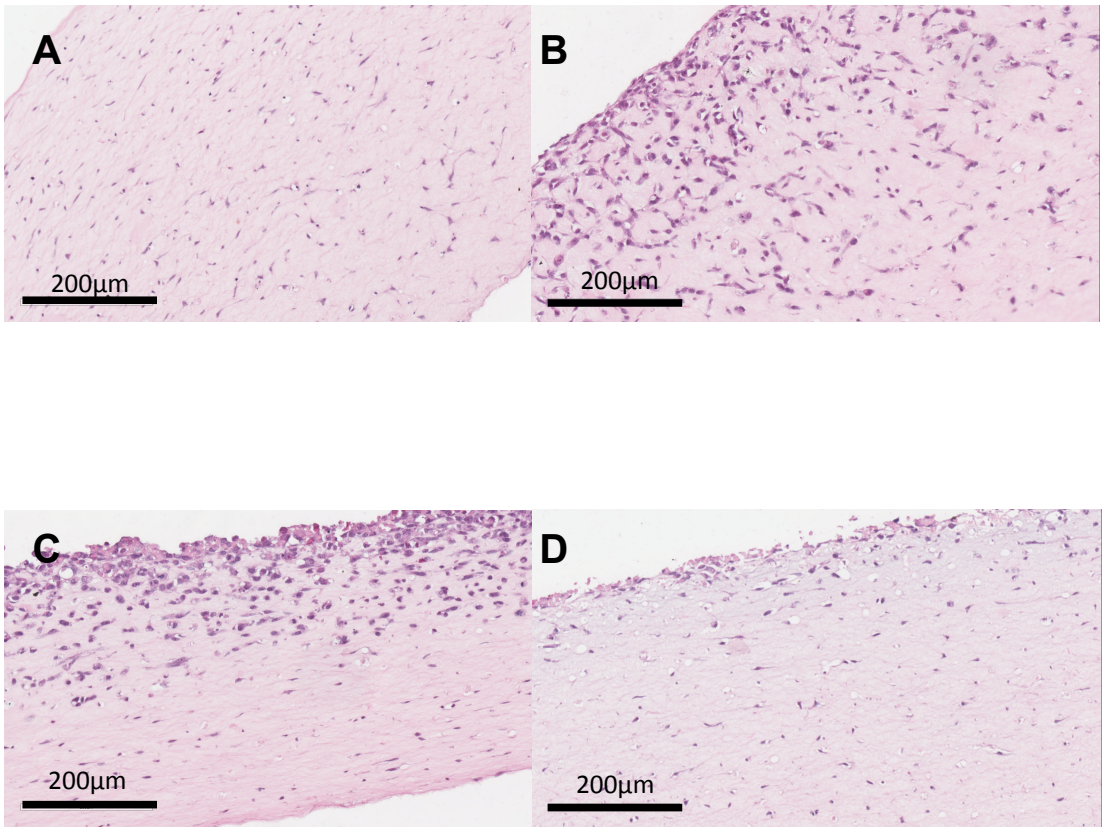

Figure 4.5. H&E stained cross sections of EJ cell three-dimensional organotypic invasion assays. A) collagen/fibroblast/matrigel matrix only, B) basal, C) AdMock, D) AdNclCD40L. Data is representative of three independent experiments.

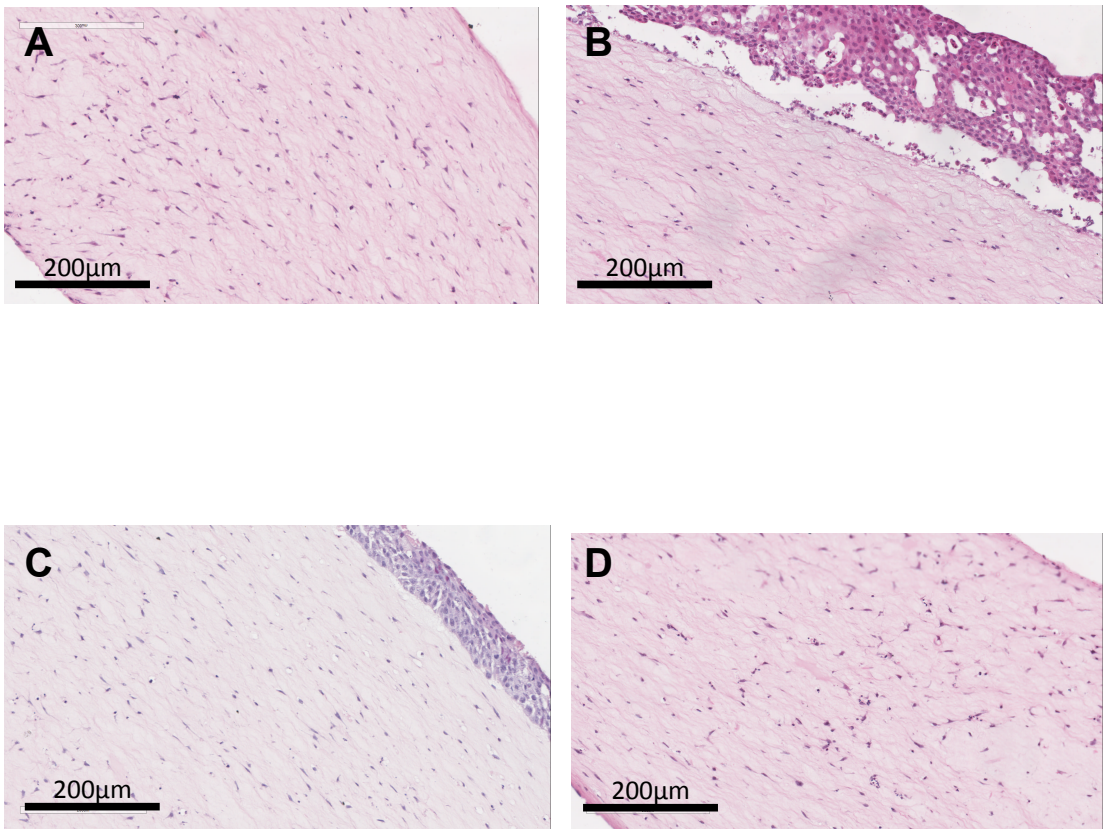

Figure 4.6. H&E stained cross sections of RT112 cell three-dimensional organotypic invasion assays. A) collagen/fibroblast/matrigel matrix only, B) basal, C) AdMock, D) AdNclCD40L. Data is representative of three independent experiments.

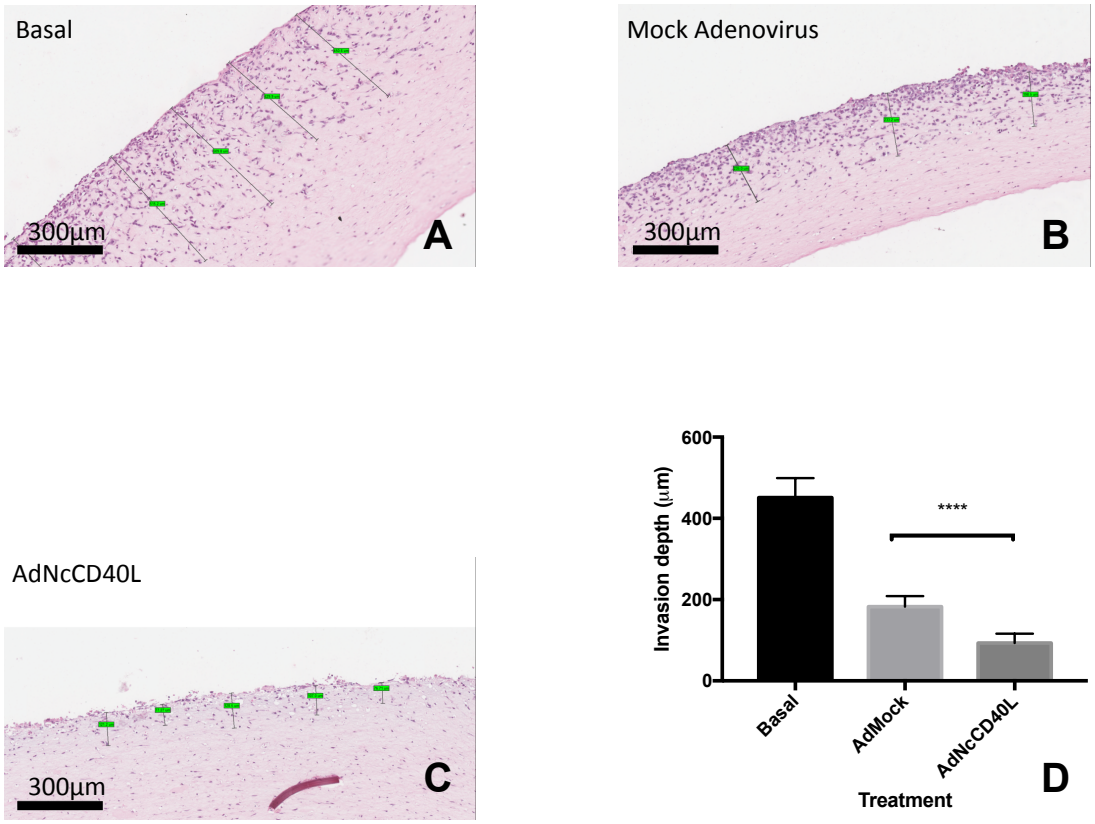

Figure 4.7. CD40-ligation limits EJ cell invasion and leads to marked cell death in an organotypic model of bladder cancer. A) Basal, B) AdMock, C) AdNclCD40L, D) Average invasion depth. A, B and C are representative images from three independent experiments. Statistical analysis performed using one-way ANOVA ($p<0.0001$). Data is representative of three separate experiments.

With some tumour cells still invading into the stroma under AdNclCD40L treated conditions, staining will be undertaken to determine whether these cells are CD40L-null. If invading cells were null, whilst non-invading cells were AdNclCD40L positive, this would further suggest a role for CD40-ligation in the attenuation of tumour invasion.

4.2.3.1 CD40L immunostaining

To determine whether invading cells were CD40L-null, whilst non-invasive cells express CD40L, organotypic sections were stained by IHC for CD40L.

4.2.3.1.1 Anti-CD40L *displays specific binding by western blotting*

Firstly, the specificity of this anti-CD40L antibody was assessed by western blot (Fig 4.8), where bands were only detected in AdNclCD40L treated EJ cells, in the appropriate region (~32kDa), whilst no expression was evident in AdMock treated, and untreated cells (Fig 4.8). The specificity of this antibody indicates a likelihood of specific behaviour in IHC.

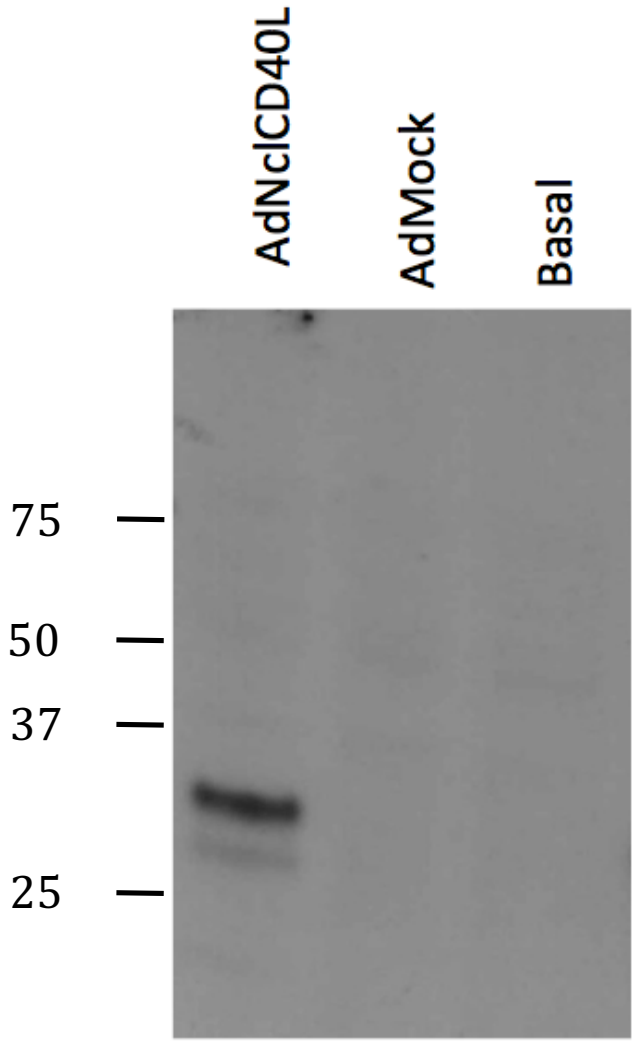

Figure 4.8. Western blot of EJ cell lysates treated as indicated. Protein lysates were prepared from untreated EJ cells, and EJ cells treated with AdNclCD40L or AdMock for 24-hours prior to western blotting. Anti-CD40L (SC978) was used to probe for CD40L. Specific binding to CD40L was displayed, with no binding in either basal or AdMock treated cells. (n=1).

4.2.3.1.2 AdNclCD40L *expression is confined to non-invading cells*

Here the expression of CD40L was tested in organotypic cross-sections treated with either AdMock or AdNclCD40L. Staining with a 1:100 dilution of anti-CD40L (Fig 4.9E,F) led to marked staining in both AdNclCD40L treated cells, and AdMock infected cells. No expression was noted in the 1:1000 AdMock control, isotype control and no primary antibody control (Fig 4.9C,D). Staining with 1:1000 anti-CD40L revealed moderate to strong diffuse expression of AdNclCD40L in the epithelial layer, whilst no expression was noted any invading tumour cells (Fig 4.9A). With only non-invading cells expression AdNclCD40L, this data indicates a potential role in the attenuation of tumour cell invasion for CD40.

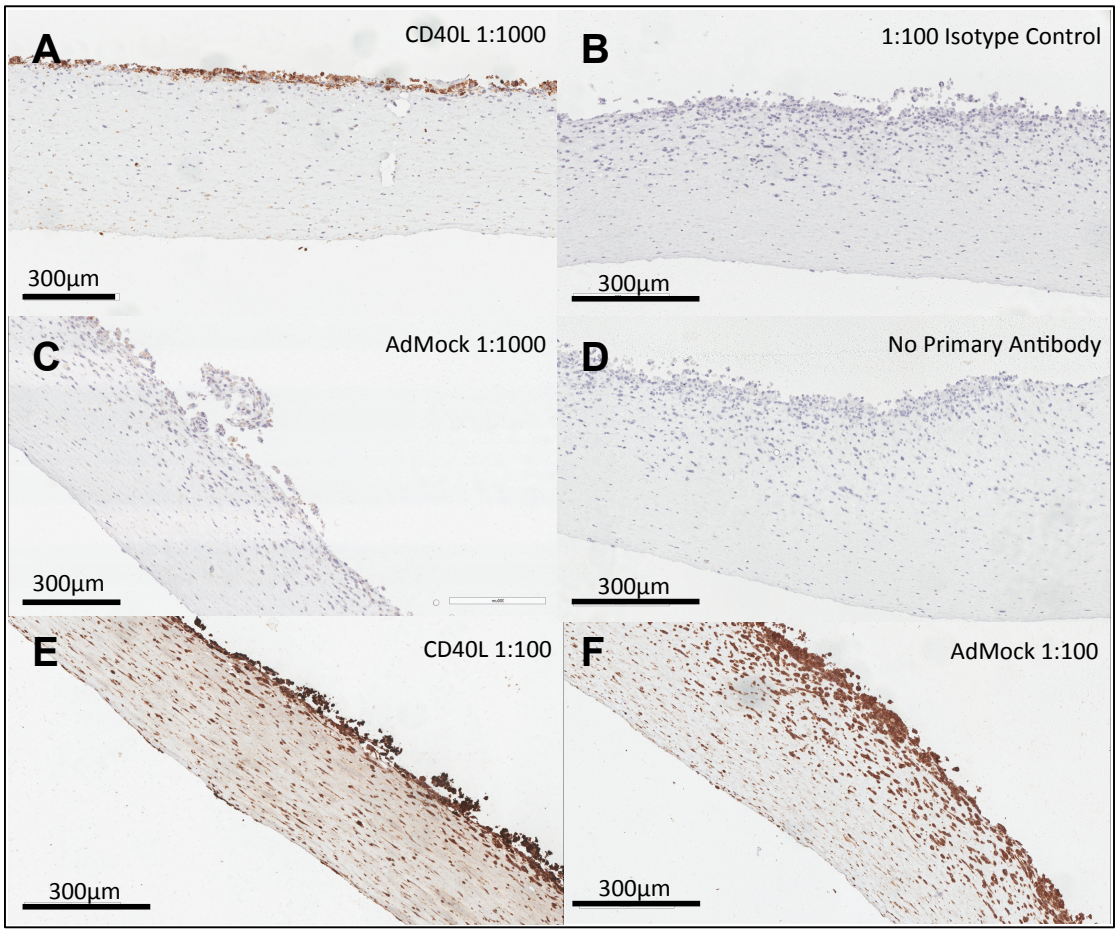

Figure 4.9. Non-invading EJ cells express mCD40L. IHC optimisation results pH9 antigen retrieval 1:100 and 1:1000 primary antibody concentration in EJ organotypic sections. A) mCD40L transfected cells stained with 1:1000 anti-CD40L exhibiting CD40L specific staining, B) Isotype control, C) AdMock control probed with 1:1000 primary antibody, D) No primary antibody control, E) mCD40L transfected cells stained with 1:100 primary antibody exhibiting non-specific staining, F) AdMock transduced cells stained with 1:100 primary antibody exhibiting non-specific staining. (n=1).

4.2.4 RNA microarray in EJ cells displays differential expression in genes implicated in tumour invasion by bladder gene expression profiling.

In order to further dissect the role of CD40-ligation in tumour cell invasion, a RNA microarray was consulted. In this microarray, performed by Taha Elmetwali, EJ cells were untreated, infected with AdMock, or infected with AdNclCD40L Differential expression was noted in a plethora of genes, therefore the UCC microarray data discussed in chapter 5 was employed to select the most dysregulated genes involved in MIBC when compared to grade 3 NMIBC. It was hypothesised that these genes may be potential drivers of muscle invasion. *OPN*, and *MMP1*, two genes dysregulated between normal bladder tissue and MIBC were included in the selection process as there is a significant body of data implicating them in tumour cell invasion [198, 200, 202, 203, 206, 222, 261, 304-307]. A literature review was conducted to determine the role of each candidate in tumour invasion (Table 4.1).

Interestingly only one queried gene was upregulated post CD40-ligation, *MMP1*, a protein implicated in remodelling of the ECM, facilitating tumour cell invasion. Seven genes were downregulated: *FAM83D* – linked with invasion in HCC; *CENP1* – implicated in mitosis; *FN1* – implicated in tumour cell invasion; *CENPF* – implicated in mitosis; *TOP2A* – alters DNA topography, TOP2A inhibitors show promise in some cancers; *TPX2* – implicated in mitosis; *ANLN* – implicated in EMT, invasion and metastasis. No change was noted in the mRNA expression of: *RARRES1* – a potential repressor of invasion; *MAN1C1*; *RASSF2* – potential TSP; *OPN/ SPP1* – implicated in BC invasion and metastasis; and *FBXW7* – TSP, regulated by FAM83D.

Based on the insight gained from these data, four genes were selected based on evidence indicating a role in invasion, and the level of change in expression observed in the AdNclCD40 RNA microarray, for use in further analysis: *MMP1*, *FN1*, *FAM83D* and *ANLN*. The relative change of expression in these genes is displayed in figure 4.10.

Table 4.1. Gene's dysregulated in MIBC when compared to grade 3 NMIBC or normal bladder tissue. Genes selected for further analysis in bold.

Gene	ID	Fold Change (MIBC vs G3 NMIBC)	Fold Change (Normal vs MIBC)	Change in EJ AdNclCD40L microarray	Role
Family with sequence similarity 83, member D	***FAM83D***	**7.87**	**-**	**Down**	**Affects proliferation and invasion in HCC, negative regulator of FBXW7 (TSP), expression linked with decreased overall survival in a number of cancers [239, 308, 309].**
Retionic Acid receptor responder (tazarotene induced) 1	*RARRES1*	5.97	-	No	May repress invasion [310].
Centromere protein I	*CENPI*	5.92	-	Down	Essential for proper mitotic progression, chromosomal alignment and segregation [311].
Fibronectin 1	***FN1***	**5.86**	**-**	**Down**	**Promotes invasion [312, 313].**
Centromere protin F (350/400KDa (mitosin)	*CENPF*	5.76	5.18	Down	Cell cycle protein, *FOXM1* and *CENPF* are synergistic drivers of prostate cancer [314].
N mannosidase, alpha, clas 1C, member 1	*MAN1C1*	5.52	-	No	Involved in maturation of Asn-linked oligosaccharides [315].

Topoisomerase (DNA) II alpha 170 Kda	*TOP2A*	5.32	7.08	Down	Alters topologic states of DNA during transcription, TOP2A inhibitors exist [316].
TPX2, microtubule-associated, homolog (Xenopus laevis)	*TPX2*	5.28	7.52	Down	Required: for normal assembly of mitotic spindles; for assembly of microtubules during apoptosis; for chbromatin and/or kinetochore dependent microtubule nucleation [317].
Ras association (RalGDS/AF-6) domain family member 2	*RASSF2*	5.05	-	No	Potential TSP, acts as a KRAS-specific effector protein, may promote apoptosis and cell cycle arrest. Stabilises STK/MST2 by protecting it from proteasomal degradation [318].
Anillin, actin binding protein	***ANLN***	**5.01**	**8.5**	**Down**	**Critical for cell division, and may promote EMT and cell migration through cytoskeletal remodelling - implicit in invasion and metastasis [250, 319].**
Osteopontin / Secreted Phosphoprotein 1 (OPN)	*SPP1*	-	10.98	No	Implicated in invasion in a number of cancers [260, 320, 321].

Matrix Metalloproteinase 1	***MMP 1***	**-**	**6.49**	**Up**	**Collagenase, involved in ECM remodelling and invasion. Secreted as a preproprotein, may cleave membrane-bound CD40 [322].**

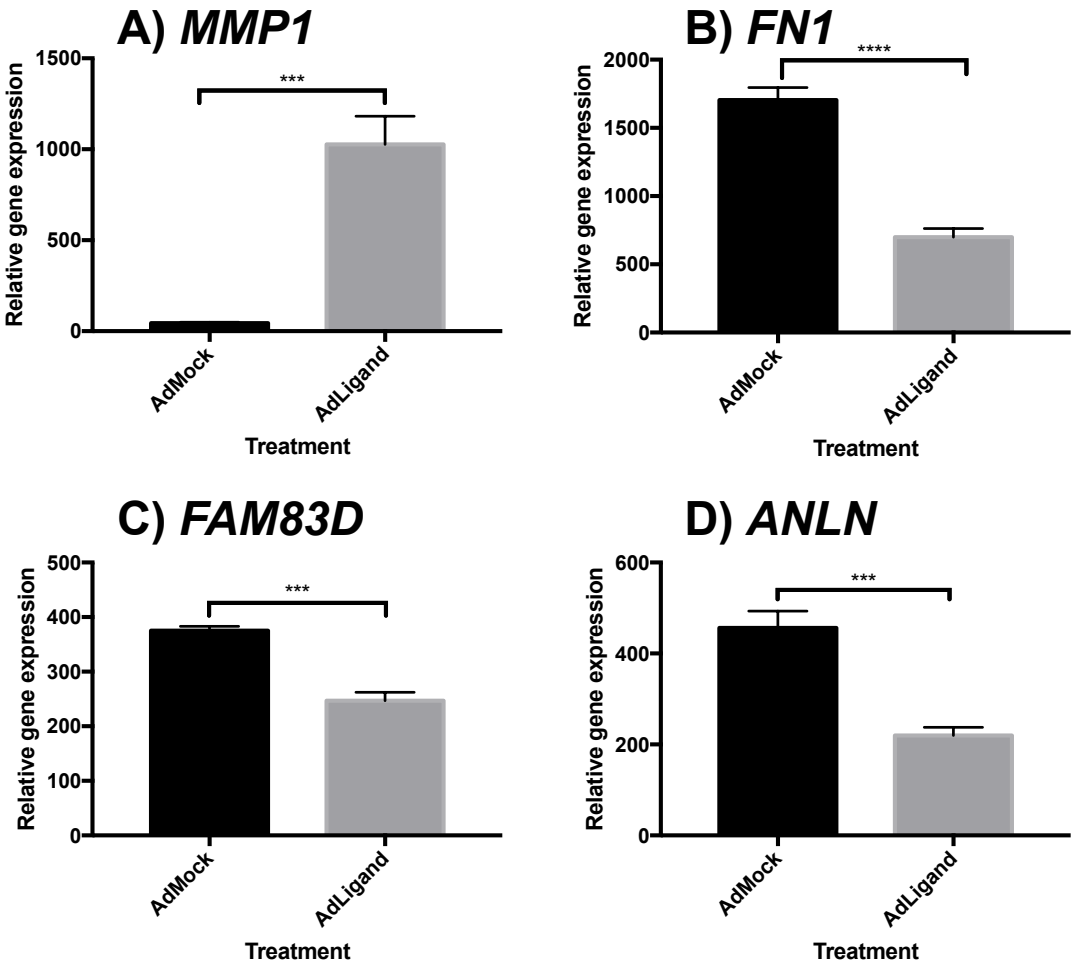

Figure 4.10. CD40-ligation induced changes in expression. Determined by RNA microarray; *MMP1* (A), *FN1* (B), *FAM83D* (C) and *ANLN* (D) relative gene expression.

4.2.4.1 Expression of the invasion markers MMP1, FAM83D, ANLN and FN1 is modulated by CD40-ligation in EJ and RT112 cells

4.2.4.1.1 Protein level

The downstream consequences of CD40-ligation were tested in EJ and RT112 cells. Here, both cell lines were infected with either AdNclCD40L or AdMock, prior to lysis 24-hours later and extraction of protein and RNA. Initially AdNclCD40L protein expression was confirmed by western blot, prior to probing for MMP1 and FN1 (Fig 4.11). The expression of MMP1 in AdMock-transduced cells was low in both cell lines. Interestingly, FN1 expression was markedly higher in RT112 cells compared to EJ cells. No significant change in the expression of either MMP1 or FN1 was observed in RT112 cells.

However, EJ cells demonstrated a marked upregulation in MMP1 levels, concordant with AdNclCD40L microarray data. Interestingly, and converse to the RNA microarray data, FN1 levels were markedly increased in EJ cells.

To confirm the expression of *FN1*, *MMP1*, FAM83D and *ANLN* at the RNA level in RT112 and EJ cells, reverse-transcription polymerase chain reaction (RT-PCR) was employed next.

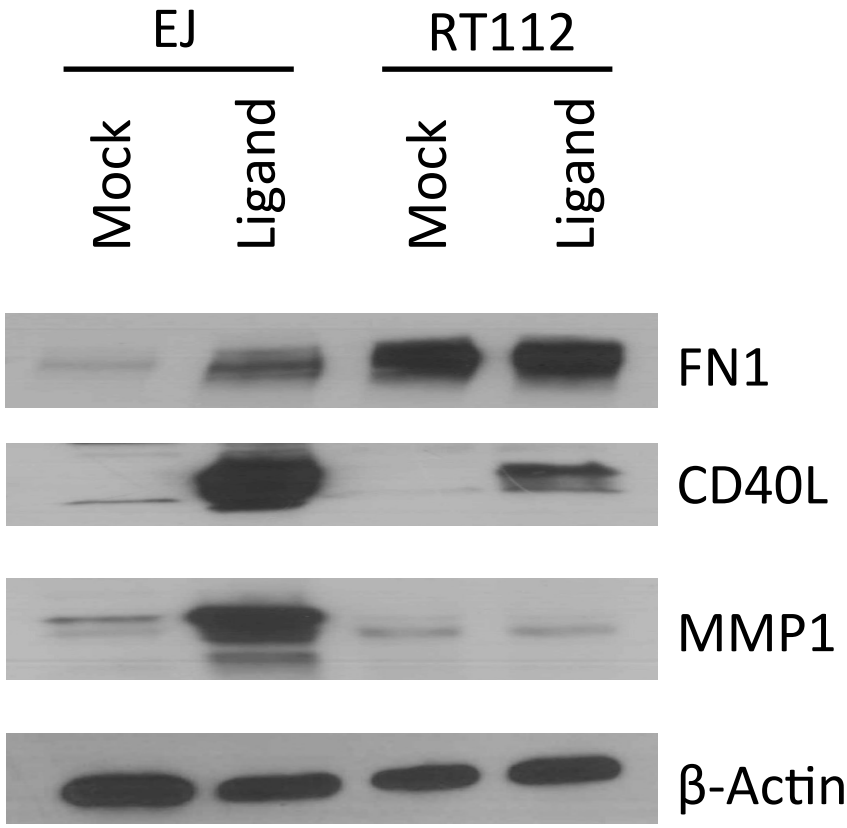

Figure 4.11. Consequences of CD40-ligation on FN1 and MMP1 expression. EJ and RT112 cells were infected either with 1MOI AdMock (Mock), or AdNcCD40L (Ligand). 50μg of protein was loaded. β-actin was used to demonstrate equal protein loading. (n=1).

4.2.4.1.2 RNA level

Endpoint RT-PCR was performed utilising cDNA generated from total RNA extracted from EJ and RT112 cells infected with AdMock, or AdNclCD40L for 24 hours. The expression of *MMP1*, *FN1*, *FAM83D* and *ANLN* was investigated together with *GAPDH* to ensure equal loading (Fig 4.12).

RT-PCR confirmed expression of *MMP1*, *FN1*, *FAM83D* and *ANLN* at the RNA level in both cell lines.

At the protein level these data suggest that CD40-ligation may increase some pro-invasive signalling in EJ cells (Fig 4.11), with increases in *MMP1* and *FN1* levels being noted in EJ cells. In contrast, the microarray data (Fig. 4.10) displays a 2.4-fold decrease in *FN1* RNA levels in EJ cells with increased RNA levels observed solely in *MMP1*. One potential explanation of the CD40L induced attenuation of invasion observed in this model is the high level of apoptotic induction resulting from membrane-bound CD40-ligation may lead to decreased cell numbers attenuating the extent of invasion.

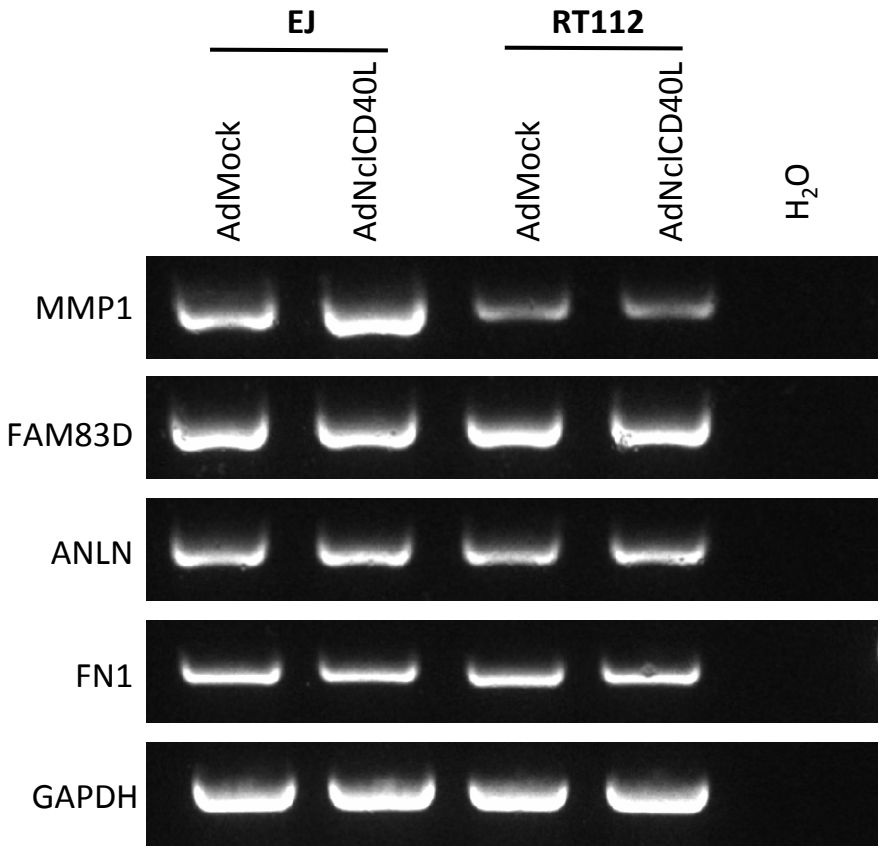

Figure 4.12. Confirmation of *MMP1*, *FAM83D*, *ANLN* and *FN1* RNA expression in EJ and RT112 cells. Agarose gel image of RT-PCR fragments of *MMP1*, *FAM83D*, *ANLN*, *FN1* and a *GAPDH* loading control (n=1).

4.3 Discussion

Over the past decade interest in CD40, a receptor studied extensively in immune biology, in cancer has grown greatly [323]. However, the role of CD40 in tumour cell invasion remains unclear. In this chapter expression of a non-cleavable membrane-bound CD40L construct, delivered by a conditionally replicating adenovirus, was initiated in UCC cells to study the consequences of CD40-ligation, in terms of tumour cell invasion and downstream effects. The primary aim of this study was to determine whether CD40-ligation plays a supportive, or inhibitory role on BC cell invasion. The secondary aim was to determine whether this effect was due to downstream CD40-ligation induced differential expression.

Initially western blot was used to determine the relative basal expression of CD40. CD40 was expressed in all cell lines tested and at highest levels in the MIBC cells, EJ and 253-J, respectively. Interestingly, NMIBCs express the highest levels of CD40 (89%), compared to a smaller proportion of MIBCs (62%) [178].

Choosing the appropriate type of CD40 ligand is essential, due to differing effects between mCD40L and sCD40L. AdNclCD40L was used after initial consideration of rsCD40L. Although rsCD40L does not cause cell death in BC cells without inhibition of protein synthesis, it only leads to short-lived transient activation of CD40, unsuitable in a multi-day assay comparatively, AdNclCD40L invokes sustained mCD40L expression, and downstream activation of CD40 pathway [180, 186]. Studies into the downstream effects of mCD40L-ligation have used high amounts of virus, in the region of 100 MOI [180, 186]. Due to apoptotic induction potential of mCD40L on EJ cells, lower MOI was utilised (1 MOI) to allow for low-level expression of mCD40L and associated downstream events without triggering apoptotic cell death induction. Following 24-hour infection with AdNclCD40L, total protein lysates were prepared and expression of mCD40L was detected by western blot. Notably, there was no phenotypic changes between different treatments, or apparent cell viability reduction at 24-hours.

Consistent with other reports, RT112 cells behaved in a non-invasive manner in an organotypic model of BC (Fig 4.13) [324]. Interestingly, RT112 cells displayed a papillary-like morphology in this model, similar to their morphology the originating tumour [272]. Consistent with their origin, EJ cells demonstrated highly invasive behaviour where invasion was seen predominantly as single cells, similar behaviour has also been noted *in vivo* [325]. In RT112 cells treated with AdMock a tighter epithelium was formed, 4-6 cells in thickness, compared to the 12-14 cells observed in untreated RT112 cells. Interestingly, inhibition in cell growth, and increased cell death has been reported with the use of adenoviral vectors [326]. The adenoviral vector also affected behaviour of EJ cells in an organotypic model, partially attenuating invasion. However, marked invasion occurred, displaying a similar diffuse pattern to untreated cells. The effect of AdNclCD40L treatment on EJ cell was marked, causing near complete inhibition tumour cell invasion, accompanied by marked cell death, whilst AdNclCD40L treatment resulted in RT112 cell death, to the extent that sections resemble the no UCC cell control. Interestingly, in EJ cells the greatest decrease in invasion correlated with adenoviral infection, where invasion depth was reduced by 60% compared to cells under basal conditions, whereas a smaller decrease of 49% was noted between AdMock and AdNclCD40L infected cells, highlighting the growth-inhibitory effects of this adenoviral vector. Additionally, assessment of efficacy of infection was not tested as published work using the same viral stocks in EJ cells has demonstrated comparable infection rates upon examination of green fluorescent protein (GFP) expression [180, 186]. Although there is potential for differential infection rates between experiments, positive CD40L staining in non-invading AdNclCD40L transduced EJ cells, compared to absence in invading cells, indicates CD40-ligation is a driver of the displayed anti-invasive behaviour.

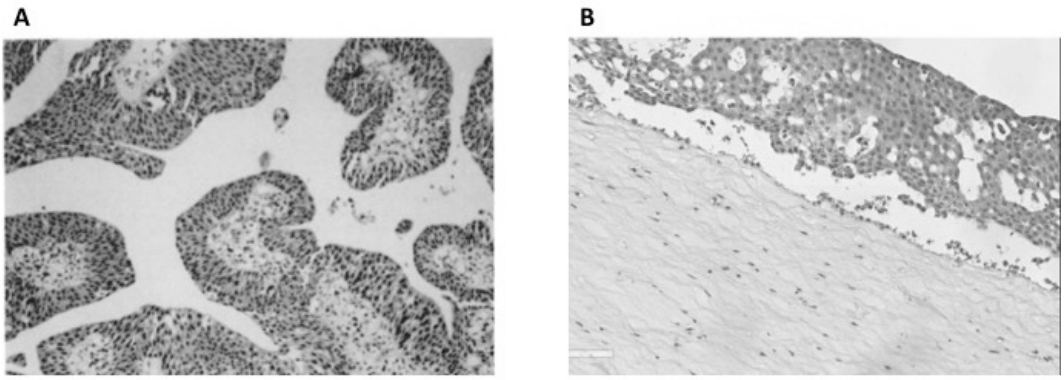

Figure 4.13. In vitro behaviour of RT112 cells is similar to that in the parent tumour of RT112. (A) Parent Tumour H&E, papillary transitional cell carcinoma of the human bladder [272]. (B) RT112 cell line in an organotypic model of BC, H&E. Shares papillary morphology of parent tumor.

Based on the observations in EJ cells, where near complete inhibition of tumour cell invasion occurred, it was hypothesised that the invasive cells do not express mCD40L. To test this hypothesis organotypic sections were stained for CD40L, staining revealed positive staining in non-invading cells, whilst all other cells were negative for CD40L expression. These data indicate an inhibitory role of CD40L, in terms of tumour cell invasion. To determine whether this effect was a result of downstream modulation of genes involved in invasion, a BC microarray, presented in chapter 5, was consulted. A table of the most differentially expressed genes between MIBC and grade 3 NMIBC was consulted (Table 4.1, 5.3), with the addition of two highly differentially expressed genes from a comparison of MIBC with normal bladder tissue, *OPN* and *MMP1*. The data in this table was cross-referenced with data from a microarray, where EJ cells were infected with AdMock or AdNclCD40L. Candidate genes were then selected based on the response to CD40-ligation, and data implicating the gene in invasion. *MMP1*, *FN1*, *FAM83D* and *ANLN* were selected for further analysis.

The expression of all four markers was confirmed at the RNA level by endpoint RT-PCR in both cell lines [327]. Relative protein levels of FN1 and MMP1 in response to AdNclCD40L were measured by western blot. In agreement with microarray data, MMP1 was markedly upregulated in EJ cells, whilst low levels

were noted in RT112 cells. In RT112 cells, relative FN1 levels were high, with little change between conditions. Interestingly, FN1 levels in EJ cells dramatically increased, in discordance with microarray data. This suggests an increase in FN1 protein stability. Potential mechanisms of increased FN1 levels are preferential translation of remaining FN1 RNAs and decreased protein breakdown [328-331].

With increases in FN1 and MMP1, and only small decreases in RNA expression of FAM83D and ANLN within this panel, evidence indicates increased levels of some markers involved in tumour invasion. However, inhibition of invasion was noted in organotypic models of BC. This may be explained by the use of a small panel of invasion markers, although these were selected from a list of 13 dysregulated genes in MIBC, it is likely other genes implicit in tumour cell invasion were not included in this panel. Furthermore, as CD40-ligation leads to altered expression of a plethora of genes, it is likely that those implicated in invasion are differentially regulated. Similarly to the effect of mCD40L-CD40-ligation on cell death, where there is evidence for TRAF3 dependent pro-apoptotic signalling and TRAF6 dependent cell survival signalling. It is possible that CD40-ligation initiates the expression of factors both positive and negative in tumour invasion promotion, with the net result leading to inhibition of tumour invasion. This notion is supported by reports of pro- and anti- invasion, proliferation and cell growth signalling resulting from CD40-ligation in several cancers [332-334]. Although, inhibition of invasion may not be due to classic invasive signalling pathways, but rather owed to the apoptosis inducing action of CD40-ligation in UCC cells [180].

Future work should focus on the development of treatments based on the apoptotic action of mCD40L. The development of mCD40L expressing liposomes may prove useful in the treatment of NMIBC. A recombinant ectodomain of apolipoprotein L1 (APOL2)/TRAIL, expressed on the surface of liposomes, has shown marked anti-tumour activity [335]. Furthermore, Systemic initiation of CD40-signalling by agonistic monoclonal antibodies (mAbs) allows for a multi-modal attack on tumour cell viability, both directly through apoptotic induction in CD40-positive cancer cells, and immune activation where antigen-presenting

cells (APCs) such as B cells, dendritic cells and monocytes are activated, facilitating an increased anti-tumour immune response [192, 336]. Furthermore, initial clinical trials of such agonistic CD40 mAbs have demonstrated very promising results, with no disabling toxicity, both as standalone agents and in combination with chemotherapy [336].

In conclusion, these data demonstrate the ability of CD40-ligation to inhibit tumour cell invasion, and to invoke marked cell death. However, changes in the expression of downstream markers, particularly increases in protein expression of FN1 and MMP1, do not explain the attenuation of invasion in EJ cells.

Chapter Five – Gene expression profiling identifies distinct segregation between histological subtypes of bladder cancer

5.1 Introduction 164

5.1.2 Chapter aims 165

5.2 Results 166

5.2.1 Bladder cancer tissue exhibits specific gene expression signatures 166

5.2.2 Further functional analysis employing Database for Annotation, Visualization, and Integrated Discovery (DAVID) 189

5.2.3 Meta-analysis of publicly available datasets 191

5.2.4 Osteopontin protein is overexpressed in MIBC tissue compared to normal urothelium * 192

5.3 Discussion 202

5.1 Introduction

Locally confined BC can be divided into NMIBC or MIBC. NMIBC may be effectively managed surgically by TURBT, and immunologically by the usage of BCG instillation. Treatment of MIBC requires radical intervention, either by cystectomy or radical radiotherapy (with or without concurrent and neo-adjuvant chemotherapy). Less than 20% of NMIBCs will recur and progress to MIBC with the passage of time. Several clinicopathological attributes are associated with disease aggressiveness, and recent findings are discussed in depth in the general introduction and general discussion sections. However current clinicopathological factors applied in the clinic include tumour grade, stage, size, presence of *Cis* and previous recurrence, all of which are associated with progression.

Unfortunately, the above factors are not sufficient to identify patients who need more radical therapy at diagnosis. In the case of MIBC, stratification of patients likely to progress to locally advanced or devastating MBC would allow a more personalised approach to therapy.

Several recent studies have employed the usage of RNA microarrays to investigate the expressional landscape of BC. Furthermore, identification of differentially expressed genes allows for the dissection aberrant of pathways and processes in BC. An increased knowledge of the expressional profiles of this remarkably heterogeneous disease may allow for increased knowledge of BC pathogenesis, and may provide clues for both non-invasive and early detection in BC, potentially unveiling novel targets for the development of new treatments.

This chapter uses gene expression analysis to identify dysregulated gene expression in BC, identifying distinct molecular subgroups with similar and opposing expressional profiles. Potential key pathways have been identified, along with a marker of aggressive MIBC. The expression of one marker, OPN, was further assessed in tissue by immunohistochemistry.

The work carried out in section 5.2 was performed in collaboration with the authors of the 2017 IJO paper "Gene expression profiling in bladder cancer identifies potential therapeutic targets". An asterisk (*) in the section heading marks experiments that I, Richard Greensmith, have performed, in sections not marked with an asterisk experiments have been undertaken by authors of the IJO paper, excluding myself.

5.1.2 Chapter aims

- To develop gene expression signatures with predictive and prognostic value
- To gain further insight into the expressional landscape of BC

Hypothesis: Gene expression analysis will identify molecularly distinct subtypes of BC.

5.2 Results

5.2.1 Bladder cancer tissue exhibits specific gene expression signatures

An aggregate of 418 genes were differentially expressed between BC and normal bladder tissue samples, with a fold change above 2.5, and a FDR of 0.05. Of this group, 368 genes displayed reduced expression in BC whilst 50 genes were increased in expression in BC. Furthermore, hierarchal clustering separated normal bladder tissue and BC into two distinct groupings (Fig 5.1).

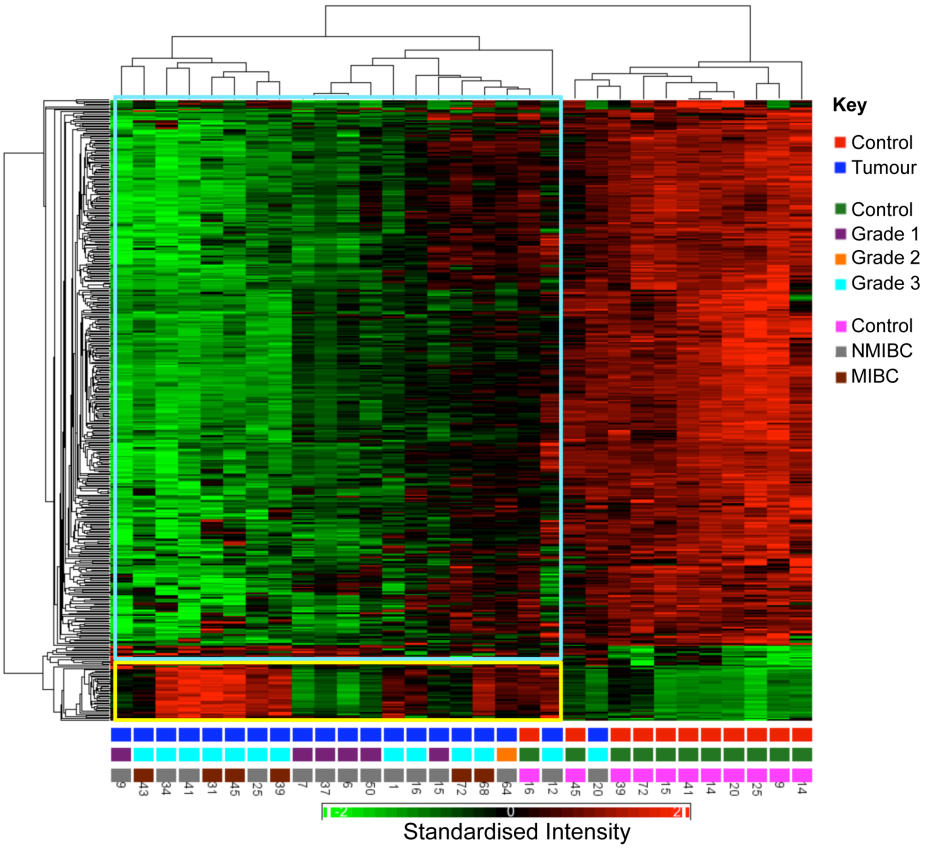

Figure 5.1. Hierarchal clustering separates BC samples from normal tissue samples. Numbers at the bottom of the figure indicate anonymised patient serial numbers.

Of the 50 genes shown to be upregulated in BC compared to normal tissue, multiple were involved in proliferation ($p = 2.59 \times 10^{-9}$), including components of the CDK1/CyclinB complex, required for progression from G2 to M-phase. Induction of Cyclin B transcription is mediated by FOXM1 (Fig 5.2). Additionally, the balance between nuclear export and import of Cyclin B1 is affected by its phosphorylation status mediated by upregulated polio-like kinase 1 (PLK1). Lamin B, a substrate of CDK1/Cyclin B, leads to the depolymerisation of the lamin nuclear-cytoskeleton, and kinesin family member 1 (KNSL1), which is linked with spindle apparatus and centrosomes.

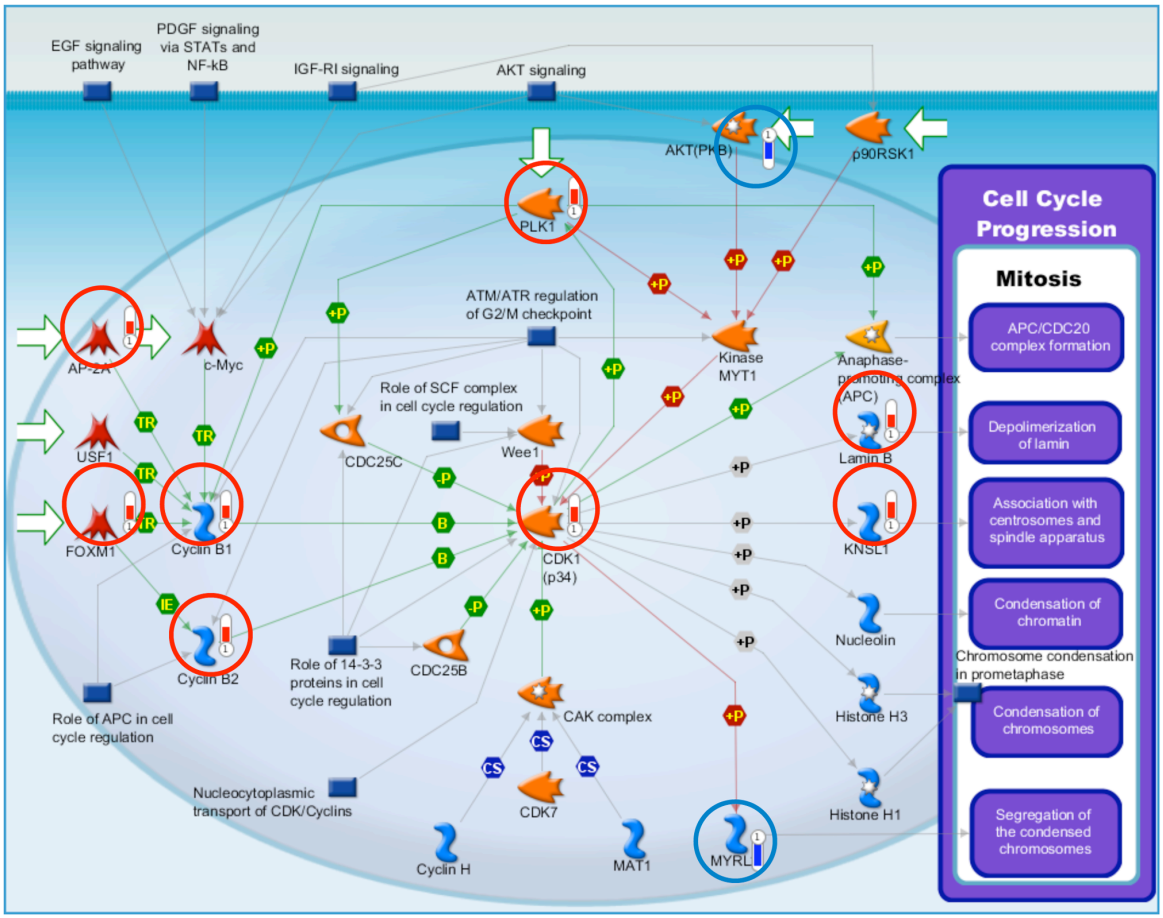

Figure 5.2. Genes implicated in mitosis are upregulated in BC (p = 2.59 x 10-9). Key: Genes c upregulated (red circled), downregulated (blue circled). The bar length is representative of the degree of expressional change.

5.2.1.1 Genes implicated in epithelial-to-mesenchymal transition and myogenesis are downregulated in bladder cancer

In comparison to normal tissue, genes downregulated in BC included a number of genes involved in myogenesis ($p = 1.22 \times 10^{-10}$) (Fig 5.3), including MEF2, expressed during myogenesis. Myocyte enhancer factor 2 (MEF2) and the myogenic regulatory factor, MyoD, interact conferring MyoD activation, leading to the expression of myosin light and heavy chains. Furthermore, genes implicated in EMT were also downregulated in BC ($p = 1.41 \times 10^{-9}$) (Fig 5.4). EMT is a key process during myogenesis as muscle precursor cells delaminate from the dermomyotome and myoblasts invade the developing tissue before differentiating into mature myocytes.

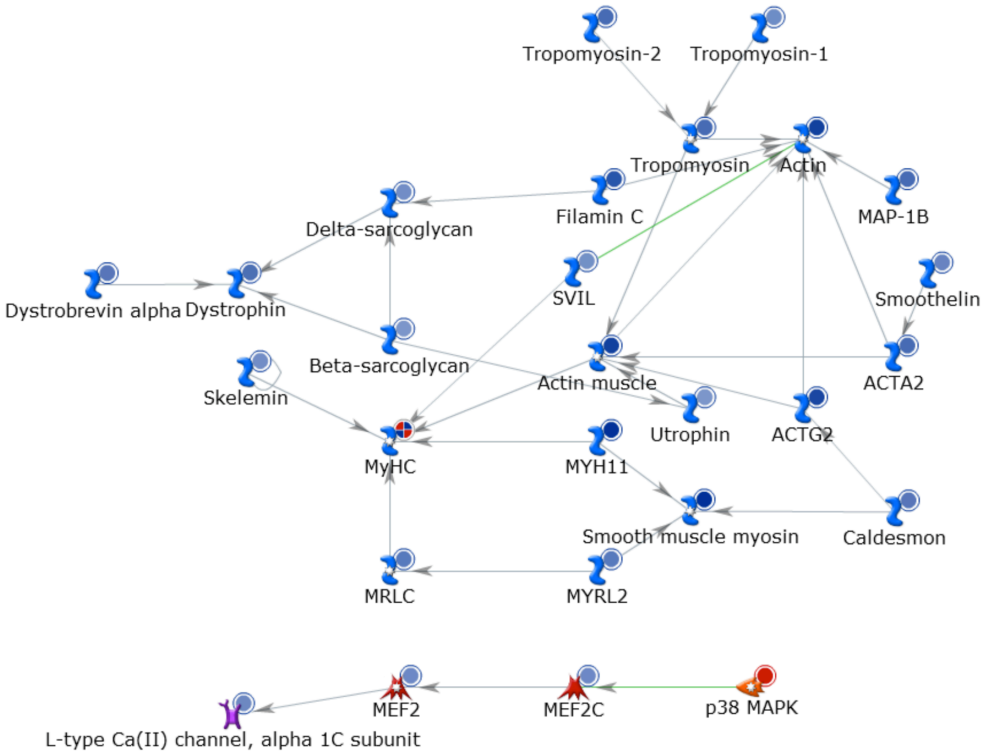

Figure 5.3. Genes implicated in myogenesis arte downregulated in BC samples (p = 1.22 x 10-10). The relative expression of each gene is represented by the colour and intensity of the circle, with blue representing downregulation and red representing upregulation.

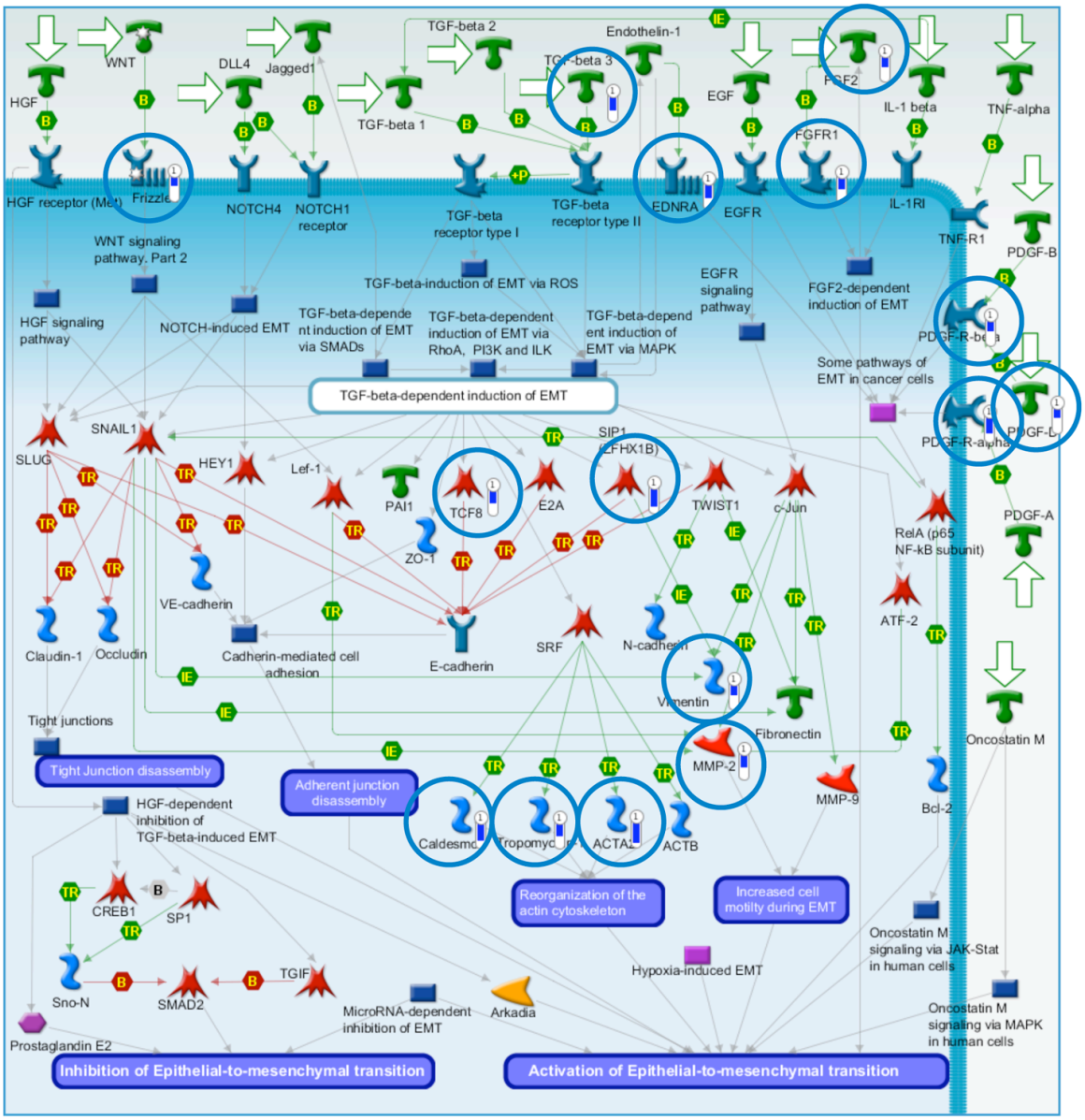

Figure 5.4. Downregulation of genes involved in EMT in BC samples (p = 1.41 x 10 -9). Key: Genes circled in blue displayed downregulation within the BC samples when compared to normal bladder tissue; the length of the adjacent blue bar depicts the extent of the downregulation.

5.2.1.2 Comparison of the expressional profiles of NMIBC and normal bladder tissue displays segregation into two groups with some branching

A comparison was made between NMIBC and normal tissue. Here 410 genes were identified with changes above 2.5-fold ($p<0.05$, FDR). Of the 410, 393 were downregulated in NIMBC, and 17 were upregulated in NMIBC (Table 5.1). Hierarchical clustering displayed segregation into two groups, but with further divergence in one cluster (Fig 5.5).

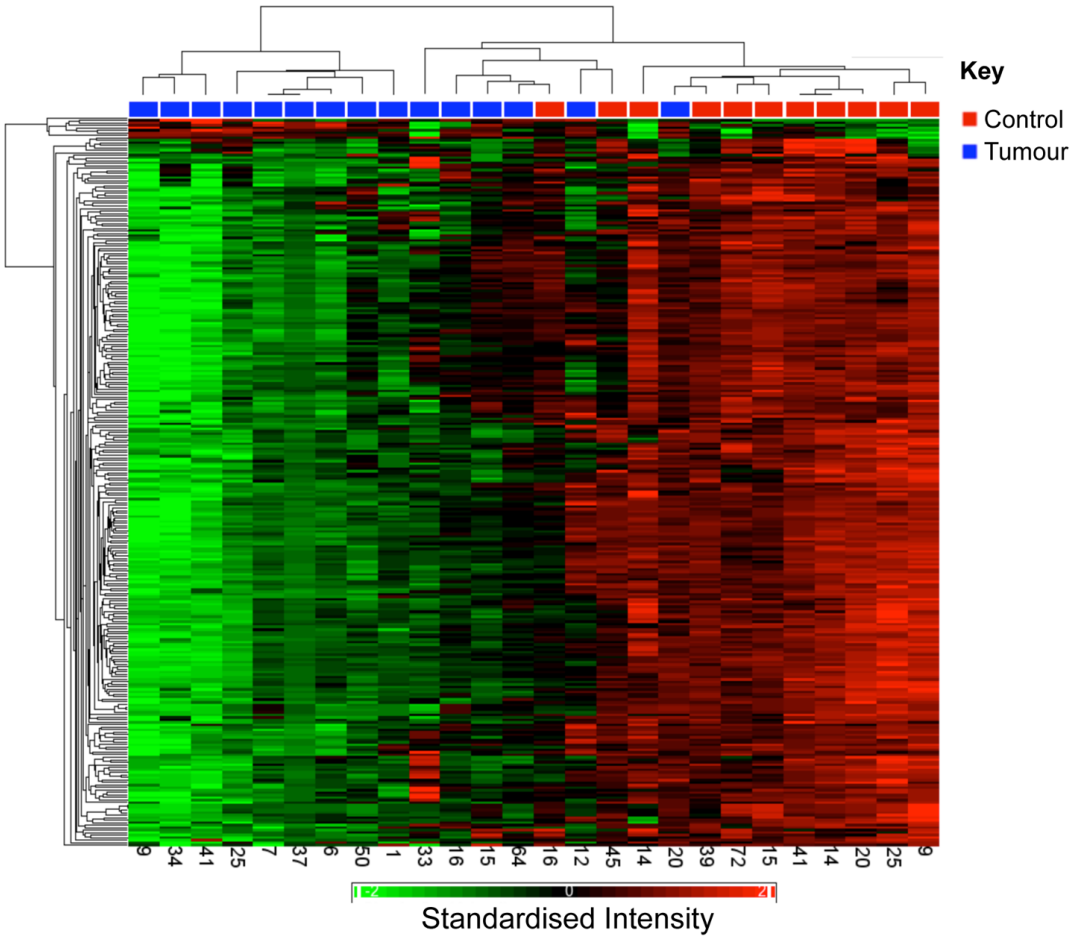

Figure 5.5. Hierarchical clustering displays clustering of NMIBC and normal bladder tissue with further branching. The key to the right of the figure denotes control and tumour sample labels, with anonymised patient serial numbers below.

Table 5.1. Genes upregulated with greatest fold change in NMIBC versus normal comparison. A fold-change cut-off of 2.5 and FDR <0.05 were used for filtration.

Gene Symbol	RefSeq	p-value	Fold-Change
HIATL1 – no obvious cancer relevance in literature	NM_032558	9.39E-05	3.39037
ESRP1 – shown in other cancers	NM_017697	0.000779	3.0231
TOX3 – Shown as a susceptibility factor in male BCR	NM_001080430	0.000469	2.80189
HK2 – role in glucose metabolism in cancer cells	NM_000189	5.14E-05	2.77546
HIST1H3F– no obvious cancer relevance in literature	NM_021018	0.00206	2.76721
CDH26 – no obvious cancer relevance in literature	NM_177980	0.00082	2.75204
ESRP2	NM_024939	4.09E-05	2.74268
ST14	NM_021978	0.000304	2.73635
MX2	NM_002463	0.000263	2.72833
CHMP4C	NM_152284	2.31E-05	2.6807
FABP6	NM_001040442	0.001337	2.67814
POF1B	NM_024921	0.000243	2.677
ZNF432	NM_014650	0.000244	2.64633
MYO5B	NM_001080467	0.000423	2.60563
ZNF841	NM_001136499	0.000197	2.56588
GRHL1	NM_198182	0.00166	2.55212
HIST1H2BH	NM_003524	0.002392	2.50504

In-line with the observed changes between BC samples and normal tissues, genes implicated in myogenesis and EMT were downregulated ($p = 4.8 \times 10^{-12}$). Intriguingly, genes implicated in the classical complement pathway were markedly underexpressed in NMIBC compared to normal tissue, indicating a potential mechanism of immune evasion ($p = 5.12 \times 10^{-10}$) (Fig 5.6).

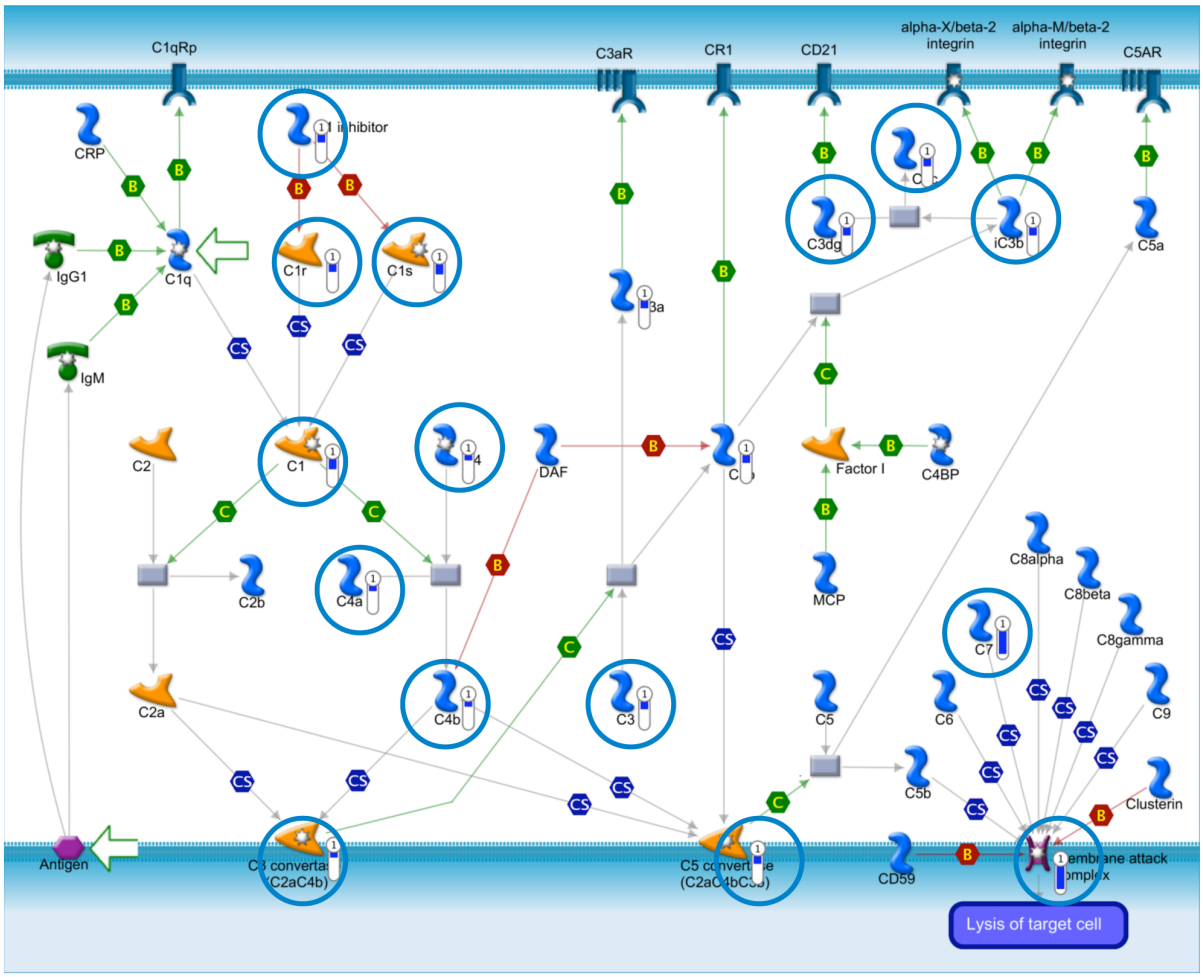

Figure 5.6. Genes implicated in the classical complement pathway are downregulated in NMIBC when compared to normal tissue (p = 5.12 x 10-10). Key: Blue circles represent downregulated genes and the blue bar to the right of each gene denotes the level of downregulation.

5.2.1.3 Comparison of MIBC and normal bladder tissue displays segregation into two distinct expressional profiles

Hierarchal clustering displays marked segregation between MIBC and normal bladder tissue samples into two distinct groups (Fig 5.7). In total 404 genes were dysregulated greater than 3-fold. ($p<0.05$ FDR). Out of the 404 genes, 107 were upregulated between MIBC and normal bladder tissue, whilst 297 were decreased in expression. Pathways augmented by these differentially expressed genes are noted in figure 5.8, with a list of genes upregulated by at least 5-fold being presented in table 5.2. Key genes implicated in chromosome condension in prometaphase were upregulated in MIBC ($p = 2.75 \times 10^{-15}$). Further cell cycle components were also upregulated, including regulators of the anaphase promoting complex (APC), including *PLK1* and *CDK1* ($p = 3.47 \times 10^{-12}$).

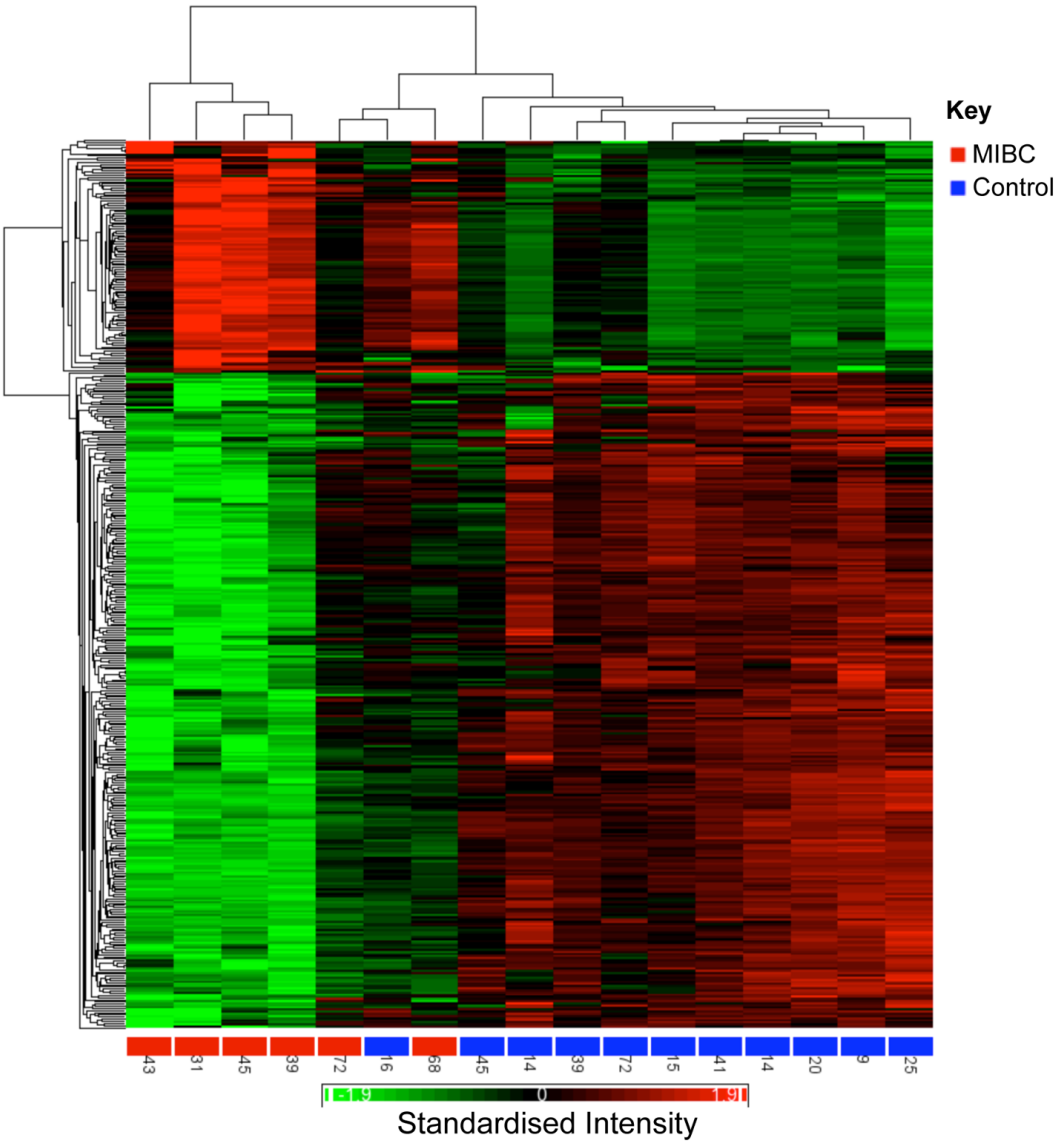

Figure 5.7. Hierarchical clustering of genes and tissue samples displays segregation of MIBC and normal bladder samples into distinct clusters. A key is displayed at the right of the figure; the numbers at the bottom of the figure denote anonymised patient serial numbers.

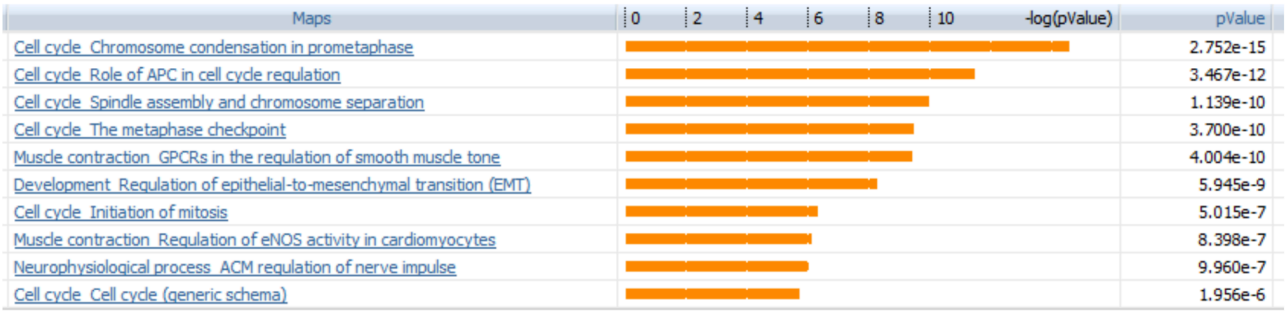

Figure 5.8. Pathway Enrichment: MIBC vs normal tissue control samples.

Table 5.2. Genes displaying greater than 5-fold increased expression in MIBC when compared to normal tissue samples.

Gene	Gene ID	RefSeq ID	p value	Fold change (MIBC versus control)
Secreted phosphoprotein 1 /osteopontin	*SPP1*	NM_001040058	0.000278942	10.9828
Anillin, actin binding protein	*ANLN*	NM_018685	0.000100265	8.49928
TPX2, microtubule-associated, homolog (Xenopus laevis)	*TPX2*	NM_012112	0.000281361	7.51978
Topoisomerase (DNA) II alpha 170kDa	*TOP2A*	NM_001067	0.000327502	7.07702
Matrix metalloproteinase 1	*MMP1*	NM_002421	4.53E-05	6.48753
Gasdermin C	*GSDMC*	NM_031415	2.47E-06	6.02525
N serpin peptidase inhibitor, clade B, member 13	*SERPINB13*	NM_012397	5.94E-06	5.98179
chloride channel accessory 2	*CLCA2*	NM_006536	0.00335894	5.61433
Antigen identified by monoclonal antibody Ki-67	*MKI67*	NM_002417	0.000992039	5.43103

Kinesin family member 23	*KIF23*	NM_138555	0.000252044	5.32734
Serpin peptidase inhibitor, clade B (ovalbumin), member3	*SERPINB3*	NM_006919	0.00367834	5.26492
Centromere protein F, 350/400ka (mitosin)	*CENPF*	NM_016343	0.00190184	5.1824
Family with sequence similarity 83, member A	*FAM83A*	NM_032899	3.54E-06	5.16728
cyclin E2	*CCNE2*	NM_057749	0.000232145	5.1512

5.2.1.4 A comparison of grade 1 and grade 3 NMIBC resulted in marked segregation between each group

A comparison between the expressional landscape of grade 1 and grade 3 NMIBCs revealed 341 genes to be differentially expressed at least 2-fold ($p<0.05$ FDR). Hierarchical clustering displayed marked segregation between grade 1 and grade 3 (Fig 5.9), enriched pathways are presented in figure 5.10. In comparison to grade 1 tumours multiple pathways associated with cell cycle progression were upregulated in grade 3 NMIBCs. Furthermore, genes implicated in the metaphase checkpoint were some of the most highly enriched ($p = 3.06 \times 10^{-17}$). A comparison was also made between genes that were upregulated in both grade 3 NMIBC compared to grade 1 NMIBC, and in MIBC compared to normal bladder tissue.

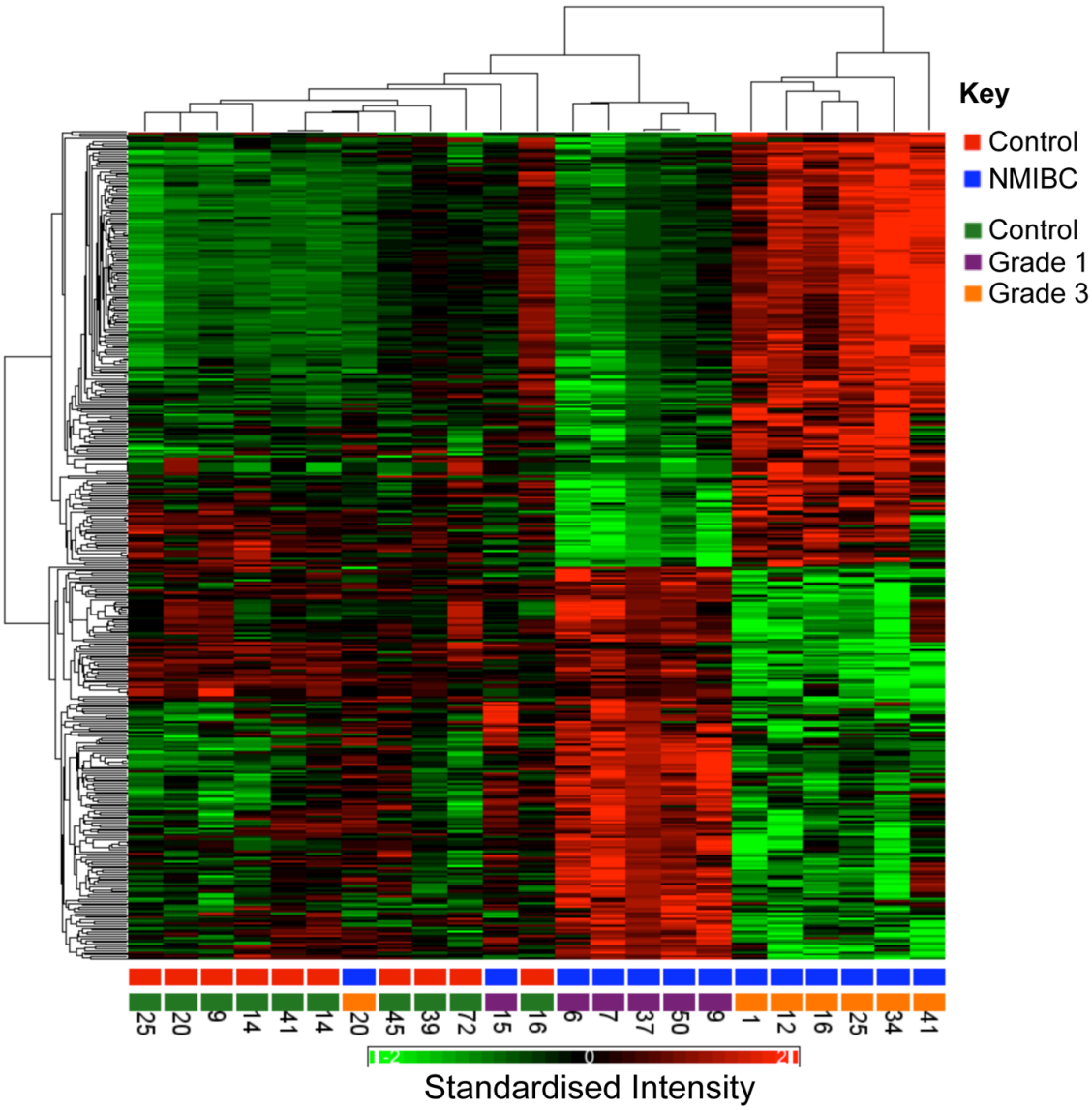

Figure 5.9. Hierarchical clustering displays well defined segregation between grade 1 and grade 3 NMIBC samples. The key is to the right of the figure; the numbers below represent anonymised patient serial numbers.

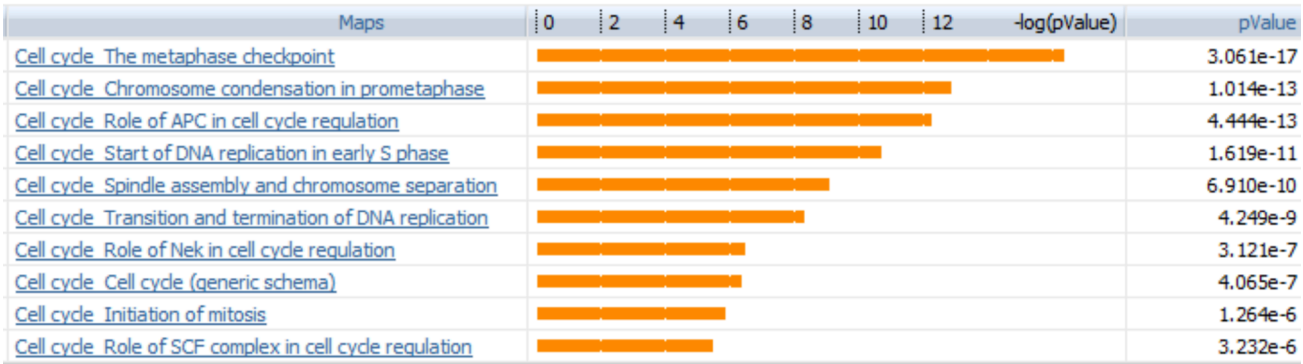

Figure 5.10. Pathway enrichment: Grade 3 NMIBC vs grade 1 NMIBC.

5.2.1.5 Comparing grade 3 NMIBC and MIBC resulted in clear segregation of both groups

A sum of 292 genes were differentially expressed greater than 2-fold ($P<0.05$). Of this group, 144 displayed increased expression in MIBC, whist 148 displayed decreased expression compared to grade 3 NMIBC. Furthermore, hierarchal clustering displayed a clear disparity between the two groups (Fig 5.11). Table 5.3 presents genes differentially expressed greater than 5-fold in grade 3 NMIBC when compared to MIBC. The proteinases were amongst the most overexpressed genes in MIBC. Overexpression and activation of proteinases is key in the remodelling of surrounding tumour-associated stroma, facilitating tumour cell invasion. The most proteolytic of these are the MMPs, which were highly overexpressed in MIBC, a family of enzymes that are collectively capable of degrading all components of the ECM. *MMP1* and *MMP16* were upregulated 4.8 and 2.6-fold respectively in MIBC compared to NMIBC. The overexpression of this group of proteins is likely imperative in the highly invasive and malignant MIBCs.

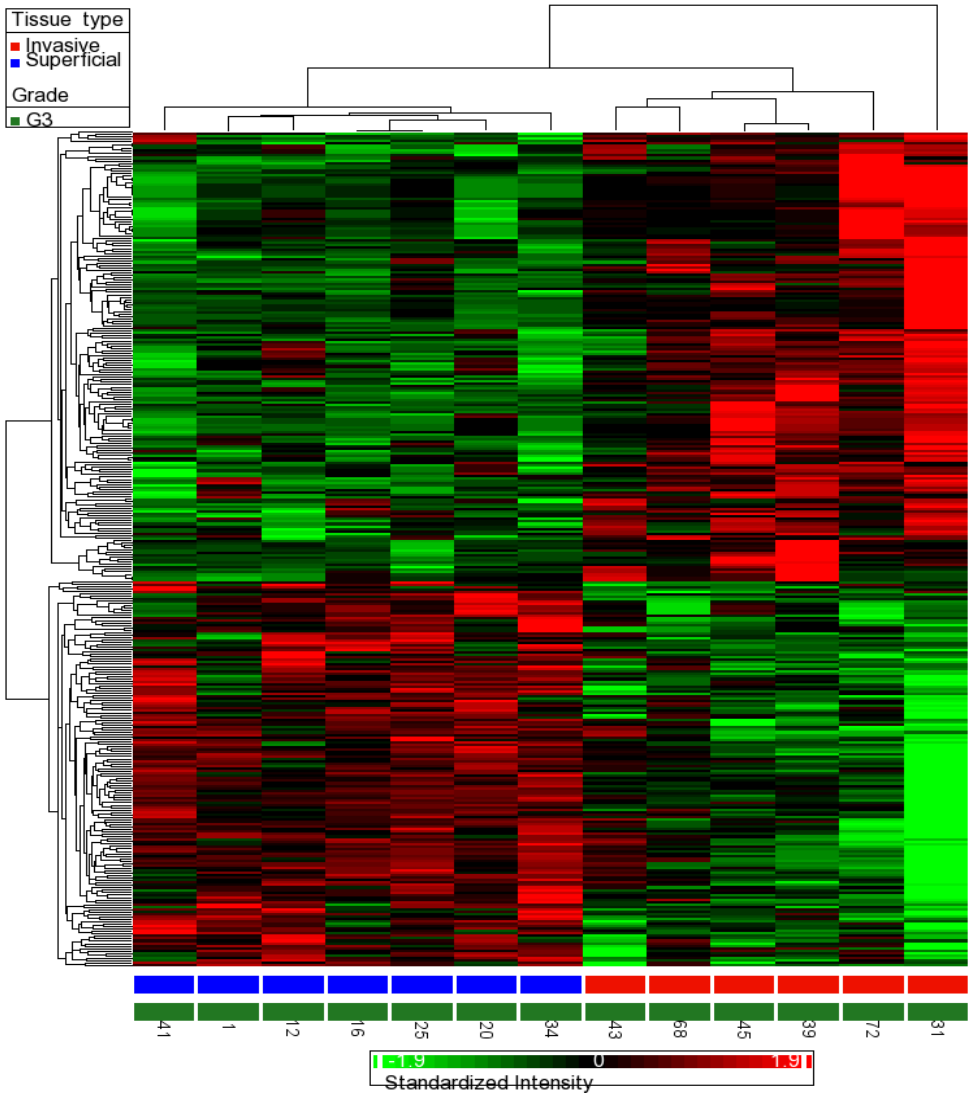

Figure 5.11. Hierarchal clustering displays a clear disparity between grade 3 NMIBC and MIBC. Key is to the right of the figure; the numbers below represent anonymised patient serial numbers.

Table 5.3. Genes displaying greater than 5-fold differential expression between grade 3 NMIBC and MIBC samples (p<0.05 FDR).

Gene	ID	RefSeq	p value	Fold change (MIBC/ NMIBC)
family with sequence similarity 83, member D	*FAM83D*	NM_030919	5.50E-06	7.87015
retinoic acid receptor responder (tazarotene induced) 1	*RARRES1*	NM_206963	0.001291	5.96921
centromere protein I	*CENPI*	NM_006733	1.35E-05	5.92042
fibronectin 1	*FN1*	NM_212482	0.000579	5.86325
centromere protein F, 350/400KDa (mitosin)	*CENPF*	NM_016343	0.000505	5.7622
N mannosidase, alpha, class 1C, member 1	*MAN1C1*	NM_020379	0.000401	5.52916
topoisomerase (DNA) II alpha 170kDa	*TOP2A*	NM_001067	0.00091	5.32363
TPX2, microtubule-associated, homolog (Xenopus laevis)	*TPX2*	NM_012112	0.000892	5.27537
Ras association (RalGDS/AF-6) domain family member 2	*RASSF2*	NM_014737	0.000644	5.04613
anillin, actin binding protein	*ANLN*	NM_018685	0.000489	5.01334

5.2.2 Further functional analysis employing Database for Annotation, Visualization, and Integrated Discovery (DAVID)

An additional analysis of 143 upregulated genes in MIBC compared to NMIBC, was performed using the DAVID database. These data are summarised in Table 5.4.

Table 5.4. Summary of DAVID analysis: functional annotation clusters.

Annotation cluster	Enrichment score	Count	p value
Extracellular glycoproteins	6.47	37	2.7E -07
Serine-type endopeptidase inhibitor activity	3.29	7	7.90E-05
Negative regulation of immune system processes	2.21	6	4.60E-04
Zymogen (proteolytic enzyme precursors)	1.85	14	5.10E -04
Cell migration	1.33	9	1.40E-03
EGF	1.18	5	1.50E-02
Response to wounding	0.95	13	8.20E-04

5.2.3 Meta-analysis of publicly available datasets

To validate these data, a meta-analysis was performed on a larger 90-sample data set, produced by merging two publicly available BC gene expression datasets [280, 281]. After the same benchmarks as used in our study were applied for classifying MIBC and NMIBC, there were 29 NMIBC and 42 MIBC cases, 14 cases were healthy bladder tissue samples, whilst the remainder represented *Cis* and were excluded from further analysis.

Meta-analysis revealed differential expression of 4513 genes in NMIBC, compared to normal tissue, when a cut off of FDR <0.05 and a fold-change of 2.5 were applied. Upon comparison with our data, there was commonality in 118 genes. Remarkably, except for pelota homolog (*PELO)*, all displayed comparable expression patterns. Including all 8 genes upregulated in NMIBC, and 109 genes downregulated in NMIBC, compared to normal bladder.

Upon comparison of MIBC to healthy bladder tissue, with a filter of FDR <0.05 and fold change >3, differential expression was noted in 3905 genes. Comparison with our data revealed 44 common differentially expressed genes. Except for SERPIN B13 (*SERPINEB13)* and *CASC5*, changes in expression shared commonality with our analyses.

5.2.4 Osteopontin protein is overexpressed in MIBC tissue compared to normal urothelium *

To determine the validity of microarray data, OPN expression was examined in MIBC (n=3), and normal urothelium (n=3) using immunohistochemistry. It was hypothesised that OPN would be expressed at a higher level in MIBC compared to healthy tissue.

5.2.4.1 Optimisation of OPN *primary antibody for immunohistochemistry* *

Firstly, the specificity of a candidate OPN antibody for IHC (AF1433 R&D Systems) was determined by western blot utilizing total protein lysates prepared from 253-J cells, and RT112 cells, representing MBC, and papillary NMIBC, respectively. Full length OPN expression was detected at the anticipated 66KDa in 253-J cells, with no non-specific binding. Interestingly, no expression was noted in RT112 cells (Fig 5.12).

The anti-OPN antibody binds specifically to OPN by western blot, in the predicted region next it will be tested for use in IHC in tissue.

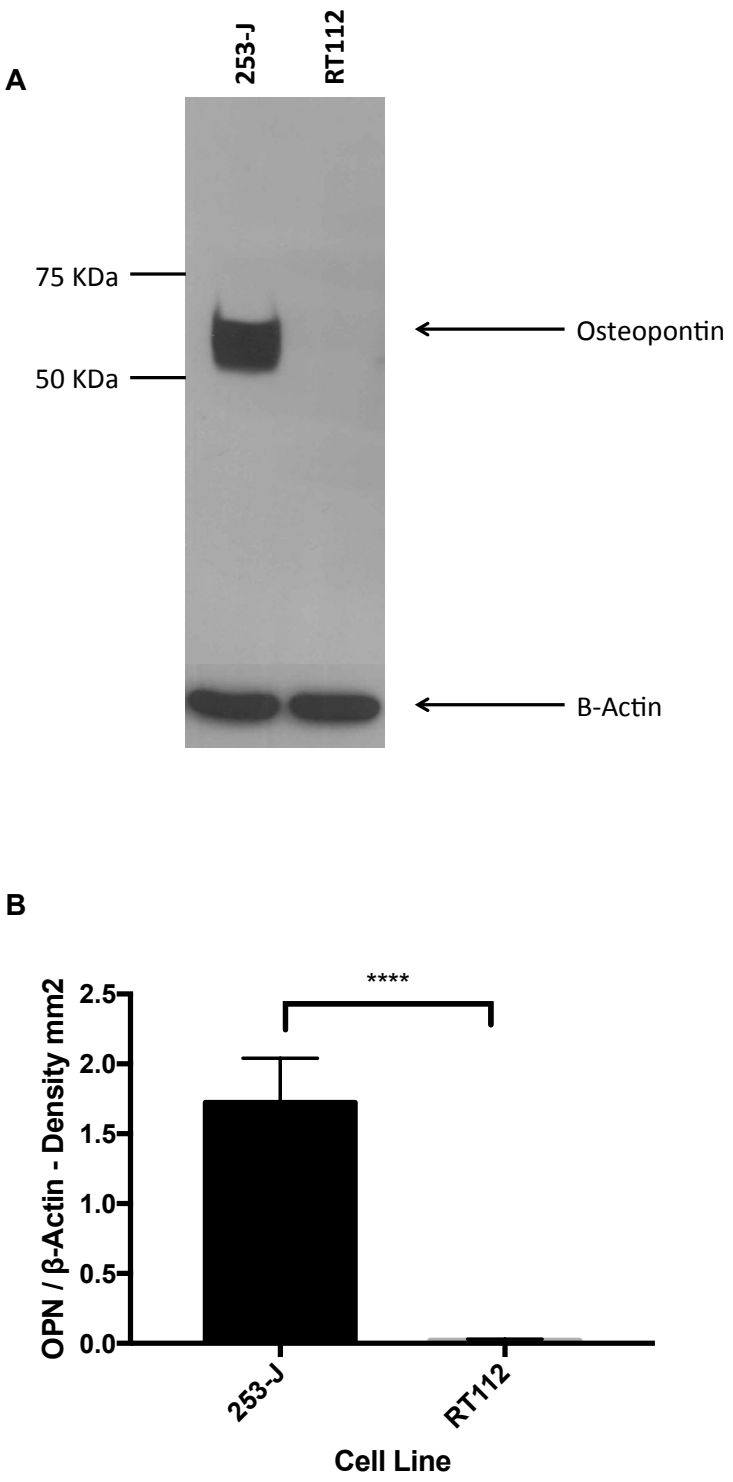

Figure 5.12. OPN expression in 253-J and RT112 cells. Anti-OPN displays specific binding, and expression of full length OPN (60-65Kda) in MBC 253-J cells, but no expression in NMIBC RT112 cells. Data is representative of four independent experiments. Statistical analysis unpaired t-test p=<0.0001.

5.2.4.1.2 Anti-OPN *binds selectively to inflammatory cells in colon adenocarcinoma, although displays weak positivity in colon adenocarcinoma cells **

To optimise the conditions for IHC, OPN-positive tissue is required. OPN highly expressed in bone, however sectioning bone tissue is technically challenging, and it may require different staining conditions than epithelial tumours. Large portions of advanced colon adenocarcinomas are reported to express high levels of OPN [337, 338]. Therefore, initial testing was performed in an advanced colon adenocarcinoma sample. Initially, three primary antibody dilutions were tested, 1:100, 1:500, 1:1000 and two secondary antibody concentrations, 1:100 and 1:200 (Fig 5.13).

No difference was apparent in staining between the two different concentrations of secondary antibody. However, staining with 1:100 anti-OPN caused unconvincing staining of adenocarcinoma cells, consistent with false positive staining. Strong positive staining was noted in areas of necrosis and in scant infiltrating inflammatory cells. False positive staining was diminished at dilutions below 1:500, with positive staining being evident in some non-adenocarcinoma cells at 1:1000.

The lack of positive staining in tumour cells may be due to too dilute primary antibody, or lack of OPN in this tissue. With the significant background staining in adenocarcinoma tissue evident at 1:100, different tissue sources for OPN will be tested, before increasing the concentration of primary antibody.

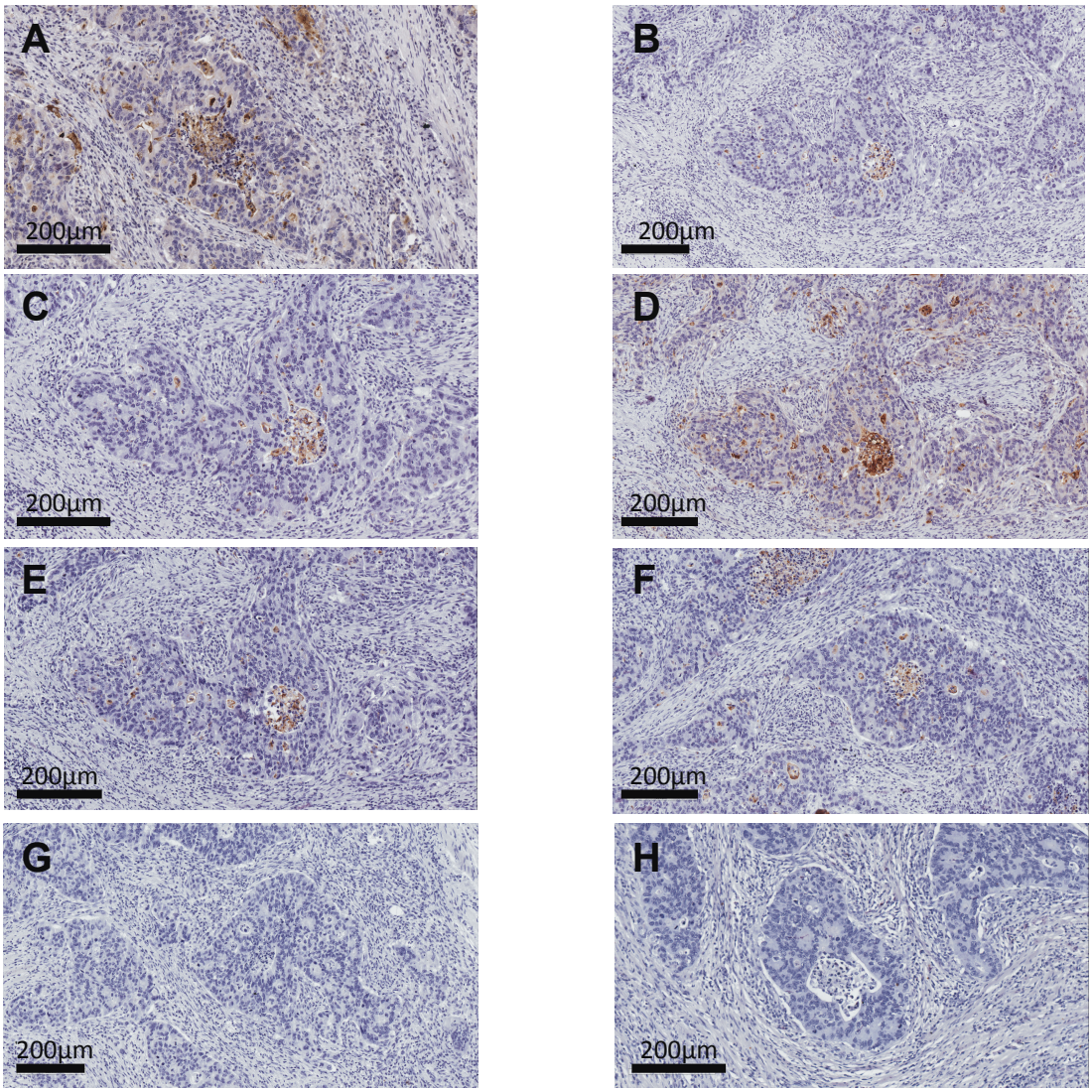

Figure 5.13. Osteopontin antibody optimisation in advanced colon adenocarcinoma. Conditions were as follows A) OPN 1°: 1:100, anti-Goat 2°: 1:100, B) OPN 1°: 1:500, anti-Goat 2°: 1:100, C) OPN 1°: 1:1000, anti-Goat 2°: 1:100, D) OPN 1°: 1:100, anti-Goat 2°: 1:200, E) OPN 1°: 1:500, anti-Goat 2°: 1:200, F) OPN 1°: 1:1000, anti-Goat 2°: 1:200, G) OPN 1°: N/A, anti-Goat 2°: 1:100, H) Isotype: 1:100, anti-Goat 2°: 1:100. (n=1).

*5.2.4.1.3 Anti-OPN displayed good staining in tubule cells of normal kidney, strong staining in clear-cell RCC cells **

Anti-OPN was tested at a dilution of 1:100 in clear cell renal carcinoma tissue, and normal kidney tissue, where OPN is reportedly expressed in the cells lining the tubules (Fig 5.14). Marked strong positive staining is evident in clear cell renal carcinoma cells. While some kidney tubules stain moderately for OPN. No staining was noted in negative controls.

With good staining being achieved in these tissues at a primary antibody dilution of 1:100, this concentration will now be tested on bladder normal bladder and tumour samples.

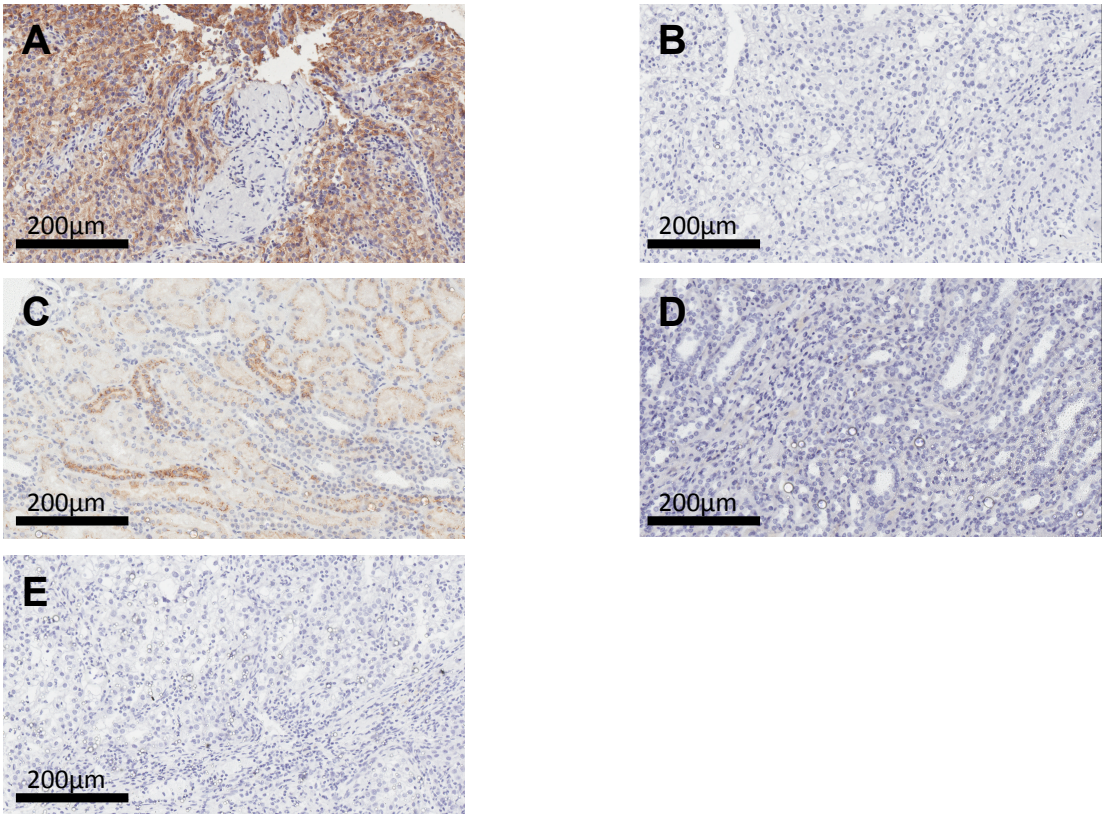

Figure 5.14. OPN staining in clear cell renal carcinoma (CCRC) and normal kidney tissue. A dilution of 1:100 primary antibody was used, and 1:100 for secondary antibody. A) CCRC stained for OPN, B) CCRC secondary antibody only, C) Normal kidney stained for OPN, D) Normal kidney secondary antibody only, E) CCRC Isotype. (n=1).

*5.2.4.1.4 Anti-OPN displays weak staining in bladder samples **

With good staining being displayed in other tissues, here six bladder tissue samples, consisting of normal bladder and MIBC samples (n=3), were stained using a primary antibody dilution of 1:100 (Fig 5.15). Strong staining was displayed in the CCRC positive control but not in normal tissue. Focal staining up-to moderate levels was apparent in MIBC samples. However, staining appeared faint in the bladder tissue. Therefore, a higher concentration of anti-OPN was attempted next.

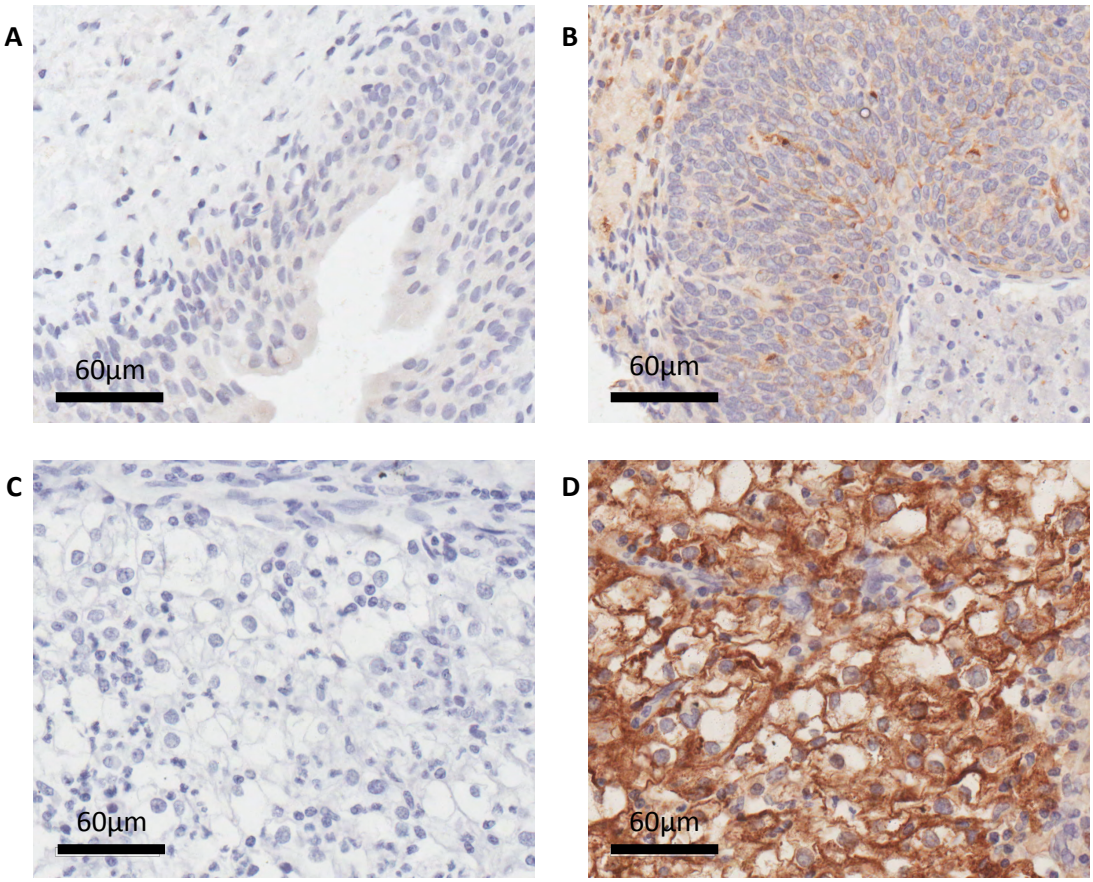

Figure 5.15. OPN staining in bladder using 1:100 anti-OPN. A) Normal urothelium, B) MIBC, C) Isotype control CCRC, D) Positive control CCRC. Images presented are representative of the cohort. (n=1).

*5.2.4.2 Osteopontin is overexpressed in MIBC samples **

To determine whether better staining could be achieved by increasing the concentration of primary antibody, a dilution of 1:50 was used. There was a marked increase in off target staining, most apparent when comparing the normal bladder sample between Fig 5.15 and Fig 5.16, OPN staining was improved.

As the paraffin embedded CCRC tissue block had ran out, kidney tissue was used for positive and negative controls.

A consultant pathologist, Dr Vijay Aachi, scored slides. Histopathological scoring a revealed moderate (++) cell membrane and cytoplasmic staining, whilst normal urothelium was typically OPN negative (-) (Fig 5.16). Non-specific background staining is evident as a uniform cytoplasmic 'blush' in normal urothelial tissue (Fig5.16A), whilst positive OPN-staining in MIBC samples is focal and granular in appearance (Fig5.16B).

There was a significant difference ($p=0.0286$) in the expression of OPN in normal bladder tissue and MIBC samples, with expression being markedly higher in MIBC tissue than normal urothelium. These data agree with that of the RNA microarray data in this chapter.

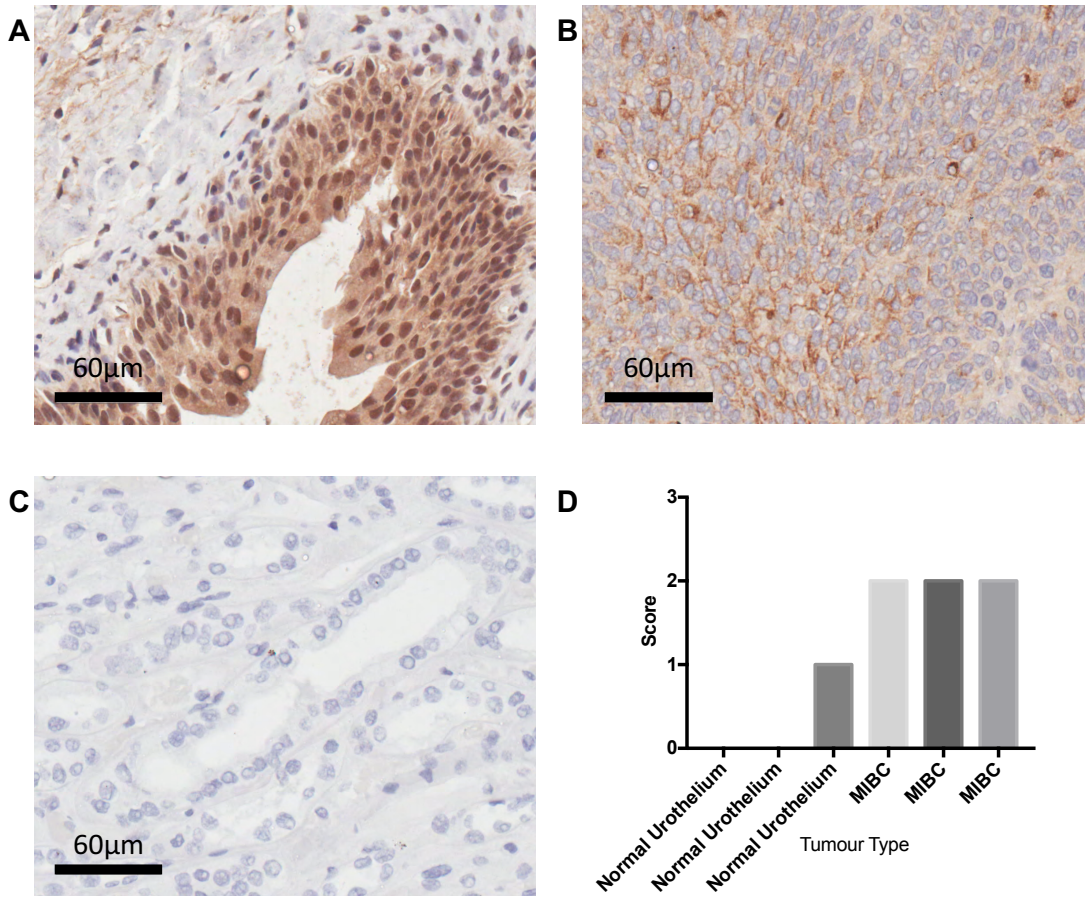

Figure 5.16. Osteopontin is overexpressed in MIBC when compared to normal bladder urothelium. A) Normal urothelium displaying negative OPN immunostaining, with the presence of non-specific binding in urothelial tissue; B) MIBC tissue exhibiting moderate (++) diffuse OPN immunostaining; C) Isotype control, OPN expressing kidney tissue with polyclonal goat IgG antibody; D) Graphical representation of staining results, results IHC staining from 3 normal urothelial samples, and 3 MIBCs, statistical analysis was performed using Welch's unpaired t test p = 0.0286. All images are representative of the cohort. (n=1).

5.3 Discussion

Work undertaken in this chapter supplements an ever-growing body of work that employs microarray data to profile BC. Allowing for new insights into pathways involved in BC pathogenesis. The primary aim of this chapter was to determine new pathways involved in BC, whilst secondary aims include the identification of drug targets and prognostic markers. This study identified distinctive patterns of gene expression differentiating between normal bladder tissue, NMIBC, and MIBC, and between high and low grade BCs.

A marked upregulation in pathways implicated in cell cycle management was seen upon comparison of MIBC and NMIBC, and between grade 1 and grade 3 NMIBCs. Interestingly, a significant overlap was apparent between genes upregulated in MIBC and in grade 3 NMIBC, compared to normal bladder. These genes were primarily those involved in cell cycle management. Potentially reflecting the increased aggressiveness, and likelihood of progression of grade 3 NMIBC, as such this panel may be useful in the prediction of progression to MIBC.

The cell cycle gene *ANLN* (upregulated >8-fold), a substrate of the APC - involved in cytokinesis [339]. *ANLN* is upregulated in a number of cancers including those of the pancreas and kidney [255, 256]. Interestingly, targeting protein for XKLP2 (*TPX2*), also involved in spindle assembly, was also upregulated [340].

The upregulation of genes in involved in the cell cycle in BC is not surprising, as similar findings have been reported previously [341]. Several upregulated genes have been identified as potential therapeutic targets for BCs. Inhibitors of TOP2A include two commonly used agents the anthacyclines, and etopopside. An example being doxorubicin, an anthacyclines, which exhibits marked anti-BC effects and is a component of the commonly used MVAC treatment combination. Polo-like kinase 1 (PLK-1) inhibitors such as volasertib have shown promise in *in vitro* models of BC, however in trials despite a favourable safety profile, insufficient anti-tumour activity was exhibited as monotherapy in a phase II trial treating MIBC [342-344]. However, its usefulness in combination therapy is yet

to be assessed in BC. Additionally, several CDK4/6 inhibitors are in trials for a range of tumours including bladder one example is recent phase I trial (ID: NCT02897375) where palbociclib, a selective inhibitor of CDK4/6, is being trailed in combination with cisplatin or carboplatin.

Overexpression of OPN has been noted in as strong tumour associated factor, with upregulation being noted in many tumours [345]. Furthermore, inhibition of OPN using RNA-silencing in significantly attenuates BC tumour cell invasion [260]. The marked (greater than 10-fold increase in RNA expression) upregulation of *OPN* levels demonstrated in this study is concordant with past studies demonstrating upregulation of *OPN* levels in BC [305, 306, 341, 346]. While *OPN* RNA expression data is well represented in BC tissue, protein expression data is more limited [305, 306, 346, 347]. Therefore OPN levels were investigated using IHC, to see if the effects on OPN RNA expression in MIBC were concordant with changes at the protein level. OPN was significantly ($p=0.0286$) overexpressed in MIBC compared to normal urothelium. This relationship is concordant with reports in cervical, gastric, oesophageal, and prostate cancers [346, 348-352]. Though, in upper urinary tract urothelial cell carcinoma significant association between OPN overexpression and poor prognosis was reported, with no relationship between with histopathological stage or grade [306]. Furthermore, it was interesting to note that the MBC cell line, 253-J, displayed OPN expression by western blot, whilst no OPN was detected in non-invasive RT112 cells. Conversely, OPN overexpression in pancreatic adenocarcinoma is linked with improved survival, highlighting the importance of cellular context on the outcome of cell signalling [353].

Elevated OPN levels have been detected in plasma of patients with advanced UCC, suggesting promise as a non-invasive biomarker of disease stage [261, 354]. However, the usefulness of OPN as a biomarker is yet to be proven [306, 346, 355]. The disparity between OPN tissue expression, and expression in plasma can partly be explained by the existence of OPN splice variants, and the cleavage of OPN by MMPs [356]. Notably, OPN splice variants, with distinct physiological functions, are differentially expressed in cancers [357]. Interestingly, expression

of CD44, a key OPN receptor, was found to be upregulated in MIBC further supporting an oncogenic role of *OPN* in UCC [354].

Upon comparison of grade 3 NMIBC and MIBC, overexpression of components in the cell-matrix interaction network was observed. Notably, upregulation was seen in proteolytic enzymes, such as the MMPs. These findings are consistent with the increased invasive ability of MIBC [195]. Mechanistically, it would be important to determine whether overexpression of certain proteolytic enzymes can cause NMIBC to invade muscle. Furthermore, overexpression of certain proteinases may predict progression of NMIBC.

Genes involved in EMT and myogenesis were downregulated in BC, chiefly between NMIBC and normal bladder tissue. Interestingly, this could represent BC exerting an inhibitory effect on the tumour microenvironment. EMT is a process where epithelial cells undergo transformation into mesenchymal cells, during this process epithelial cells lose their apical-basal polarity, intercellular junctions, epithelial markers, and up-regulate the expression of mesenchymal markers, developing front-rear polarity, and undergoing cytoskeletal reorganisation [358]. In cancer, EMT is associated with tumour invasion and metastasis, indicative of a poor prognosis [359]. Importantly this study did not use micro-dissection during sample preparation, it is therefore possible that the 'admixture' may have confounded the analysis of genes involved in EMT and myogenesis.

A novel discovery in this work is the downregulation of classical complement pathway genes in NMIBC. Consistent with these findings, the upregulation of complement inhibitors including CD46, and complement factor H (CFH) has previously been reported in BC [360]. These data suggest repression of complement activity is potentially important in BC pathogenesis. Interestingly, CFH may alter OPN activity through masking of enzyme cleavage sites [361].

Epithelial splicing regulatory proteins 1 and 2 (ESRP1 & ESRP2), involved in FGFR2 splicing, are upregulated in NMIBC, compared to normal tissue [362].

Interestingly, decreased variant FGFR2b expression has been observed in one group of BCs, whilst upregulation of FGFR2c was observed in a model of MBC [363, 364]. In agreement with the notion that different transcriptional isoforms are expressed during early carcinogenesis, this data supports a hypothesis implicating differential expression of FGFR2 splice variants as a key process in bladder carcinogenesis.

Availability of long-term clinical outcome data would have allowed for stronger conclusions to be drawn from the small cohort. However, meta-analysis of two further microarray data sets, together with the protein expression data highlight the significance of the presented data, and the role of OPN in tumour invasion [260]. Additionally, this work complements an increasingly rich wealth of molecular data in BC, allowing further understanding of this incredibly diverse, multifaceted disease.

In conclusion, this work supplements published literature and displays associations between certain gene expression landscapes with tumour stage and grade. Top dysregulated genes are potential gene signatures, which may be clinically useful when determining treatment options, where a more aggressive approach can be taken in those likely to progress. Notably, several pathways and genes were identified, including OPN and the classical complement pathway, shows marked dysregulation in BC, and may serve as drug targets.

Chapter Six – General discussion

6.1 Introduction 207

6.2 The utility of brusatol in BC and the future of NRF2 inhibition in cancer .. 208

6.3 The significance of CD40-signalling in bladder cancer 211

6.4 The importance gene expression analysis and biomarker identification in the advancement of bladder cancer care 213

6.5 Insight into the near and distant future of bladder cancer care 215

6.6 Concluding statements 218

6.1 Introduction

In recent decades little progress has been achieved to improve overall survival in BC, this includes the usage of systemic-GC in place of MVAC, allowing a lower incidence of adverse events and comparable response rates [17]. Furthermore, the outcome of the BC2001, a multi-centre phase 3 trial where 360 patients with MIBC were randomly assigned to undergo treatment with radiotherapy with or without concurrent chemotherapy, displayed a significant improvement in locoregional tumour control in patients treated with synchronous chemotherapy (5-Flourouracil and Mitomycin C), without a significant increase in adverse events [365, 366]. Importantly, the implementation of bladder-sparing treatment resulted in a significant increase in the quality of life for patients with BC [367, 368]. However, despite these progressions, the advancement of care in BC in terms of overall survival is severely lagging when compared to other high-incidence cancers.

This chapter will discuss how findings in this thesis fit-in with recent advances in BC, future pathways for the development of ideas presented in this thesis and the future of BC treatment, both in terms of impending advances, and long-term goals.

6.2 The utility of brusatol in BC and the future of NRF2 inhibition in cancer

Cisplatin based chemotherapy is often highly effective. However, a key barrier to successful treatment is the high incidence of acquired chemotherapy resistance associated with MIBC. Furthermore, a sub-classification of BC has been identified as intrinsically drug resistant [369]. Thus, attenuation of cisplatin resistance in BC would have significant implications in BC outcomes. The normally cytoprotective transcription factor, NRF2, has been implicated in chemotherapy resistance, as well as displaying oncogenic traits, promoting cell growth and proliferation [129]. Notably, inhibition of NRF2 levels by siRNA partially restores sensitivity to cisplatin in UCC cells [134]. In this work brusatol did increase the sensitivity of the majority of UCC cells to cisplatin although published data and that presented in this thesis do not indicate this is as a result of NRF2 inhibition.

Future work should follow up on two key findings of chapter three. Firstly, in most cell lines, the combination of brusatol and cisplatin led to increased sensitivity to cisplatin, which is in agreement with findings from *Ren et al,* where they demonstrate a marked reduction in tumour volume following brusatol and cisplatin combination therapy, when compared to control or either agent alone. Therefore, the benefit of combining brusatol and cisplatin should be explored further, using different dosage intervals and frequencies to determine the most effective regime. A key option to explore is pulsatile-dosing of brusatol to evoke sustained protein synthesis inhibition, theoretically allowing for the time-dependent depletion of proteins involved in cisplatin metabolism, once a time point for sufficient depletion of these genes is identified cisplatin may elicit increased efficacy. If further promise is found *in vitro*, *in vivo* experiments should be employed in order to evaluate the safety and efficacy of this combination.

Secondly, since brusatol displayed marked concentration-dependent inhibition of UCC and similar compounds such as silvestrol have displayed potential as anti-cancer treatments, the utility of brusatol as a standalone setting should be explored further in BC. Furthermore, *Ren et al* reports a reduction in tumour size, greater than that of cisplatin alone, when brusatol was used alone in a

murine xenograft model using A549 lung cancer cells. *In vitro* studies may begin by comparing the response in normal urothelial cell lines with UCC cells, whilst *in vivo* studies would be required to determine the systemic tolerability of brusatol and its efficacy in accepted murine models of BC such as the BBN-induced model of BC.

Brusatol may not be a specific inhibitor but the rationale behind NRF2 inhibition as a treatment for cisplatin-resistant BC is robust. Aside from its role in chemotherapy resistance, this is further exemplified by findings in recent years where NRF2 is described in an oncogenic context, highlighting the potential of NRF2 inhibition as a mode of promoting tumour death. Unfortunately, whilst there are some examples of NRF2 inducers such a dimethyl fumarate approved for clinical use, and a number in under investigation, including bardoxolone methyl (CDDO-Me), there are no approved inhibitors of NRF2, nor any currently in clinical trials.

Encouragingly, there have been reports of several potential inhibitors of NRF2, (For more information please see this comprehensive review of potential inhibitors of NRF2 [370]. Briefly, In A549 cells luteolin, a flavonoid, has been reported to reduce both mRNA and protein expression of NRF2 and increase sensitivity to chemotherapy, through increased *NRF2* mRNA degradation [371, 372]. Furthermore, luteolin has been demonstrated to display selective cytotoxicity to cancer cells, compared to non-cancer cells, including peripheral blood monocytes [372-374]. Similar effects have been noted in the flavanoids apigenin, and chrysin [375, 376]. Conversely, in rat cells luteolin initiates NRF2 and MAPK signalling, exerting a cytoprotective role [377]. The antitubercular drug, isoniazid, has been demonstrated to inhibit the NRF2-pathway, purportedly through the inhibition of NRF2 mRNA [378]. Other drugs used in the antitubercular class including ethanbutol, dihydrochloride, ethionamide, rifampicin and sparfloxacin have also been demonstrated to have inhibitory effects on NRF2 [370]. Vitamin C, ascorbic acid, a well-recognised antioxidant, has been shown to inhibit NRF2 activation through the inhibition of NRF2 nuclear translocation, showing chemopotentiating effects in cancer cell lines

[379]. Finally, retinoic acid has been demonstrated as an inhibitor of NRF2 activation through the heterodimerisation of retinoid acid receptor α and retinoid X receptor α, and subsequent inhibitor binding of NRF2 [380].

6.3 The significance of CD40-signalling in bladder cancer

CD40 receptor activation leads to a plethora of context-dependent changes in cellular behaviour. CD40 regulates the immune response and cell defence, in some cases, inducing the maturation of immune cells including peripheral blood monocytes. Although the effects of CD40-ligation are not confined to the immune system. In BC cell lines CD40-ligation with mCD40L leads to marked apoptotic induction. This response is the net outcome of pro-apoptotic, and anti-apoptotic signalling mediated by the TRAFs. Furthermore, CD40 is highly expressed in BC, making it an interesting putative drug target. Interestingly, CD40-ligation has been implicated in direct tumour cell death and immune-activation that can increase the anti-tumour response to CD40-directed therapy, furthermore CD40-ligation is reported to enhance immune cell motility and infiltration, however little is known about the role of CD40-ligation in tumour cell invasion [323].

Using an organotypic three-dimensional model of BC, chapter 4 aimed to determine whether CD40-ligation induced pro- or anti- invasive effects. A key secondary aim was to identify genes involved invasive change. Notably, marked cell death, and attenuation of invasion was observed, whilst CD40-expressing tumour cells did not invade. The BC tissue gene expression microarray data presented in chapter 5 and a microarray comparing gene expression between AdMock and AdNclCD40L treated EJ cells were cross-referenced, *MMP1*, *FN1*, *FAM83D* and *ANLN* were selected for further analysis, due to marked differential expression in both datasets, supported by evidence for their implementation in tumour invasion, growth or proliferation. Expression of all four genes was confirmed by endpoint RT-PCR and FN1 and MMP1 expression was examined at the protein level by western blot. Interestingly, discordance was noted between mRNA and protein levels of FN1 were noted in EJ cells. However, these data did not explain the marked inhibition of tumour-invasion noted in organotypic models.

In order to determine the mode of invasion inhibition further experimentation is needed. Initially the potential anti-invasive effect of apoptotic induction should

be explored, using current knowledge of CD40-ligation mediated apoptosis to identify targets for commercially available inhibitors of apoptosis, or siRNAs. If tumour invasion is not attenuated by inhibition of apoptosis, the downstream effects of CD40-ligation should be scrutinised further. Due to the broad-reaching effects of CD40-ligation, scrutinisation of differentially expressed genes may be an extensive process. Therefore, a similar rational design to chapter 4, where large datasets are used to identify a small panel of potential effectors may be the most-time efficient method. Additionally, as we understand more about molecularly distinct subtypes of BC, candidate effectors can be selected with increased confidence. Exploration of the effects of on tumour motility and invasion can be performed using siRNA in monolayer experiments such as scratch-assays. Markers displaying promise can be analysed in more complex models, such as an organotypic model of BC where lentiviral silencing and adenoviral infection can be added to determine the effects of up, and down-regulation of specific genes.

The immune activating and cell-death inducing effects of CD40-ligation have led to marked interest as a drug target. Agonistic antibodies have shown encouraging results in pre-clinical and phase I studies. A recent phase I study in solid tumours has reported activation of B and NK cells at well tolerated doses, indicating potential in combination with chemotherapy [381]. In pancreatic cancer the usage of a CD40 agonistic antibody, CP-870, 893, in a phase I trial revealed promising anti-tumour activity in combination with chemotherapy, whilst a phase I study of the same agonistic antibody with carboplatin and paclitaxel, for advanced solid tumours, produced promising results warranting phase II studies [382, 383]. Finally, in murine models a locally delivered CD40 agonistic antibody leads to eradication of MBC [384].

6.4 The importance gene expression analysis and biomarker identification in the advancement of bladder cancer care

In NMIBC 20% of patients will progress to MIBC, whilst under half of MIBC patients will survive 5 years' post-diagnosis, with survival down to only 6% of patients with MBC. The current histological staging and grading system does not accurately determine which tumours are most likely to progress to life threatening disease. Thus, there is rationale for the exploration of alternative methods of disease stratification for more accurate diagnosis. Gene-expression analyses in cancer can allow for the association of distinct expressional profiles, with disease stage and grade. Additionally, expressional profiles can be used to determine traits involved in progression, useful in prognostication.

In this study, distinct clustering was noted in a number of different comparisons between normal bladder tissue, NMIBC tissue, and MIBC tissue. Furthermore, expressional signatures were suggested that might be predictive of stage and grade, also highlighting some genes that may be involved in tumour progression, notably between grade 3 NMIBC and MIBC.

In recent years, there has been an extensive effort to define the expressional, mutational, epigenetic and proteomic landscape of BCs. These analyses have resulted in the formation of molecularly distinct subsets of BC, some with similarities to tumours at different anatomical sites, that may be predictive of response to therapy, survival and disease progression [369, 385-387]. Further integration of multiple-'omics' data with clinicopathological features and outcomes may allow the development of diagnostic tests with predictive and prognostic value.

Overexpressed in the plasma of patients with MIBC, in this thesis OPN expression was also upregulated in MIBC tissues, indicating prognostic potential. However, exploration of OPN as a blood biomarker of BC should be pursued prior to tissue, as a non-invasive method of disease monitoring is direly needed.

In order to determine the validity of OPN as a plasma available model of BC, blood samples could be collected from groups of healthy volunteers, NMIBC patients, and MIBC patients. After plasma preparation, detection of various OPN isoforms by the enzyme-linked immunosorbent assay (ELISA) could then be correlated with clinicopathological features, and outcomes.

6.5 Insight into the near and distant future of bladder cancer care

One of the key challenges in developing new regimens for the treatment of BC is the demographic of BC patients. The target population is elderly, often harbouring co-morbidities, some smoking associated such as renal dysfunction, and poor performance status. These traits necessitate the development of well-tolerated regimes. The usage of novel targeted-therapies in BC aims to deliver potent tumour killing, with fewer systemic side effects than conventional cytotoxic chemotherapy. Promising emerging treatments include inhibitors of T-cell checkpoint molecules, programmed cell death protein 1 (PD1) and programmed death-ligand 1 (PD-L1), and anti-angiogenics. Inhibition of both PD1 and PD-L1 durable responses in patients with advanced MIBC, previously challenged with platinum-based chemotherapy [388, 389]. Interestingly, when treated with the PD-L1 inhibitor, atezolizumab, response-rates were increased in patients with higher expression of PD-L1 in immune cells [388, 390]. Atezolizumab and the PD1 inhibitor, pembrolizumab, are both being investigated in phase III trials as second line treatments, in comparison to vinfluinine or taxanes. Additionally, several checkpoint inhibitors are being investigated as a first line treatment in platinum-ineligible patients, one example being durvalumab, a recent PD-L1 inhibitor, which is under-investigation in a three-arm phase III trial, where it is being tested in cisplatin-ineligible and –eligible patients: comparing GC, durvalumab alone, and durvalumab plus tremeliumab, an inhibitor of cytotoxic T-lymphocyte-associated antigen 4 (CTLA4). With adjuvant atezolizumab, nivolumab, and pembrolizumab being under phase III investigation, post-cystectomy, in patients with- or without neoadjuvant chemotherapy for MIBC.

Interestingly, cabozatinib, responsible for the inhibition of vascular endothelial growth factor receptors (VEGFRs) and c-MET, displays activity in preliminary studies and is associated with an increase in PD1 expression in regulatory T-cells, suggesting potential in combination with PD1 inhibition [391]. Although a number of VEGFR tyrosine kinase inhibitors (TKIs) have not demonstrated significant benefit in phase II trains, both alone (pazopanib, sunitinib) and in

combination with chemotherapy (sorafenib, vandetanib) [392-395]. Conversely, the VEGFR-2 inhibitor, ramucirumab, extended progression free survival (PFS) in combination with docetaxel in a phase II trial and is currently under phase III analysis [396]. A multicentre phase II trial, NEOBLADE, is currently assessing the benefit of the triple angiokinase (VEGFR, FGFR, platelet derived growth factor receptor (PDGFR)) inhibitor Nintedanib, in addition to GC in the neoadjuvant setting. Additionally, regorafenib, a TKI that inhibits VEGFRs, FGFR1 and the angiopoietin-tyrosine kinase 2-axis, is under phase II evaluation in the second line setting for advanced BC.

Several other agents have performed well in select groups of patients. Molecular profiling of tumour tissue has suggested a number of potential therapeutic targets including constituents of the EGFR family, mTOR pathway, MAPK pathway and pathways controlling the G1/S phase checkpoint [385, 397]. Moreover, patients with tumours containing tuberous sclerosis 1 (TSC1) and mTOR mutations display marked response to everolimus [398, 399]. Contrarily, the human epidermal growth factor receptor (HER)-2 inhibitors trastuzumab and lapatinib did not improve outcomes in HER2 or EGFR-expressing MBC patients [400, 401]. However, afatinib demonstrated activity in patients with tumours containing HER2, or HER3 mutation or amplification [402]. Differences in response have been demonstrated between TKIs of divergent potency. The use of FGFR inhibitors in patients harbouring FGFR2 and FGFR3 alterations is associated with durable response, however, the usage of the less potent inhibitor, dovitinib, does not display significant activity in FGFR3-altered patients. These findings highlight the importance of both target and drug [403-405]. The CDK(4/6) inhibitor, palbociclib, approved in breast cancer, is currently under rational evaluation in a population of patients with functional retinoblastoma protein (RB) and either CDK inhibitor 2A-negative tumours, or cyclin D1 protein overexpression by IHC. Interestingly, histone deacetylase inhibitors are also under investigation in BC, due to the enhanced expression of these targets in BC [385]. Interestingly, novel preparations of current cytotoxic drugs are also under investigation with encouraging results, one example being nanoparticle albumin-bound-paclitaxel [406].

The identification of discreet molecular subtypes of BC by gene expression profiling may have consequences in the implementation of personalised care [369, 385, 387, 407]. Briefly, the basal subclassification is proposed as being more chemosensetive, whilst the luminal subclassification identifies FGFR, HER2 and HER3 as targets, finally the mesenchymal/claudin-low subclassification is rich in T-cell checkpoint targets [369, 407].

The ever-growing number of clinical trials in BC is a direct result of our-increased understanding of the molecular underpinnings of this disease. Translational medicine allows for the integration of high-throughput target mining techniques such as gene expression profiling, and next generation sequencing, with pre-clinical *in vitro and in vivo* analyses, which feed into clinical trials. Work in this thesis identifies potential targets such as OPN, whilst recently published work chiefly that by *Choi et al,* Damrauer *et al* and TGCA highlights a range of targets [369, 385, 407]. With further integration of data spanning multiple-'omics', more targets will be discovered in BC, fuelling the generation of multimodal therapies in BC. Excitingly, the future of BC care looks brighter with new better tolerated treatments in phase II and III trials, offering advantageous survival, treatments building upon recent findings may offer a new-generation in treatment for BC, where the implementation of checkpoint inhibitors, angiokinase inhibitors and CD40-agonsits in the clinic is the first phase in this personalised approach. Furthermore, with an increased number of putative targets and therapies the implementation of umbrella trials is an interesting trial design for personalised therapy – here patient treatment is stratified by target expression. Finally, as pan-cancer gene-expression profiles emerge, the basket trial design is very attractive; in this approach eligibility is based on the tumour expression profile, rather than location.

6.6 Concluding statements

This thesis demonstrates techniques used in the identification of drug targets, prognostic markers, and pre-clinical development of cancer therapies.

Here the molecular aspects of BC have been analysed in BC tissue using gene expression profiling techniques, allowing for more insight into gene expression patterns in BC and their relation to stage and grade. Here a number of potential expressional signatures were proposed and expression of OPN was revealed to be associated with MIBC. However, further studies are required to determine the clinical validity of the proposed expressional signatures, whilst mechanistic investigations are needed to determine the passenger/driver status of the presented alterations.

Targeted inhibition of NRF2 was evaluated with its putative inhibitor, brusatol, whilst brusatol inhibited NRF2 expression, it did not affect downstream protein expression. Furthermore, recently published work by *Vartanian et al* questioned the specificity of brusatol to NRF2, describing it as a global inhibitor or protein synthesis. However, brusatol does increase the sensitivity of UCC cells to cisplatin, and as a stand-alone agent it potently evokes marked toxicity on UCC cells, warranting further research in this setting – especially considering the promise of similar molecules such as silvesterol.

The implication of CD40-ligation on CD40-positive UCC invasion was investigated in an organotypic model of BC. Marked cell death was observed in NMIBC RT112 cells treated with AdNclCD40L, whilst distinct attenuation of invasion was observed in MIBC EJ cells, accompanied by marked cell death. IHC staining for CD40L revealed a lack of CD40 expression on invading cells. Gene-expression analysis data comparing grade 3 NMIBC and MIBC highlighted genes potentially involved in invasion, this data was cross-referenced with gene expression data comparing EJ cells treated with AdMock or AdNclCD40L. The expression of four candidates were confirmed in EJ and RT112 cells at the mRNA level, whilst relative changes in FN1 and MMP1 expression in response to

AdNclCD40L-ligation were observed, indicating increased expression of proteins involved in tumour invasion, with discordance between *FN1* and FN1 expression. These data highlight a role of CD40-ligation in the attenuation of tumour cell invasion, however, the mechanisms for this process are yet to be determined. Further analysis should determine whether apoptotic-induction plays a role in the inhibition of tumour-cell invasion. Furthermore, pharmacological inhibition and gene silencing should be employed in-order to determine the role of altered downstream genes in invasion.

Chapter Seven – Bibliography

1. Hanahan, D.a.W., R. , *The Hallmarks of Cancer.* Cell 2000. **100**: p. 57-70.
2. Hanahan, D. and R.A. Weinberg, *Hallmarks of cancer: the next generation.* Cell, 2011. **144**(5): p. 646-74.
3. Hussain, S. and N. James, *Molecular markers in bladder cancer.* Seminars in Radiation Oncology, 2005. **15**(1): p. 3-9.
4. Derrickson, G.J.T.a.B.H., *Principles of Anatomy and Physiology* 12 ed. Principles of Anatomy and Physiology Vol. 1. 2009: Wiley Publishing Group 1200.
5. Truschel, S.T., et al., *Primary uroepithelial cultures. A model system to analyze umbrella cell barrier function.* J Biol Chem, 1999. **274**(21): p. 15020-9.
6. Jost, S.P., J.A. Gosling, and J.S. Dixon, *The morphology of normal human bladder urothelium.* Journal of Anatomy, 1989. **167**: p. 103-115.
7. Hicks, R.M., *THE MAMMALIAN URINARY BLADDERAN ACCOMMODATING ORGAN.* Biological Reviews, 1975. **50**(2): p. 215-246.
8. Wu, X.-R., et al., *Uroplakins in Urothelial Biology, Function and Disease.* Kidney international, 2009. **75**(11): p. 1153-1165.
9. Andersson, K.E. and K.D. McCloskey, *Lamina propria: the functional center of the bladder?* Neurourol Urodyn, 2014. **33**(1): p. 9-16.
10. Mitra, A.P. and R.J. Cote, *Molecular pathogenesis and diagnostics of bladder cancer.* Annu Rev Pathol, 2009. **4**: p. 251-85.
11. Mitra, A.P., M. Jorda, and R.J. Cote, *Pathological possibilities and pitfalls in detecting aggressive bladder cancer.* Curr Opin Urol, 2012. **22**(5): p. 397-404.
12. UK, C.R., http://www.cancerresearchuk.org. Website, 2015.
13. UK, C.R., *Survival statistics for bladder cancer.* Cancer Research UK Website, 2014.
14. Sangar, V.K., et al., *The economic consequences of prostate and bladder cancer in the UK.* BJU Int, 2005. **95**(1): p. 59-63.
15. Avritscher, E.B., et al., *Clinical model of lifetime cost of treating bladder cancer and associated complications.* Urology, 2006. **68**(3): p. 549-53.
16. Tomlinson, D.C., et al., *FGFR1-induced epithelial to mesenchymal transition through MAPK/PLCgamma/COX-2-mediated mechanisms.* PLoS One, 2012. **7**(6): p. e38972.
17. Galsky, M.D., et al., *Comparative effectiveness of gemcitabine plus cisplatin versus methotrexate, vinblastine, doxorubicin, plus cisplatin as neoadjuvant therapy for muscle-invasive bladder cancer.* Cancer, 2015. **121**(15): p. 2586-93.
18. Excellence, N.I.f.H.a.C., *Bladder cancer: diagnosis and managment* in *Diagnosis and managment* 2016, National Institute for Health and Care Excellence https://http://www.nice.org.uk/guidance/ng2/resources.
19. Als, A.B., et al., *Emmprin and survivin predict response and survival following cisplatin-containing chemotherapy in patients with advanced bladder cancer.* Clin Cancer Res, 2007. **13**(15 Pt 1): p. 4407-14.
20. Clavel, J., et al., *Tobacco and bladder cancer in males: increased risk for inhalers and smokers of black tobacco.* Int J Cancer, 1989. **44**(4): p. 605-10.

21. Burch, J.D., et al., *Risk of bladder cancer by source and type of tobacco exposure: a case-control study.* Int J Cancer, 1989. **44**(4): p. 622-8.
22. Hoffman, D., Y. Masuda, and E.L. Wynder, *Alpha-naphthylamine and beta-naphthylamine in cigarette smoke.* Nature, 1969. **221**(5177): p. 255-6.
23. Pfeifer, G.P., et al., *Tobacco smoke carcinogens, DNA damage and p53 mutations in smoking-associated cancers.* Oncogene, 2002. **21**(48): p. 7435-51.
24. Case, R.A.M. and M.E. Hosker, *Tumour of the Urinary Bladder as an Occupational Disease in the Rubber Industry in England and Wales.* British Journal of Preventive and Social Medicine, 1954. **8**(2): p. 39-50.
25. Brown, T., R. Slack, and L. Rushton, *Occupational cancer in Britain. Urinary tract cancers: bladder and kidney.* Br J Cancer, 2012. **107 Suppl 1**: p. S76-84.
26. Burger, M., et al., *Epidemiology and risk factors of urothelial bladder cancer.* Eur Urol, 2013. **63**(2): p. 234-41.
27. Stadler, W., *Molecular events in the initiation and progression of bladder-cancer (review).* Int J Oncol, 1993. **3**(4): p. 549-57.
28. Cole, P., *Originally published as Volume 1, Issue 7713COFFEE-DRINKING AND CANCER OF THE LOWER URINARY TRACT.* The Lancet, 1971. **297**(7713): p. 1335-1337.
29. Hartge, P., et al., *Coffee drinking and risk of bladder cancer.* J Natl Cancer Inst, 1983. **70**(6): p. 1021-6.
30. D'Avanzo, B., et al., *Coffee consumption and bladder cancer risk.* Eur J Cancer, 1992. **28A**(8-9): p. 1480-4.
31. Hoover, R.N. and P.H. Strasser, *Artificial sweeteners and human bladder cancer. Preliminary results.* Lancet, 1980. **1**(8173): p. 837-40.
32. Reuber, M.D., *Carcinogenicity of saccharin.* Environmental Health Perspectives, 1978. **25**: p. 173-200.
33. Brinkman, M., et al., *Use of selenium in chemoprevention of bladder cancer.* Lancet Oncol, 2006. **7**(9): p. 766-74.
34. Amaral, A.F., et al., *Selenium and bladder cancer risk: a meta-analysis.* Cancer Epidemiol Biomarkers Prev, 2010. **19**(9): p. 2407-15.
35. Chen, F., et al., *Association of vitamin C, vitamin D, vitamin E and risk of bladder cancer: a dose-response meta-analysis.* Scientific Reports, 2015. **5**: p. 9599.
36. Piper, J.M., J. Tonascia, and G.M. Matanoski, *Heavy phenacetin use and bladder cancer in women aged 20 to 49 years.* N Engl J Med, 1985. **313**(5): p. 292-5.
37. Antoni, S., et al., *The ban on phenacetin is associated with changes in the incidence trends of upper-urinary tract cancers in Australia.* Aust N Z J Public Health, 2014. **38**(5): p. 455-8.
38. Kaye, J.A., M.W. Myers, and H. Jick, *Acetaminophen and the risk of renal and bladder cancer in the general practice research database.* Epidemiology, 2001. **12**(6): p. 690-4.
39. Fairchild, W.V., et al., *The incidence of bladder cancer after cyclophosphamide therapy.* J Urol, 1979. **122**(2): p. 163-4.
40. Shaw, I.C. and M.I. Graham, *Mesna--a short review.* Cancer Treat Rev, 1987. **14**(2): p. 67-86.

41. Habs, M.R. and D. Schmahl, *Prevention of urinary bladder tumors in cyclophosphamide-treated rats by additional medication with the uroprotectors sodium 2-mercaptoethane sulfonate (mesna) and disodium 2,2'-dithio-bis-ethane sulfonate (dimesna).* Cancer, 1983. **51**(4): p. 606-9.
42. Duncan, R.E., et al., *Radiation-induced bladder tumors.* J Urol, 1977. **118**(1 Pt 1): p. 43-5.
43. Kaldor, J.M., et al., *Bladder tumours following chemotherapy and radiotherapy for ovarian cancer: a case-control study.* Int J Cancer, 1995. **63**(1): p. 1-6.
44. Rausch, S., et al., *[Squamous cell lesions of the urinary bladder].* Urologe A, 2014. **53**(3): p. 368, 370-4.
45. Welk, B., et al., *Bladder cancer in individuals with spinal cord injuries.* Spinal Cord, 2013. **51**(7): p. 516-521.
46. Pannek, J., *Transitional cell carcinoma in patients with spinal cord injury: a high risk malignancy?* Urology, 2002. **59**(2): p. 240-4.
47. Locke, J.R., D.E. Hill, and Y. Walzer, *Incidence of squamous cell carcinoma in patients with long-term catheter drainage.* J Urol, 1985. **133**(6): p. 1034-5.
48. Groah, S.L., et al., *Excess risk of bladder cancer in spinal cord injury: evidence for an association between indwelling catheter use and bladder cancer.* Arch Phys Med Rehabil, 2002. **83**(3): p. 346-51.
49. Silverman, D.T., et al., *Epidemiology of bladder cancer.* Hematol Oncol Clin North Am, 1992. **6**(1): p. 1-30.
50. Lucey, D.R. and J.H. Maguire, *Schistosomiasis.* Infect Dis Clin North Am, 1993. **7**(3): p. 635-53.
51. Badawi, A.F., *Molecular and genetic events in schistosomiasis-associated human bladder cancer: role of oncogenes and tumor suppressor genes.* Cancer Lett, 1996. **105**(2): p. 123-38.
52. *<Rang Pharmacology.pdf>.*
53. Alberg, A.J., et al., *N-acetyltransferase 2 (NAT2) genotypes, cigarette smoking, and the risk of breast cancer.* Cancer Detect Prev, 2004. **28**(3): p. 187-93.
54. Marcus, P.M., P. Vineis, and N. Rothman, *NAT2 slow acetylation and bladder cancer risk: a meta-analysis of 22 case-control studies conducted in the general population.* Pharmacogenetics, 2000. **10**(2): p. 115-22.
55. McIlwain, C.C., D.M. Townsend, and K.D. Tew, *Glutathione S-transferase polymorphisms: cancer incidence and therapy.* Oncogene, 0000. **25**(11): p. 1639-1648.
56. Sobti, R.C., et al., *Genetic polymorphisms of CYP2D6, GSTM1, and GSTT1 genes and bladder cancer risk in North India.* Cancer Genet Cytogenet, 2005. **156**(1): p. 68-73.
57. Ouerhani, S., et al., *The role of CYP2D6*4 variant in bladder cancer susceptibility in Tunisian patients.* Bull Cancer, 2008. **95**(2): p. E1-4.
58. Anwar, W.A., et al., *Genetic polymorphism of GSTM1, CYP2E1 and CYP2D6 in Egyptian bladder cancer patients.* Carcinogenesis, 1996. **17**(9): p. 1923-9.
59. van der Post, R.S., et al., *Risk of urothelial bladder cancer in Lynch syndrome is increased, in particular among MSH2 mutation carriers.* Journal of Medical Genetics, 2010. **47**(7): p. 464-470.

60. Fletcher, O., et al., *Lifetime risks of common cancers among retinoblastoma survivors.* J Natl Cancer Inst, 2004. **96**(5): p. 357-63.
61. Marees, T., et al., *Risk of second malignancies in survivors of retinoblastoma: more than 40 years of follow-up.* J Natl Cancer Inst, 2008. **100**(24): p. 1771-9.
62. Gallagher, D.J., A. Feifer, and J.A. Coleman, *Genitourinary cancer predisposition syndromes.* Hematol Oncol Clin North Am, 2010. **24**(5): p. 861-83.
63. Lindor, N.M., et al., *Concise handbook of familial cancer susceptibility syndromes - second edition.* J Natl Cancer Inst Monogr, 2008(38): p. 1-93.
64. Letasiova, S., et al., *Bladder cancer, a review of the environmental risk factors.* Environ Health, 2012. **11 Suppl 1**: p. S11.
65. Fernandez, M.I., et al., *Long-term impact of arsenic in drinking water on bladder cancer health care and mortality rates 20 years after end of exposure.* J Urol, 2012. **187**(3): p. 856-61.
66. Villanueva, C.M., et al., *Bladder cancer and exposure to water disinfection by-products through ingestion, bathing, showering, and swimming in pools.* Am J Epidemiol, 2007. **165**(2): p. 148-56.
67. Cosyns, J.P., *Aristolochic acid and 'Chinese herbs nephropathy': a review of the evidence to date.* Drug Saf, 2003. **26**(1): p. 33-48.
68. Yang, H.Y., P.C. Chen, and J.D. Wang, *Chinese herbs containing aristolochic acid associated with renal failure and urothelial carcinoma: a review from epidemiologic observations to causal inference.* Biomed Res Int, 2014. **2014**: p. 569325.
69. Shinagare, A.B., et al., *Metastatic Pattern of Bladder Cancer: Correlation With the Characteristics of the Primary Tumor.* American Journal of Roentgenology, 2011. **196**(1): p. 117-122.
70. Grignon, D.J., *The current classification of urothelial neoplasms.* Mod Pathol, 0000. **22**(S2): p. S60-S69.
71. Chou, R., et al., *Treatment of muscle-invasive bladder cancer: A systematic review.* Cancer, 2016. **122**(6): p. 842-51.
72. Bohle, A. and P.R. Bock, *Intravesical bacille Calmette-Guerin versus mitomycin C in superficial bladder cancer: formal meta-analysis of comparative studies on tumor progression.* Urology, 2004. **63**(4): p. 682-6; discussion 686-7.
73. Shen, Z., et al., *Intravesical Treatments of Bladder Cancer: Review.* Pharmaceutical Research, 2008. **25**(7): p. 1500-1510.
74. Manoharan, M., *Intravesical therapy for urothelial carcinoma of the bladder.* Indian J Urol, 2011. **27**(2): p. 252-61.
75. Furuse, H. and S. Ozono, *Transurethral resection of the bladder tumour (TURBT) for non-muscle invasive bladder cancer: basic skills.* Int J Urol, 2010. **17**(8): p. 698-9.
76. Lee, S.E., et al., *Impact of transurethral resection of bladder tumor: analysis of cystectomy specimens to evaluate for residual tumor.* Urology, 2004. **63**(5): p. 873-7; discussion 877.
77. Aldousari, S. and W. Kassouf, *Update on the management of non-muscle invasive bladder cancer.* Canadian Urological Association Journal, 2010. **4**(1): p. 56-64.

78. Engilbertsson, H., et al., *Transurethral bladder tumor resection can cause seeding of cancer cells into the bloodstream.* J Urol, 2015. **193**(1): p. 53-7.
79. Antoniewicz, A.A., et al., *Lack of evidence for increased level of circulating urothelial cells in the peripheral blood after transurethral resection of bladder tumors.* International Urology and Nephrology, 2012. **44**(3): p. 761-767.
80. King, M.J. and W.H. Park, *Effect of Calmette's BCG Vaccine on Experimental Animals.* Am J Public Health Nations Health, 1929. **19**(2): p. 179-92.
81. Morales, A., D. Eidinger, and A.W. Bruce, *Intracavitary Bacillus Calmette-Guerin in the treatment of superficial bladder tumors.* J Urol, 1976. **116**(2): p. 180-3.
82. Chapman, P.B. and A.N. Houghton, *Non-antibody immunotherapy of cancer.* Curr Opin Immunol, 1993. **5**(5): p. 726-31.
83. Sylvester, R.J., M.A. van der, and D.L. Lamm, *Intravesical bacillus Calmette-Guerin reduces the risk of progression in patients with superficial bladder cancer: a meta-analysis of the published results of randomized clinical trials.* J Urol, 2002. **168**(5): p. 1964-70.
84. Shelley, M.D., et al., *A systematic review of intravesical bacillus Calmette-Guerin plus transurethral resection vs transurethral resection alone in Ta and T1 bladder cancer.* BJU Int, 2001. **88**(3): p. 209-16.
85. Kapoor, R., V. Vijjan, and P. Singh, *Bacillus Calmette-Guérin in the management of superficial bladder cancer.* Indian Journal of Urology : IJU : Journal of the Urological Society of India, 2008. **24**(1): p. 72-76.
86. Mendez-Samperio, P. and E. Garcia-Martinez, *CD40 ligand expression in mycobacterium bovis BCG infection and its regulation by cytokines: a direct role of interleukin 12.* Arch Med Res, 2001. **32**(2): p. 108-12.
87. Redelman-Sidi, G., M.S. Glickman, and B.H. Bochner, *The mechanism of action of BCG therapy for bladder cancer--a current perspective.* Nat Rev Urol, 2014. **11**(3): p. 153-62.
88. Hofbauer, S.L., et al., *The Moreau Strain of Bacillus Calmette-Guerin (BCG) for High-Risk Non-Muscle Invasive Bladder Cancer: An Alternative during Worldwide BCG Shortage?* Urol Int, 2016. **96**(1): p. 46-50.
89. Torti, F.M., et al., *Alpha-interferon in superficial bladder cancer: a Northern California Oncology Group Study.* J Clin Oncol, 1988. **6**(3): p. 476-83.
90. Belldegrun, A.S., et al., *Superficial bladder cancer: the role of interferon-alpha.* J Urol, 1998. **159**(6): p. 1793-801.
91. Glashan, R.W., *A randomized controlled study of intravesical alpha-2b-interferon in carcinoma in situ of the bladder.* J Urol, 1990. **144**(3): p. 658-61.
92. Kalble, T., et al., *[BCG vs interferon A for prevention of recurrence of superficial bladder cancer. A prospective randomized study].* Urologe A, 1994. **33**(2): p. 133-7.
93. Ghoneim, M.A., et al., *Radical cystectomy for carcinoma of the bladder: critical evaluation of the results in 1,026 cases.* J Urol, 1997. **158**(2): p. 393-9.
94. Sweeney, P., E.D. Kursh, and M.I. Resnick, *Partial cystectomy.* Urol Clin North Am, 1992. **19**(4): p. 701-11.
95. James, N.D., et al., *Radiotherapy with or without chemotherapy in muscle-invasive bladder cancer.* N Engl J Med, 2012. **366**(16): p. 1477-88.

96. Hussain, S.A., et al., *A study of split-dose cisplatin-based neo-adjuvant chemotherapy in muscle-invasive bladder cancer.* Oncol Lett, 2012. **3**(4): p. 855-859.
97. Siddik, Z.H., *Cisplatin: mode of cytotoxic action and molecular basis of resistance.* Oncogene, 2003. **22**(47): p. 7265-79.
98. von der Maase, H., *Gemcitabine and cisplatin in locally advanced and/or metastatic bladder cancer.* Eur J Cancer, 2000. **36 Suppl 2**: p. 13-6.
99. von der Maase, H., et al., *Gemcitabine and cisplatin versus methotrexate, vinblastine, doxorubicin, and cisplatin in advanced or metastatic bladder cancer: results of a large, randomized, multinational, multicenter, phase III study.* J Clin Oncol, 2000. **18**(17): p. 3068-77.
100. Koster, R., et al., *Unravelling mechanisms of cisplatin sensitivity and resistance in testicular cancer.* Expert Rev Mol Med, 2013. **15**: p. e12.
101. Dimri, K., et al., *Conventional radiotherapy with concurrent weekly Cisplatin in locally advanced head and neck cancers of squamous cell origin - a single institution experience.* Asian Pac J Cancer Prev, 2013. **14**(11): p. 6883-8.
102. Johnson, D.H., *Evolution of cisplatin-based chemotherapy in non-small cell lung cancer: a historical perspective and the eastern cooperative oncology group experience.* Chest, 2000. **117**(4 Suppl 1): p. 133S-137S.
103. Helm, C.W. and J.C. States, *Enhancing the efficacy of cisplatin in ovarian cancer treatment – could arsenic have a role.* Journal of Ovarian Research, 2009. **2**: p. 2-2.
104. Dasari, S. and P.B. Tchounwou, *Cisplatin in cancer therapy: molecular mechanisms of action.* European journal of pharmacology, 2014. **0**: p. 364-378.
105. Marechal, R., et al., *Human equilibrative nucleoside transporter 1 and human concentrative nucleoside transporter 3 predict survival after adjuvant gemcitabine therapy in resected pancreatic adenocarcinoma.* Clin Cancer Res, 2009. **15**(8): p. 2913-9.
106. Matsumura, N., et al., *The prognostic significance of human equilibrative nucleoside transporter 1 expression in patients with metastatic bladder cancer treated with gemcitabine-cisplatin-based combination chemotherapy.* BJU Int, 2011. **108**(2 Pt 2): p. E110-6.
107. Kim, R., et al., *Prognostic roles of human equilibrative transporter 1 (hENT-1) and ribonucleoside reductase subunit M1 (RRM1) in resected pancreatic cancer.* Cancer, 2011. **117**(14): p. 3126-34.
108. Greenhalf, W., et al., *Pancreatic cancer hENT1 expression and survival from gemcitabine in patients from the ESPAC-3 trial.* J Natl Cancer Inst, 2014. **106**(1): p. djt347.
109. Jordheim, L.P., et al., *Increased expression of the large subunit of ribonucleotide reductase is involved in resistance to gemcitabine in human mammary adenocarcinoma cells.* Mol Cancer Ther, 2005. **4**(8): p. 1268-76.
110. Vollrath, V., et al., *Role of Nrf2 in the regulation of the Mrp2 (ABCC2) gene.* Biochem J, 2006. **395**(3): p. 599-609.
111. Rocha, C.R.R., et al., *Glutathione depletion sensitizes cisplatin- and temozolomide-resistant glioma cells in vitro and in vivo.* Cell Death Dis, 2014. **5**: p. e1505.

112. Chen, H.H.W. and M.T. Kuo, *Role of Glutathione in the Regulation of Cisplatin Resistance in Cancer Chemotherapy.* Metal-Based Drugs, 2010. **2010**.
113. Zhang, K., et al., *Modulation of cisplatin cytotoxicity and cisplatin-induced DNA cross-links in HepG2 cells by regulation of glutathione-related mechanisms.* Mol Pharmacol, 2001. **59**(4): p. 837-43.
114. Reed, E., *ERCC1 and Clinical Resistance to Platinum-Based Therapy.* Clinical Cancer Research, 2005. **11**(17): p. 6100-6102.
115. Britten, R.A., et al., *ERCC1 expression as a molecular marker of cisplatin resistance in human cervical tumor cells.* Int J Cancer, 2000. **89**(5): p. 453-7.
116. Chiu, T.J., et al., *High ERCC1 expression predicts cisplatin-based chemotherapy resistance and poor outcome in unresectable squamous cell carcinoma of head and neck in a betel-chewing area.* J Transl Med, 2011. **9**: p. 31.
117. Muallem, M.Z., et al., *ERCC1 expression as a predictor of resistance to platinum-based chemotherapy in primary ovarian cancer.* Anticancer Res, 2014. **34**(1): p. 393-9.
118. Olaussen , K.A., et al., *DNA Repair by ERCC1 in Non–Small-Cell Lung Cancer and Cisplatin-Based Adjuvant Chemotherapy.* New England Journal of Medicine, 2006. **355**(10): p. 983-991.
119. Horibe, S., et al., *Cisplatin resistance in human lung cancer cells is linked with dysregulation of cell cycle associated proteins.* Life Sci, 2015. **124**: p. 31-40.
120. Lee, J.M., et al., *Nrf2, a multi-organ protector?* FASEB J, 2005. **19**(9): p. 1061-6.
121. Kansanen, E., et al., *The Keap1-Nrf2 pathway: Mechanisms of activation and dysregulation in cancer.* Redox Biol, 2013. **1**: p. 45-9.
122. Osburn, W.O. and T.W. Kensler, *Nrf2 signaling: an adaptive response pathway for protection against environmental toxic insults.* Mutat Res, 2008. **659**(1-2): p. 31-9.
123. Ishii, T., *Transcription Factor Nrf2 Coordinately Regulates a Group of Oxidative Stress-inducible Genes in Macrophages.* Journal of Biological Chemistry, 2000. **275**(21): p. 16023-16029.
124. Harder, B., et al., *Molecular mechanisms of Nrf2 regulation and how these influence chemical modulation for disease intervention.* Biochemical Society Transactions, 2015. **43**(4): p. 680-686.
125. Bryan, H.K., et al., *The Nrf2 cell defence pathway: Keap1-dependent and -independent mechanisms of regulation.* Biochem Pharmacol, 2013. **85**(6): p. 705-17.
126. Kaspar, J.W. and A.K. Jaiswal, *An autoregulatory loop between Nrf2 and Cul3-Rbx1 controls their cellular abundance.* J Biol Chem, 2010. **285**(28): p. 21349-58.
127. Kwak, M.K., et al., *Enhanced expression of the transcription factor Nrf2 by cancer chemopreventive agents: role of antioxidant response element-like sequences in the nrf2 promoter.* Mol Cell Biol, 2002. **22**(9): p. 2883-92.
128. Kitteringham, N.R., et al., *Proteomic analysis of Nrf2 deficient transgenic mice reveals cellular defence and lipid metabolism as primary Nrf2-*

dependent pathways in the liver. Journal of Proteomics, 2010. **73**(8): p. 1612-1631.
129. Geismann, C., et al., *Cytoprotection "gone astray": Nrf2 and its role in cancer.* Onco Targets Ther, 2014. **7**: p. 1497-518.
130. Yu, X. and T. Kensler, *Nrf2 as a target for cancer chemoprevention.* Mutat Res, 2005. **591**(1-2): p. 93-102.
131. Satoh, H., et al., *Nrf2-deficiency creates a responsive microenvironment for metastasis to the lung.* Carcinogenesis, 2010. **31**(10): p. 1833-43.
132. Rachakonda, G., et al., *Increased cell migration and plasticity in Nrf2-deficient cancer cell lines.* Oncogene, 2010. **29**(25): p. 3703-14.
133. Lau, A., et al., *Dual roles of Nrf2 in cancer.* Pharmacol Res, 2008. **58**(5-6): p. 262-70.
134. Hayden, A., et al., *The Nrf2 transcription factor contributes to resistance to cisplatin in bladder cancer.* Urol Oncol, 2014. **32**(6): p. 806-14.
135. Lister, A., et al., *Nrf2 is overexpressed in pancreatic cancer: implications for cell proliferation and therapy.* Mol Cancer, 2011. **10**: p. 37.
136. Bao, L.J., et al., *Nrf2 induces cisplatin resistance through activation of autophagy in ovarian carcinoma.* Int J Clin Exp Pathol, 2014. **7**(4): p. 1502-13.
137. Ji, L., et al., *Nrf2 pathway regulates multidrug-resistance-associated protein 1 in small cell lung cancer.* PLoS One, 2013. **8**(5): p. e63404.
138. Cho, J.M., et al., *Role of the Nrf2-antioxidant system in cytotoxicity mediated by anticancer cisplatin: implication to cancer cell resistance.* Cancer Lett, 2008. **260**(1-2): p. 96-108.
139. Syu, J.P., J.T. Chi, and H.N. Kung, *Nrf2 is the key to chemotherapy resistance in MCF7 breast cancer cells under hypoxia.* Oncotarget, 2016. **7**(12): p. 14659-72.
140. Payen, L., et al., *The drug efflux pump MRP2: Regulation of expression in physiopathological situations and by endogenous and exogenous compounds.* Cell Biology and Toxicology, 2002. **18**(4): p. 221-233.
141. Yamasaki, M., et al., *Role of multidrug resistance protein 2 (MRP2) in chemoresistance and clinical outcome in oesophageal squamous cell carcinoma.* Br J Cancer, 2011. **104**(4): p. 707-13.
142. Schondorf, T., et al., *Cisplatin, doxorubicin and paclitaxel induce mdr1 gene transcription in ovarian cancer cell lines.* Recent Results Cancer Res, 2003. **161**: p. 111-6.
143. Godwin, A.K., et al., *High resistance to cisplatin in human ovarian cancer cell lines is associated with marked increase of glutathione synthesis.* Proc Natl Acad Sci U S A, 1992. **89**(7): p. 3070-4.
144. Cullen, K.J., et al., *Glutathione S-transferase pi amplification is associated with cisplatin resistance in head and neck squamous cell carcinoma cell lines and primary tumors.* Cancer Res, 2003. **63**(23): p. 8097-102.
145. Srivastava, A.N., et al., *Cisplatin combination chemotherapy induces oxidative stress in advance non small cell lung cancer patients.* Asian Pac J Cancer Prev, 2010. **11**(2): p. 465-71.
146. Ooi, A., et al., *CUL3 and NRF2 mutations confer an NRF2 activation phenotype in a sporadic form of papillary renal cell carcinoma.* Cancer Res, 2013. **73**(7): p. 2044-51.

147. Singh, A., et al., *Dysfunctional KEAP1–NRF2 Interaction in Non-Small-Cell Lung Cancer.* PLoS Medicine, 2006. **3**(10): p. e420.
148. Wang, D., et al., *Hypermethylation of the Keap1 gene inactivates its function, promotes Nrf2 nuclear accumulation, and is involved in arsenite-induced human keratinocyte transformation.* Free Radical Biology and Medicine, 2015. **89**: p. 209-219.
149. Grau, L., et al., *A quantitative proteomic analysis uncovers the relevance of CUL3 in bladder cancer aggressiveness.* PLoS One, 2013. **8**(1): p. e53328.
150. Abazeed, M., et al., *NRF2 Is a Novel Oncogene and Biomarker of Therapeutic Resistance in Non-Small Cell Lung Cancer.* International Journal of Radiation Oncology • Biology • Physics. **90**(5): p. S53.
151. Homma, S., et al., *Nrf2 enhances cell proliferation and resistance to anticancer drugs in human lung cancer.* Clin Cancer Res, 2009. **15**(10): p. 3423-32.
152. Wang, X.J., et al., *Nrf2 enhances resistance of cancer cells to chemotherapeutic drugs, the dark side of Nrf2.* Carcinogenesis, 2008. **29**(6): p. 1235-43.
153. Kim, Y.R., et al., *Oncogenic NRF2 mutations in squamous cell carcinomas of oesophagus and skin.* J Pathol, 2010. **220**(4): p. 446-51.
154. Anna Kowalik, M., et al., *Metabolic reprogramming identifies the most aggressive lesions at early phases of hepatic carcinogenesis*. 2016. 2016.
155. Gatenby, R.A. and E.T. Gawlinski, *A reaction-diffusion model of cancer invasion.* Cancer Res, 1996. **56**(24): p. 5745-53.
156. Estrella, V., et al., *Acidity generated by the tumor microenvironment drives local invasion.* Cancer Res, 2013. **73**(5): p. 1524-35.
157. Xie, J., et al., *Beyond Warburg effect – dual metabolic nature of cancer cells.* Scientific Reports, 2014. **4**: p. 4927.
158. Satoh, H., et al., *Nrf2 Prevents Initiation but Accelerates Progression through the Kras Signaling Pathway during Lung Carcinogenesis.* Cancer Research, 2013. **73**(13): p. 4158-4168.
159. Yang, C.R., et al., *Intracellular glutathione content of urothelial cancer in correlation to chemotherapy response.* Cancer Lett, 1997. **119**(2): p. 157-62.
160. Savic-Radojevic, A., et al., *Glutathione S-transferase-P1 expression correlates with increased antioxidant capacity in transitional cell carcinoma of the urinary bladder.* Eur Urol, 2007. **52**(2): p. 470-7.
161. Byun, S.S., et al., *Augmentation of cisplatin sensitivity in cisplatin-resistant human bladder cancer cells by modulating glutathione concentrations and glutathione-related enzyme activities.* BJU Int, 2005. **95**(7): p. 1086-90.
162. Siegsmund, M.J., et al., *Cisplatin-resistant bladder carcinoma cells: enhanced expression of metallothioneins.* Urol Res, 1999. **27**(3): p. 157-63.
163. Wulfing, C., et al., *Metallothionein in bladder cancer: correlation of overexpression with poor outcome after chemotherapy.* World J Urol, 2007. **25**(2): p. 199-205.
164. Miyake, M., et al., *Clinical significance of heme oxygenase-1 expression in non-muscle-invasive bladder cancer.* Urol Int, 2010. **85**(3): p. 355-63.
165. Miyake, M., et al., *Inhibition of heme oxygenase-1 enhances the cytotoxic effect of gemcitabine in urothelial cancer cells.* Anticancer Res, 2010. **30**(6): p. 2145-52.

166. Hoffmann, A.C., et al., *MDR1 and ERCC1 expression predict outcome of patients with locally advanced bladder cancer receiving adjuvant chemotherapy.* Neoplasia, 2010. **12**(8): p. 628-36.
167. Tada, Y., et al., *Increased expression of multidrug resistance-associated proteins in bladder cancer during clinical course and drug resistance to doxorubicin.* Int J Cancer, 2002. **98**(4): p. 630-5.
168. Iida, K., et al., *Nrf2 and p53 cooperatively protect against BBN-induced urinary bladder carcinogenesis.* Carcinogenesis, 2007. **28**(11): p. 2398-403.
169. Atilano-Roque, A., L.M. Aleksunes, and M.S. Joy, *Bardoxolone methyl modulates efflux transporter and detoxifying enzyme expression in cisplatin-induced kidney cell injury.* Toxicol Lett, 2016. **259**: p. 52-9.
170. Arlt, A., et al., *Inhibition of the Nrf2 transcription factor by the alkaloid trigonelline renders pancreatic cancer cells more susceptible to apoptosis through decreased proteasomal gene expression and proteasome activity.* Oncogene, 2013. **32**(40): p. 4825-35.
171. Tarumoto, T., et al., *Ascorbic acid restores sensitivity to imatinib via suppression of Nrf2-dependent gene expression in the imatinib-resistant cell line.* Exp Hematol, 2004. **32**(4): p. 375-81.
172. Ren, D., et al., *Brusatol enhances the efficacy of chemotherapy by inhibiting the Nrf2-mediated defense mechanism.* Proc Natl Acad Sci U S A, 2011. **108**(4): p. 1433-8.
173. Kansanen, E., et al., *The Keap1-Nrf2 pathway: Mechanisms of activation and dysregulation in cancer.* Redox Biology, 2013. **1**(1): p. 45-49.
174. Olayanju, A., et al., *Brusatol provokes a rapid and transient inhibition of Nrf2 signaling and sensitizes mammalian cells to chemical toxicity-implications for therapeutic targeting of Nrf2.* Free Radic Biol Med, 2015. **78**: p. 202-12.
175. Hill, S.C., et al., *Activation of CD40 in cervical carcinoma cells facilitates CTL responses and augments chemotherapy-induced apoptosis.* J Immunol, 2005. **174**(1): p. 41-50.
176. Elgueta, R., et al., *Molecular mechanism and function of CD40/CD40L engagement in the immune system.* Immunol Rev, 2009. **229**(1): p. 152-72.
177. van Kooten, C. and J. Banchereau, *CD40-CD40 ligand.* J Leukoc Biol, 2000. **67**(1): p. 2-17.
178. Cooke, P.W., et al., *CD40 expression in bladder cancer.* The Journal of Pathology, 1999. **188**(1): p. 38-43.
179. Paulie, S., et al., *Monoclonal antibodies to antigens associated with transitional cell carcinoma of the human urinary bladder. II. Identification of the cellular target structures by immunoprecipitation and SDS-PAGE analysis.* Cancer Immunol Immunother, 1984. **17**(3): p. 173-9.
180. Elmetwali, T., L.S. Young, and D.H. Palmer, *CD40 ligand-induced carcinoma cell death: a balance between activation of TNFR-associated factor (TRAF) 3-dependent death signals and suppression of TRAF6-dependent survival signals.* J Immunol, 2010. **184**(2): p. 1111-20.
181. Eliopoulos, A.G. and L.S. Young, *The role of the CD40 pathway in the pathogenesis and treatment of cancer.* Current Opinion in Pharmacology, 2004. **4**(4): p. 360-367.

182. Eliopoulos, A.G. and L.S. Young, *The role of the CD40 pathway in the pathogenesis and treatment of cancer.* Curr Opin Pharmacol, 2004. **4**(4): p. 360-7.
183. Tong, A.W. and M.J. Stone, *Prospects for CD40-directed experimental therapy of human cancer.* Cancer Gene Ther, 2003. **10**(1): p. 1-13.
184. Lederman, S., et al., *Identification of a novel surface protein on activated CD4+ T cells that induces contact-dependent B cell differentiation (help).* J Exp Med, 1992. **175**(4): p. 1091-101.
185. Lobo, F.M., P.R. Scholl, and R.L. Fuleihan, *CD40 ligand-deficient T cells from X-linked hyper-IgM syndrome carriers have intrinsic priming capability.* J Immunol, 2002. **168**(3): p. 1473-8.
186. Elmetwali, T., et al., *CD40 ligand induced cytotoxicity in carcinoma cells is enhanced by inhibition of metalloproteinase cleavage and delivery via a conditionally-replicating adenovirus.* Mol Cancer, 2010. **9**: p. 52.
187. Eliopoulos, A.G., et al., *CD40 Induces Apoptosis in Carcinoma Cells through Activation of Cytotoxic Ligands of the Tumor Necrosis Factor Superfamily.* Molecular and Cellular Biology, 2000. **20**(15): p. 5503-5515.
188. Georgopoulos, N.T., et al., *A novel mechanism of CD40-induced apoptosis of carcinoma cells involving TRAF3 and JNK/AP-1 activation.* Cell Death Differ, 2006. **13**(10): p. 1789-801.
189. Yamamoto, K., H. Ichijo, and S.J. Korsmeyer, *BCL-2 is phosphorylated and inactivated by an ASK1/Jun N-terminal protein kinase pathway normally activated at G(2)/M.* Mol Cell Biol, 1999. **19**(12): p. 8469-78.
190. Chen, Y.R. and T.H. Tan, *The c-Jun N-terminal kinase pathway and apoptotic signaling (review).* Int J Oncol, 2000. **16**(4): p. 651-62.
191. Malmstrom, P.U., et al., *AdCD40L immunogene therapy for bladder carcinoma--the first phase I/IIa trial.* Clin Cancer Res, 2010. **16**(12): p. 3279-87.
192. Vonderheide, R.H., et al., *Clinical activity and immune modulation in cancer patients treated with CP-870,893, a novel CD40 agonist monoclonal antibody.* J Clin Oncol, 2007. **25**(7): p. 876-83.
193. Lu, P., et al., *Extracellular Matrix Degradation and Remodeling in Development and Disease.* Cold Spring Harb Perspect Biol, 2011. **3**(12).
194. Bonnans, C., J. Chou, and Z. Werb, *Remodelling the extracellular matrix in development and disease.* Nat Rev Mol Cell Biol, 2014. **15**(12): p. 786-801.
195. Rodriguez Faba, O., et al., *Matrix Metalloproteinases and Bladder Cancer: What is New?* ISRN Urology, 2012. **2012**: p. 9.
196. Zucker, S., J. Cao, and W.T. Chen, *Critical appraisal of the use of matrix metalloproteinase inhibitors in cancer treatment.* Oncogene, 2000. **19**(56): p. 6642-50.
197. Löffek, S., O. Schilling, and C.-W. Franzke, *Biological role of matrix metalloproteinases: a critical balance.* European Respiratory Journal, 2011. **38**(1): p. 191-208.
198. Liu, H., et al., *The role of MMP-1 in breast cancer growth and metastasis to the brain in a xenograft model.* BMC Cancer, 2012. **12**: p. 583.
199. Poola, I., et al., *Identification of MMP-1 as a putative breast cancer predictive marker by global gene expression analysis.* Nat Med, 2005. **11**(5): p. 481-483.

200. Sunami, E., et al., *MMP-1 is a prognostic marker for hematogenous metastasis of colorectal cancer.* Oncologist, 2000. **5**(2): p. 108-14.
201. Du, X., et al., *MMP-1 and Pro-MMP-10 as potential urinary pharmacodynamic biomarkers of FGFR3-targeted therapy in patients with bladder cancer.* Clin Cancer Res, 2014. **20**(24): p. 6324-35.
202. Yan, Y., et al., *The MMP-1, MMP-2, and MMP-9 gene polymorphisms and susceptibility to bladder cancer: a meta-analysis.* Tumour Biol, 2014. **35**(4): p. 3047-52.
203. Srivastava, P., et al., *Bladder cancer risk associated with genotypic polymorphism of the matrix metalloproteinase-1 and 7 in North Indian population.* Dis Markers, 2010. **29**(1): p. 37-46.
204. Tasci, A.I., et al., *A single-nucleotide polymorphism in the matrix metalloproteinase-1 promoter enhances bladder cancer susceptibility.* BJU International, 2008. **101**(4): p. 503-507.
205. Rothenberg, M.L., A.R. Nelson, and K.R. Hande, *New Drugs on the Horizon: Matrix Metalloproteinase Inhibitors.* Oncologist, 1998. **3**(4): p. 271-274.
206. Cathcart, J., A. Pulkoski-Gross, and J. Cao, *Targeting matrix metalloproteinases in cancer: Bringing new life to old ideas.* Genes & Diseases, 2015. **2**(1): p. 26-34.
207. Sparano, J.A., et al., *Randomized phase III trial of marimastat versus placebo in patients with metastatic breast cancer who have responding or stable disease after first-line chemotherapy: Eastern Cooperative Oncology Group trial E2196.* J Clin Oncol, 2004. **22**(23): p. 4683-90.
208. Bissett, D., et al., *Phase III study of matrix metalloproteinase inhibitor prinomastat in non-small-cell lung cancer.* J Clin Oncol, 2005. **23**(4): p. 842-9.
209. Hirte, H., et al., *A phase III randomized trial of BAY 12-9566 (tanomastat) as maintenance therapy in patients with advanced ovarian cancer responsive to primary surgery and paclitaxel/platinum containing chemotherapy: a National Cancer Institute of Canada Clinical Trials Group Study.* Gynecol Oncol, 2006. **102**(2): p. 300-8.
210. Vandenbroucke, R.E. and C. Libert, *Is there new hope for therapeutic matrix metalloproteinase inhibition?* Nat Rev Drug Discov, 2014. **13**(12): p. 904-927.
211. Said, A.H., J.P. Raufman, and G. Xie, *The Role of Matrix Metalloproteinases in Colorectal Cancer.* Cancers (Basel), 2014. **6**(1): p. 366-75.
212. Rigas, J.R., et al., *O-107 Adjuvant targeted therapy in unresectable lung cancer: The results of two randomized placebo-controlled trials of BAY 12-9566, a matrix metalloproteinase inhibitor (MMPI).* Lung Cancer, 2003. **41**: p. S34.
213. Hirte, H., et al., *A phase III randomized trial of BAY 12-9566 (tanomastat) as maintenance therapy in patients with advanced ovarian cancer responsive to primary surgery and paclitaxel/platinum containing chemotherapy: A National Cancer Institute of Canada Clinical Trials Group Study.* Gynecologic Oncology, 2006. **102**(2): p. 300-308.
214. Pankov, R. and K.M. Yamada, *Fibronectin at a glance.* Journal of Cell Science, 2002. **115**(20): p. 3861-3863.

215. To, W.S. and K.S. Midwood, *Plasma and cellular fibronectin: distinct and independent functions during tissue repair.* Fibrogenesis & Tissue Repair, 2011. **4**(1): p. 21.
216. Ruoslahti, E., *Fibronectin in cell adhesion and invasion.* Cancer and Metastasis Reviews, 1984. **3**(1): p. 43-51.
217. Lenselink, E.A., *Role of fibronectin in normal wound healing.* Int Wound J, 2015. **12**(3): p. 313-6.
218. Thery, M., et al., *The extracellular matrix guides the orientation of the cell division axis.* Nat Cell Biol, 2005. **7**(10): p. 947-953.
219. Sottile, J., D.C. Hocking, and P.J. Swiatek, *Fibronectin matrix assembly enhances adhesion-dependent cell growth.* J Cell Sci, 1998. **111 (Pt 19)**: p. 2933-43.
220. Ylätupa, S., et al., *Cellular fibronectin in serum and plasma: a potential new tumour marker?* Br J Cancer, 1995. **71**(3): p. 578-82.
221. Ruiz-Garcia, E., et al., *Gene expression profiling identifies Fibronectin 1 and CXCL9 as candidate biomarkers for breast cancer screening.* Br J Cancer, 2010. **102**(3): p. 462-468.
222. Fernandez-Garcia, B., et al., *Expression and prognostic significance of fibronectin and matrix metalloproteases in breast cancer metastasis.* Histopathology, 2014. **64**(4): p. 512-22.
223. Kaplan, R.N., et al., *VEGFR1-positive haematopoietic bone marrow progenitors initiate the pre-metastatic niche.* Nature, 2005. **438**(7069): p. 820-7.
224. Quail, D. and J. Joyce, *Microenvironmental regulation of tumor progression and metastasis.* Nat Med, 2013. **19**(11): p. 1423-37.
225. Joyce, J.A. and J.W. Pollard, *Microenvironmental regulation of metastasis.* Nat Rev Cancer, 2009. **9**(4): p. 239-52.
226. Kenny, H.A., et al., *Mesothelial cells promote early ovarian cancer metastasis through fibronectin secretion.* J Clin Invest, 2014. **124**(10): p. 4614-28.
227. Liotta, L.A., C.N. Rao, and U.M. Wewer, *Biochemical interactions of tumor cells with the basement membrane.* Annu Rev Biochem, 1986. **55**: p. 1037-57.
228. Schaffner, F., A.M. Ray, and M. Dontenwill, *Integrin alpha5beta1, the Fibronectin Receptor, as a Pertinent Therapeutic Target in Solid Tumors.* Cancers (Basel), 2013. **5**(1): p. 27-47.
229. Tsafrir, D., et al., *Relationship of gene expression and chromosomal abnormalities in colorectal cancer.* Cancer Res, 2006. **66**(4): p. 2129-37.
230. Scotto, L., et al., *Identification of copy number gain and overexpressed genes on chromosome arm 20q by an integrative genomic approach in cervical cancer: potential role in progression.* Genes Chromosomes Cancer, 2008. **47**(9): p. 755-65.
231. Ramakrishna, M., et al., *Identification of Candidate Growth Promoting Genes in Ovarian Cancer through Integrated Copy Number and Expression Analysis.* PLoS One, 2010. **5**(4).
232. Karhu, R., E. Mahlamaki, and A. Kallioniemi, *Pancreatic adenocarcinoma -- genetic portrait from chromosomes to microarrays.* Genes Chromosomes Cancer, 2006. **45**(8): p. 721-30.

233. van Dekken, H., et al., *Evaluation of genetic patterns in different tumor areas of intermediate-grade prostatic adenocarcinomas by high-resolution genomic array analysis.* Genes, Chromosomes and Cancer, 2004. **39**(3): p. 249-256.
234. Wullich, B., et al., *Evidence for gains at 15q and 20q in brain metastases of prostate cancer.* Cancer Genet Cytogenet, 2004. **154**(2): p. 119-23.
235. Sauer, G., et al., *Proteome analysis of the human mitotic spindle.* Mol Cell Proteomics, 2005. **4**(1): p. 35-43.
236. Santamaria, A., et al., *The spindle protein CHICA mediates localization of the chromokinesin Kid to the mitotic spindle.* Curr Biol, 2008. **18**(10): p. 723-9.
237. Chang, Q., et al., *JNK1 activation predicts the prognostic outcome of the human hepatocellular carcinoma.* Mol Cancer, 2009. **8**: p. 64.
238. Inamura, K., et al., *A metastatic signature in entire lung adenocarcinomas irrespective of morphological heterogeneity.* Hum Pathol, 2007. **38**(5): p. 702-9.
239. Wang, Z., et al., *FAM83D promotes cell proliferation and motility by downregulating tumor suppressor gene FBXW7.* Oncotarget, 2013. **4**(12): p. 2476-86.
240. Welcker, M. and B.E. Clurman, *FBW7 ubiquitin ligase: a tumour suppressor at the crossroads of cell division, growth and differentiation.* Nat Rev Cancer, 2008. **8**(2): p. 83-93.
241. Welcker, M., et al., *A Nucleolar Isoform of the Fbw7 Ubiquitin Ligase Regulates c-Myc and Cell Size.* Current Biology. **14**(20): p. 1852-1857.
242. Wei, W., et al., *The v-Jun point mutation allows c-Jun to escape GSK3-dependent recognition and destruction by the Fbw7 ubiquitin ligase.* Cancer Cell, 2005. **8**(1): p. 25-33.
243. Koepp, D.M., et al., *Phosphorylation-dependent ubiquitination of cyclin E by the SCFFbw7 ubiquitin ligase.* Science, 2001. **294**(5540): p. 173-7.
244. Liu, N., et al., *The Fbw7/human CDC4 tumor suppressor targets proproliferative factor KLF5 for ubiquitination and degradation through multiple phosphodegron motifs.* J Biol Chem, 2010. **285**(24): p. 18858-67.
245. Oberg, C., et al., *The Notch intracellular domain is ubiquitinated and negatively regulated by the mammalian Sel-10 homolog.* J Biol Chem, 2001. **276**(38): p. 35847-53.
246. Mao, J.H., et al., *FBXW7 targets mTOR for degradation and cooperates with PTEN in tumor suppression.* Science, 2008. **321**(5895): p. 1499-502.
247. Piekny, A.J. and M. Glotzer, *Anillin Is a Scaffold Protein That Links RhoA, Actin, and Myosin during Cytokinesis.* Current Biology. **18**(1): p. 30-36.
248. Tian, D., et al., *Anillin Regulates Neuronal Migration and Neurite Growth by Linking RhoG to the Actin Cytoskeleton.* Curr Biol, 2015. **25**(9): p. 1135-45.
249. Wang, D., et al., *F-actin binding protein, anillin, regulates integrity of intercellular junctions in human epithelial cells.* Cellular and Molecular Life Sciences, 2015. **72**(16): p. 3185-3200.
250. Wang, G., et al., *Overexpression of Anillin (ANLN) is correlated with colorectal cancer progression and poor prognosis.* Cancer Biomark, 2016. **16**(3): p. 459-65.
251. Hall, P.A., et al., *The septin-binding protein anillin is overexpressed in diverse human tumors.* Clin Cancer Res, 2005. **11**(19 Pt 1): p. 6780-6.

252. Liang, P.I., et al., *Subcellular localisation of anillin is associated with different survival outcomes in upper urinary tract urothelial carcinoma.* J Clin Pathol, 2015. **68**(12): p. 1026-32.
253. Kim, H., et al., *Development of biomarkers for screening hepatocellular carcinoma using global data mining and multiple reaction monitoring.* PLoS One, 2013. **8**(5): p. e63468.
254. PC, O.L., et al., *Systematic antibody generation and validation via tissue microarray technology leading to identification of a novel protein prognostic panel in breast cancer.* BMC Cancer, 2013. **13**: p. 175.
255. Olakowski, M., et al., *NBL1 and anillin (ANLN) genes over-expression in pancreatic carcinoma.* Folia Histochem Cytobiol, 2009. **47**(2): p. 249-55.
256. Ronkainen, H., et al., *Anillin expression is a marker of favourable prognosis in patients with renal cell carcinoma.* Oncol Rep, 2011. **25**(1): p. 129-33.
257. Zhou, W., et al., *Knockdown of ANLN by lentivirus inhibits cell growth and migration in human breast cancer.* Mol Cell Biochem, 2015. **398**(1-2): p. 11-9.
258. Henry, N.L. and D.F. Hayes, *Cancer biomarkers.* Molecular Oncology, 2012. **6**(2): p. 140-146.
259. Rodrigues, L.R., et al., *The role of osteopontin in tumor progression and metastasis in breast cancer.* Cancer Epidemiol Biomarkers Prev, 2007. **16**(6): p. 1087-97.
260. Xu, S.T., et al., *Role of osteopontin in the regulation of human bladder cancer proliferation and migration in T24 cells.* Mol Med Rep, 2015. **11**(5): p. 3701-7.
261. Zhao, L., et al., *Significance of plasma osteopontin levels in patients with bladder urothelial carcinomas.* Mol Diagn Ther, 2012. **16**(5): p. 311-6.
262. Cui, B.K., et al., *[Osteopontin as a potential biomarker of metastasis and recurrence for hepatocellular carcinoma].* Ai Zheng, 2006. **25**(7): p. 876-9.
263. Zhang, H., et al., *The prognostic significance of preoperative plasma levels of osteopontin in patients with hepatocellular carcinoma.* J Cancer Res Clin Oncol, 2006. **132**(11): p. 709-17.
264. Xie, H., et al., *Prognostic significance of osteopontin in hepatitis B virus-related hepatocellular carcinoma.* Dig Liver Dis, 2007. **39**(2): p. 167-72.
265. Shijubo, N., et al., *Vascular endothelial growth factor and osteopontin in stage I lung adenocarcinoma.* Am J Respir Crit Care Med, 1999. **160**(4): p. 1269-73.
266. Yang, G.H., et al., *Osteopontin combined with CD44, a novel prognostic biomarker for patients with hepatocellular carcinoma undergoing curative resection.* Oncologist, 2008. **13**(11): p. 1155-65.
267. Hotte, S.J., et al., *Plasma osteopontin: associations with survival and metastasis to bone in men with hormone-refractory prostate carcinoma.* Cancer, 2002. **95**(3): p. 506-12.
268. Wu, Y., D.T. Denhardt, and S.R. Rittling, *Osteopontin is required for full expression of the transformed phenotype by the ras oncogene.* Br J Cancer, 2000. **83**(2): p. 156-63.
269. Cook, A.C., et al., *Osteopontin induction of hyaluronan synthase 2 expression promotes breast cancer malignancy.* J Biol Chem, 2006. **281**(34): p. 24381-9.

270. Lin, C.W., J.C. Lin, and G.R. Prout, Jr., *Establishment and characterization of four human bladder tumor cell lines and sublines with different degrees of malignancy.* Cancer Res, 1985. **45**(10): p. 5070-9.
271. Elliott, A.Y., et al., *Characterization of a Cell Line From Human Transitional Cell Cancer of the Urinary Tract.* Journal of the National Cancer Institute, 1974. **53**(5): p. 1341-1349.
272. Masters, J.R.W., et al., *Tissue Culture Model of Transitional Cell Carcinoma: Characterization of Twenty-two Human Urothelial Cell Lines.* Cancer Research, 1986. **46**(7): p. 3630-3636.
273. Walker, M.C., et al., *Development and characterization of cisplatin-resistant human testicular and bladder tumour cell lines.* Eur J Cancer, 1990. **26**(6): p. 742-7.
274. standards, L. *STR Database* 2015 [cited 2015 09/09/2015]; Available from: https://http://www.lgcstandards-atcc.org/STRDatabase.aspx?geo_country=gb&slp=1.
275. Cellosaurus, *Cellosaurus.* 2015.
276. Expasy, *Cellosaurus.* 2015.
277. Standards, L., *STR Database.* 2015.
278. England, P.H. *PHE - Culture Collections ECACC General Cell Collection RT112/84*. [cited 2015 01/09/15]; Available from: http://www.phe-culturecollections.org.uk/products/celllines/generalcell/detail.jsp?refId=85061106&collection=ecacc_gc
279. Moutasim, K.A., M.L. Nystrom, and G.J. Thomas, *Cell migration and invasion assays.* Methods Mol Biol, 2011. **731**: p. 333-43.
280. Irizarry, R.A., et al., *Exploration, normalization, and summaries of high density oligonucleotide array probe level data.* Biostatistics, 2003. **4**(2): p. 249-64.
281. Wu, Z., et al., *A Model-Based Background Adjustment for Oligonucleotide Expression Arrays.* Journal of the American Statistical Association, 2004. **99**(468): p. 909-917.
282. Bolstad, B.M., et al., *Experimental design and low-level analysis of microarray data.* Int Rev Neurobiol, 2004. **60**: p. 25-58.
283. Hochberg, Y. and Y. Benjamini, *More powerful procedures for multiple significance testing.* Stat Med, 1990. **9**(7): p. 811-8.
284. Huang da, W., B.T. Sherman, and R.A. Lempicki, *Systematic and integrative analysis of large gene lists using DAVID bioinformatics resources.* Nat Protoc, 2009. **4**(1): p. 44-57.
285. Edgar, R., M. Domrachev, and A.E. Lash, *Gene Expression Omnibus: NCBI gene expression and hybridization array data repository.* Nucleic Acids Res, 2002. **30**(1): p. 207-10.
286. Dyrskjot, L., et al., *Gene expression in the urinary bladder: a common carcinoma in situ gene expression signature exists disregarding histopathological classification.* Cancer Res, 2004. **64**(11): p. 4040-8.
287. Hall, M.D., et al., *Say no to DMSO: dimethylsulfoxide inactivates cisplatin, carboplatin, and other platinum complexes.* Cancer Res, 2014. **74**(14): p. 3913-22.
288. Loboda, A., et al., *Role of Nrf2/HO-1 system in development, oxidative stress response and diseases: an evolutionarily conserved mechanism.* Cell Mol Life Sci, 2016. **73**(17): p. 3221-47.

289. Yim, M.S., et al., *HMOX1 is an important prognostic indicator of nonmuscle invasive bladder cancer recurrence and progression.* Journal of Urology, 2011. **185**(2): p. 701-705.
290. Miyake, M., et al., *Clinical significance of heme oxygenase-1 expression in non-muscle-invasive bladder cancer.* Urologia Internationalis, 2010. **85**(3): p. 355-363.
291. Miyata, Y., et al., *Heme oxygenase-1 expression is associated with tumor aggressiveness and outcomes in patients with bladder cancer: A correlation with smoking intensity.* Translational Research, 2014. **164**(6): p. 468-476.
292. Henry, J., *The response to chemical stress: Development of preclinical and translational biomarkers of Nrf2 activity*, in *Medical Research Council, Centre for Drug Saftey Science, Department of Molecular and Clinical Pharmacology* 2012, University of Liverpool University of Liverpool Library Repositary p. 198.
293. Zhang, B., et al., *MBD1 is an Epigenetic Regulator of KEAP1 in Pancreatic Cancer.* Curr Mol Med, 2016. **16**(4): p. 404-11.
294. Vartanian, S., et al., *Application of Mass Spectrometry Profiling to Establish Brusatol as an Inhibitor of Global Protein Synthesis.* Mol Cell Proteomics, 2016. **15**(4): p. 1220-31.
295. Miller, R.P., et al., *Mechanisms of Cisplatin Nephrotoxicity.* Toxins (Basel), 2010. **2**(11): p. 2490-518.
296. Sporn, M.B. and K.T. Liby, *NRF2 and cancer: the good, the bad and the importance of context.* Nat Rev Cancer, 2012. **12**(8): p. 564-71.
297. Anwar, A., et al., *Interaction of the molecular chaperone Hsp70 with human NAD(P)H:quinone oxidoreductase 1.* J Biol Chem, 2002. **277**(16): p. 14060-7.
298. Nguyen, T., P. Nioi, and C.B. Pickett, *The Nrf2-Antioxidant Response Element Signaling Pathway and Its.* J Biol Chem, 2009. **284**(20): p. 13291-5.
299. Greig, M.E. and A.J. Gibbons, *An antidote to cycloheximide (actidione) poisoning.* Toxicol Appl Pharmacol, 1959. **1**: p. 598-601.
300. Kim, S., et al., *Silvestrol, a potential anticancer rocaglate derivative from Aglaia foveolata, induces apoptosis in LNCaP cells through the mitochondrial/apoptosome pathway without activation of executioner caspase-3 or -7.* Anticancer Res, 2007. **27**(4B): p. 2175-83.
301. Daker, M., et al., *Inhibition of nasopharyngeal carcinoma cell proliferation and synergism of cisplatin with silvestrol and episilvestrol isolated from Aglaia stellatopilosa.* Exp Ther Med, 2016. **11**(6): p. 2117-26.
302. Kogure, T., et al., *Therapeutic Potential of the Translation Inhibitor Silvestrol in Hepatocellular Cancer.* PLoS One, 2013. **8**(9).
303. Lucas, D.M., et al., *The novel plant-derived agent silvestrol has B-cell selective activity in chronic lymphocytic leukemia and acute lymphoblastic leukemia in vitro and in vivo.* Blood, 2009. **113**(19): p. 4656-66.
304. Shevde, L.A. and R.S. Samant, *Role of osteopontin in the pathophysiology of cancer.* Matrix Biol, 2014. **37**: p. 131-41.
305. Zaravinos, A., et al., *Role of the angiogenic components, VEGFA, FGF2, OPN and RHOC, in urothelial cell carcinoma of the urinary bladder.* Oncol Rep, 2012. **28**(4): p. 1159-66.

306. Ke, H.L., et al., *Osteopontin overexpression predicts poor prognosis of upper urinary tract urothelial carcinoma.* Urol Oncol, 2011. **29**(6): p. 703-9.
307. Celetti, A., et al., *Overexpression of the cytokine osteopontin identifies aggressive laryngeal squamous cell carcinomas and enhances carcinoma cell proliferation and invasiveness.* Clin Cancer Res, 2005. **11**(22): p. 8019-27.
308. Liao, W., et al., *Upregulation of FAM83D affects the proliferation and invasion of hepatocellular carcinoma.* Oncotarget, 2015. **6**(27): p. 24132-47.
309. Walian, P.J., B. Hang, and J.H. Mao, *Prognostic significance of FAM83D gene expression across human cancer types.* Oncotarget, 2016. **7**(3): p. 3332-40.
310. Oldridge, E.E., et al., *Retinoic acid represses invasion and stem cell phenotype by induction of the metastasis suppressors RARRES1 and LXN.* Oncogenesis, 2013. **2**: p. e45.
311. Okada, M., et al., *The CENP-H–I complex is required for the efficient incorporation of newly synthesized CENP-A into centromeres.* Nat Cell Biol, 2006. **8**(5): p. 446-457.
312. Lou, X., et al., *SOX2 targets fibronectin 1 to promote cell migration and invasion in ovarian cancer: new molecular leads for therapeutic intervention.* OMICS, 2013. **17**(10): p. 510-8.
313. Sponziello, M., et al., *Fibronectin-1 expression is increased in aggressive thyroid cancer and favors the migration and invasion of cancer cells.* Mol Cell Endocrinol, 2016. **431**: p. 123-32.
314. Aytes, A., et al., *Cross-species regulatory network analysis identifies a synergistic interaction between FOXM1 and CENPF that drives prostate cancer malignancy.* Cancer Cell, 2014. **25**(5): p. 638-51.
315. Ninagawa, S., et al., *EDEM2 initiates mammalian glycoprotein ERAD by catalyzing the first mannose trimming step.* The Journal of cell biology, 2014. **206**(3): p. 347-356.
316. Jain, M., et al., *TOP2A is overexpressed and is a therapeutic target for adrenocortical carcinoma.* Endocr Relat Cancer, 2013. **20**(3): p. 361-70.
317. Perez de Castro, I. and M. Malumbres, *Mitotic Stress and Chromosomal Instability in Cancer: The Case for TPX2.* Genes Cancer, 2012. **3**(11-12): p. 721-30.
318. Akino, K., et al., *The Ras effector RASSF2 is a novel tumor-suppressor gene in human colorectal cancer.* Gastroenterology, 2005. **129**(1): p. 156-69.
319. Wang, D., et al., *F-actin binding protein, anillin, regulates integrity of intercellular junctions in human epithelial cells.* Cell Mol Life Sci, 2015. **72**(16): p. 3185-200.
320. Lin, J., et al., *Osteopontin (OPN/SPP1) isoforms collectively enhance tumor cell invasion and dissemination in esophageal adenocarcinoma.* Oncotarget, 2015. **6**(26): p. 22239-57.
321. Sun, B.S., et al., *Osteopontin knockdown suppresses non-small cell lung cancer cell invasion and metastasis.* Chin Med J (Engl), 2013. **126**(9): p. 1683-8.
322. Pulukuri, S.M. and J.S. Rao, *Matrix metalloproteinase-1 promotes prostate tumor growth and metastasis.* Int J Oncol, 2008. **32**(4): p. 757-65.
323. Elgueta, R., et al., *Molecular mechanism and function of CD40/CD40L engagement in the immune system.* Immunol Rev, 2009. **229**(1).

324. Fujiyama, C., et al., *Human bladder cancer invasion model using rat bladder in vitro and its use to test mechanisms and therapeutic inhibitors of invasion.* Br J Cancer, 2001. **84**(4): p. 558-564.
325. Cheng, L., et al., *Staging and reporting of urothelial carcinoma of the urinary bladder.* Mod Pathol, 0000. **22**(S2): p. S70-S95.
326. Teramoto, S., et al., *Effect of adenoviral vector infection on cell proliferation in cultured primary human airway epithelial cells.* Hum Gene Ther, 1995. **6**(8): p. 1045-53.
327. Marone, M., et al., *Semiquantitative RT-PCR analysis to assess the expression levels of multiple transcripts from the same sample.* Biological Procedures Online, 2001. **3**: p. 19-25.
328. Young, S.K. and R.C. Wek, *Upstream Open Reading Frames Differentially Regulate Gene-specific Translation in the Integrated Stress Response.* J Biol Chem, 2016. **291**(33): p. 16927-35.
329. Young, S.K., et al., *Ribosome Reinitiation Directs Gene-specific Translation and Regulates the Integrated Stress Response.* J Biol Chem, 2015. **290**(47): p. 28257-71.
330. Young, S.K., et al., *Ribosome Elongation Stall Directs Gene-specific Translation in the Integrated Stress Response.* J Biol Chem, 2016. **291**(12): p. 6546-58.
331. Dai, C.L., et al., *Inhibition of Protein Synthesis Alters Protein Degradation through Activation of Protein Kinase B (AKT).* J Biol Chem, 2013. **288**(33): p. 23875-83.
332. Baxendale, A.J., et al., *Constitutive activation of the CD40 pathway promotes cell transformation and neoplastic growth.* Oncogene, 2005. **24**(53): p. 7913-23.
333. Posner, M.R., et al., *Surface membrane-expressed CD40 is present on tumor cells from squamous cell cancer of the head and neck in vitro and in vivo and regulates cell growth in tumor cell lines.* Clin Cancer Res, 1999. **5**(8): p. 2261-70.
334. Tai, Y.T., et al., *CD40 induces human multiple myeloma cell migration via phosphatidylinositol 3-kinase/AKT/NF-kappa B signaling.* Blood, 2003. **101**(7): p. 2762-9.
335. Nair, P.M., et al., *Enhancing the antitumor efficacy of a cell-surface death ligand by covalent membrane display.* Proceedings of the National Academy of Sciences, 2015. **112**(18): p. 5679-5684.
336. Vonderheide, R.H. and M.J. Glennie, *Agonistic CD40 antibodies and cancer therapy.* Clin Cancer Res, 2013. **19**(5): p. 1035-43.
337. Agrawal, D., et al., *Osteopontin Identified as Lead Marker of Colon Cancer Progression, Using Pooled Sample Expression Profiling.* Journal of the National Cancer Institute, 2002. **94**(7): p. 513-521.
338. Huang, J., et al., *Osteopontin-Enhanced Hepatic Metastasis of Colorectal Cancer Cells.* PLoS ONE, 2012. **7**(10): p. e47901.
339. Zhao, W.M. and G. Fang, *Anillin is a substrate of anaphase-promoting complex/cyclosome (APC/C) that controls spatial contractility of myosin during late cytokinesis.* J Biol Chem, 2005. **280**(39): p. 33516-24.
340. Gruss, O.J. and I. Vernos, *The mechanism of spindle assembly: functions of Ran and its target TPX2.* J Cell Biol, 2004. **166**(7): p. 949-55.

341. Zaravinos, A., et al., *Spotlight on Differentially Expressed Genes in Urinary Bladder Cancer.* PLoS One, 2011. **6**(4).
342. Brassesco Mí, S., et al., *In vitro targeting of Polo-like kinase 1 in bladder carcinoma: Comparative effects of four potent inhibitors.* Cancer Biol Ther, 2013. **14**(7): p. 648-57.
343. Stadler, W.M., et al., *An Open-Label, Single-Arm, Phase 2 Trial of the Polo-Like Kinase Inhibitor Volasertib (BI 6727) in Patients With Locally Advanced or Metastatic Urothelial Cancer.* Cancer, 2014. **120**(7): p. 976-82.
344. Zhang, Z., G. Zhang, and C. Kong, *High expression of polo-like kinase 1 is associated with the metastasis and recurrence in urothelial carcinoma of bladder.* Urol Oncol, 2013. **31**(7): p. 1222-30.
345. Ahmed, M., et al., *Osteopontin: a potentially important therapeutic target in cancer.* Expert Opin Ther Targets, 2011. **15**(9): p. 1113-26.
346. Coppola, D., et al., *Correlation of osteopontin protein expression and pathological stage across a wide variety of tumor histologies.* Clin Cancer Res, 2004. **10**(1 Pt 1): p. 184-90.
347. Fang, Z.Q., et al., *Gene expression profile and enrichment pathways in different stages of bladder cancer.* Genet Mol Res, 2013. **12**(2): p. 1479-89.
348. Imano, M., et al., *Immunohistochemical expression of osteopontin in gastric cancer.* J Gastrointest Surg, 2009. **13**(9): p. 1577-82.
349. Kita, Y., et al., *Expression of Osteopontin in oesophageal squamous cell carcinoma.* Br J Cancer, 2006. **95**(5): p. 634-638.
350. Song, J.Y., et al., *Osteopontin expression correlates with invasiveness in cervical cancer.* Aust N Z J Obstet Gynaecol, 2009. **49**(4): p. 434-8.
351. Forootan, S.S., et al., *Prognostic significance of osteopontin expression in human prostate cancer.* Int J Cancer, 2006. **118**(9): p. 2255-61.
352. Weber, G.F., G.S. Lett, and N.C. Haubein, *Osteopontin is a marker for cancer aggressiveness and patient survival.* Br J Cancer, 2010. **103**(6): p. 861-9.
353. Collins, A.L., et al., *Osteopontin expression is associated with improved survival in patients with pancreatic adenocarcinoma.* Ann Surg Oncol, 2012. **19**(8): p. 2673-8.
354. Naor, D., R.V. Sionov, and D. Ish-Shalom, *CD44: structure, function, and association with the malignant process.* Adv Cancer Res, 1997. **71**: p. 241-319.
355. Ang, C., et al., *Plasma osteopontin levels are predictive of disease stage in patients with transitional cell carcinoma of the bladder.* BJU Int, 2005. **96**(6): p. 803-5.
356. Agnihotri, R., et al., *Osteopontin, a Novel Substrate for Matrix Metalloproteinase-3 (Stromelysin-1) and Matrix Metalloproteinase-7 (Matrilysin).* Journal of Biological Chemistry, 2001. **276**(30): p. 28261-28267.
357. Zduniak, K., et al., *Osteopontin splice variants are differential predictors of breast cancer treatment responses.* BMC Cancer, 2016. **16**.
358. Lim, J. and J.P. Thiery, *Epithelial-mesenchymal transitions: insights from development.* Development, 2012. **139**(19): p. 3471-86.
359. Baumgart, E., et al., *Identification and prognostic significance of an epithelial-mesenchymal transition expression profile in human bladder tumors.* Clin Cancer Res, 2007. **13**(6): p. 1685-94.

360. Varela, J.C., et al., *Upregulated expression of complement inhibitory proteins on bladder cancer cells and anti-MUC1 antibody immune selection.* Int J Cancer, 2008. **123**(6): p. 1357-63.
361. Fedarko, N.S., et al., *Factor H binding to bone sialoprotein and osteopontin enables tumor cell evasion of complement-mediated attack.* J Biol Chem, 2000. **275**(22): p. 16666-72.
362. Warzecha, C.C., et al., *ESRP1 and ESRP2 are epithelial cell-type-specific regulators of FGFR2 splicing.* Mol Cell, 2009. **33**(5): p. 591-601.
363. Diez de Medina, S.G., et al., *Decreased expression of keratinocyte growth factor receptor in a subset of human transitional cell bladder carcinomas.* Oncogene, 1997. **14**(3): p. 323-30.
364. Chaffer, C.L., et al., *Mesenchymal-to-epithelial transition facilitates bladder cancer metastasis: role of fibroblast growth factor receptor-2.* Cancer Res, 2006. **66**(23): p. 11271-8.
365. James , N.D., et al., *Radiotherapy with or without Chemotherapy in Muscle-Invasive Bladder Cancer.* New England Journal of Medicine, 2012. **366**(16): p. 1477-1488.
366. James, N.D. and S.A. Hussain, *A multidisciplinary approach in muscle-invasive disease: novel chemotherapy combinations and targets in chemoradiation.* Am Soc Clin Oncol Educ Book, 2013: p. 200-6.
367. El-Taji, O.M.S., S. Alam, and S.A. Hussain, *Bladder Sparing Approaches for Muscle-Invasive Bladder Cancers.* Curr Treat Options Oncol, 2016. **17**.
368. Hafeez, S., et al., *Selective organ preservation with neo-adjuvant chemotherapy for the treatment of muscle invasive transitional cell carcinoma of the bladder.* Br J Cancer, 2015. **112**(10): p. 1626-1635.
369. Choi, W., et al., *Identification of distinct basal and luminal subtypes of muscle-invasive bladder cancer with different sensitivities to frontline chemotherapy.* Cancer Cell, 2014. **25**(2): p. 152-65.
370. Zhu, J., et al., *An overview of chemical inhibitors of the Nrf2-ARE signaling pathway and their potential applications in cancer therapy.* Free Radic Biol Med, 2016. **99**: p. 544-556.
371. Tang, X., et al., *Luteolin inhibits Nrf2 leading to negative regulation of the Nrf2/ARE pathway and sensitization of human lung carcinoma A549 cells to therapeutic drugs.* Free Radical Biology and Medicine, 2011. **50**(11): p. 1599-1609.
372. Chian, S., et al., *Luteolin inhibits the Nrf2 signaling pathway and tumor growth in vivo.* Biochemical and Biophysical Research Communications, 2014. **447**(4): p. 602-608.
373. Horinaka, M., et al., *Luteolin induces apoptosis via death receptor 5 upregulation in human malignant tumor cells.* Oncogene, 2005. **24**(48): p. 7180-7189.
374. Xu, H., et al., *Luteolin synergizes the antitumor effects of 5-fluorouracil against human hepatocellular carcinoma cells through apoptosis induction and metabolism.* Life Sciences, 2016. **144**: p. 138-147.
375. Gao, A.-M., et al., *Chrysin enhances sensitivity of BEL-7402/ADM cells to doxorubicin by suppressing PI3K/Akt/Nrf2 and ERK/Nrf2 pathway.* Chemico-Biological Interactions, 2013. **206**(1): p. 100-108.

376. Gao, A.-M., et al., *Apigenin sensitizes doxorubicin-resistant hepatocellular carcinoma BEL-7402/ADM cells to doxorubicin via inhibiting PI3K/Akt/Nrf2 pathway.* Carcinogenesis, 2013. **34**(8): p. 1806-1814.
377. Lin, C.W., et al., *Neurotrophic and cytoprotective action of luteolin in PC12 cells through ERK-dependent induction of Nrf2-driven HO-1 expression.* J Agric Food Chem, 2010. **58**(7): p. 4477-86.
378. Verma, A.K., et al., *Isoniazid prevents Nrf2 translocation by inhibiting ERK1 phosphorylation and induces oxidative stress and apoptosis.* Redox Biology, 2015. **6**: p. 80-92.
379. Tarumoto, T., et al., *Ascorbic acid restores sensitivity to imatinib via suppression of Nrf2-dependent gene expression in the imatinib-resistant cell line.* Experimental Hematology, 2004. **32**(4): p. 375-381.
380. Wang, H., et al., *RXRalpha inhibits the NRF2-ARE signaling pathway through a direct interaction with the Neh7 domain of NRF2.* Cancer Res, 2013. **73**(10): p. 3097-108.
381. Johnson, P., et al., *Clinical and biological effects of an agonist anti-CD40 antibody: a Cancer Research UK phase I study.* Clin Cancer Res, 2015. **21**(6): p. 1321-8.
382. Beatty, G.L., et al., *A phase I study of an agonist CD40 monoclonal antibody (CP-870,893) in combination with gemcitabine in patients with advanced pancreatic ductal adenocarcinoma.* Clin Cancer Res, 2013. **19**(22): p. 6286-95.
383. Vonderheide, R.H., et al., *Phase I study of the CD40 agonist antibody CP-870,893 combined with carboplatin and paclitaxel in patients with advanced solid tumors.* Oncoimmunology, 2013. **2**(1): p. e23033.
384. Sandin, L.C., et al., *Locally delivered CD40 agonist antibody accumulates in secondary lymphoid organs and eradicates experimental disseminated bladder cancer.* Cancer Immunol Res, 2014. **2**(1): p. 80-90.
385. The Cancer Genome Atlas Research, N., *Comprehensive molecular characterization of urothelial bladder carcinoma.* Nature, 2014. **507**(7492): p. 315-322.
386. Hoadley, K.A., et al., *Multiplatform analysis of 12 cancer types reveals molecular classification within and across tissues of origin.* Cell, 2014. **158**(4): p. 929-44.
387. Sjodahl, G., et al., *Toward a molecular pathologic classification of urothelial carcinoma.* Am J Pathol, 2013. **183**(3): p. 681-91.
388. Rosenberg, J.E., et al., *Atezolizumab in patients with locally advanced and metastatic urothelial carcinoma who have progressed following treatment with platinum-based chemotherapy: a single-arm, multicentre, phase 2 trial.* The Lancet. **387**(10031): p. 1909-1920.
389. Plimack, E.R., et al., *LBA23A PHASE 1B STUDY OF PEMBROLIZUMAB (PEMBRO; MK-3475) IN PATIENTS (PTS) WITH ADVANCED UROTHELIAL TRACT CANCER.* Annals of Oncology, 2014. **25**(suppl 4).
390. Powles, T., et al., *MPDL3280A (anti-PD-L1) treatment leads to clinical activity in metastatic bladder cancer.* Nature, 2014. **515**(7528): p. 558-562.
391. Andrea Borghese Apolo, Y.T., Min-Jung Lee, Sunmin Lee, Ari Frosch, Seth M. Steinberg, James L. Gulley, Jeffrey Schlom, Donald P Bottaro, Jane B. Trepe. *Effect of cabozantinib on immunosuppressive subsets in metastatic*

urothelial carcinoma. in *American Society for Clinical Oncology* 2014. Chicago, IL: J Clin Oncol 32:5s, 2014 (suppl; abstr 4501).
392. Grivas, P.D., et al., *Double-blind, randomized, phase 2 trial of maintenance sunitinib versus placebo after response to chemotherapy in patients with advanced urothelial carcinoma.* Cancer, 2014. **120**(5): p. 692-701.
393. Jones, R.J., et al., *Pazopanib versus paclitaxel in relapsed urothelial tumors: A randomized phase II study investigating pazopanib versus weekly paclitaxel in relapsed or progressive transitional cell carcinoma of the urothelium (PLUTO).* J Clin Oncol (Meeting Abstracts), 2014. **32**(15_suppl): p. TPS4589-.
394. Choueiri, T.K., et al., *Double-blind, randomized trial of docetaxel plus vandetanib versus docetaxel plus placebo in platinum-pretreated metastatic urothelial cancer.* J Clin Oncol, 2012. **30**(5): p. 507-12.
395. Krege, S., et al., *Prospective randomized double-blind multicentre phase II study comparing gemcitabine and cisplatin plus sorafenib chemotherapy with gemcitabine and cisplatin plus placebo in locally advanced and/or metastasized urothelial cancer: SUSE (AUO-AB 31/05).* BJU Int, 2014. **113**(3): p. 429-36.
396. Petrylak, D.P., et al., *Docetaxel As Monotherapy or Combined With Ramucirumab or Icrucumab in Second-Line Treatment for Locally Advanced or Metastatic Urothelial Carcinoma: An Open-Label, Three-Arm, Randomized Controlled Phase II Trial.* Journal of Clinical Oncology, 2016. **34**(13): p. 1500-1509.
397. Iyer, G., et al., *Prevalence and Co-Occurrence of Actionable Genomic Alterations in High-Grade Bladder Cancer.* J Clin Oncol, 2013. **31**(25): p. 3133-40.
398. Iyer, G., et al., *Genome sequencing identifies a basis for everolimus sensitivity.* Science, 2012. **338**(6104): p. 221.
399. Wagle, N., et al., *Activating mTOR mutations in a patient with an extraordinary response on a phase I trial of everolimus and pazopanib.* Cancer Discov, 2014. **4**(5): p. 546-53.
400. Oudard, S., et al., *Multicentre randomised phase II trial of gemcitabine+platinum, with or without trastuzumab, in advanced or metastatic urothelial carcinoma overexpressing Her2.* Eur J Cancer, 2015. **51**(1): p. 45-54.
401. Thomas Powles, R.A.H., Tony Elliott, Robert Jones, Syed A. Hussain, Simon J. Crabb, Charlotte Ackerman, Satinder Jagdev, John D. Chester, Serena Hilman, Mark Beresford, A. Graham Macdonald, Santhanam Sundar, John A. Frew, Andrew Stockdale, Shah-Jalal Sarker, Daniel Berney, Simon Chowdhury. *A phase II/III, double-blind, randomized trial comparing maintenance lapatinib versus placebo after first line chemotherapy in HER1/2 positive metastatic bladder cancer patients.* in *American Society for Clinical Oncology* 2015. J Clin Oncol 33, 2015 (suppl; abstr 4505)

.
402. Choudhury, N.J., et al., *Afatinib Activity in Platinum-Refractory Metastatic Urothelial Carcinoma in Patients With ERBB Alterations.* J Clin Oncol, 2016. **34**(18): p. 2165-71.

403. Tabernero, J., et al., *Phase I Dose-Escalation Study of JNJ-42756493, an Oral Pan-Fibroblast Growth Factor Receptor Inhibitor, in Patients With Advanced Solid Tumors.* J Clin Oncol, 2015. **33**(30): p. 3401-8.
404. Sequist, L.V., et al., *Abstract CT326: Phase I study of BGJ398, a selective pan-FGFR inhibitor in genetically preselected advanced solid tumors.* Cancer Research, 2014. **74**(19 Supplement): p. CT326-CT326.
405. Milowsky, M.I., et al., *Phase 2 trial of dovitinib in patients with progressive FGFR3-mutated or FGFR3 wild-type advanced urothelial carcinoma.* Eur J Cancer, 2014. **50**(18): p. 3145-52.
406. Ko, Y.J., et al., *Nanoparticle albumin-bound paclitaxel for second-line treatment of metastatic urothelial carcinoma: a single group, multicentre, phase 2 study.* Lancet Oncol, 2013. **14**(8): p. 769-76.
407. Damrauer, J.S., et al., *Intrinsic subtypes of high-grade bladder cancer reflect the hallmarks of breast cancer biology.* Proc Natl Acad Sci U S A, 2014. **111**(8): p. 3110-5.

Appendix I – Publication: Gene expression profiling in bladder cancer identifies potential therapeutic targets

INTERNATIONAL JOURNAL OF ONCOLOGY

Gene expression profiling in bladder cancer identifies potential therapeutic targets

SYED A. HUSSAIN[1*], DANIEL H. PALMER[1*], WING-KIN SYN[2,3], JOSEPH J. SACCO[1], RICHARD M.D. GREENSMITH[1], TAHA ELMETWALI[1], VIJAY AACHI[4], BRYONY H. LLOYD[1], PUTHEN V. JITHESH[1], JOHN ARRAND[5], DARREN BARTON[5], JAWAHER ANSARI[6], D. ROSS SIBSON[1] and NICHOLAS D. JAMES[5]

[1]Department of Molecular and Clinical Cancer Medicine, University of Liverpool, Liverpool L69 3GA; [2]Regeneration and Repair Group, The Institute of Hepatology, Foundation of Liver Research, London SE5 9NT, UK; [3]Department of Physiology, University of the Basque Country, 48940 Leioa, Spain; [4]The Royal Liverpool and Broadgreen University Hospital Trust, Liverpool L7 8XP; [5]School of Cancer Sciences, University of Birmingham, Birmingham B15 2TT; [6]Beatson West Scotland Cancer Centre, Glasgow G12 0YN, UK

Received November 22, 2016; Accepted January 27, 2017

DOI: 10.3892/ijo.2017.3893

Abstract. Despite advances in management, bladder cancer remains a major cause of cancer related complications. Characterisation of gene expression patterns in bladder cancer allows the identification of pathways involved in its pathogenesis, and may stimulate the development of novel therapies targeting these pathways. Between 2004 and 2005, cystoscopic bladder biopsies were obtained from 19 patients and 11 controls. These were subjected to whole transcript-based microarray analysis. Unsupervised hierarchical clustering was used to identify samples with similar expression profiles. Hypergeometric analysis was used to identify canonical pathways and curated networks having statistically significant enrichment of differentially expressed genes. Osteopontin (OPN) expression was validated by immunohistochemistry. Hierarchical clustering defined signatures, which differentiated between cancer and healthy tissue, muscle-invasive or non-muscle invasive cancer and healthy tissue, grade 1 and grade 3. Pathways associated with cell cycle and proliferation were markedly upregulated in muscle-invasive and grade 3 cancers. Genes associated with the classical complement pathway were downregulated in non-muscle invasive cancer. Osteopontin was markedly over-expressed in invasive cancer compared to healthy tissue. The present study contributes to a growing body of work on gene expression signatures in bladder cancer. The data support an important role for osteopontin in bladder cancer, and identify several pathways worthy of further investigation.

Correspondence to: Dr Syed A. Hussain, Department of Molecular and Clinical Cancer Medicine, University of Liverpool, Duncan Building, Daulby Street, Liverpool, L69 3GA, UK
E-mail: syed.hussain@liverpool.ac.uk

*Contributed equally

Abbreviations: NMIBC, non-muscle invasive bladder cancer; MIBC, muscle invasive bladder cancer; CDK1, cyclin-dependent kinase 1; FOXM1, forkhead box protein M1; PLK1, polo-like kinase 1; KNSL1, kinesin family member 11; Mef2, myocyte enhancer factor-2; MyoD, myogenic differentiation 1; EMT, epithelial to mesenchymal transition; MMPs, matrix metalloproteinases; MMP1, matrix metalloproteinase 1; MMP16, matrix metalloproteinase 16; PELO, protein pelota homolog; SERPINB13, Serpin peptidase inhibitor, clade B (ovalbumin), member 13; CASC5, cancer susceptiility candidate 5; APC, anaphase promoting complex; TPX2, targeting protein for Xklp2; TOP2A, topoisomerase 2-alpha; MVAC, methotrexate, vinblastine, adriamycin and cisplatin; OPN, osteopontin; TCC, transitional cell carcinoma; CFH, compliment factor H; ESRP1, epithelial splicing regulatory protein 1; ESRP2, epithelial splicing regularoty protein 2; FGFR2(b,c), fibroblast growth factor receptor 2 (b isoform, c isoform); IHC, immunohistochemistry

Key words: bladder cancer, osteopontin, gene expression analysis, molecular classification, microarray, muscle invasive

Introduction

Carcinoma of the bladder is the most common urothelial malignancy, and is the 6th commonest cancer in the world by incidence (1). Despite significant improvements in management, bladder cancer remains one of the commonest causes of cancer related mortality, ranked 6th and 11th in the UK in 2008 in men and women, respectively (2). Additionally, curative surgery or radiotherapy commonly results in significant long-term morbidity.

Localised bladder cancer may be divided into either non-muscle invasive bladder cancer (NMIBC) or into muscle invasive bladder cancer (MIBC). While the former may be cured by transurethral resection, treatment of the latter requires radical local management using either cystectomy

Table I. Patient demographics.

Demographics	Controls (n=11)	NMIBC (n=14)	MIBC (n=6)
Age in years			
Median, range	79.2 (64-85.8)	70.8 (47.0-81.9)	80.14 (65.3-85.8)
Gender			
Male	8 (72.2)	11 (78.6)	3 (60.0)
Female	3 (27.2)	3 (21.4)	2 (40.0)
Grade			
G1	N/A	6 (42.8)	0 (0)
G2	N/A	1 (7.1)	0 (0)
G3	N/A	7 (50.0)	6 (100)
T stage			
PT1	N/A	5 (35.7)	0 (0)
PT1B	N/A	1 (7.1)	0 (0)
Pta	N/A	8 (57.1)	0 (0)
PT2	N/A	0 (0)	6 (100)
Recurrence			
No	N/A	12 (92.3)	0 (0)
Yes	N/A	1 (7.7)	5 (100)
Survival in months (95% CI)	N/A	81.2 (73.3-not estimatable)	12.26 (0-35.6)

N/A, not applicable.

or radical radiotherapy (with or without concurrent chemotherapy). Approximately a third of NMIBC tumours will recur and progress to muscle invasive over time (3). Several clinicopathological factors including tumour grade, stage, size, presence of carcinoma *in situ*, previous recurrence (4), and p53 status are associated with increased likelihood of progression. However, these factors are not currently clearly sufficient to identify patients who need more radical therapy at the outset. Similarly, stratification of patients with muscle invasive cancer into those most likely to recur or progress following local therapy would enable a more personalised approach to treatment.

Previous studies have employed microarrays to investigate gene expression profiles in bladder cancer (5-8). The identification of differentially regulated genes and gene networks allows the dissection of pathways and processes that are dysregulated in bladder cancer. This, in turn, provides invaluable clues relating to pathogenesis and moreover, may provide novel targets for drug development.

Here, we describe a study in which we profiled gene expression in 20 bladder cancer samples and compared this to 11 healthy urothelial samples. In addition to defining gene expression signatures for different subgroups, the study identified several genes and gene networks which are significantly deregulated in bladder cancer. These include osteopontin and the classical complement pathway. In this study we used the Affymetrix Human Gene 1.0 ST array which is a whole transcript based array compared to many other studies which used arrays querying only the 3' end of transcripts.

Materials and methods

Patients and tumour samples. Cystoscopic tissue biopsies were collected between May 2004 and November 2005. Prior to undergoing cystoscopy, participants gave written informed consent for additional biopsies to be taken for this study during their medical procedure. Patients eligible for inclusion were those aged 18-80 years with a diagnosis of histologically confirmed superficial (NMIBC) or muscle invasive (MIBC) transitional cell carcinoma (n=14 and n=6, respectively), and who had not received any prior therapy. Control (C) samples were obtained from uninvolved tissues, for which no abnormalities were observed upon histological examination (n=11). Ten of these were paired with bladder cancer biopsies (4 non-muscle invasive and 5 muscle invasive), while the last was from a patient without a diagnosis of malignancy. Demographic characteristics of the patient cohort are presented in Table I. MIBC samples displayed a basal immuno-phenotype.

Tumour samples for IHC analysis were obtained from the Liverpool Bioinnovation Hub Biobank (Liverpool, UK). Pathologically assessed samples used healthy bladder tissue (n=3) and MIBC tumour tissue (n=3).

Ethical considerations. Approval for the present study was obtained from the South Birmingham Local Research Ethics Committee. All participants gave written informed consent for their respective biopsies to be utilized in this study. Approval for further anaylsis was granted by the Liverpool Tissue Bank Ethics Committee (application no. 12-09). All participants

gave written informed consent for their respective biopsies to be used in biomedical analysis.

Tissue sample preparation. Tissue biopsy samples were snap-frozen and stored in liquid nitrogen prior to RNA extraction.

RNA isolation. Total RNA was extracted from each tissue using TRIzol (Invitrogen) prior to purification on silica (RNeasy Mini columns; Qiagen, Hilden, Germany) according to the manufacturer's recommendation. An Agilent Bioanalyser was used to confirm RNA integrity and only samples having a RIN of 6.0 or more were used.

cDNA probe synthesis. A total of 200 ng of total RNA was converted to cDNA including targeted depletion of rRNA transcripts using a WT Expression kit (Ambion, Cambridge, MA, USA) according to the manufacturer's procedures. Resultant cDNA was fragmented and biotin end labelled using an Affymetrix WT Terminal Labelling kit (Affymetrix, Santa Clara, CA, USA).

Microarray hybridisation analysis. Labelled cDNA was hybridised to Affymetrix Human Gene 1.0 ST whole transcript-based arrays followed by washing and staining on an Affymetrix FS450 fluidics station. The Human Gene 1.0 ST Array (Affymetrix) comprised 764,885 distinct 25-nt probes interrogating 28,869 annotated genes based on the March 2006 (UCSC hg18, NCBI Build 36) human genome sequence assembly with comprehensive coverage of RefSeq, Ensembl and putative complete CDS GenBank transcripts.

Signal collection and analysis. Arrays were scanned using an Affymetrix Scanner 3000 7G. Affymetrix Command Console was used for instrument control and data acquisition. All procedures were carried out according to the standard Affymetrix protocols. Raw microarray data were submitted to ArrayExpress (Accession: E-MTAB-1560).

Statistical analysis of microarray data

Data transformation. Robust multi-array averaging, adjusted for non-specific binding, (GCRMA) was used for normalisation and summarisation of the probe intensity signals (9,10). Data were subject to RMA background correction and quantile normalisation across all chips (to ensure comparable mean and standard deviation of the probe intensities), prior to log2 transformation and median polish probe set summarisation.

Array data quality estimation. The normalised unscaled standard error (NUSE) of each array was calculated to compare data variability between and within arrays (11). A NUSE value of 1.05 was set as the upper limit of acceptable quality.

Data analysis. Principal components analysis using a covariance dispersion matrix was performed to map high dimensional data of each sample to 3 dimensions for estimation of clustering according to classification and identification of outlying samples.

A mixed model analysis of variance (ANOVA) including methods of moments estimation was used to identify differential expression between non-invasive tumours, invasive tumours and healthy bladder tissue. Batch effects were taken into consideration within the model. ANOVA was conducted including 'patient' as a factor, taking the paired samples into consideration. Differences in gene expression between tumours of differing grade, and also differential expression between tumour samples were assessed using the t-test. To correct for multiple testing, genes were considered to be significantly differentially expressed if a false discovery rate (FDR) adjusted $P<0.05$ was obtained. The false discovery rate was calculated as previously described (12). Those genes whose fold change expression level was found to significantly differ by ±2x or greater were used for further analysis.

Unsupervised hierarchical agglomerative clustering (Euclidean distance with average linkage clustering) was used to identify samples with similar expression profiles.

MetaCore version 6.7 (GeneGo, Inc., St. Joseph, MI, USA), IPA (Ingenuity Systems, Redwood City, CA, USA) and DAVID Bioinformatics resource v 6.7 (13) were employed to identify canonical pathways and curated networks having statistically significant enrichment of differentially expressed genes. Pathways from MetaCore analysis filtered on FDR <0.05 are presented in Results, unless otherwise stated. Univariate Cox proportional hazards regression analysis was performed to evaluate the association between disease progression and differential gene expression.

Meta-analysis. Meta-analysis was conducted using publicly available gene expression data from Gene Expression Omnibus (14). Out of the possible 12 datasets identified (GSE88, GSE89, GSE7476, GSE30522, GSE24152, GSE3167, GSE5287, GSE12630, GSE27448, GSE19915, GSE13507 and GSE5479), we selected two datasets using the same microarray platform (Affymetrix Human Genome U133A array) with a large number of samples for further analysis. Raw CEL files from GSE3167 (15) with 60 samples and GSE5287 (16) with 30 samples were imported into Partek Genomic Suite (Partek, Inc., Chesterfield, MO, USA) and data were processed and differential genes identified following the same protocol described earlier for our own data. Clinico-pathological data for the datasets were kindly provided by the authors. The GSE3167 dataset contains superficial transitional cell carcinoma (NMIBC) with surrounding carcinoma *in situ* (CIS) (13 patients), without surrounding CIS lesions (15 patients), muscle invasive carcinoma (MIBC, 13 patients), CIS only (n=5) and healthy bladder (n=14). The GSE2587 dataset contains 30 samples from patients with muscle invasive bladder cancer.

Immunostaining

Western blotting. Western blotting was performed to validate the specificity of anti-OPN antibody (AF1433; R&D Systems, Inc., Minneapolis, MN, USA) for subsequent IHC analysis. Protein lysates were prepared in RIPA buffer from a MIBC cell line, 253-J and a NMIBC cell line, RT112. Bradford was used for protein quantification. Proteins were separated by SDS-PAGE prior to transferring onto a PDVF membrane. Blocking was performed for 1 h with 10% milk, prior to overnight incubation in 1:1,000 dilution of AF1433. Secondary antibody was applied for 1 h before visualising using ECL. β-actin (ab8227; Abcam) was used to demonstrate equal protein loading.

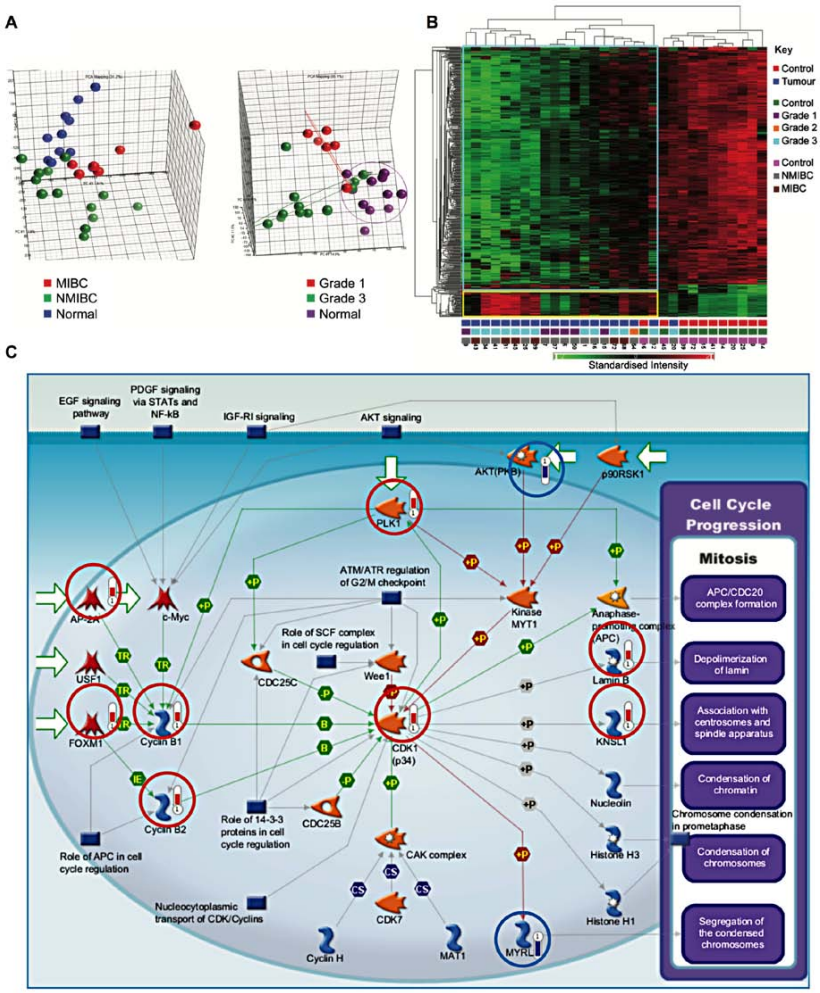

Figure 1. Cell proliferation genes are upregulated in bladder cancer. (A) Principal components analysis. Segregation into groups by tissue type and tumour grade was assessed. (B) Hierarchical clustering segregates tumour samples from healthy tissue. Key shown on the right. The numbers at the bottom of each column correspond to patient serial numbers. Standardised intensity range -2 (green) to 2 (red), 0 (black) fold change. (C) Genes involved in the initiation of mitosis are upregulated in bladder cancer ($P=2.59\times10^{-9}$). Genes circled in red and blue were, respectively, upregulated or downregulated in cancer samples. The length of the bar is proportional to the degree of change in expression.

Immunohistochemistry. Conditions for IHC with AF1433 were optimised in clear cell renal carcinoma and kidney FFPE sections, using a no primary antibody control, a goat IgG isotype control (AB-108-C; R&D Systems) and a negative tissue control-breast skin. Antigen retreval was performed using the PT-link at pH 9.0, prior to peroxidase block (Dako), 1-h primary antibody (1:50 AF1433) incubation at RT, 1-h secondary antibody incubation at RT (1:100) prior to visualisation with DAB Chromagen (Dako). Staining intensity was scored by a consultant pathologist. Briefly, staining intensity was graded as 0 (negative), + (weak), ++ (moderate) and +++ (strong).

Results

Bladder cancer tissues exhibit specific gene signatures. A total of 418 genes were differentially expressed between

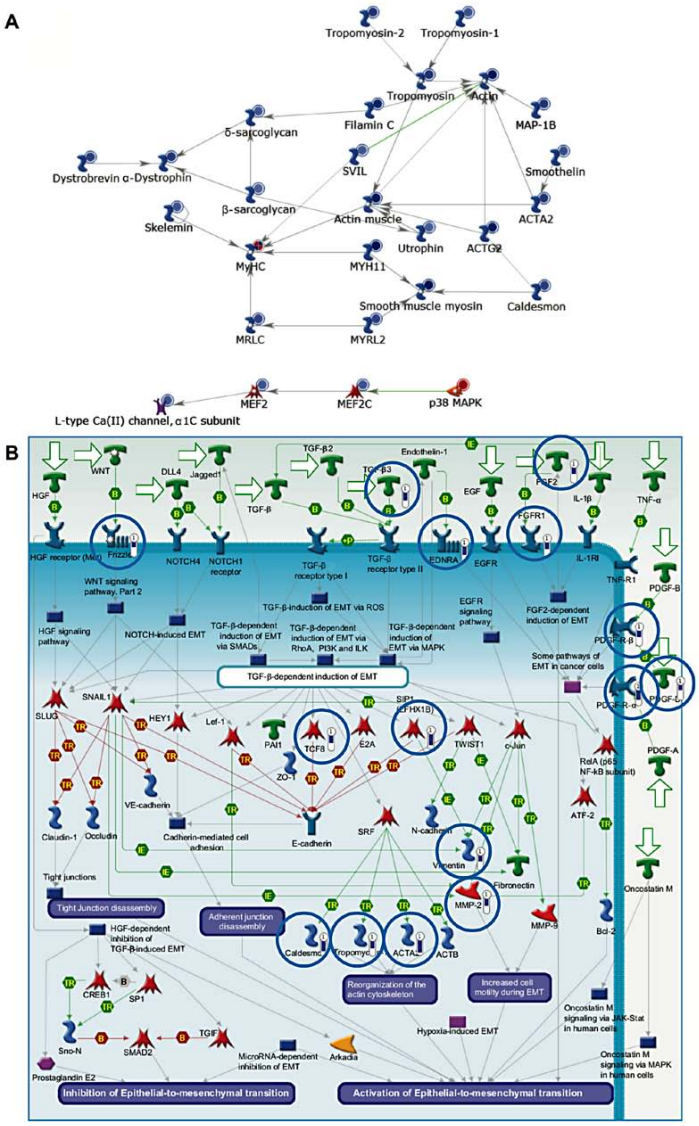

Figure 2. Genes involved in myogenesis and EMT are dysregulated in bladder cancer. (A) Genes involved in myogenesis were downregulated in cancer samples ($P=1.22x10^{-10}$). The relative expression for each gene is depicted by the colour and intensity of the circle (blue, downregulation; red, upregulation). (B) Downregulation of genes involved in EMT in cancer samples ($P=1.41x10^{-9}$). Genes circled in blue exhibited reduced expression within the tumour samples relative to healthy bladder tissue. The length of the blue bar is proportional to the extent of downregulation.

cancer and control samples, using a fold change of at least 2.5, and a false discovery rate (FDR) of 0.05. Of these, 368 genes showed reduced expression in tumours, while 50 genes showed increased expression in tumours. Principal components analysis demonstrated segregation of samples by tissue type and tumour grade (Fig. 1A). Similarly, hierarchical clustering

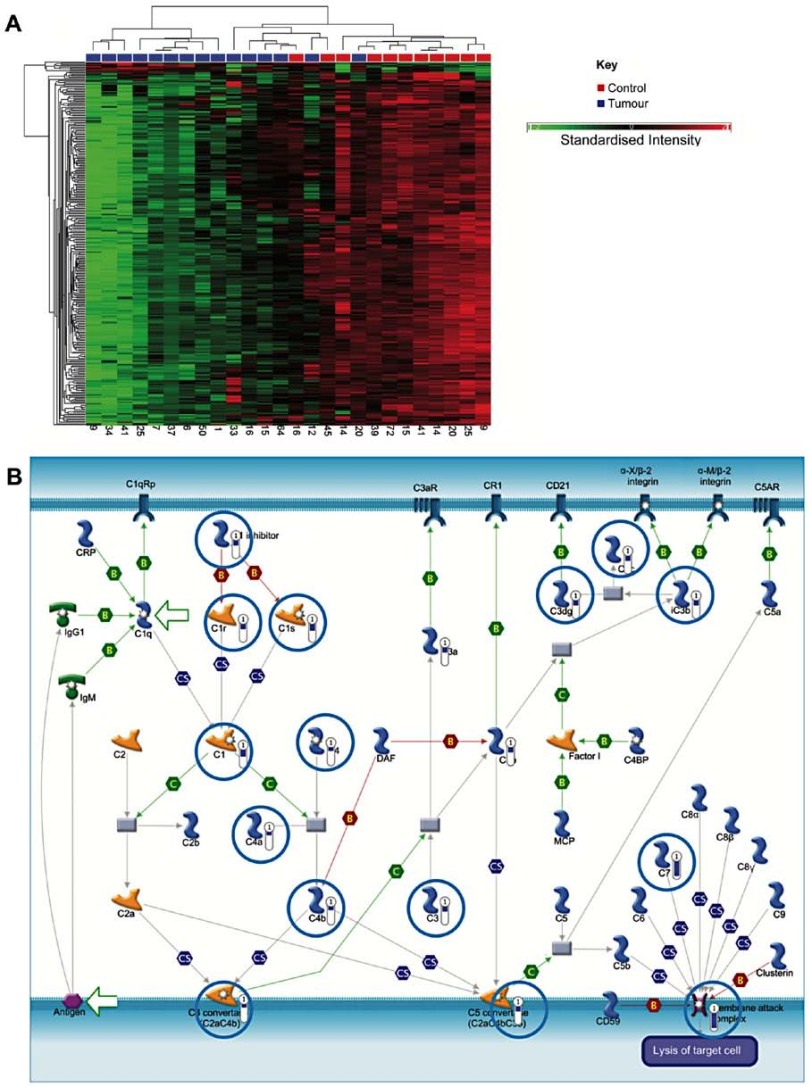

Figure 3. Classical complement genes are downregulated in NMIBC. (A) Hierarchical clustering showing clustering of NMIBC and healthy tissue samples, though complete separation is not established. A key is given on the right of the figure. The numbers at the bottom of each column correspond to patient serial numbers. Standardised intensity range -2 (green) to 2 (red), 0 (black) fold change. (B) Genes associated with the classical complement pathway are downregulated in NMIBC ($P=5.12x10^{-10}$).

segregated healthy bladder tissue and bladder cancer into two groups (Fig. 1B).

Multiple genes involved in proliferation were upregulated in bladder cancer samples as compared to healthy samples ($P=2.59x10^{-9}$) (Fig. 1C). These included components of the cyclin-dependent kinase 1 (CDK1)/cyclin B complex, activation of which is required to drive progression from G2- to M-phase. Initiation of cyclin B transcription is carried out by FOXM1. Moreover, the equilibrium between nuclear import and export of cyclin B1 is influenced by its phosphorylation

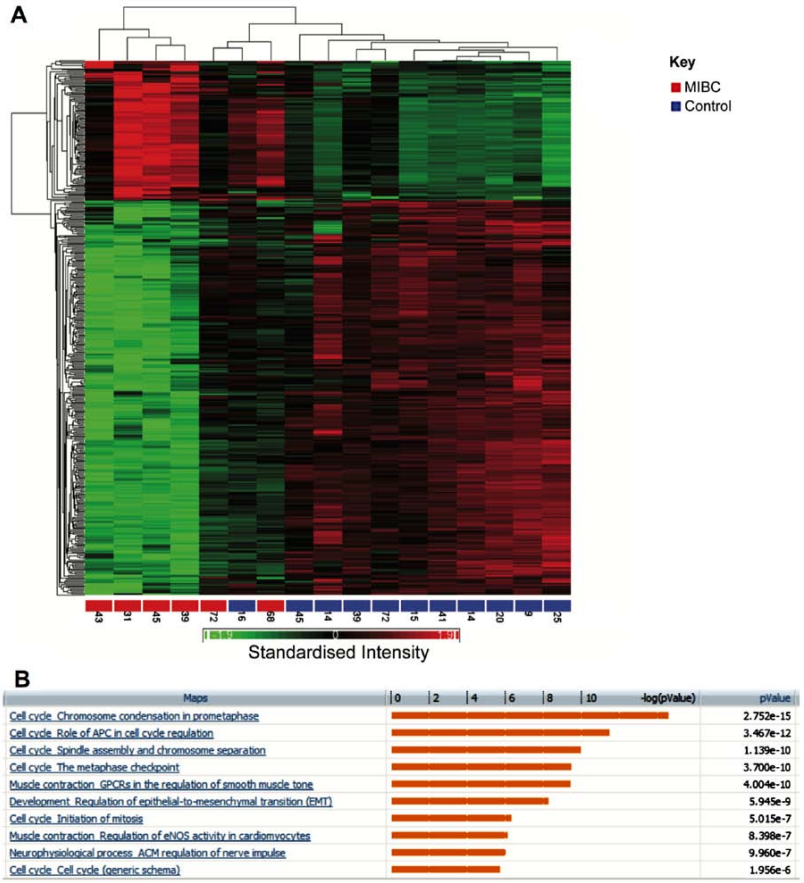

Figure 4. Dysregulation of pathways in MIBC. (A) Hierarchical clustering of genes and samples showing segregation of muscle-invasive tumour samples and control samples into different clusters. A key is shown on the right of the figure. The numbers at the bottom of each column correspond to patient serial numbers. Standardised intensity range -1.9 (green) to 1.9 (red), 0 (black) fold change. (B) Pathway enrichment (MIBC vs. control samples).

status by PLK1, which was also upregulated. The substrates of CDK1/cyclin B include Lamin B, leading to depolymerization of the lamin nuclear-cytoskeleton, and Kinesin-related motor protein Eg5 (KNSL1), which associates with centrosomes and spindle apparatus.

Genes involved in myogenesis and epithelial-to-mesenchymal transition (EMT) are downregulated in cancer samples. Genes downregulated in cancer (compared to healthy tissue) included several which are involved in myogenesis ($P=1.22x10^{-10}$) (Fig. 2A). These included the myocyte enhancer factor, Mef2, which is expressed during myogenesis. Mef2 and MyoD interact leading to MyoD activation and hence the expression of myosin heavy and light chains. In addition, genes involved in EMT were also downregulated ($P=1.41x10^{-9}$) (Fig. 2B). EMT is critical during myogenesis, particularly as the muscle precursor cells delaminate from the dermomyotome. Muscle precursors invade the developing tissue and differentiate into mature muscle cells.

Comparison of NMIBC and healthy bladder tissue. A specific comparison was also made between NMIBC and healthy tissue. This identified 410 genes, which were differentially expressed by ≥2.5-fold ($P<0.05$, false discovery rate). Of these, 393 were downregulated in cancer, while increased expression was observed in 17 (data not shown). Hierarchical clustering generally segregated into two groups, but with additional branching in one cluster as shown in Fig. 3A.

Similar to the analysis comparing all bladder cancer samples to healthy samples, genes involved in smooth muscle

Table II. Genes exhibiting >5 fold differential expression between grade 3 and MIBC (FDR P<0.05).

Gene	ID	RefSeq	P-value	Fold change (MIBC/NMIBC
Family with sequence similarity 83, member D	FAM83D	NM_030919	5.50E-06	7.87015
Retinoic acid receptor responder (tazarotene induced) 1	RARRES1	NM_206963	0.001291	5.96921
Centromere protein I	CENPI	NM_006733	1.35E-05	5.92042
Fibronectin 1	FN1	NM_212482	0.000579	5.86325
Centromere protein F, 350/400 ka (mitosin)	CENPF	NM_016343	0.000505	5.7622
N mannosidase, α, class 1C, member 1	MAN1C1	NM_020379	0.000401	5.52916
Topoisomerase (DNA) II α 170 kDa	TOP2A	NM_001067	0.00091	5.32363
TPX2, microtubule-associated, homolog (*Xenopus laevis*)	TPX2	NM_012112	0.000892	5.27537
Ras association (RalGDS/AF-6) domain family member 2	RASSF2	NM_014737	0.000644	5.04613
Anillin, actin binding protein	ANLN	NM_018685	0.000489	5.01334

Table III. DAVID functional annotation clusters.

Annotation cluster	Enrichment score	Count	P-value
Extracellular glycoproteins	6.47	37	2.7E-07
Serine-type endopeptidase inhibitor activity	3.29	7	7.90E-05
Negative regulation of immune system processes	2.21	6	4.60E-04
Zymogen (proteolytic enzyme precursors)	1.85	14	5.10E -04
Cell migration	1.33	9	1.40E-03
EGF	1.18	5	1.50E-02
Response to wounding	0.95	13	8.20E-04

development and EMT were downregulated ($P=4.8x10^{-12}$). Notably, genes associated with the classical complement pathway were strongly downregulated in NMIBC samples, which may indicate a mechanism for immune evasion ($P=5.12x10^{-10}$) (Fig. 3B).

MIBC vs. healthy tissue. Hierarchical clustering showed segregation of MIBC and healthy samples into two groups (Fig. 4A). There were 404 genes that were altered by at least 3-fold (P<0.05 false discovery rate). Out of these, 107 showed increased expression between invasive tumours and healthy samples, while 297 were decreased in expression. Pathways enriched for these differentially regulated genes are shown in Fig. 4B. Genes involved in chromosome condensation in prometaphase were upregulated in invasive bladder cancer ($P=2.75x10^{-15}$). Similarly, several regulators of the anaphase promoting complex (APC) were also upregulated ($P=3.47x10^{-12}$). These included the kinases, PLK1 and CDK1.

Comparison of grade 1 and 3 NMIBC. A further comparison was made between gene expression profiles in grade 1 and 3 bladder cancers, which identified 341 genes that were differentially regulated by at least 2-fold (FDR P<0.05). Hierarchical clustering clearly segregates between grade 1 and 3 (Fig. 5A). Enriched pathways are shown in Fig. 5B. Notably multiple pathways associated with cell cycle progression were upregulated in grade 3 tumours and multiple core cell cycle components were upregulated in grade 3 tumours. Genes involved in the metaphase checkpoint were particularly upregulated ($P=3.06x10^{-17}$). A comparison was also made of genes that were upregulated both in grade 3 compared to grade 1 NMIBC and in MIBC compared to healthy samples.

Comparing grade 3 NMIBC and MIBC. A total of 292 genes were differentially expressed 2 or more fold (P<0.05). Of these, 144 showed increased expression in MIBC while the remaining 148 exhibited decreased expression in MIBC. Hierarchical clustering resulted in clear segregation between the two groups. Table II lists genes that were differentially expressed by >5-fold in grade 3 NMIBC compared to MIBC. Among the genes most upregulated in MIBC were the proteinases. Overexpression and activation of proteinases, that destroy the connective tissue, are involved in various pathological processes including tumour progression. The most proteolytic of enzymes are the metalloproteinases. The matrix metalloproteinases (MMPs) comprise a family of enzymes that collectively can degrade all components of the extracellular matrix (ECM), these were upregulated in this study. For example, the matrix metalloproteinases MMP1 and MMP16 were upregulated 4.8- and 2.6-fold, respectively in MIBC compared to NMIBC.

Further functional analysis using Database for Annotation, Visualization and Integrated Discovery (DAVID). A further analysis of 143 genes, which were upregulated in MIBC

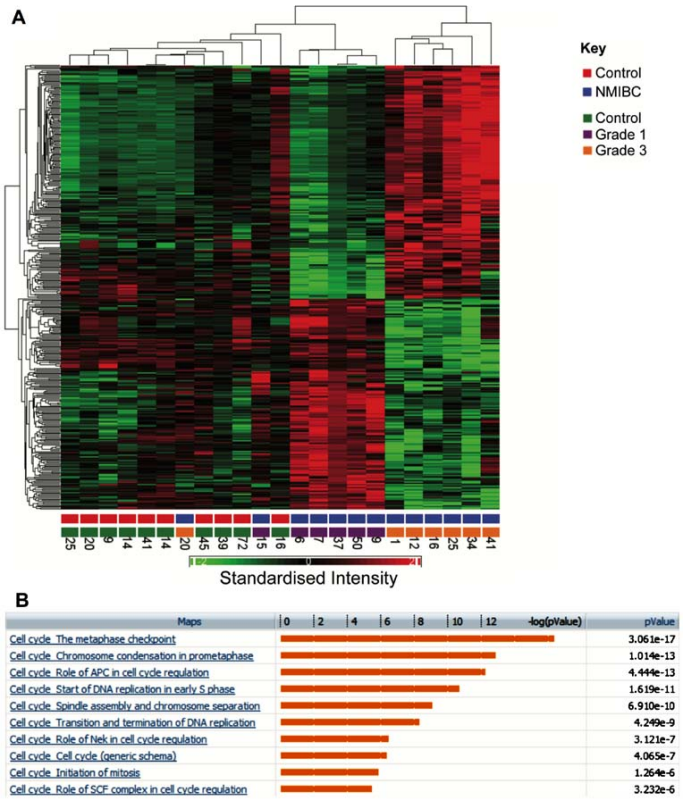

Figure 5. Comparing grade 3 and 1 NMIBC. (A) Hierarchical clustering segregates grade 1 and 3 NMIBC samples. The numbers at the bottom of each column correspond to patient serial numbers. Standardised intensity range -2 (green) to 2 (red), 0 (black) fold change. (B) Pathway enrichment (grade 3 vs. grade 1 NMIBC).

compared to NMIBC was performed using the DAVID database. A summary of annotation clusters is given in Table III.

Meta-analysis of gene expression data. In order to validate our results, we used a meta-analysis of a larger dataset consisting of 90 samples, generated by the combination of two publicly available bladder cancer gene expression datasets (15,16). When we followed the same criteria used with our dataset for classifying MIBC and NMIBC, there were 29 NMIBC samples and 42 MIBC samples in the meta-analysis dataset. There were also 14 healthy bladder tissue samples, while the rest of the samples (carcinoma *in situ*) were not used in analysis.

A total of 4513 genes were differentially expressed in NMIBC compared to healthy tissue, when a cut-off of FDR <0.05 and fold-change >2.5 were applied. When compared with differential genes from our data, there were 118 genes common in both analyses. Surprisingly except for one gene, PELO, all the other genes showed concordant expression. This included all the 8 genes upregulated in NMIBC and 109 genes downregulated in NMIBC compared to healthy bladder tissue (data not shown).

When MIBC samples were compared with healthy bladder samples, with a filter of FDR <0.05 and fold-change >3, 3905 genes were differentially expressed in the meta-analysis. A comparison with differential genes from our data under similar conditions and filtrations revealed 44 common genes. Similarly, the expressions of all except 2 genes (SERPINEB13 and CASC5) were concordant in both the analyses. All the 30 genes downregulated in MIBC compared to healthy tissue showed concordant expression, while 12 out of 14 genes highly expressed in MIBC in this study showed similar expression in the meta-analysis (data not shown).

Osteopontin protein is overexpressed in MIBC compared to healthy urothelium. In order to determine the validity of the

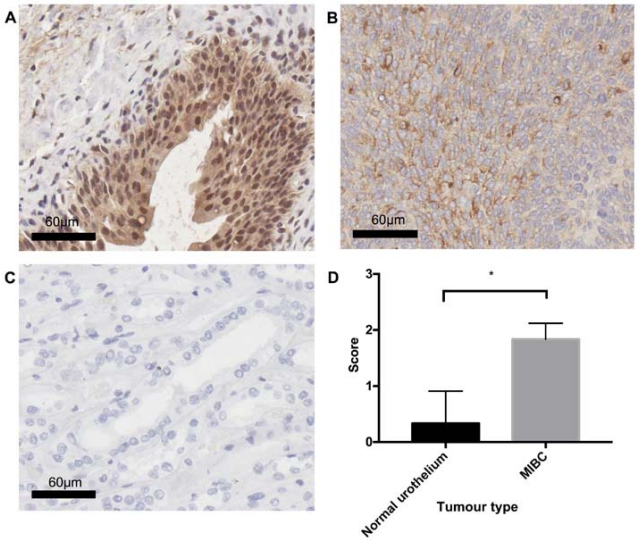

Figure 6. Comparing OPN protein expression in MIBC and healthy urothelial tissue. (A) Healthy urothelium displaying negative OPN immunostaining, with the presence of non-specific binding in urothelial tissue; (B) MIBC tissue exhibiting moderate (++) diffuse OPN immunostaining; (C) Isotype control, OPN expressing kidney tissue with polyclonal goat IgG antibody; (D) graphical representation of staining results, results are average of staining from 3 healthy urothelial samples, and 3 MIBCs, statistical analysis was performed using Welch's unpaired t-test (P=0.0286). All images are representative of the cohort. Scoring was performed by a pathologist.

microarray data, OPN expression was examined in MIBC (n=3) and healthy urothelial tissue (n=3) using the IHC technique. Statistical analysis using Welch's unpaired t-test revealed a significant difference (P=0.0286) between MIBC and healthy tissue, with MIBC displaying diffuse cytoplasmic OPN staining of moderate (++) intensity, whilst healthy urothelium was typically OPN negative (-) (Fig. 6).

Discussion

The present study contributes to a body of work that uses microarray data to profile bladder cancer, and provides fresh insights into pathways involved in its pathogenesis. Distinctive patterns of gene expression differentiating between NMIBC and MIBC, and between high and low grade cancers were identified.

A striking upregulation in pathways involved in cell cycle control was observed in comparisons of MIBC and NMIBC, and between grade 3 and grade 1 NMIBC tumours. A significant overlap was observed between genes upregulated in grade 3 NMIBC tumours and those upregulated in MIBC compared to healthy tissue and these genes were predominantly mapped to cell cycle control pathways. This is likely to reflect the increased aggressiveness and likelihood of progression of grade 3 NMIBC. This panel of genes may therefore be useful in predicting progression of NMIBC.

Cell cycle genes which were upregulated included anillin (>8-fold upregulation), a substrate of APC, which is involved in cytokinesis (17). Anillin is upregulated in various cancers including pancreatic (18) and renal carcinoma (19). TPX2, which is involved in spindle assembly (20), was also upregulated.

This upregulation of cell cycle related genes in bladder cancer is not unexpected, and was similarly shown in a study by Zaravinos *et al* (21). Notably, several of the upregulated genes have been identified as potential therapeutic targets for bladder cancers. Inhibitors of TOP2A include anthracyclines and etoposide, two well-established chemotherapy agents. The anthracycline doxorubicin, for example, exhibits anti-bladder cancer effects and is a component of the commonly employed MVAC regimen. PLK1 inhibitors are currently in phase 1 and 2 trials, and preliminary studies suggest that PLK1 inhibitors may reduce proliferation of bladder cancer cell lines (22). However, results obtained from a recent phase 2 study evaluating the efficacy of the PLK1 inhbitor volasertib as a second-line treatment in patients with locally advanced or metastatic urothelial cancer, suggests that although volasertib was well-tolerated with an acceptable safety profile the antitumour activity of volasertib was not suffecient for further evaluation as a monotherapy (23). Several CDK inhibitors are also currently in phase 1 and 2 clinical trials.

The expression of osteopontin (OPN) 'secreted phosphoprotein 1', a matricellular protein, is strongly associated with malignancies (reviewed in ref. 24). Furthermore, OPN RNA-silencing in BC significantly attenuates tumour cell

invasion (25). The finding that OPN expression was strikingly upregulated (>10-fold) in invasive bladder cancers compared with the healthy tissue is consistent with previous studies demonstrating upregulation of OPN in urothelial malignancy (22,26-28). Whilst OPN RNA expression data is well represented in BC tissue (28,29), protein expression data are limited (26,27). Therefore, OPN expression was examined between MIBC and healthy urothelium to determine whether commonality between RNA and protein expression exists in BC. OPN was found to be signifcantly (P=0.0286) overexpressed in MIBC compared to healthy urothelium. These data are consistent with obeservations in gastric (30), oesophageal (31), cervical (32) and prostate (33) cancers (26,34). Whilst a significant relationship between OPN and poor prognosis was noted in upper urinary tract urothelial cell carcinoma no correlation between stage and grades was found (27). Conversely, OPN expression is associated with improved survival in pancreatic adenocarcinoma (35).

Elevated levels of osteopontin have also been detected in the plasma of patients with advanced transitional cell carcinoma (TCC), suggesting that OPN could be a novel biomarker of disease stage (36,37). The utility of OPN expression as a prognostic marker (and/or predictor of treatment response), however, remains unproven (26,27,38). The differences in OPN expression (in blood and tissue) observed in studies could be explained, at least in part, by the expression of OPN isoforms. Specifically, OPN splice variants which exhibit divergent biological functions are differentially expressed in cancers. Intriguingly, CD44, the hyaluronic acid receptor, for which osteopontin is a key ligand (37), was found to be upregulated among invasive bladder cancers, further supporting a potential role for OPN in pathogenesis of TCC.

When comparing grade 3 NMIBC with MIBC, we observed an overexpression of the cell-matrix interaction network. In particular, there was upregulation in proteolytic enzymes such as the matrix metalloproteases (MMPs). This is consistent with the increased ability of MIBC to invade local tissues. It would be important to evaluate if overexpression of MMPs predicts NMIBC progression.

Genes involved in myogenesis and epithelial-to-mesenchymal transition (EMT) were downregulated in tumours, and this was particularly noted in NMIBC samples compared with the healthy tissue. This is intriguing, and could represent an inhibitory effect of bladder cancer on normal bladder muscle growth. EMT describes a process by which epithelial cells lose their characteristic apical-basal polarity, intercellular junctions and epithelial markers, while upregulating mesenchymal markers, acquiring front-rear polarity, and undergoing cytoskeleton reorganization into mesenchymal cells (39). EMT is associated with invasive cancers and metastases, portends a poor prognosis in patients with bladder cancer (40). In the present study, tumour samples were not micro-dissected, and the possible 'admixture' with normal muscle tissue within samples could have confounded the analysis of myogenesis and EMT genes.

One novel finding in this study is the downregulation of genes involved in the classical complement pathway within the NMIBC group. Previously, others have shown that complement inhibitors such as CD46 and complement factor H (CFH) are upregulated in bladder cancers (41). The aggregate data suggest that repression of complement activity is an important pathogenic mechanism in bladder cancer development. Intriguingly, CFH binds to the OPN protein and masks putative enzymatic-cleavage sites, and could thereby, alter OPN activity. Urinary levels of CFH were also investigated as markers of bladder malignancy (42,43), but were found to exhibit low sensitivity and specificity. This could be explained by changes in CFH levels during disease progression, and supports our findings that downregulation of complement genes occurred in NMIBC rather than MIBC samples.

ESRP1 and ESRP2 are upregulated in NMIBC (compared to healthy tissue), and are involved in the regulation of FGFR2 splicing (44). While decreased expression of FGFR2b (one of the FGFR2 splice variants) was observed in a subset of bladder cancers (45), upregulation of FGFR2c (another splice variant) was detected in a bladder cancer metastasis model (46). Consistent with reports on differential protein isoforms during cancer development, our findings support the hypothesis that differential expression of FGFR2 splice variants is an important pathogenic mechanism in bladder cancer. In agreement with data published from the Cancer Genome Atlas Reseach Network in 2013 (47) which comprehensively evaluated the molecular signature of 131 urothelial carcinomas and revealed that mutational spectrum was involved in cell cycle regulation, chromatin regulation, and kinase signalling pathways with potential therapeutic application, the present study highlights several dysregulated transcripts in BC that potentially could be targeted in BC treatment.

Whilst the long-term clinical outcome data would have allowed more robust conclusions to be drawn from the small cohort, meta-analysis of the microarray data together with the protein expression experiment highlight the importance of the presented data, in addition to the role of OPN in invasion (25). Furthermore, this study supplements a growing body of molecular data in bladder cancer allowing further understanding of this complex and heterogeneous disease.

In conclusion, this study complements the published literature, and gives credence to observed associations between patterns of gene signatures with the stage and grade of bladder cancers. Ultimately such signatures would be most clinically useful if they improve prognostication of disease, particularly among NMIBC, where a more aggressive therapeutic approach could be employed in cancers that were more likely to progress. The present study identified expression patterns, which may help this prediction (such as proteolytic enzymes), and these may be incorporated into future prospective studies. Significantly, we also identified several genes and pathways (such as OPN and the classical complement pathway) which were strikingly deregulated in bladder cancer, and which may be valuable drug targets.

Acknowledgements

We thank Sim Sihota for her skilled technical assistance in the extraction and microarray analysis of RNA.

References

1. IARC: Cancer incidence and mortality Worldwide. IARC CancerBase No. 10. Journal, 2015. http://globocan.iarc.fr.

2. Cancer Research UK: Bladder cancer statistics, 2015. http://www.cancerresearchuk.org/health-professional/cancer-statistics/statistics-by-cancer-type/bladder-cancer.
3. Kaufman DS, Shipley WU and Feldman AS: Bladder cancer. Lancet 374: 239-249, 2009.
4. Sylvester RJ, van der Meijden AP, Oosterlinck W, Witjes JA, Bouffioux C, Denis L, Newling DW and Kurth K: Predicting recurrence and progression in individual patients with stage Ta T1 bladder cancer using EORTC risk tables: a combined analysis of 2596 patients from seven EORTC trials. Eur Urol 475-467, 2006.
5. Blaveri E, Simko JP, Korkola JE, Brewer JL, Baehner F, Mehta K, Devries S, Koppie T, Pejavar S, Carroll P, *et al*: Bladder cancer outcome and subtype classification by gene expression. Clin Cancer Res 11: 4044-4055, 2005.
6. Elsamman E, Fukumori T, Ewis AA, Ali N, Kajimoto K, Shinohara Y, Ishikawa M, Takahashi M, Nishitani MA, Baba Y, *et al*: Differences in gene expression between noninvasive and invasive transitional cell carcinoma of the human bladder using complementary deoxyribonucleic acid microarray: Preliminary results. Urol Oncol 24: 109-115, 2006.
7. Riester M, Taylor JM, Feifer A, Koppie T, Rosenberg JE, Downey RJ, Bochner BH and Michor F: Combination of a novel gene expression signature with a clinical nomogram improves the prediction of survival in high-risk bladder cancer. Clin Cancer Res 18: 1323-1333, 2012.
8. Sanchez-Carbayo M, Socci ND, Lozano J, Saint F and Cordon-Cardo C: Defining molecular profiles of poor outcome in patients with invasive bladder cancer using oligonucleotide microarrays. J Clin Oncol 24: 778-789, 2006.
9. Irizarry RA, Hobbs B, Collin F, Beazer-Barclay YD, Antonellis KJ, Scherf U and Speed TP: Exploration, normalization, and summaries of high density oligonucleotide array probe level data. Biostatistics 4: 249-264, 2003.
10. Wu Z, Irizarry RA, Gentleman R, Martinez-Murillo F and Spencer F: A Model-based background adjustment for oligonucleotide expression arrays. J Am Stat Assoc 99: 909-917, 2004.
11. Bolstad BM, Collin F, Simpson KM, Irizarry RA and Speed TP: Experimental design and low-level analysis of microarray data. Int Rev Neurobiol 60: 25-58, 2004.
12. Pawitan Y, Michiels S, Koscielny S, Gusnanto A and Ploner A: False discovery rate, sensitivity and sample size for microarray studies. Bioinformatics 21: 3017-3024, 2005.
13. Huang W, Sherman BT and Lempicki RA: Systematic and integrative analysis of large gene lists using DAVID bioinformatics resources. Nat Protoc 4: 44-57, 2009.
14. Edgar R, Domrachev M and Lash AE: Gene Expression Omnibus: NCBI gene expression and hybridization array data repository. Nucleic Acids Res 30: 207-210, 2002.
15. Dyrskjøt L, Kruhøffer M, Thykjaer T, Marcussen N, Jensen JL, Møller K and Ørntoft TF: Gene expression in the urinary bladder: A common carcinoma in situ gene expression signature exists disregarding histopathological classification. Cancer Res 64: 4040-4048, 2004.
16. Als AB, Dyrskjøt L, von der Maase H, Koed K, Mansilla F, Toldbod HE, Jensen JL, Ulhøi BP, Sengeløv L, Jensen KM, *et al*: Emmprin and survivin predict response and survival following cisplatin-containing chemotherapy in patients with advanced bladder cancer. Clin Cancer Res 13: 4407-4414, 2007.
17. Zhao WM and Fang G: Anillin is a substrate of anaphase-promoting complex/cyclosome (APC/C) that controls spatial contractility of myosin during late cytokinesis. J Biol Chem 280: 33516-33524, 2005.
18. Olakowski M, Tyszkiewicz T, Jarzab M, Król R, Oczko-Wojciechowska M, Kowalska M, Kowal M, Gala GM, Kajor M, Lange D, *et al*: NBL1 and anillin (ANLN) genes over-expression in pancreatic carcinoma. Folia Histochem Cytobiol 47: 249-255, 2009.
19. Gruss OJ and Vernos I: The mechanism of spindle assembly: Functions of Ran and its target TPX2. J Cell Biol 166: 949-955, 2004.
20. Ronkainen H, Hirvikoski P, Kauppila S and Vaarala MH: Anillin expression is a marker of favourable prognosis in patients with renal cell carcinoma. Oncol Rep 25: 129-133, 2011.
21. Zaravinos A, Lambrou GI, Volanis D, Delakas D and Spandidos DA: Spotlight on differentially expressed genes in urinary bladder cancer. PLoS One 6: e18255, 2011.
22. Zhang Z, Zhang G and Kong C: High expression of polo-like kinase 1 is associated with the metastasis and recurrence in urothelial carcinoma of bladder. Urol Oncol 31: 1222-1230, 2013.
23. Stadler WM, Vaughn DJ, Sonpavde G, Vogelzang NJ, Tagawa ST, Petrylak DP, Rosen P, Lin CC, Mahoney J, Modi S, *et al*: An open-label, single-arm, phase 2 trial of the Polo-like kinase inhibitor volasertib (BI 6727) in patients with locally advanced or metastatic urothelial cancer. Cancer 120: 976-982, 2014.
24. Ahmed M, Behera R, Chakraborty G, Jain S, Kumar V, Sharma P, Bulbule A, Kale S, Kumar S, Mishra R, *et al*: Osteopontin: A potentially important therapeutic target in cancer. Expert Opin Ther Targets 15: 1113-1126, 2011.
25. Xu ST, Guo C, Ding X, Fan WJ, Zhang FH, Xu WL and Ma YC: Role of osteopontin in the regulation of human bladder cancer proliferation and migration in T24 cells. Mol Med Rep 11: 3701-3707, 2015.
26. Coppola D, Szabo M, Boulware D, Muraca P, Alsarraj M, Chambers AF and Yeatman TJ: Correlation of osteopontin protein expression and pathological stage across a wide variety of tumor histologies. Clin Cancer Res 10: 184-190, 2004.
27. Ke HL, Chang LL, Yang SF, Lin HH, Li CC, Wu DC and Wu WJ: Osteopontin overexpression predicts poor prognosis of upper urinary tract urothelial carcinoma. Urol Oncol 29: 703-709, 2011.
28. Zaravinos A, Volanis D, Lambrou GI, Delakas D and Spandidos DA: Role of the angiogenic components, VEGFA, FGF2, OPN and RHOC, in urothelial cell carcinoma of the urinary bladder. Oncol Rep 28: 1159-1166, 2012.
29. Fang ZQ, Zang WD, Chen R, Ye BW, Wang XW, Yi SH, Chen W, He F and Ye G: Gene expression profile and enrichment pathways in different stages of bladder cancer. Genet Mol Res 12: 1479-1489, 2013.
30. Imano M, Satou T, Itoh T, Sakai K, Ishimaru E, Yasuda A, Peng YF, Shinkai M, Akai F, Yasuda T, *et al*: Immunohistochemical expression of osteopontin in gastric cancer. JJ Gastrointest Surg 13: 1577-1582, 2009.
31. Kita Y, Natsugoe S, Okumura H, Matsumoto M, Uchikado Y, Setoyama T, Owaki T, Ishigami S and Aikou T: Expression of osteopontin in oesophageal squamous cell carcinoma. Br J Cancer 95: 634-638, 2006.
32. Song JY, Lee JK, Lee NW, Yeom BW, Kim SH and Lee KW: Osteopontin expression correlates with invasiveness in cervical cancer. Aust N Z J Obstet Gynaecol 49: 434-438, 2009.
33. Forootan SS, Foster CS, Aachi VR, Adamson J, Smith PH, Lin K and Ke Y: Prognostic significance of osteopontin expression in human prostate cancer. Int J Cancer 118: 2255-2261, 2006.
34. Weber GF, Lett GS and Haubein NC: Osteopontin is a marker for cancer aggressiveness and patient survival. Br J Cancer 103: 861-869, 2010.
35. Collins AL, Rock J, Malhotra L, Frankel WL and Bloomston M: Osteopontin expression is associated with improved survival in patients with pancreatic adenocarcinoma. Ann Surg Oncol 19: 2673-2678, 2012.
36. Zhao L, Wang Y, Qu N, Huang C and Chen L: Significance of plasma osteopontin levels in patients with bladder urothelial carcinomas. Mol Diagn Ther 16: 311-316, 2012.
37. Naor D, Sionov RV and Ish-Shalom D: CD44: Structure, function, and association with the malignant process. Adv Cancer Res 71: 241-319, 1997.
38. Ang C, Chambers AF, Tuck AB, Winquist E and Izawa JI: Plasma osteopontin levels are predictive of disease stage in patients with transitional cell carcinoma of the bladder. BJU Int 96: 803-805, 2005.
39. Lim J and Thiery JP: Epithelial-mesenchymal transitions: Insights from development. Development 139: 3471-3486, 2012.
40. Baumgart E, Cohen MS, Silva Neto B, Jacobs MA, Wotkowicz C, Rieger-Christ KM, Biolo A, Zeheb R, Loda M, Libertino JA, *et al*: Identification and prognostic significance of an epithelial-mesenchymal transition expression profile in human bladder tumors. Clin Cancer Res 13: 1685-1694, 2007.
41. Varela JC, Atkinson C, Woolson R, Keane TE and Tomlinson S: Upregulated expression of complement inhibitory proteins on bladder cancer cells and anti-MUC1 antibody immune selection. Int J Cancer 123: 1357-1363, 2008.
42. Babjuk M, Soukup V, Pešl M, Kostírová M, Drncová E, Smolová H, Szakacsová M, Getzenberg R, Pavlík I and Dvorácek J: Urinary cytology and quantitative BTA and UBC tests in surveillance of patients with pTapT1 bladder urothelial carcinoma. Urology 71: 718-722, 2008.

43. Cheng ZZ, Corey MJ, Pärepalo M, Majno S, Hellwage J, Zipfel PF, Kinders RJ, Raitanen M, Meri S and Jokiranta TS: Complement factor H as a marker for detection of bladder cancer. Clin Chem 51: 856-863, 2005.
44. Warzecha CC, Sato TK, Nabet B, Hogenesch JB and Carstens RP: ESRP1 and ESRP2 are epithelial cell-type-specific regulators of FGFR2 splicing. Mol Cell 33: 591-601, 2009.
45. Diez de Medina SG, Chopin D, El Marjou A, Delouvée A, LaRochelle WJ, Hoznek A, Abbou C, Aaronson SA, Thiery JP and Radvanyi F: Decreased expression of keratinocyte growth factor receptor in a subset of human transitional cell bladder carcinomas. Oncogene 14: 323-330, 1997.
46. Chaffer CL, Brennan JP, Slavin JL, Blick T, Thompson EW and Williams ED: Mesenchymal-to-epithelial transition facilitates bladder cancer metastasis: Role of fibroblast growth factor receptor-2. Cancer Res 66: 11271-11278, 2006.
47. Cancer Genome Atlas Research Network: Comprehensive molecular characterization of urothelial bladder carcinoma. Nature 507: 315-322, 2014.

Appendix II – Grant: Characterisation of dendritic cell function in the three-dimensional model of urothelial carcinoma in response to soluble CD40L based immunotherapy

CCC Charitable funds for early / novel R&D projects
Application for funding

In 2013/14 'Clatterbridge Cancer Centre' has committed £100,000 to support very early / novel R&D projects that are not suitable for established national funding routes. Projects must fit with local / national priorities and applications must not exceed £25,000. Projects can be run over more than one year but must be funded in the entirety at the outset. If you would like to discuss your proposals in advance of submission, please do not hesitate to contact Maria Maguire (Acting Research Manager) on ext: 4181 or **maria.maguire@clatterbridgecc.nhs.uk**. Please also refer to guidance document for further information. **The deadline for this call is 5pm on Friday 14TH March 2014.**

Name and job title of main applicant:	Dr Syed A. Hussain – Consultant and senior lecturer in medical oncology
Names of collaborators:	**Professor Daniel H. Palmer** (Chair of Medical Oncology), **Professor D. Ross Sibson** (Professor in Applied Cancer Biology), **Dr Taha El-Metwalli** (Senior post-doc), **Dr Asmaa Salman** (post-doc), **Mr Richard M. D. Greensmith** (PhD student)
Amount of funding requested:	**Item** / **Cost** Matrigel, collagen, CD40L and other organotypic assay reagents: £9,900 IHC antibodies/reagents: £5,000 Cell culture media/plasticware: £1,580 General laboratory consumables: £1,400 **Tot: £17,880**
Project Title:	***Characterisation of dendritic cell function in the three-dimensional model of urothelial carcinoma in response to soluble CD40L based immunotherapy.***

Project details (MAXIMUM 4 SIDES A4)
(please include background, aim of study, patients numbers, eligibility criteria, study design, statistical considerations, outcome measures / endpoints)

Bladder cancer (BC) is the fifth commonest cause of cancer-related morbidity in the UK, with 10,335 new cases and 4,907 BC-related deaths in 2010 (CR-UK). The vast majority (90%) of cases of BC are histologically classified as urothelial cell carcinomas (UCC) (*Bryan et al 2004*). Median survival for metastatic BC is approximately 12-15 months, after 5 years a meager 6% of patients survive and this has not improved significantly over the last 10 years. Non-muscle invasive disease is associated with a better outcome, with 86% of patients with non-invasive disease showing a complete response to intravesicular Bacillus Calmette-Guérin (BCG) instillation. Muscle invasive and metastatic BC requires aggressive management through radical surgery and radiotherapy, often with neo-adjuvant platinum-based chemotherapy prior to radical treatment *(James et al. 2012*). The response rate from different treatment regimens in phase II trials varies between 20-60%, but with modest survival advantage in randomised trial settings (*Hussain and James, 2003; Huddart et al., 2013*).

Due to the age and the presence of co-morbidities often as a result of a history of tobacco smoking and/or occupational exposure to aromatic amines of the average BC patient, systemic platinum based chemotherapy may not be a viable option due to toxicities including nephrotoxicity and severe neutropenia which may lead to chemotherapy related death, patients then being put on best supportive care (*Mitra & Cote 2009*). The poor response of patients to standard first line therapy, the lack of more efficacious second line treatments, and the ineligibility of a proportion of patients for cytotoxic chemotherapy leads to the immediate requirement for a novel treatment option for bladder cancer.

Over the past decade, the overexpression of key immune proteins in a large number of solid tumors

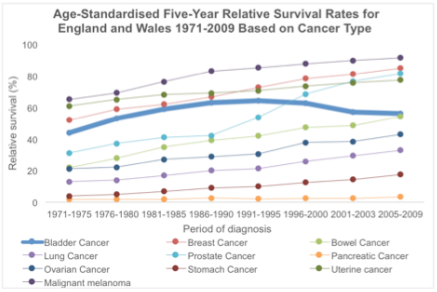

Figure 1, The relative survival of the top 10 most fatal cancers since 1971. *The relative survival of bladder cancer has been decreasing since 1990, due to slow progress in the development of new treatment options for urothelial neoplasms* (CR-UK).

including bladder has become apparent. Expressional studies have found of immunogenic markers including the co-stimulatory protein CD40 (*Cook et al 1999)*. A 48kDa member of the TNF receptor family, CD40 is a key regulator of humoral and cellular immunity expressed on a range of immune cells including B-cells, DCs and monocytes (*Vonderheide 2007, Cook et al 1999),* and also a key player in immune evasion of malignant cells *(Scarlett et al 2009)*. CD40 has been shown to be overexpressed in the majority (84%) of cases of BC (Hussain et al BJC 2003, Cooke et al 1990 J Path), with patients overexpressing CD40 having a near significant (p=0.12) increase in 5 year survival (figure 3).

The CD40 agonist, CD40-Ligand (CD40L) a 33-kDa-membrane protein is a member of the TNF family, which is mainly expressed on CD4+ T-cells in response to T-cell receptor (TCR) activation, is overexpressed in most (83%) of BCs, associated with a significant (p=0.036) increase in 5 year survival (figure 2). Due to the apparent immunogenicity of bladder cancer immunotherapy has become an attractive conceivable future therapeutic option (*Hussain et al 2003, Cooke et al 1999)*.

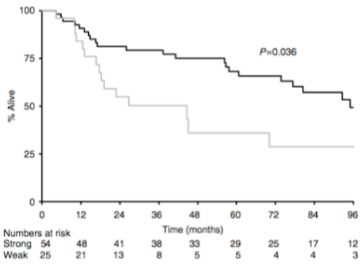

Figure 2 Survival by CD40L (— strong; — weak).

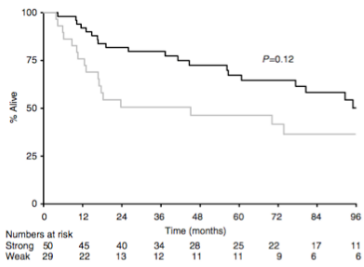

Figure 3 Survival by CD40 (— strong; — weak).

Figure 2. The effect on of strong vs weak CD40L staining on 5 year survival. *Shows a significant increase in 5-year survival for those patients whos tumours strongly express CD40L (p=0.06).* ***Figure 3. The effect of strong vs weak CD40 staining on 5 year survival.*** *Shows a near significant increase in 5-year survival for those patients whos tumours strongly express CD40 (p=0.13). (Hussain et al 2003)*

CD40L related activation of CD40 pathway has 2 effects:

1. DC licensing for priming of T-Cells and generation of a specific immune response
2. Direct activation of cell death initiating mechanism of tumor cells.

Point 1 is thought to be responsible for the bystander effect, due to uptake of tumor antigens from dead tumor cells, allowing the immune system to surmount an attack on remaining tumor cells (*Tong & Stone 2003)*.

Immunostimulating gene therapy using viral vectors which express a CD40-L construct (vCD40L) and co-culture with membrane bound CD40L expressing fibroblasts have been successful at initiating cancer cell death in different cancer models *(Dzojic et al 2006, Georgupoulos et al 2007, Kimura et al 2003, Malmstrom et al 2010, Vonderheide 2001, Beatty et al 2011*), through direct CD40-CD40L dependent tumor cell death signaling and recruitment of immune cells such as T-cells, macrophages and dendritic cells (DCs), (Malmström et al 2010).

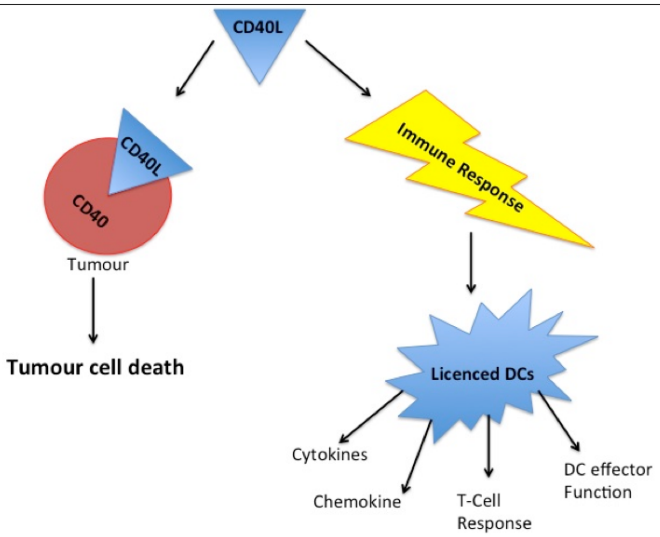

Figure 4. Differential responses to CD40 ligation. CD40L is responsible for direct tumour cell death through activation of TRAF/NF-κB/JNK/MAPK signaling pathways and DC licensing for priming of T-cells and generation of a tumour specific immune response, leading to the bystander tumour killing effect.

A phase I/IIa trial-using intravesicular Adenoviral vCD40L in the treatment of BC showed that therapy was safe, increased immune activation with heavy T-cell infiltration noted, and was generally well tolerated (Malmstrom et al 2010). Vonnderheide et all showed that human CD40L in advanced solid tumors demonstrated encouraging anti-tumour activity, including a complete response and long term remission (*Vonderheide et al 2001*).

The plan of this investigation is to explore the effect of soluble CD40L (sCD40L) on secondary 7 UCC cell lines, a range of primary UCC cell lines, in the orgaotypic model (figure 5.) of bladder cancer developed in or laboratory at the University of Liverpool, with modifications taking lessons from *Hoang et al 2011*. The organotypic model combines tumor (UCCs), immune (DCs, T-Cells, Macrophages) and stromal cells (HFFs) together in a manner, which shares homology with the setting of bladder cancer in vivo.

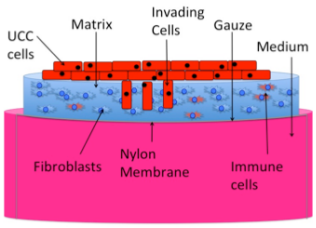

Figure 5. The three-dimensional model of bladder cancer. Showing UCC cells plated on a collagen-matrigel matrix embedded with stromal and immune cells.

This investigation will look into the effects of sCD40L dosing in the three dimensional model; on the invasion, recruitment of immune cells, activation and infiltration of immune cells, and the ratio of M2:M1 macrophages and effector function of DCs will be assessed.

Along with the expression of a number of key cytokines and chemokines involved in DC licencing and immune response including: HLA-DR, DC-SIGN, CD11c, CSF-2, IL4, IL-1B, TNF, IL10, IL13, TGFB, CX3CL1, CXCL8, CCL17, CCL18 and CCL22 *(Hoang et al 2011).*

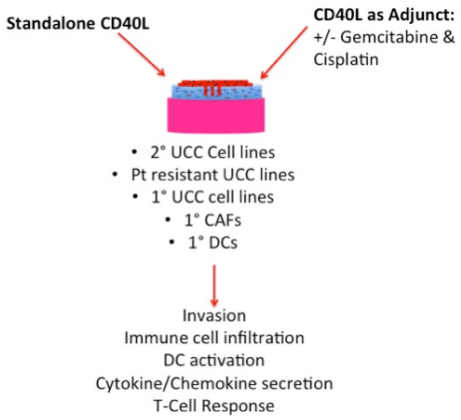

Figure 6. Plan of investigation. *With 9 secondary UCC cell lines available, 1 Platinum resistant UCC line, and a growing number of primary UCC cell lines being isolated in-house at the University of Liverpool. Organotypic assays will be assessed using H&E staining, and immunohistochemistry (IHC).*

CR-UK website (http://www.cancerresearchuk.org/cancer-info/cancerstats/types/bladder).
Bryan RT, Hussain SA, James ND, Jankowski JA, Wallace MA (2004). *Molecular pathways in bladder cancer: Part 1* BJUI 95, 485-490.
James ND, Hussain SA, Hall E, Jenkins P, Tremlett J, Rawlings C, Crundwell M, Sizer B, Sreenivasan T, Hendron C, Lewis R, Waters R, Huddart R for the investigators of BC2001 (2012) Radiotherapy with or without chemotherapy in muscle invasive bladder cancer. N Engl J Med 366, 1477-88.
Hussain SA and James ND (2003) The systemic treatment of advanced and metastatic bladder cancer. Lancet Oncol 4(8):489-497. Huddart R, Hall E,
Hussain S, Crundwell M, Tremlett J, Jenkins P, Rawlings C, James N (2013) A randomised non-inferiority trial of reduced high dose volume versus standard volume radiotherapy for muscle-invasive bladder cancer: results of BC2001 trial (CRUK/01/004) International journal of radiation oncology, biology, physics vol 87 issue 2 261-9. Mitra AP, Cote RJ (2009) Molecular pathogenesis and diagnostics of bladder cancer. Annu. Rev. Pathol. Mechan. Dis 4, 251-85
Cook PW, James ND, Ganesan R, Wallace M, Burton A, Young LS (1999) CD40 expression in bladder cancer. J. Pathol 188, 38-43 Vonderheide RH
(2007) Prospect of targeting the CD40 pathway for cancer therapy. Clin Cancer Res 15;13(4), 1083-8 Hussain SA, Ganesan R, Hiller L, Murray PG, El-Magraby MM, Young L, James ND (2003) Proapoptotic genes BAX and CD40L are predictors of survival in transitional cell carcinoma of the bladder BJC 88, 586-592. Tong AW and Stone MJ (2003)
Prospects for CD40-directed experimental therapy of human cancer. Cancer Gene Therapy 10, 1-13
Dzojic H, Loskog A, Totterman TH, Essand M (2006) Adenovirus-mediated CD40 Ligand therapy induces tumour cell apoptosis and systemic immunity in the TRAMP-C2 mouse prostate cancer model. The prostate 66, 831, 838. Georgopoulos NT, Merrick A, Scott N, Selby PJ, Melcher A, Trejdosiewicz (2007) CD40-mediated death and cytokine secretion in colorectal cancer: a potential target for inflammatory tumour cell killing. Int. J. Cancer 121, 1373-1381 Kimura T, Ohashi T, Kikuchi T, Kiyota H, Eto Y, Ohishi Y (2003) Antitumour immunity against bladder cancer induced by ex vivo expression of CD40 ligand gene using retrovirus vector. Cancer Gene Therapy 10, 833-839. Malmström P, Loskog ASI, Lindqvist CA, Mangsbo SM, Fransson M, Wanders A, Gardmark T, Torterman T (2010) AdCD40L immunogene therapy for bladder carcinoma- the first phase I/IIa trial. Clin. Cancer. Res 16 (12) 3279-87 Vonderheide RH, Dutcher JP, Anderson JA, Eckhardt GS, Stephans KF, Razvillas B, Garl S, Butine MD, Perry VP, Armitage RJ, Ghalie R, Caron DA, Gribben JG. (2001) Journal of Clinical Oncology 19 (13) 3280-3287. Beatty GL, Chiorean EG, Fishman MP, Saboury B, Teitelbaum UR, Sun W, Huhn R, Song W, Li D, Sharp LL, Torigian DA, O'Dwyer PJ, Vonderheide RH. (2011) CD40 agonists alter tumour stroma and show efficacy against pancreatic carcinoma in mice and humans. Science 331, 1612
Hoang ATN, Chen P, Juarez J, Sachmitr P, Billing B, Bosnjak L, Dahien B, Coles M, Svensson M (2011) Dendritic cell functional properties in a three-dimensional tussue model of human lung mucosa. Am J Physiol Lung Cell Mol Physiol 302, L226-37